

CRANFIELD UNIVERISTY

Binxu Zeng

Validation of Energy Saving Novel Single Shot Melting
Process for Foundry Industry

SCHOOL OF APPLIED SCIENCES
SMSC Manufacturing and materials Department

PhD THESIS

Academic Year 2010-2013

Supervisor: Mark Jolly

December 2013

CRANFIELD UNIVERSITY

SCHOOL OF APPLIED SCIENCES

SMSC Manufacturing and materials Department

PhD THESIS

Academic Year 2010-2013

Binxu Zeng

Validation of Energy Saving Novel Single Shot Melting
Process for Foundry Industry

Supervisor: Mark Jolly

December 2013

This thesis is submitted in partial fulfilment of the requirements for
the degree of Doctor of Philosophy

© Cranfield University 2013. All rights reserved. No part of this
publication may be reproduced without written permission of the
copyright owner

Executive Summary

Casting is a metal forming process: Pouring the melt metal into a desired shaped mould wait it solidifies. It is often used to manufacture complex parts, which are too expensive or time consuming to produce by other methods. However, casting probably is one of the most challenging manufacturing process. It is a highly technical engineering process requiring deep scientific understanding. A typical modern casting process contains six different stages, which named as melting, alloying, moulding, pouring, solidification and finishing respectively. At each stage, high level and precision of process control is required. Casting process also is one of the most energy intensive manufacturing processes. The metal melting consumes over half of the energy in a casting process. Therefore, the expenses on the casting process has been a significant concern due to the rising of the energy prices.

A new casting process, CRIMSON (Constrained Rapid Induction Melting Single Shot Up-casting), has been developed by teams from Cranfield University and the N-TEC Ltd. It can improve the energy efficiency of a casting process without reducing the quality. The process, firstly, uses the rapid induction furnace to melt just enough metal for one single casting; then transfer the molten charge to a computer controlled counter gravity casting platform. Finally, the highly controlled metal flow is pushed into the mould to finish the pouring and solidification. Such process reduces the defect generation and energy consumption by rapid melting, minimum holding and smooth filling of the mould.

Since the CRIMSON process is a relatively new casting production process. The main objective of this dissertation is to validate the CRIMSON process by different approaches. Firstly, the concept of the sound casting running system design and the principle of the novel CRIMSON process has been introduced. Secondly, Flow3D (A comprehensive, general-purpose computational fluid dynamics software) has been used to investigate the filling patterns of the novel CRIMSON process and the gravity sand casting process. Thirdly, life cycle assessment (LCA) method has been used in this project to review the energy consumption of the conventional casting sector and the novel CRIMSON process. The inventory data was used to assess the environmental impacts of the both casting processes. Moreover, this project investigated the productivity of the CRIMSON process. The productivity of the CRIMSON process for certain range of the casting product has been investigated and compared with the conventional casting process. Finally, the cost of the

CRIMSON process has been estimated. The total variable cost of the CRIMSON process was investigated and compared with the conventional casting process as well.

Key conclusions can be addressed as below:

- Because of the geometry requirement, the gravity poured running system cannot avoid generating double oxide film defect during the filling.
- For the CRIMSON process, all the important parameters (such as temperature, time, and velocity) are under control. The piston only needs to move at low speed to guarantee the liquid metal is delivered smoothly and the double oxide films are not formed or entrapped.
- The material flow and the embedded energy of the casting making can be evaluated by the lift cycle inventory data collection method. The embedded energy of the sand casting is about 55 MJ/kg. However, to consider the recycling and reusing the internal material, the energy burden of the CRIMSON and the conventional sand casting are 16 MJ/kg and 18 MJ/kg respectively. Considering the energy burden for saleable casting, the CRIMSON process consumes 230 MJ/kg to make saleable casting; the conventional process consumes 449 MJ/kg to make saleable casting.
- By using the collected inventory data, the environmental impact assessment can be carried out for both the casting process. The results indicate that the CRIMSON process is environmental friendly compared with the conventional sand casting process.
- A complete foundry model was developed in order to investigate the productivity of the CRIMSON process. The WITNESS simulation tool was used to assess the productivity investigation. For casting size less than 2 kg, the conventional sand casting process is productive. However, as the casting size increases, the CRIMSON process becomes more productive.
- Cost estimation also carried out for the CRIMSON process. The total variable cost of the casting process was investigated. It was found that the most expensive variable cost is the raw material cost, which can be 80% of the total variable cost. Furthermore, it is concluded that the CRIMSON process has less variable cost compared with the conventional sand casting process under most of the circumstances.

ACKNOWLEDGEMENTS

Firstly, I want to heartily thank my supervisor Professor Mark Jolly, who have been inspirational and a joy to work with. I also want to thank Professor Mark Jolly for his guidance, stimulating advice, encouragement and patience during my research and study. With his help and support, my research life at Cranfield University became a wonderful journey.

My sincere thanks go to co-supervisor Dr Konstantinos Salonitis. His wide ranging and in-depth knowledge of Life Cycle Assessment and discrete event simulation has enlightened me about investigate the CRIMSON process from different points of view.

My fellow group members, Dr. Xiaojun Dai, and Mrs Nasim Soleimanian made this group a source of friendship as well as good advice and collaboration. I'm very grateful for their continuous encouragement and benefit a lot from those stimulating discussions and sharing ideas.

Special thanks also need to give to Dr. Carl Reilly. Without his e flow3D programming of the sub-routines, many of the achievements of this thesis would not have been possible. Also thanks to the David Souders at Flow Science and Simon Olive at MAGMASoft. Their technical support has being influential in casting filling and solidification simulation.

I greatly appreciate Phil Enright from N-Tec Limited and Martin Wood from GRAINGER & WORRALL LTD. They have provided a wealth of experience, enthusiasm and technical support within this thesis. Their humour has being greatly appreciated and made it a pleasure to work with them.

The School of Applied Science at the Cranfield University have financially supported me through the years of this degree with a Departmental Scholarship. For this generous support I am truly grateful.

Finally, I owe my deepest gratitude to my family, who, as always have been supportive and encouraging, in this as with every endeavour. Thank you all for your love and belief in me!

Table of Contents

Chapter 1 Introduction	1
1 Background.....	1
2 Aim	1
3 Objectives	1
4 Research Outline and Outcome	2
Chapter 2 Literature review	5
2.1 Modern Casting.....	5
2.1.1 Sand casting method.....	5
2.1.2 Investment casting process.....	5
2.1.3 The novel CRIMSON casting process	6
2.2 Casting defects.....	7
2.2.1 Pouring defects in casting	8
2.2.1.1 Air entrainment.....	8
2.2.1.2 Bubble damage	9
2.2.1.3 Oxide film.....	10
2.2.1.4 Double oxide film (DOF)	11
2.2.2 Solidification defects.....	12
2.2.2.1 Porosity.....	13
2.2.2.2 Hot tears.....	15
2.2.2.3 Cold cracks	15
2.2.3 Summary	15
2.3 Energy during casting process	15
2.3.1 Current situation.....	15
2.3.2 Research on energy saving.....	18

2.3.3 Opportunities for saving.....	21
2.3.3.1 Direct saving.....	23
2.3.3.2 Savings through indirect saving	26
2.3.3.3 Savings through plant management.....	29
2.3.4 The CRIMSON process	30
2.4 Summary of chapter	32
Chapter 3 : Validation of the CRIMSON process through numerical simulation	33
3.1. General introduction	33
3.1.1 Software validation	33
3.1.1.1 Parameters used in the filling simulation	34
3.1.1.2 Solidification & mechanical property.....	35
3.1.2 Process introduction	36
3.1.2.1 Gravity filling method	36
3.1.2.2 The CRIMSON process.....	36
3.1.3 Methodology	37
3.1.3.1 CRIMSON casting running system	37
3.1.3.2 Gravity pouring running system design.....	38
3.1.3.3 Summary.....	43
3.1.4 Software and hardware introduction	43
3.1.5 Results	44
3.1.6 Discussion	46
3.1.7 Conclusion.....	49
3.2 Design and optimisation of an investment CRIMSON casting running system.....	49
3.2.1 Methodology	50
3.2.2 First approach.....	51
3.2.3 Running system design	53
3.2.3.1 Runner design	53

3.2.3.2 Feeder design	57
3.2.3.3 Parameter settings	58
3.2.4 Simulation results for version One	61
3.2.5 Version Two	63
3.3 Development of the CRIMSON running system design spreadsheet	64
3.4 Summary of chapter	67
Chapter 4 Validation of the CRIMSON process through Life Cycle Assessment	68
4.1 Introduction	68
4.1.1 About Life Cycle Assessment	68
4.1.1.1 Goal definition/scoping	68
4.1.1.2 System boundaries	69
4.1.1.3 Life cycle inventory data collection	70
4.1.1.4 Life cycle impact assessment	72
4.2 Inventory data collection for casting	72
4.2.1 Energy input data collection for sand mould making	72
4.2.1.1 Introduction	72
4.2.1.2 Sand additives	76
4.2.1.3 Sand mix	77
4.2.1.4 Mould making (compaction)	79
4.2.1.5 Sand reclamation	80
4.2.1.6 Transportation	84
4.2.2 Energy input data collection for metal preparation	85
4.2.2.1 Aluminium foundry energy consumption investigation	86
4.2.3 Multiple recycling inventory data collection	88
4.2.3.1 Methodology for multiple life cycle method	88
4.2.3.2 Material flow during the casting process	89
4.2.3.3 Energy burden for casting	90

4.2.3.4 Energy burden for saleable casting.....	91
4.2.4 Spreadsheet.....	93
4.2.4.1 How the spreadsheet works	94
4.2.4.2 Results	96
4.2.4.3 Discussion.....	96
4.3 Simple impact assessments: greenhouse gas emission	98
4.4 Environmental impact assessment	99
4.4.1 Data input for simulation.....	99
4.4.2 Simulation setup.....	99
4.4.3 Life cycle impact assessment	102
4.4.3.1 Greenhouse gas emission.....	102
4.4.3.2 ECO-indicator.....	103
4.4.3.3 ECO-points 97	104
4.4.4 Discussion	106
4.5 Summary of chapter.....	107
4.5.1 Inventory data for mould making.....	107
4.5.2 Inventory data for casting production	107
4.5.3 Environmental impact assessment	108
Chapter 5 Validation of the CRIMSON process through productivity investigation ...	110
5.1 Assumptions for model development	110
5.1.1 Casting weight.....	110
5.1.2 Cycle time for Melting	111
5.1.3 Customer requirements	111
5.1.4 Supplier information	111
5.1.5 Information flow	112
5.1.6 Special assumptions for shop floor operation	112
5.2 Simulation approach	113

5.2.1 Simulation model setup.....	114
5.2.2 Simulation results.....	117
5.2.3 More results and discussion	118
5.3 Summary of chapter.....	122
Chapter 6 Validation of the CRIMSON process through cost analysis.....	124
6.1 Introduction to cost estimation.....	124
6.1.1 Intuitive cost estimation techniques	125
6.1.2 Analogical cost estimation techniques	125
6.1.3 Parametric cost estimation techniques	125
6.1.4 Analytical cost estimation techniques	125
6.2 Suitable technique for current project.....	126
6.3 Model development	127
6.4 Development of casting cost estimation model	127
6.4.1 Raw material cost.....	127
6.4.2 Energy cost.....	129
6.4.3 Labour cost.....	130
6.5 Development of the cost calculation spreadsheet	131
6.5.1 Calculation spreadsheet introduction	132
6.5.1.1 Raw material cost	132
6.5.1.2 Energy cost for melting and holding	133
6.5.1.3 Labour cost	133
6.5.2 Case study	133
6.5.2.1 Case study 1: tensile test bar.....	133
6.5.2.2 Case study 2: piston head	136
6.6 More results and discussions	137
6.6.1 Recovery ratio influence	138
6.6.2 Material influence	139

6.6.3 Casting size influence.....	140
6.6.4 Batch size influence	141
6.6.5 Power output influence.....	143
6.7 Summary of chapter.....	144
Chapter 7 All-In-One spreadsheet development.....	147
7.1 The all in one spreadsheet	147
7.2 Share information.....	148
7.2.1 Casting weight	148
7.2.2 Casting yield.....	148
7.2.3 OME and RR	148
7.3 Running system design.....	148
7.4 Energy consumption estimation	149
7.5 Variable cost estimation	149
7.6 Case study	150
7.6.1 Calliper production	150
7.6.2 Sliding block.....	152
7.6.3 Casing	154
7.7 Summary of chapter	156
Chapter 8 conclusions.....	157
8.1 Simulation approach.....	157
8.2 Life Cycle Assessment approach	157
8.3 Productivity investigation	158
8.4 Cost estimation.....	159
8.5 Final conclusions.....	160
Chapter 9 Future Work.....	161
Chapter 10 Reference	162
Chapter 11 Appendix.....	170

Appendix 1: Material and energy flow chart of the conventional sand casting	170
Appendix 2 knowledge of the lean manufacturing.....	171
Appendix 3 Material and energy flow chart of the CRIMSON sand casting.....	172
11.2 Numerical casting simulation.....	173
Appendix 4 the geometry of benchmark test.....	173
Appendix 5 the simulation results	173
Appendix 6 layout of the CRIMSON facility.....	178
Appendix 7 Flow chart of velocity control in gravity casting.....	179
Appendix 8 First version of the running system design	180
Appendix 9 Second approach of the CRIMSON filter housing system	182
Appendix 10 The third approach for filter housing running system design	184
Appendix 11 the final design of the filter housing design.....	186
Appendix 12 the CRIMSON running system design spreadsheet.....	188
11.3 LCA Investigation of the casting process	189
Appendix 13 life cycle of the sand casting product (also can be found on DVD)	189
Appendix 14 Average values for “Q” for Fabric Belts	190
Appendix 15 Energy burden result from 1993 to 2010.....	191
Appendix 16 Saleable casting per unit melting of aluminium, process yield, recovery ratio and recycling efficiency for different casting products 15.....	192
Appendix 17 sand casting energy consumption calculation spreadsheet	193
Appendix 18 Energy burden of sand mould making and total energy burden of casting	194
Appendix 19 Energy burden of sand mould making through secondary reclamation method and total energy burden of the casting.....	194
Appendix 20 Energy burden of sand mould making through thermal reclamation method and total energy burden of the casting.....	195
Appendix 21 Total energy burden for different recycle and non-recycle models.....	195

Appendix 22 Metal loss during each step of casting operation for the CRIMSON and the conventional casting processes	196
Appendix 23 Impact assessment: GWP, AC, HTA due to emissions from the casting process and raw materials.....	196
Appendix 24 ECO-indicator single score results for four casting scenarios	197
Appendix 25 Weighting comparison using ECO-Points 97 method.....	198
Appendix 26 ECO-point single score results for four casting scenarios.....	199
11.4 Productivity investigation: foundry survey and response	200
Appendix 27 the foundry survey	200
Appendix 28 the foundry survey response from GKN.....	202
Appendix 29 the foundry survey response from himangshu patel	202
Appendix 30 the foundry survey response from RD casting.....	202
Appendix 31 the foundry survey response from zac ulsinger	202
11.5 Data of cost estimation.....	202
Appendix 32 the comparison of the simulation results and the calculation results for different power output.	202
Appendix 33 the conversation with Martin Wood from GW Cast about sand cost	202
Appendix 34 the cost estimation spreadsheet.....	204
Appendix 35 gravity pour casting running system design spreadsheet.....	205
Appendix 36 All-in-one spreadsheet	206
11.6 Machineries for sand making	207
Appendix 37 specification of machineries for sand making	207
11.7 Publication.....	216
Appendix 38 Publications.....	216

Table of Figure

Figure 2-1 Investment casting process. Photo comes from PREVAIL casting LTD	6
Figure 2-2 Schematic of the constrained melting furnace (Jolly, 2010).....	6
Figure 2-3 Photograph of the CRIMSON melting facility (Jolly, 2010).....	7
Figure 2-4 Impingement at the bottom of the down-sprue	9
Figure 2-5 Bubble trail generation, movement and trail collapse mechanisms.....	10
Figure 2-6 Surface entrainment event.....	11
Figure 2-7 Schematic of entrainment defects	11
Figure 2- 8 Schematic of the progress of gas precipitation at the dendrite arm space	14
Figure 2- 9 UK annual casting production.....	17
Figure 2-10 Material and energy flow chart of a conventional sand casting process.....	22
Figure 2-11 Metal flow in the foundry	27
Figure 2-12 typical energy use in a foundry.	29
Figure 2-13 Energy and metal flow of the CRIMSON casting process.	31
Figure 3-1 the entire CRIMSON facility (top view). The arrow represents operation sequence. + High resolution layout can be seen in Appendix 5	37
Figure 3-2 CRIMSON up-casting runner	37
Figure 3-3 Typical gravity poured running system.....	38
Figure 3-4 Schematic of the recommended pouring basin (Jolly, 2002).....	39
Figure 3-5 Flow chart of the velocity control in the gravity poured running system (Zeng, 2010). High resolution flow chart can be seen in Appendix 6 (pp185).....	42
Figure 3-6 Key dimensions of the running system	43
Figure 3-7 Tb stands for tensile test bar; it counts from left to right. ig represents ingate.....	45
Figure 3-8 Schematics of the fluid behaviour in the pouring basin.....	47
Figure 3-9 Schematic of DOF generation during falling. Parts c and d show DOFs stuck on the taper-shaped down-sprue	48
Figure 3-10 Demonstrating fluid behaviour during the CRIMSON filling process. Fluid is moving very smoothly in the runner.	48
Figure 3-11 schematic of the geometry of the filter housing.....	50
Figure 3-12 Ground design adapted from tensile test bar.....	51
Figure 3-13 Solidification results. Left to right: porosity, FS time and Hot spot FS time	52
Figure 3- 14 shows the thinnest cross section area of the filter housing	53
Figure 3-15 Critical height of the sessile drop (Jolly, 2002)	54

Figure 3-16 typical shape of the runner bar	55
Figure 3-17 Velocity profile for different heights of runner.....	56
Figure 3-18 schematics of fluid pattern for different heights of runner	56
Figure 3-19 DOFs count for different casting running systems	57
Figure 3-20 Schematic of the shape of the feeders and their locations	58
Figure 3-21 Main effects plot for SN ratios. Indicates that a good casting should have pouring temperature of 700 °C, a mould temperature of 500 °C, a filling rate of 0.25l/s and a 6-mm thickness shell.....	61
Figure 3-22 First version of the filter housing design and key parameter settings.....	62
Figure 3-23 Schematics of the smooth and uniform filling process for Version One	62
Figure 3-24 Configuration of Version Two. All of the feeders are located out of the filter housing.....	64
Figure 3- 25 schematics the system approach to design the CRIMSON running system	65
Figure 3- 26 shows three different situations for the CRIMSON casting production	66
Figure 3- 27 shows the guide provided by the spreadsheet.	67
Figure 4-1 System boundaries for both casting process	69
Figure 4-2 Schematic of the entire life cycle of the sand casting product. High resolution version can be found in appendix 12	71
Figure 4-3 Process flow chart of sand mould construction.....	73
Figure 4-4 Process flow chart of sand making. Please note every arrow in this graph represents transportation by conveyor belt or bucket elevator	74
Figure 4-5 Schematic of a continuous mixer (muller) for chemical bonded sand (Brown, 1999)	78
Figure 4-6 Typical structure of a continuous mixer , containing a muller wheel and plough blade (A-Yite-group-Limited, 2012)	78
Figure 4-7 Process flow chart of primary mechanical reclamation. Every arrow in this graph represents a conveyor or bucket elevator, which means energy is consumed in the transportation	81
Figure 4-8 Process flow chart of full mechanical reclamation typical for resin bonded sand. Every arrow in the graph represents a conveyor or bucket elevator, which means energy is consumed by transportation	82
Figure 4-9 Process flow chart of full thermal reclamation. Every arrow in the graph represents a conveyor or bucket elevator, which means energy is consumed by transportation	82

Figure 4-10 Box plot showing the distribution of energy burden from 1993 to 2010.....	87
Figure 4-11 Energy burden for different foundry sectors.....	90
Figure 4-12 Process flow of sand in a foundry	94
Figure 4-13 Flow chart of new simulation.....	101
Figure 4-14 ECO-indicator single score results for four casting scenarios. High resolution table can be seen in appendix 24.....	104
Figure 4-15 ECO-point single score results for four casting scenarios. High resolution table can be seen in appendix 26	105
Figure 5-1 Process flow of the Witness simulation for conventional casting sand process. In current simulation, the container in the process only takes one piece at a time	115
Figure 5-2 Process flow of the Witness simulation for the CRIMSON casting process. In current simulation, the container in the process only takes one piece at a time	116
Figure 5-3 Layout of the conventional casting sand process in WITNESS. The process starts from raw metal 1 on the left side. Followed by the assumption there are no inventories from preheating to holding. After casting, buffers are applied to represent the work-in-process inventory	116
Figure 5-4 Schematic of the current state of CRIMSON process. A part arrives every 4.8 minutes. The capacity of the container is 20.....	117
Figure 5-5 Simulation results of output for both casting processes under different casting weights for one-year period	117
Figure 5-6 Comparison of busy status between the CRIMSON and the conventional casting processes. Maximum, minimum and mean difference between the processes are shown. Above base line means conventional has higher utilization, below base line means CRIMSON has higher utilization.....	118
Figure 5-7 CRIMSON product output under different power outputs	119
Figure 5-8 Machine utilisation for different casting settings; higher utilisation means higher productivity	120
Figure 5-9 Machine utilisation in producing 3 kg castings under different power outputs...	120
Figure 5-10 Utilisation to produce 8 kg castings under different power outputs	121
Figure 6-1 Typical classification of cost estimation techniques (Niazi, et al., 2006).....	125
Figure 6-2 Difference between simulated and calculated results for the CRIMSON process under 100 kW power output. Clearly, as the casting size and shipment increase, the simulated results and calculated results become identical	131
Figure 6-3 Schematic of the relation between variable cost and variables.....	131

Figure 6-4 Illustration of the colour system in the spreadsheet	132
Figure 6-5 Schematics of the running system design for piston head. The left-hand side is the CRIMSON running system and the right-hand side is the conventional sand casting system. The casting yield for the CRIMSON system is 58% and the casting yield for the conventional system is 52%	136
Figure 6-6 Cost breakdown for the two case studies	138
Figure 6-7 Cost contribution for different sand reclamation methods (different recovery ratios)	139
Figure 6-8 Contribution of the different variable costs	140
Figure 6-9 Total variable cost for different sizes of casting and the cost per kg as the casting size increases.....	141
Figure 6-10 Results show total variable costs vary with batch size and unit cost to produce one casting	142
Figure 6-11 Total variable costs for different power outputs for the CRIMSON process	143
Figure 6-12 Comparison of the CRIMSON and conventional sand casting processes. The red line is the base line of the comparison. Left-hand side of the red line means that conventional casting is expensive, the right-hand side of the red line means that the CRIMSON process is expensive and the red line means both casting processes have the same cost.....	144
Figure 6-13 Average cost contribution and distribution of each variable cost	145
Figure 7- 1 schematics the flow chart of the all in one spreadsheet. Because of the shared information, each function can be connected	147
Figure 7- 2 schematics the simplified spreadsheet for gravity running system design, the blue cells are the user input data, the red cells are the output results, the green one are the shared information with other sheet, and the black cell is the default value.....	149
Figure 7- 3a left side is the geometry of the calliper. Figure 7- 3b right side is the casting orientation with feeder and cooling fin	150
Figure 7- 4 running system on the left is for the CRIMSON process, the running system on the right is for the gravity sand casting process. Both are designed to the highest specification	151
Figure 7- 5the geometry of the sliding block.....	152
Figure 7- 6 the left side shows the casting orientation and the right side shows the casting feeder and cooling fin location	153
Figure 7- 8 shows the geometry and casting orientation of the casing.....	154

Figure 7- 9 the left side is the CRIMSON running system, and the right side is the gravity poured running system.....155

Table of Table

Table 2- 1 Assessment of applicability of lean tools in the steel industry.....	20
Table 2-2 Capacity, fuel type and energy efficiency of different furnaces.	23
Table 2-3 General metal loss during each operation.	27
Table 2-4 Summary of energy loss and opportunities for energy saving	30
Table 3-1 Parameters used in the simulations.....	34
Table 3- 2 Comparison of the benchmark and the different simulation results.....	35
Table 3-3 Initial data for mould design.....	39
Table 3-4 DOFs generated in the gravity sand casting running system	45
Table 3-5 DOFs generated in the CRIMSON running system	46
Table 3-6 General settings and results	52
Table 3-7 Dimensions of the feeders	58
Table 3-8 Parameters that need to be tested for filter housing	59
Table 3-9 Parameter combination of orthogonal array L9 (3*4).....	60
Table 3-10 Response table for signal-to-noise ratios Smaller	60
Table 3-11 Porosity volume for Version One.....	62
Table 4- 1 Example of various types of vibrating feeders	75
Table 4-2 Embedded energy of sand	76
Table 4-3 Energy contents of the sands, additives and mixed sands.....	77
Table 4-4 Energy burden of the mixer and moulding machines.....	80
Table 4-5 Energy burden of primary reclamation.....	83
Table 4-6 Energy burden of secondary reclamation	83
Table 4-7 Energy burden of thermal reclamation	83
Table 4-8 Summary of the energy burden of making sand moulds using different materials and processes	85
Table 4-9 Database used to collect data.....	86
Table 4-10 Energy burden result from 1993 to 2010.....	87
Table 4-11 Summary of weight loss for different casting foundry sectors.....	89
Table 4-12 Saleable casting per unit melting of aluminium, process yield, recovery ratio and recycling efficiency for different casting products.	90
Table 4-13 Operational material efficiency of the different foundry sectors	92

Table 4-14 Energy burden of saleable castings for different casting processes under critical condition	92
Table 4-15 Energy burden of saleable castings for different casting processes under multiple recycling method.....	93
Table 4-16 Energy burden of sand mould making and total energy burden of casting.	96
Table 4-17 Energy burden of sand mould making through secondary reclamation method and total energy burden of the casting.	96
Table 4-18 Energy burden of sand mould making through thermal reclamation method and total energy burden of the casting.	96
Table 4-19 Table of the unit energy consumption and energy consumption of sand mould making for different mould making methods	97
Table 4-20 Total energy burden for different recycle and non-recycle models.	98
Table 4-21 Equivalent CO ₂ emissions for four different situations.....	99
Table 4-22 Metal loss during each step of casting operation for the CRIMSON and the conventional casting processes.	100
Table 4-23 Total aluminium used to produce the test bar	101
Table 4-24 CO ₂ emission resulting from the simulation and the spreadsheet	102
Table 4-25 Impact assessment: GWP, AC, HTA due to emissions from the casting process and raw materials.	103
Table 4-26 Environmental impact contribution sorted by process type under ECO-indicator method.....	104
Table 4-27 Weighting comparison using ECO-Points 97 method.	105
Table 4-28 Environmental impact contribution sorted by process type under ECO-point method.....	106
Table 4-29 Summary of the embedded energy of casting before and after recycling	108
Table 5-1 Depending on the capacity of the CRIMSON furnace, a maximum 10 kg aluminium casting can be produced.....	111
Table 5-2 Time required to melt different weights of metal to make one casting under the CRIMSON process	111
Table 5-3 Time required to melt different weights of metal to make one casting under the conventional process.....	111
Table 5-4 Assumptions of setup time, cycle time, changeover time, availability and up time for different equipment used in conventional sand casting process	113

Table 5-5 Assumptions of setup time, cycle time, changeover time, availability and up time for different equipment used in the CRIMSON process.....	113
Table 5-6 Theoretical calculation results of casting products made in one year under the assumptions.....	113
Table 5-7 Labour productivity results for both casting processes. The conventional casting sand process is more productive than the CRIMSON process	118
Table 5-8 Labour productivity for different casting processes for different casting sizes and power outputs.....	122
Table 6-1 Quantity of the shipment by customer requirement	127
Table 6-2 Operation cycles to consume the recycled metal and total weight of recycled metal and new metal	134
Table 6-3 Key variables used to calculate the variable cost	136
Table 6-4 Total variable costs for both casting processes	136
Table 6-5 Key variables used to calculate the variable cost	137
Table 6-6 Total variable cost for case study 2	137
Table 6-7 Parameters used to investigate the influence of recovery ratio	138
Table 6-8 Parameters used to compare the variable costs	140
Table 6-9 Parameters used to investigate the influence of size	141
Table 6-10 Parameters used to investigate the influence of batch size.....	142
Table 6-11 Parameters used to investigate the influence of power	143
Table 7- 1 the casting yield and OME results from the spreadsheet	151
Table 7- 2 energy burden and energy consumption of each operations	151
Table 7- 3 the production time and variable cost estimation	152
Table 7- 4 the casting yield and OME results from the spreadsheet	153
Table 7- 5 energy burden and energy consumption of each operations	153
Table 7- 6 the production time and variable cost estimation	154
Table 7- 7 the casting yield and OME results from the spreadsheet	155
Table 7- 8 energy burden and energy consumption of each operations	155
Table 7- 9 the production time and variable cost estimation.....	156
Table 8- 1 shows the guides of the power selection for the CRIMSON process.....	159

Chapter 1 Introduction

1 Background

Despite years of decline in traditional, high volume foundries, the UK remains in ahead light metal alloy casting and investment casting, especially in the aerospace and automotive sectors (Jolly, 2010). As a result, foundry engineers in these sectors normally view the quality of the casting product as the most important factor. According to author's knowledge, only few investigation or optimisation of the energy efficiency of the casting process has ever been performed with a view to reducing energy consumption in a light alloy foundry. This research project works with several different light alloy foundries to quantify and model their energy usage. The results are then compared with the novel Constrained Rapid Induction Melting Single Shot Method (CRIMSON) to identify opportunities for reductions in energy usage in the foundry industry. This project is aimed at the light metal industry in general but the bulk of the work focuses on the production of aluminium alloy.

2 Aim

The aim of this PhD study is to quantify and model achievable energy savings when using a novel single shot casting process compared with traditional foundry processes.

3 Objectives

- Assessing the energy required to heat bulk metal, maintain it at temperature and transfer into the mould
- Measuring the energy input for the equivalent casting using CRIMSON melting
- Estimating the energy of quality, e.g., measuring waste/scrap metal that can be re-melted from the traditional and CRIMSON methods
- Developing a model of foundry processes using the information gathered above, such that a practical tool can be developed for use by foundry staff to assess energy usage for a range of casting types and foundry processes.

4 Research Outline and Outcome

1. Stage One: Literature review.

Outlines:

- Review on typical casting defects in a casting product
- Review on the mechanisms of casting defects
- Review on concept of good casting running system design
- Review on the energy usage of a conventional casting foundry and the novel CRIMSON process
- Review on the current energy saving method

Outcome:

- Understanding typical casting defects and their mechanisms of formation
- Understanding the theories used to design the sound casting running system and be able to design good casting running to minimise casting defects
- Understanding how energy is used in a conventional casting foundry and be able to calculate the energy consumption
- Understanding how energy is used in the novel CRIMSON method and be able to calculate the energy consumption

2. Stage Two: Using a numerical simulation tool to compare the conventional gravity sand casting process with the novel CRIMSON process. Using the advantages of the CRIMSON process, design the casting running system for an investment casting running system for a partner foundry.

Outlines:

- Use casting simulation package for validation, Flow3D[®]¹ or MAGMA5²
- Design and optimise a gravity poured sand casting running system
- Establish the gravity sand casting filling model based on real pouring conditions
- Establish the CRIMSON filling model based on experiment data and real pouring conditions

¹ Flow science: <http://www.flow3d.com/index.html>

² MAGMASOFT[®]: <http://www.magmaflow.com/en/>

- Use the combination of Flow3D and Magmasoft 5 to design and optimise the CRIMSON runner
- Work with the factory to validate the design

Outcome:

- Be able to use of Flow3D and Magmasoft 5 establish simulation for filling and solidification
 - Be able to design a sound casting running system using running system design concept
 - Developing the CRIMSON running system design guidelines, which can be used as a standard CRIMSON running system design guide
3. Stage Three: Using the Life Cycle Assessment (LCA) method, investigate the environmental impact of using the CRIMSON process.

Outlines:

- Investigating the energy and material consumption of sand mould making process
- Using multiple recycling methods to investigate the energy consumption and material recycling
- Using the Life Cycle Inventory analysis to collect the energy and material consumption of the casting process
- Using the SimaPro Life Cycle Assessment simulation package to assess the environmental impact of the casting process

Outcome:

- Understanding the methods of material and process selection during construction of sand moulds
- Be able to calculate the energy consumption of the process of sand mould construction
- Be able to calculate the energy consumption of the casting process
- Be able to calculate the energy consumption of the casting process under recycling
- Be able to develop an LCA model for environmental impact assessment

4. Stage Four: Develop a complete foundry model to investigate the productivity of the CRIMSON process.

Outline:

- Developing a survey to investigate the cycle time for different casting operations
- Applying lean thinking such as value stream mapping (VSM) to develop a foundry model
- Use the process simulation package WITNESS to investigate the productivity of the casting process under a range of conditions

Outcome:

- Be able to identify waste within the process
- From the investigation results, be able to choose the suitable casting process for specific casting products

5. Stage Five: Develop a complete foundry model to estimate the cost of the casting production.

Outline:

- Choose an appropriate cost estimation method to investigate the total production costs
- Use the process simulation package WITNESS to investigate the production time of the casting process under different variables

Outcome:

- Understand the differences between different cost estimation methods
- Develop a cost estimation spreadsheet to integrate all variables
- Identify those variable most influential on total production cost
- Identify methods that could possibly reduce the cost of production

Chapter 2 Literature review

2.1 Modern Casting

Casting is the name of the manufacturing process of pouring molten metal into a mould and then allowing it to solidify. It is often used to manufacture complex parts, which are too expensive or too time consuming to produce by other methods. The casting methods used in this project will be introduced briefly below.

2.1.1 Sand casting method

Sand casting is a casting process that uses an expendable sand mould. The mould is normally made from a sand and clay mixture. It can be used in ferrous and non-ferrous foundries. Although it requires significant quantities of sand, it remains the most cost-effective casting method. Owing to the easy operational feature of gravity pouring, most sand castings are poured by this method. Therefore, the sand casting process is the most widely used casting method throughout the world; over 70% of all cast products are made by this method (Rao, 2010).

2.1.2 Investment casting process

Investment casting is a metal-forming process that uses expendable patterns. This is a standard casting technique and is used widely to produce high quality parts. The investment casting process was developed from the lost wax process, which was invented at the beginning of the Bronze Age (Jolly, 2002). Since then, copper, silver or bronze metals have been used in this process to produce artistic products or jewellery. During World War 2, because of the urgent military demands burdening the industry, the lost wax process provided a shortcut for producing complete geometry and near net shape precision (IndiaMART, 2012) (NPC, nd). Nowadays, the lost wax process is known as the investment casting process. Its accuracy, versatility and integrity tie it to the aerospace industry and subsequently, to other high quality engineering components. A single crystal compressor blade for a gas turbine is one of the best examples of the use of the investment casting process (Jolly, 2002). The process is shown schematically in figure 2.1 (PREVAIL, 2012)

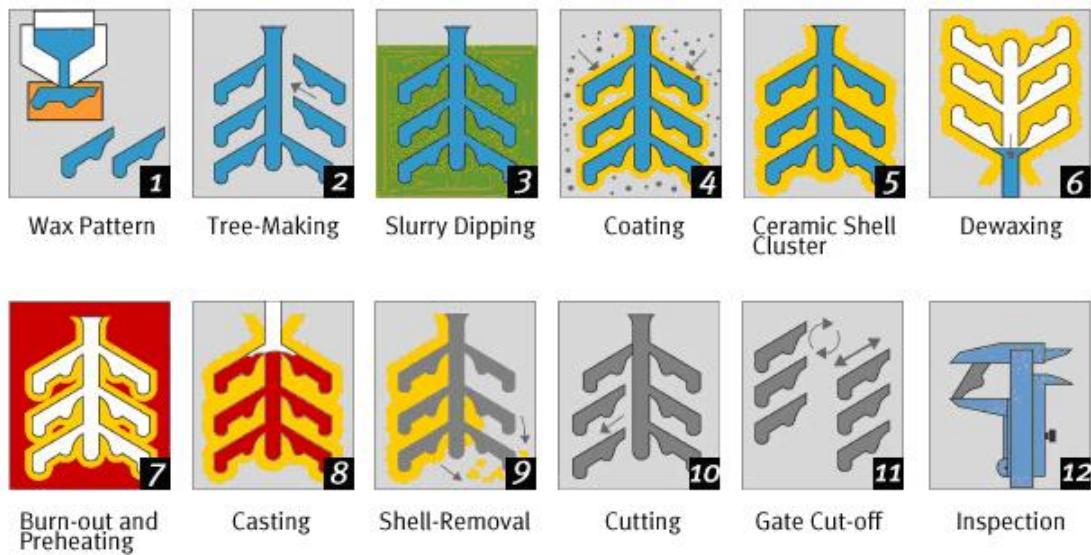


Figure 2-1 Investment casting process. Photo comes from PREVAIL casting LTD

2.1.3 The novel CRIMSON casting process

For the purpose of improving casting quality within the light metal casting industry and related energy issues, the researchers and engineers from the Birmingham university, Cranfield University and a local company called N-Tec LTD., co-invented CRIMSON, a patented up-casting method (Jolly, 2010). The CRIMSON method uses a rapid induction furnace to melt just enough metal for a single mould rather than bulk melting used in traditional processing (Figure 2.2). The molten metal is then transferred to a computer-controlled platform to complete the counter-gravity up filling (Figure 2.3) (Dai, et al., 2010).

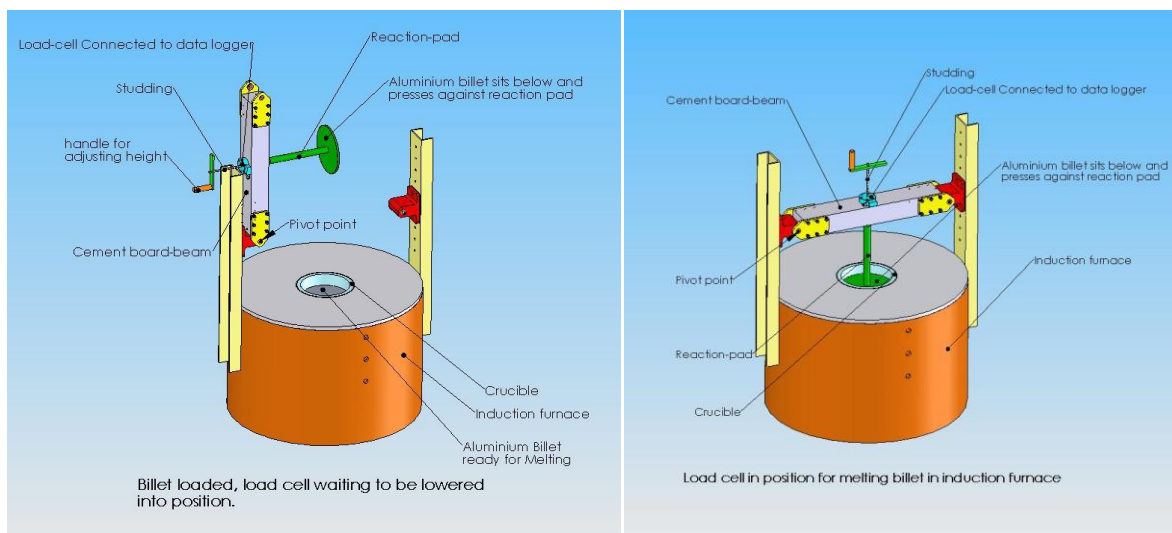


Figure 2-2 Schematic of the constrained melting furnace (Jolly, 2010)



Figure 2-3 Photograph of the CRIMSON up-casting facility (Jolly, 2010)

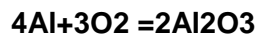
Figure 2-2 shows the constrained melting unit of the CRIMSON process. The furnace melts the correct amount of metal for a single-shot casting. During the melting, the proximity of the lid helps achieve fast melting and precision. Thus, the molten metal has less chance to react with the atmosphere to form an oxide film or to absorb hydrogen; and degassing and drossing become unnecessary processes in this casting process. Figure 2-3 shows the up-casting facility used in the CRIMSON process. This up-casting facility is attached to a computer-controlled servo-motor, which offers precise control of the filling to any desired level. Thus, quiescent and turbulence-free filling can be achieved, which reduces the generation of defects during this stage and ultimately, reduces the quantity of scrap (Campbell, 2004).

2.2 Casting defects

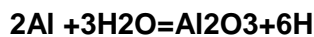
Casting is possibly the most challenging manufacturing process. In fact, it is a highly technical engineering process requiring significant scientific understanding. A typical modern casting process contains six different sub-processes: melting, alloying, moulding, pouring, solidification and finishing (Campbell, 2004). At every stage, the accuracy of process control is very strict.

To demonstrate how easily a defect can form, an example of porosity is introduced. Casting has suffered a poor reputation mainly because of small holes within the castings; which are known as porosity. There are many reasons for porosity to appear in the casting. In many foundries, the melting process is achieved in an open environment. For aluminium foundries,

the highly active molten metal not only reacts with oxygen (Eq. 1) but it also reacts with water vapour (Eq. 2) in the air. As the reaction equations show, hydrogen then decompose as nascent hydrogen in the molten metal. As a result, the degassing, refining, reduction of the hydrogen content and modification of the composition are essential (BCS, 2005). If the drossing and degassing are not applied, the nascent hydrogen can remain in the molten metal until the solidification stage, whereupon, because of the different solubilities in the liquid and solid states, it diffuses from the melt causing the problem of porosity.



Equation 1



Equation 2

Secondly, the mould design is very important. It needs to be well vented during the filling, it has to control the velocity of the filling metal and it has to supply sufficient metal for feeding during solidification; otherwise, filling and solidification defects will occur, leading to porosity problems within the casting. The details of pouring and solidification defects will be introduced in later in the review.

Many factors can cause porosity defects: composition of the alloy, temperature of the melt and mould, velocity of the filling and the quality of the mould/die, etc. Only if the process is correct at every single step can a sound and reliable casting be produced. This example has already indicated how easily porosity can occur. Later on, different mechanisms for the formation of porosity will be introduced in detail. Porosity is only one kind of defect in casting products; other serious casting defects that can occur will be introduced later. In the following review, casting defects are divided into two categories: pouring defects and solidification defects.

2.2.1 Pouring defects in casting

Once the liquid metal exceeds a critical velocity during filling, surface turbulence of the liquid flow usually leads to entrainment defects, including air entrainment, bubble damage and double oxide films (DOFs). These defects reduce the reliability of the castings significantly.

2.2.1.1 Air entrainment

Bubbles can become entrained into castings in many different ways. The most common is due to the impingement mechanism of the metal stream against a solid surface or other liquid metal. The base of the pouring basin and the down-sprue are the most common places for air

entrainment (Jolly, 2002). Typically, these places are areas in which there is a combination of the impingement of the metal stream on the mould surface and on the pool of liquid metal in the running system (Figure 2-4).

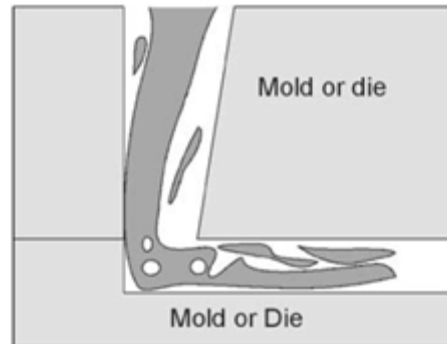


Figure 2-4 Impingement at the bottom of the down-sprue

Figure 2-4 shows the impingement at the bottom of the down-sprue but it also indicates the occurrence of a phenomenon called Vena Contracta, which is where the liquid reduces in cross-sectional area as it falls (Falkovich, 2011). As a result, the shape of the down-sprue has to be tapered. There are two reasons for this arrangement. First, the tapered shape is more likely to match the falling metal stream as it experiences the Vena Contracta phenomenon. The liquid metal can then be constrained easily inside the down-sprue. Secondly, the tapered shape can fill the down-sprue more quickly; otherwise, low pressure is experienced in the down-sprue, which sucks more air into the running system (Jolly, 2002).

2.2.1.2 Bubble damage

Once bubbles have been sucked or entrapped into the running system, the story does not end. Owing to their buoyancy, the bubbles will float up. As mentioned before, oxide films can be formed when in contact with air. Thus, the air bubbles react with the surrounding liquid metal as they pass through it, which causes channels, the surfaces of which are coated with a layer of oxide film. Because there is no residual liquid on the surface of the oxide film, there is no adhesiveness on the surface of the oxide film; therefore, the channel never heals. Because of the pressure of the liquid metal, each channel may collapse and leave a 'star-shaped' oxide and these oxide channels quickly form a complex mesh, although in some instances, this mesh can block the movement of other bubbles (Campbell, 2004). Thus, hollow structures can be formed inside the casting products, which weaken its performance (Figure 2-5).

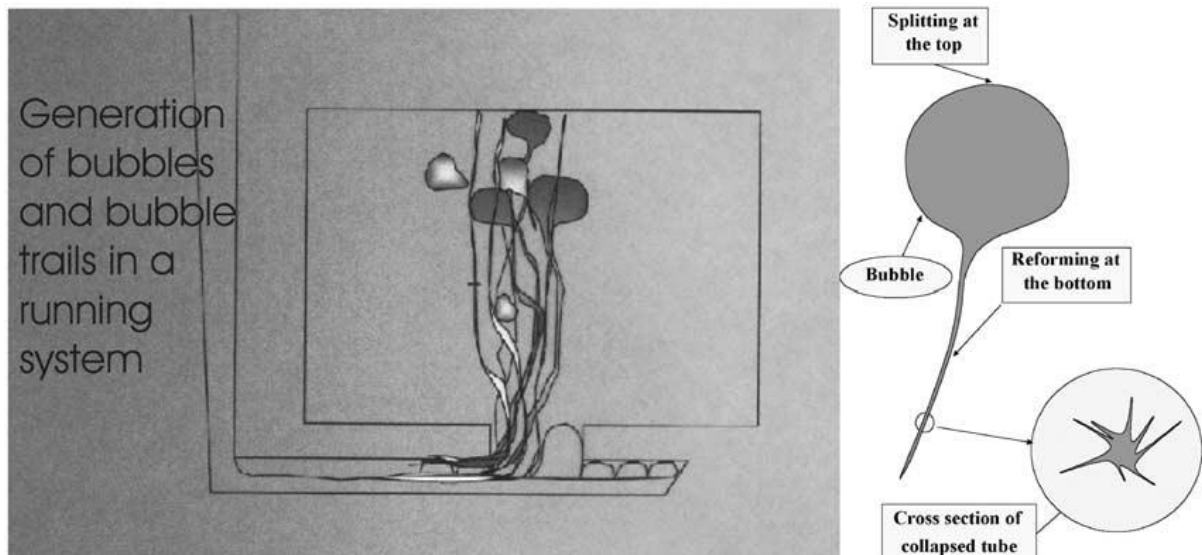


Figure 2-5 Bubble trail generation, movement and trail collapse mechanisms in liquid metals (Divandari, 2001)

2.2.1.3 Oxide film

When liquid metal comes into contact with air, oxides are formed on its surface. In the case of aluminium, the oxide is solid, continuous, forms extremely rapidly and is difficult to break up. In aluminium casting, oxide films derive mainly from two sources: melt preparation, and filling. Oxide films from the melting process can be called ‘old’ oxide films because of the long duration of oxidation. Some of this kind of oxide film can be removed easily in the melt preparation stage (drossing). On the other hand, oxide films that form during the filling process can be termed ‘young’ oxide films. These types of film are usually very thin because of the short time of the reaction. As the filling time for a casting is normally less than 60 seconds, the thickness of oxide films is normally between 0.01 and 0.1 μm (Campbell, 1991) (Reilly, 2010). During an entraining event, parts of the thin layer of oxide film can easily become detached and spread into the bulk liquid. Figure 2-6 displays a surface entrainment event at the filling stage. Owing to the mechanism of surface turbulence, the surface oxide film breaks and folds on itself before becoming entrapped within the bulk liquid. In many cases, the oxide film is a layer of dry film. Therefore, the fragments of folded double oxide film cannot bond with each other and leave a gap in between. Eventually, these randomly sized defects can act as sites for pore initiation in the solidification stage, or for crack initiation in the final casting product (Green & Campbell, 1994).

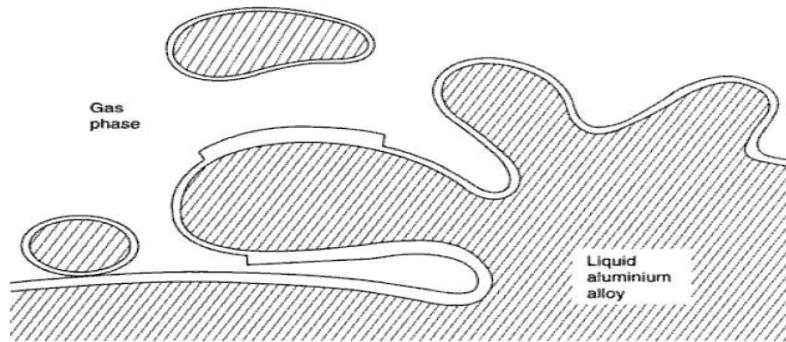


Figure 2-6 Surface entrainment event (Campbell, 1991)

2.2.1.4 Double oxide film (DOF)

As discussed in the previous section, DOF is a defect caused by surface turbulent flow during filling, which leads to the action of folding. For film-forming metals such as aluminium alloy, the folding action breaks the surface oxide film and it folds on itself. Eventually, the folded films will become entrained into the bulk liquid due to the surface turbulent flow and function as cracks in the casting. Back waves, bubble entrapment, colliding fluid fronts and both plunging and rising jets during the filling can cause the entrainment of DOFs into the bulk liquid (Reilly, 2009).

The generation of DOF is via a folding-in action, which means that not only air can become entrapped between the films but other inclusions can be trapped as well. Campbell (2004) summarised six different entrappings between oxide films, as shown in Figure 2-7.

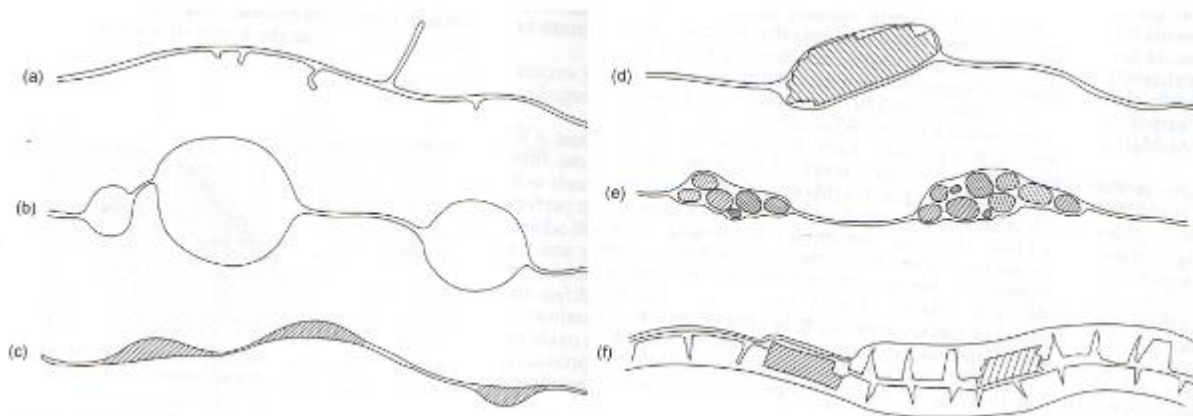


Figure 2-7 Schematic of entrainment defects: (a) a new DOF; (b) bubbles entrained as an integral part of the DOF; (c) liquid flux trapped in a DOF; (d) surface debris entrained with the DOF; (e) sand inclusions entrained in the DOF; (f) an entrained old film containing integral debris (Campbell, 2004)

Generally, DOFs entrapped with inclusions (cases c, d, e and f in [Figure 2-7](#)) are quite ‘inert’ in the liquid casting. The only problem for these defects may relate to the porosity during the solidification stage. Oxide films with inclusions may work as solid impurities that initiate gas pore nucleation. The details of this nucleation can be found in Campbell’s book (2004). This review focuses only on the problems caused by new films and films with air inside.

[Figure 2-7a](#) shows a new DOF that is only few nanometres thick (this is why DOFs are invisible to most inspection methods). It has been mentioned already that this kind of DOF can reduce the mechanical properties of the casting. The most harmful DOF defect is shown in [Figure 2-7b](#). Once air has become entrapped within the DOFs, the combination of the DOF and bubble damage can be observed in the casting.

Pouring the liquid metal into the pouring basin generates huge amounts of DOFs due to the plunging jet mechanism (Reilly, 2010). Air can then become trapped within the DOFs during this chaotic filling pattern. The effect of the DOFs depends on the sizes of the entrapped air bubbles. Small bubbles of air entrapped between films can cause porosity defects in the casting products. Because of the enclosed air, the density of the DOF is quite similar to that of aluminium (the oxide is slightly heavier than pure aluminium). Thus, it can travel easily within the metal stream to any random location. This is why the porosities observed are scattered within the casting. On the other hand, it is a different matter if the bubble inside the film exceeds 5 mm in diameter. Similar to the bubble damage discussed before, the bubble will float up due to buoyancy effects. Owing to this powerful buoyancy, large bubbles are found rarely inside casting products, because their buoyancy can drive them through any barriers and they quickly escape from the upper surface of the casting. However, large bubble oxide films can damage other oxide films and can bend or break dendrite meshes in partially solidified regions. Finally, the passage of the bubble leaves a trail through the casting, which never heals up.

2.2.2 Solidification defects

Solidification is the phenomenon of phase change during which a liquid turns into a solid as its temperature is lowered below its freezing point. It is a very important stage of the casting process and requires very precise control. Normally, porosity, shrinkage, hot tears and cracks can occur during the solidification stage. The following text will explain the details of these defects.

2.2.2.1 Porosity

Porosity is a very complex defect that occurs during the solidification stage. Generally, it can be divided into two types: that caused by gas and that caused by solidification shrinkage. Porosity caused by gas can be subdivided into three further classes: that caused by turbulent flow during the pouring stage, that caused by gas diffusing from the molten metal on freezing and that due to the sand core or mould blow when in contact with the molten metal. Shrinkage porosity can also be subdivided into two different categories: macroporosity and microporosity. The formation of each type of porosity will be discussed later.

2.2.2.1.1 Gas porosity

Air entrapment

The entraining mechanism, caused by surface turbulence during the filling stage has been explained earlier. The chaotic surface turbulence entraps air into the liquid with random sizes. However, it transpires that pores formed by air entrapment fall into the size range of 0.5 to 5 mm. To reduce air entrapment during filling, the solution almost certainly relies on the design of the casting running system.

Gas precipitation

This type of porosity defect is due to the gas that dissolves out from solution in the liquid metal. In the case of aluminium, hydrogen is the main type of gas precipitated. Gas pores are normally within the range of 0.05 to 0.5 mm in diameter and are located 1 or 2 mm under the surface of the casting (Campbell, et al., 1994).

In most cases, solidification starts from the mould/metal interface because of the greater contact and the higher temperature gradient (Campbell, 2004). Therefore, the solidified metal at this early stage of the process often forms a planar freezing front (Campbell, 2004). As the solidification starts, the solution is reduced and thus, a 'snowplough' build-up of solute occurs. When the solidification front progresses beyond 1–2 mm, the solute reaches the critical level of solubility for liquid aluminium (Campbell, et al., 1994) and hydrogen in solution precipitates from the liquid. However, as the metal has been solidified at front. Hydrogen has no way to escape and forms gas pores (Figure 2.8).

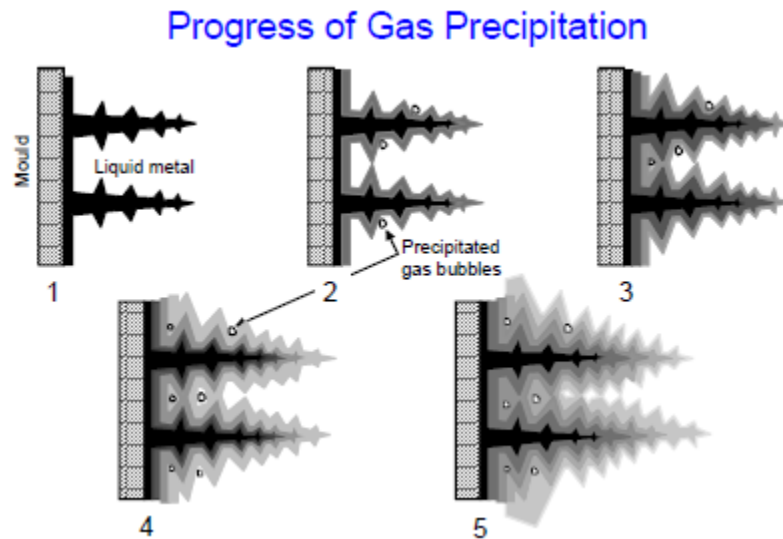


Figure 2- 8 Schematic of the progress of gas precipitation at the dendrite arm space (Campbell, et al., 1994)

Gas coming from cores

The final type of the gas defect is blowholes (named by Campbell) from sand cores (Campbell, 2004). As the heat diffuses into the core, the gas present in the core expands and attempts to escape. In addition, the resin binders inside the core start to decompose and generate additional gas. The sizes of this type of gas pore are the biggest of all the gas porosity defects. The final sizes of the blowholes can vary from 10 to 100 mm in diameter (Campbell, et al., 1994). Because time is required to transfer heat into the core, the blowholes normally occur during the latter stages of the casting. Therefore, the position of the blowholes is usually several millimetres below the uppermost surface of the casting (Campbell, et al., 1994).

2.2.2.1.2 Shrinkage porosity

The volume of molten metal is considerably greater than that of the solidified metal that is ultimately produced. This phenomenon raises several problems for founders; one of which is shrinkage porosity. In general, shrinkage can be described as atoms becoming rearranged from a rather open ‘randomly close-packed’ form, to a regular crystalline array of significantly denser packing (Campbell, 2004). During the solidification process, if the feeding is insufficient to compensate the volume shrinkage of the casting, then shrinkage porosity may occur inside the casting product. Depending on the size of the shrinkage porosity, it can be subdivided as macro- or microporosity.

2.2.2.2 Hot tears

A hot tear is another serious defect that can occur in castings and it is perhaps the most important factor defining a casting's performance (Green & Campbell, 1994). Once it occurs, the casting has to be returned for repair or rejected as scrap. A hot tear is a ragged, branching crack defect in casting products. During the solidification process, the linear contraction of the casting pulls the grains and dendrites apart. A true crack will form if there is insufficient feeding to fill the increased volume. Normally, hot tears are located at hot spots and heavily oxidised failure surfaces (Reilly & Jolly, 2009).

2.2.2.3 Cold cracks

The final type of solidification defect is a cold crack. Compared with hot tearing, the cold crack emphasises the different nature of the failure: it occurs below the temperature of the solidus. Whereas a hot tear exhibits a ragged and branching form, the cold crack is straighter and smoother (Campbell, et al., 1994). Because it happens below the solidus temperature, it builds up residual stress to tear the material. Reducing stress concentration can prevent cold cracks.

2.2.3 Summary

Most pouring and solidification defects have been introduced. For the pouring process, the fluid behaviour is very important. Chaotic filling can cause air entrapment, bubble damage and DOF entrapment, which can lead subsequently to problems, such as a poor surface finish and gas porosity. For the solidification process, sufficient feeding is essential, because inadequate feeding may lead to shrinkage porosity and hot tears occurring in the casting products. Based on this review, the sound casting running system design will be presented in chapter 3. All the casting products comparisons that will be shown later on are produced by those sound casting running systems.

2.3 Energy during casting process

2.3.1 Current situation

The modernisation of the world economy has benefited from energy derived from fossil fuels, such as oil, gas, and coal. The conflicts that have happened in the Middle East, The Gulf and Africa have affected the fossil energy configuration and distribution and the price of fossil fuel may be expected to rise continually. From the projection provided by the Department of

Energy and Climate Change (DECC, October 2012), the oil price will increase from \$115 per barrel to \$135 per barrel during the period of 2012 to 2030, i.e., the price may go up by at least 15%. It is expected to be the same for other resources; gas prices may go up by 20% and the cost of coal may increase by 16% during the same period. Sadly, the fossil fuel price and inflation are often seen as being connected in a cause and effect relationship (Investopedia, 2013). The inflation follows same direction as the fossil fuel price moves up or down. Therefore, the inflation will keep increase as the fuel price increase. No doubt that the energy and raw material price will keep increase as well.

In addition to the issue of price, the use of energy derived from fossil fuels results in an environment impact. The combustion of fossil fuel to generate electricity, provide heat or to drive a car generates sulphuric, carbonic and nitric acids, which result in acid rain (Anon., n.d.). Burning coal also generates significant quantities of coal ash, which may cause health problems for people (Klopffer, 1997). Most importantly, burning fossil fuels generate huge amounts of carbon dioxide (a greenhouse gas), which is considered a key trigger of global climate change.

Reducing emissions of greenhouse gases has become a major international imperative. Since the early 1990s, environmental legislation and international environment agreements have expanded greatly, driving global environmental policy changes. In December 1997, the Kyoto Protocol was announced in Kyoto (UNFCCC, 2013). Under this protocol, the developed countries committed themselves to reducing their emissions of carbon dioxide (CO₂), methane (CH₄) and nitrous oxide (N₂O) by 6% to 8% compared with their 1990 levels by the period of 2008–2012 (Yih-Liang, et al., 2007). Irrespective of international protocols, some countries also established their own standards to manage energy and emission issues. For example, the Clean Air Act 1993 was announced by the United Kingdom to reduce air pollution nationally (Legislation, 2013).

Regardless of the energy price or of the environmental issues, the energy efficiency of a product during its lifetime is becoming increasingly important. Generally, the heavier a product is, the greater the energy required to move it. During the lifetime of a product, the total energy consumption is higher for heavier products than lightweight products. Therefore, lightweight materials are becoming increasingly popular in industrial sectors. In particular, in the automotive and aerospace industries, aluminium and other light alloy metals are used widely. Thus, aluminium is becoming increasingly important for industrial sectors.

A survey carried out by MODERN CASTING (Dahlouist, 2011) in 2011 confirmed that aluminium is the dominant casting material in the United States. Out of 1617 metal casting facilities in the US, 882 (55%) produce aluminium castings. This is higher than the number of facilities producing iron (499). Despite the fact that iron has higher production tonnages, such result indicates that aluminium becomes more and more popular. Furthermore, despite years of general decline in production, the data of the Annual Census of World Casting Production show that the proportion of aluminium casting is increasing. Therefore, these results indicate that the increasing demand for aluminium is a universal phenomenon.

This is especially true for UK-based industry. Because the UK remains at the forefront of light metal casting and investment casting technologies, it has wide experience in the design and manufacture of energy efficient products, which are hugely beneficial for the aerospace and automotive industries (Jolly, 2010). Therefore, even with the high volume of foundry decline, the proportion of aluminium casting has increased from 9% to 20% from 1999 to 2010 (Figure 2.9). According to author’s knowledge, despite the energy efficiency of the final products, only fewer energy efficiency of the non-ferrous casting process has been investigated. Therefore, this research project seeks to identify the energy usage in non-ferrous foundries, particularly aluminium foundries.

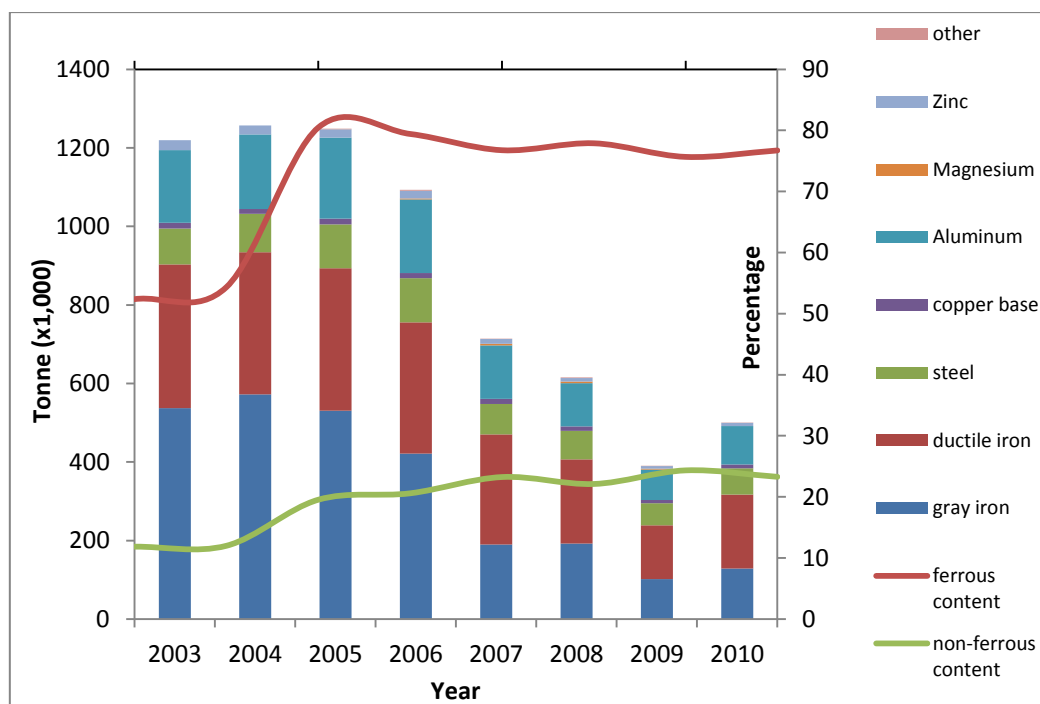


Figure 2- 9 figure shows UK annual casting production. The total production is declines through the period mainly due to the shrinkage of ferrous foundry sector. The non-ferrous foundries steadily increase its proportion over time. The UK foundry data comes from 34th, 38th, 39th,40th, 41st, 42nd, 43rd, 44th, and 45th Annual Census of World Casting

Production (1999) (2003) (2004) (2005) (2006) (42c) (2008) (2009) (2010). Because there is no data reported from UK, 2000,2001,and 2002 are not includes in the graph

Fossil fuels boost the economy but impact on the global climate. As the price of fossil fuels increases, the cost of manufactured products goes up as well, especially for the energy intensive smelter and foundry industries. Saving energy in these sectors would not only help the organisation reduce production costs but it would also help them meet government emission regulations, which is one of the reasons that led to the development of the CRIMSON casting process. The following discussion reviews several energy saving methods against which the performance of the CRIMSON process will be analysed.

2.3.2 Research on energy saving

The energy intensity of a process has a positive relation with the share of the energy cost in the total variable costs and of the value of the product (Subrahmanya, 2006). The more energy intense a process is, the greater the cost of the process. As a result of these pressures, industrial energy saving is becoming increasingly important from the aspect of the economy. For this reason, a number of research works have been performed to identify opportunities for energy saving. Generally, energy saving can be achieved through several techniques and methods, a few of which are outlined below:

Klugman and his colleagues performed an energy audit at a chemical wood pulp mill in Sweden (Klugman, et al., 2006). They used the surveyed data from the pulp mill to identify the saving potential. Their work revealed that the company should update their equipment to reduce their energy consumption by 50%. Furthermore, they found that compressed air has a significant energy overhead and that it would be better to reduce the usage of compressed air. Kabir and Abubakar performed a similar audit in a cement production plant (Kabir, et al., 2010). They discovered that the thermal energy efficiency was quite low; significant thermal energy escaped through the exhaust gas and kiln shell. They suggested that a new waste heat recovery steam generator should be introduced into plant to increase the thermal efficiency.

However, audit methods only provide theoretical figures about energy saving and often simply suggest major equipment updates or exchange. This kind of energy efficiency management often requires significant capital investment on new equipment. Comparing energy saving and capital investment, Anderson pointed out that plants are 40% more responsive to initial cost rather than annual saving (Anderson & Newell, 2003). With regard to new equipment and the adoption of new technology for long-term savings, organisations prefer projects with shorter payback times, lower costs and greater annual saving. Therefore,

it is not surprising that Thollander's (2010) research indicates that about one-half of the foundries in Sweden lack a long-term energy strategy and only about 25% may be categorised as having a successful energy management practice (Ottosson, 2010).

Further evidence for this can be found in the Climate Change Agreement published by UK Government (Department of Energy & Climate Change, 2011). According to the agreement, the foundries sector needs to attain an energy burden target of 25.7 GJ/tonne by 2010. However, the average energy burden for the UK foundry sector is 55 GJ/tonne. A company runs its business for profit. No matter what strategy is employed by the company, the priority is profit and energy saving could be one of the many goals within that strategy. It is more likely that a firm may operate based purely on the benefits of cost saving rather than energy saving. Furthermore, according to Thollander's research (Thollander & Ottosson 2008, 2010), there are several barriers that prevent a company from becoming energy efficient. He identified that the main barriers are technical risks, such as the risk/cost/hassle/inconvenience of production disruptions, inappropriate technology for the operation, lack of time and priorities, lack of access to capital and slim organisation. In particular, for SME foundries, the lack of time, proper personnel and insufficient resources are the largest barriers to energy efficiency (Trianni, et al., 2012). Unfortunately, this is quite true for most UK foundries; many of the UK's foundries are small and medium enterprises (UKFoundries, 2013), (UKcasting, 2013).

Instead of direct energy saving through big investments in new technology and equipment, a lean philosophy was introduced to eliminate waste, improve quality and eventually, achieve the goal of energy saving. This is a less radical way to achieve energy saving.

The concept behind lean manufacturing is simple; it is to spot and eliminate waste in a production process rather than inspect and repair afterwards. In the lean philosophy, the word 'waste' is complicated. It can represent a machine breakdown, product defects and physical waste during the production process. Most importantly, it represents those resources or processes that do not create products or services directly (US Environmental Protection Agency, 2003). By implementing lean tools such as Just in Time (JIT), cellular manufacturing, value stream mapping, waste caused by machine breakdowns, product defects, physical waste and non-value added processes could be reduced or eliminated. The consequence of such an implementation reduces the production resource requirements, costs

and lead-time³, while increasing the product quality, customer responsiveness and boosting competitiveness (US Environmental Protection Agency, 2003).

However, lean tools are implemented less in continuous manufacturing sectors such as the foundry sector. This is because of the large stocks of input raw materials and the long setup times that are required and the general difficulty in producing small batches (Abdulmalek & Rajgopal, 2007) (Besta, et al., 2011). Therefore, Abdulmalek (Abdulmalek & Rajgopal, 2007) undertook research on the steel foundry and investigated which lean tools could be implemented. The summary of his work is shown in Table 2.1.

Lean Tool	Applicability
Cellular manufacturing	Probably inapplicable
Setup reduction	Partially applicable
5S	Universally applicable
Value stream mapping (VSM)	Universally applicable
Just in time	Partially applicable
Production levelling	Partially applicable
Total productive maintenance (TPM)	Partially applicable
Visual system	Universally applicable

Table 2- 1 Assessment of applicability of lean tools in the steel industry. Please refer to the Appendix 2 for detail of each lean tool (Abdulmalek & Rajgopal, 2007)

Pude (Girishi, et al., 2012) conducted research on the implementation of Value Stream Mapping (VSM) in a foundry. He investigated the entire production flow of the casting process and identified the waste during each operational step. It was discovered that without significant change, this foundry could reduce waste by 23%, which corresponds to significant energy savings if converting the waste to energy. Abeulmalek (Abdulmalek & Rajgopal, 2007) also performed VSM for the steel industry. After implementation of VSM, that company was able to reduce their non-value added time dramatically. Some other lean tools are also used in the foundry sector. Kukla confirmed that the implementation of Total Productive Maintenance (TPM) in a casting industry will allow for efficient management of machinery and increase its effectiveness, resulting in improved production flow and lower production costs (Kukla, 2011).

However, fewer research works link the elimination of waste with the practice of energy saving in casting industry. Therefore, this project uses lean thinking to identify waste and to analyse the energy saving potential for casting industry.

³ The total amount of time required to complete the customers' orders.

2.3.3 Opportunities for saving

By adopting some concepts from VSM, the entire operation of the casting process can be investigated. In this section, suggestions regarding waste and other possible savings will be examined.

Energy saving can be achieved in two ways: direct savings through lower fuel consumption and indirect savings through lower material consumption. Therefore, the rule for energy saving in the foundry sector is simple; use less fuel and less material in making a certain quantity of sound products. To accomplish this, an understanding of the flows of energy and materials in the casting process is required. [Figure 2-9](#) presents the process flow for the conventional casting. This can be divided into six sub-processes: melting, refining, holding, fettling, machining and inspection. The melting, refining and holding activities consume most of the energy involved in casting (at least 60%); thus, the direct energy savings should be achieved in this step (DETR, 1997). Fettling, machining, and scrap contain at least 70% metal by weight of the total melting (Jolly, 2010); thus, the indirect saving should come from these three processes.

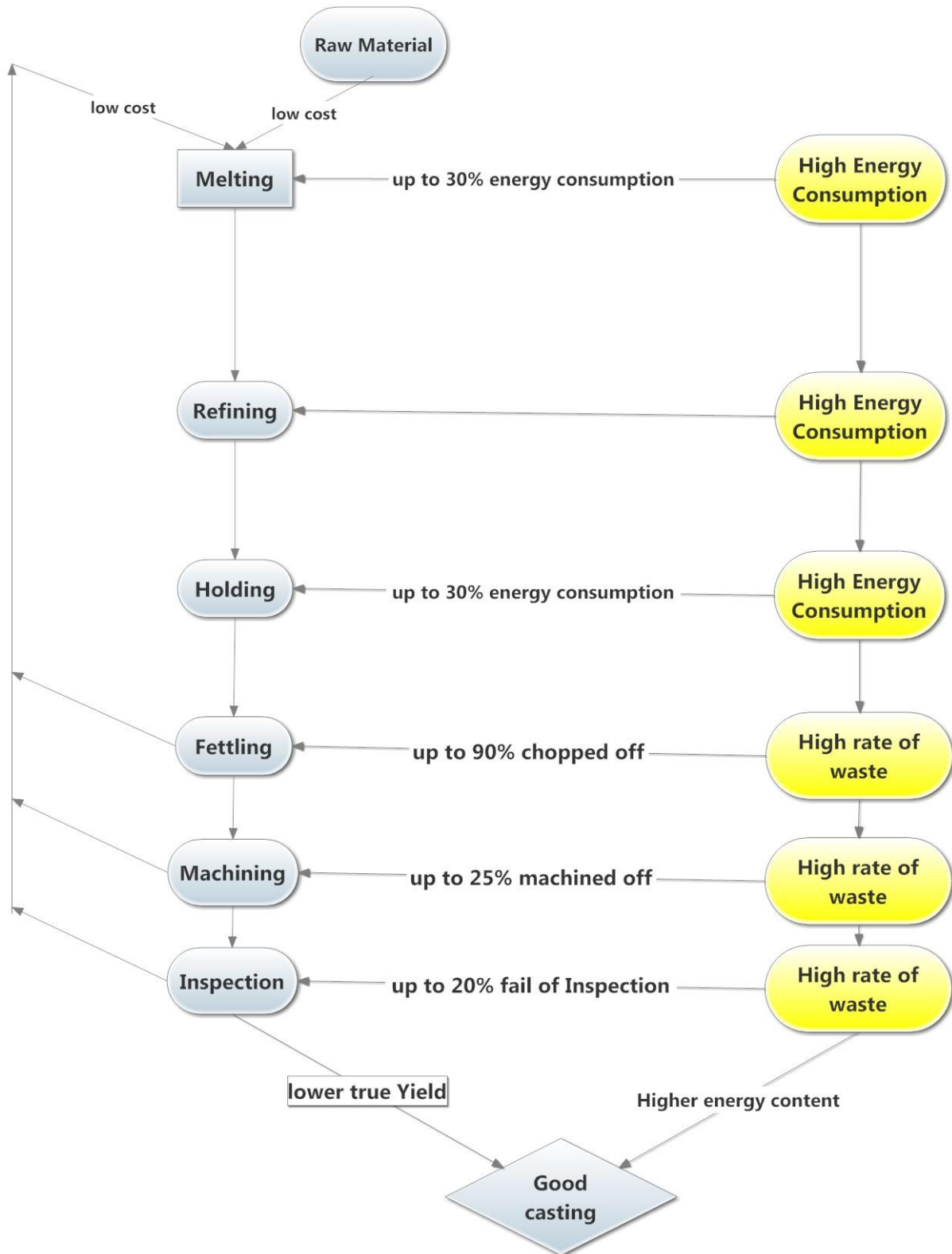


Figure 2-10 Material and energy flow chart of a conventional sand casting process. High resolution figure can be seen in appendix 1 (pp168)

2.3.3.1 Direct saving

2.3.3.1.1 Savings through preheating the metal and loading

This is the first step of the melting process. Most foundries employ this step to preheat or dry their charge metals. There are several advantages related to preheating: it can remove moisture and other organics, which helps preventing explosion in the furnace; it can increase the melting capacity of the furnace; and it can reduce the energy required for melting. Especially for aluminium alloy, preheating can inhibit slag formation when the hot aluminium comes into contact with moisture (Dalquist, et al., 2004).

Nowadays, foundries often use hot flue gases from the melting furnace to preheat the metal. Mefferta (1999) presented results of a study that investigated how much energy could be saved by preheating in the iron foundry sector. The recommendation of that work was that using recovered exhaust gases should be seen as the primary method of reheating. However, loading or transferring the preheated metal may cause the loss of vast amounts of heat. When transferring the preheated metal to the melting furnace, the metal loses heat through convection and radiation. Therefore, reducing the energy lost during transportation can retain significant amounts of energy and reduce the energy required by melting. To achieve this efficiently, the pre-heating and melting operations should be close to each other and a lean tool such as 5S could be employed (tidy up work floor to reduce the time of movement).

2.3.3.1.2 Savings through melting

As mentioned in the previous section, the melting operation consumes 30% of the energy of the casting process. Thus, saving energy through the melting operation logically becomes a primary consideration. When considering energy saving via the melting operation, people normally think about the efficiency of the furnace. If the efficiency of the furnace increases, the energy consumed per unit mass of metal reduces.

	Melt capacity	Fuel Type	Efficiency
Crucible furnace	Several Kg to Tonne	Natural gas / coal / Oil	7-19%
Reverberatory furnace	1 t—75,000 t	Natural gas / coal / Oil	20-25%
Induction Furnace	several Kg to 30 t	Electricity	85-97%

Table 2-2 Capacity, fuel type and energy efficiency of different furnaces. Data from Advanced Melting Technologies (BCS, 2005)

The table above shows several popular furnace types used in the aluminium foundry industry. Clearly, the induction furnace is the most efficient melting method compared with the other two furnaces. However, 60% of the energy currently used in melting is provided by natural gas and only 27% of the melting is provided by electricity (BCS, 2005).

Therefore, this raises another debate between energy saving and cost saving. Using a gas-fired furnace can save money but the quality of the melt is poor. The quality of the melting influences the subsequent sub-processes. As highlighted in the section on casting quality in the review literature introduced before, hydrogen content is normally higher in gas-fired furnaces owing to the moisture-rich exhaust gases. Removing hydrogen is essential because it causes serious damage later on. Therefore, compared with metal melted by using electrical means, the metal melted by using gas requires additional treatment in degassing. In other words, spending less during the melting process requires additional expense during degassing. If considering cost savings over the long term, the story may differ.

Irrespective of the purpose for cost or energy savings, some recommendations are introduced for the improvement of energy efficiency.

1. Improving the air compressor that controls the fuel-fired furnace (Meffert, 1999). Oxygen enrichment can lead to higher heat transfer rates and thus, reduce melting times. In turn, this would reduce the overall fuel consumption (BCS, 2005).
2. Reducing the frequency of metal charging (Chan & Yang, 2010). This can reduce the metal loss and the radiation heat loss. Metal loss refers to losses through oxidation when in contact with air. Radiation loss refers to heat losses when the furnace lid or door is opened (BCS, 2005).
3. When considering lean manufacturing, it is recommended to use high-quality raw material. Using high-quality raw material may increase the initial cost. However, in return, it can reduce overall metal losses through oxidation and drossing⁴. Lowering the metal loss requires less energy and metal to compensate.
4. Providing training for the furnace operators. It has already been shown that operator performance can influence energy usage by as much as 10% (ETSU, 1998).

⁴ Dross is a mass of solid impurities floating on the surface of melting metal. Drossing is an operation remove those impurities.

In addition to increasing energy efficiency, there is also a positive way for engineering energy savings. This refers to other strands of lean manufacturing; use correctly sized equipment to produce the desired amount of products (US Environmental Protection Agency, 2003). For the aluminium sector, it is recommended to use the correct size and a rapid-melting coreless induction furnace for the melting (DETR, 1997). The advantages of such a furnace are list below:

1. High-efficiency furnace saves energy during melting
2. Cleaner energy leads to cleaner metal, lower hydrogen content and less need for other treatments
3. The correct size furnace can ensure no waste during casting; it can smooth the casting process and no residual liquid needs to be held
4. Fast melting reduces the chance of oxidation; thus, reducing the need for additional metal to compensate the metal loss

2.3.3.1.3 Savings through treating and refining molten metal

Following the melting operation, the molten metal is not clean. Normally, it includes impurities, such as oxides and slag and undesired gas content such as hydrogen. As a result, degassing and flotation are necessary requirements.

Normally, the hydrogen in aluminium comes from the decomposition of water vapour. Following the reaction, hydrogen gas dissociates and forms hydrogen atoms, which diffuse into the melt (Smithells, 1976). As the aluminium solidifies, the dissolved hydrogen escapes from the melt to form undesirable porosity, unfurl DOFs (ASM Handbook Committee, 1979), or even form cracks. Therefore, reducing the hydrogen content is essential during the degassing operation. Nowadays, the technology used for degassing is purging with an inert gas via a rapidly rotating nozzle (Smithells, 1976) (ASM Handbook Committee, 1979). This technology is based on the equilibrium relationship between the hydrogen in the melt and the hydrogen in the atmosphere (Otsuka, n.d.). By injecting the inert gas, the molten metal is put under an inert atmosphere. To maintain the balance, hydrogen needs to transfer into the inert gas bubble and diffuse to the surface of the melt. As the purging of the melt by the inert gas continues, the hydrogen content gradually drops to the required level.

According to the literature (Jolly, 2010), the metal loss during the treating and refining operations can be as high as 5% in terms of mass. Assuming a melt of 1 tonne of aluminium uses 2.2 GJ of energy. The loss of 5% of the metal requires an additional 0.11 GJ of energy to melt. Energy is also consumed by the degassing unit; the rotating motor, the inert gassing and the flux pumping all require energy. A mid-range degassing unit is usually powered by a 3.5 KW motor for period of 15 minutes. Therefore, the energy consumed is 3.15 MJ. Furthermore, the embedded energy required to compress the inert gas into the container also needs to be considered. Assuming the purging rate of the inert gas is $20 \text{ L}\cdot\text{min}^{-1}$, which gives 300 L of gas in total, the embedded energy of the inert gas would be about 0.5 MJ (Jolly, 2010). Combined with the consumption by the motor, the total energy consumption could be 3.65 MJ.

In order to save energy through refining and treating, the quality of the raw metal is very important. It not only reduces metal loss during refining but also reduces the frequency of refining. In addition, there are the corresponding savings of inert gas and electricity to be considered as well.

2.3.3.1.4 Savings through holding

Holding is another significant consumer of energy in the casting process, demanding another 30% of the energy of the casting production. The purpose of holding is to maintain a continuous supply of liquid for casting with constant composition and quality (BCS, 2005). Owing to its characteristics, the holding furnace can operate as long as a working shift (8 hours). In most non-ferrous foundries, the holding process requires more energy and money than the melting process does. (DETR, 1997) Reducing the holding time is one of the most efficient ways for energy saving. To achieve this, a smooth and continuous production plan is essential. Lean tools, such as TPM, VSM, production levelling and planning can be used to assess the holding time reduction.

2.3.3.2 Savings through indirect saving

2.3.3.2.1 Savings through operational material efficiency improvement

Operational material efficiency (OME) is the ratio between the good casting shipped to customer and the total metal melted (Eq. 3) (Jolly, 2010).

$$OME = \frac{\text{mass of Good casting shipped}}{\text{mass of Total metal melted}}$$

Equation 3

Improving the true yield is probably the simplest way in which foundries can save energy, because this method focuses on increasing good casting production and reducing the total metal melted. It deals mainly with the production process itself, seeking opportunities to save material. It has less relation with the performance of the production equipment. To be able to understand the true yield of the casting process, the entire casting operation needs to be analysed. Using a traditional sand casting as an example, the casting process is analysed briefly in the following.

Aluminium is a highly reactive material. In particular, when it is liquefied at high temperature, it can react with air, moisture, the furnace lining and other metals. The metal loss during the melting process is due mainly to this characteristic. As discussed before, a casting process can be divided into seven sub-processes: melting, holding, refining, pouring, fettling, machining and inspection. Apart from pouring, six out of seven have a direct relation with metal loss.

	Melting	Holding	Refining	Fettling	Machining	Inspection
Metal Loss	2%	2%	5%	50%	25%	20%

Table 2-3 General metal loss during each operation. Data based on general/automotive sand casting production (Jolly, 2010)

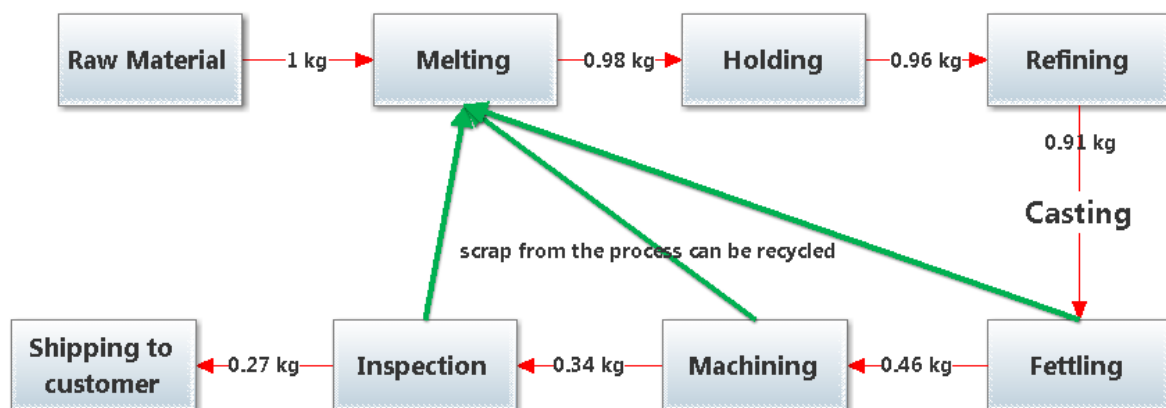


Figure 2-11 Metal flow in the foundry

Figure 2-11 shows a representation of a conventional sand casting process. By assuming 1 Kg of metal is melted, then after the different stages of the operation, the final casting despatched to customer only weighs about 0.27 Kg. Therefore, the operational material efficiency of this casting process is about 27%. For conventional casting, 1 Kg of good casting requires 3.7 Kg

of raw materials. Therefore, if the true yield of the casting can be improved, less metal will be required to produce the casting and the energy consumption for the melting could be reduced.

Opportunities to improve the true yield require that the metal loss during each operation must be reduced. Starting with the melting operation, 2% of the metal loss is mainly due to the oxidation of the aluminium at the surface of the melt. Thus, keeping the melt away from contact with air can reduce the level of oxidation. Normally, this can be done by keeping the lid of the furnace shut and reducing the metal charge time. Secondly, the holding process also contributes 2% of the loss, which can also be attributed to oxidation (long term exposure). Therefore, reducing the holding time can reduce the metal loss. Thirdly, the refining / cleaning operation contributes 5% of the metal loss. The loss at this stage of the operation is due mainly to oxidation, hydrogen degassing and impurities. The rate of the loss depends on the cleanliness of the raw material. Again, good quality raw material is essential.

After pouring, solidification and shakeout, the casting system is sent to the fettling operation. Fettling is used to separate the casting and its running system. Generally, the casting itself is only about 50% (casting yield⁵) by weight of the entire casting system. This means that at least half of the metal is chopped off and scrapped. This is the principal cause of metal loss during the casting process. For foundries producing aerospace castings, the metal loss during fettling can be as high as 90% owing to the strict quality regulations (Jolly, 2010). Thus, reducing the weight of the running system can reduce the metal loss in fettling. The concept of a good casting running system will be introduced later.

The fifth cause of losses relates to machining. This process transforms the casting into its final shape. It involves grinding, drilling, boring, turning, polishing and any other necessary operations. The metal loss during this stage of the operation is mainly in the form of fine scrap or swarf. If the casting can be produced closer to net shape, then the need for machining operations can be reduced. The final type of loss is that of castings that fail the inspection process. Defects such as a poor tolerance, poor surface finish, inclusions and porosity lead to rejection during the inspection. To reduce the level of rejections, the processes of melting, alloying and refining and the design of the running system are very important.

The losses in first three steps are permanent losses, which cannot be easily recovered or reused⁶. They can only be reduced by the methods mentioned. The last three types of loss are

⁵ Casting yield = casting/ (casting + casting running system). Please do not confuse this with true yield.

⁶ Dross can be recovered. However, most foundries don't have facility to recover it.

assigned as internal scrap. Energy has been used to make and melt this metal and because these losses can contribute up to 90% of the metal loss in the casting process, energy savings must be achieved by reducing such losses during the casting process.

2.3.3.2.2 Savings through using numerical simulation

Starting from the product design, the behaviour of the fluid inside the casting running system and the performance of the feeder during solidification can be predicted by using a numerical simulation package. This allows foundry engineers to develop sound products without doing physical experiments of trial and error. This can help at both initial production and during long runs when an energy saving method is being sought. Taking advantage of the simulation package, this research uses numerical simulation to design and to compare the quality between conventional casting and the novel CRIMSON process.

2.3.3.3 Savings through plant management

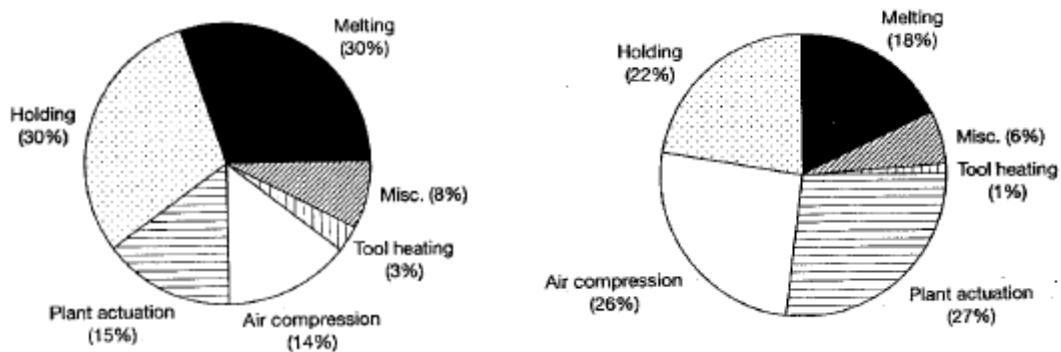


Figure 2-12 Left: typical energy use in a foundry. Right: typical energy cost in a foundry (DETR, 1997)

As Figure 2-11 shows, a typical foundry consumes 14% of its energy on air compression, which costs even more money than melting or holding. There are many reasons for using compressed air in a foundry; the most important is for combustion. Generally, compressed air can provide more oxygen for combustion. Efficient burning of fuels can provide a hotter flame temperature, which gives a higher heat transfer rate and reduces the time required for melting (BCS, 2005). Furthermore, it not only reduces the heat loss during combustion but also reduces the environmental impact. Again, there are always two sides to everything. Compressed air helps reducing the fuel consumption during combustion but it consumes significant quantities of electricity. Therefore, ensuring that there is no excess air in the burner will help greatly in reducing the need for compressed air. Furthermore, using the correct size of compressor and routine maintenance can also save energy. Ultimately, using

an induction furnace will eliminate the requirement for compressed air and lean tool such as TPM can be extremely helpful for this purpose.

2.3.4 The CRIMSON process

Direct and indirect methods of saving energy during the casting process have been introduced. At the starting point of the casting process, using the correct size of rapid induction furnace with matched billet size for high susception not only saves energy during melting but can also reduce metal loss as well; both direct and indirect savings can be achieved. Refining is the second step in the casting process and savings during this stage rely mainly on loss reductions. This requires good quality charging materials and clean melting. Savings during the holding process can be achieved both directly and indirectly. Reducing the time of the holding can reduce energy consumption and metal loss. Savings achieved during the fettling, machining and inspection stages of the process are all indirect savings. All of these processes achieve savings by increasing the casting yield. Simulation methods can be used to achieve casting yield improvements. Therefore, a good running system with high casting yield not only guarantees the quality of the casting but also saves energy.

	Energy loss reason	Saving method	Saving type
Melting	1. Inefficient melting 2. Permanent metal loss	1. Correct size of furnace 2. Rapid melting 3. Keep melt away from air	Direct / Indirect
Refining	Permanent metal loss	1. Using high-quality charging metal 2. Cleaning melting	Indirect
Holding	1. Long-term holding 2. Permanent metal loss	Reducing the holding time	Direct / Indirect
Fettling	Low casting yield	Increasing the casting yield	Indirect
Machining	Rough shape of casting	Making net shape casting	Indirect
Inspection	Defects such as inclusion, poor surface finish, porosity	1. High-quality melting 2. Good running system	Indirect

Table 2-4 Summary of energy loss and opportunities for energy saving during each operation

Based on these concepts, the CRIMSON casting process combines direct and indirect saving methods; thus, achieving energy savings in a more efficient way. The energy and material flow diagram of the CRIMSON process is shown below:

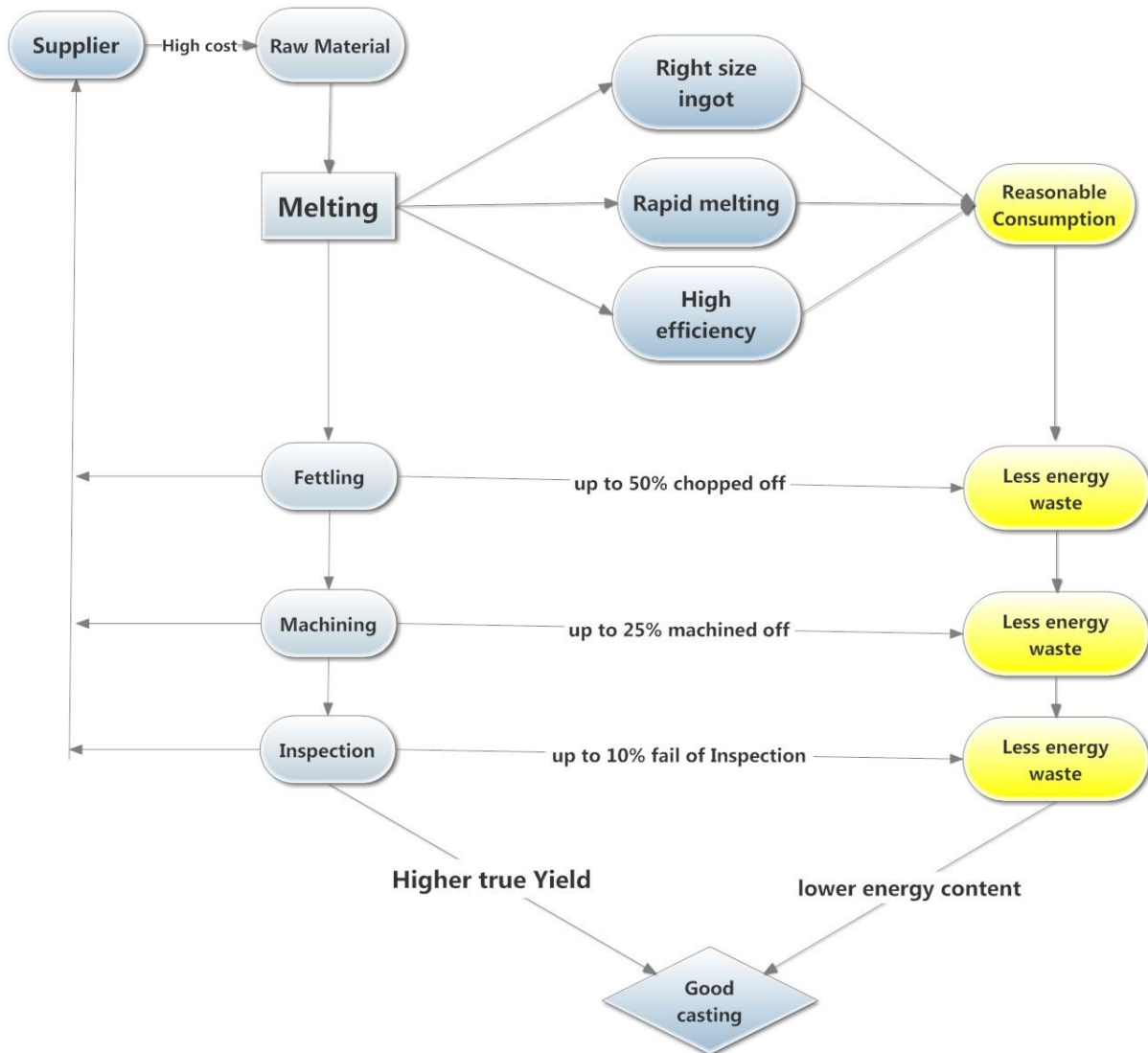


Figure 2-13 Energy and metal flow of the CRIMSON casting process. High resolution figure can be seen in appendix 9.1, appendix 2 (pp169).

Instead of using cheap bulk metal, the CRIMSON process uses pre-alloyed high-quality metal for the casting process. Moreover, the CRIMSON casting process uses a rapid induction furnace to melt just enough metal for a single casting. The time for melting is normally under 10 minutes, which reduces significantly the chance of the oxidation and hydrogen absorption. Therefore, the refining stage of the operation is no longer necessary. Because of the single melting, the melt can be transfer to the pouring operation immediately; thus, the holding operation can be also removed from the casting process. Considering that

the holding process can consume up to 30% of the casting energy, eliminating this stage can plug a significant drain of energy consumption.

Owing to the new filling feature of the CRIMSON process, the liquid metal is pushed into the casting system through a bottom gate. This up-casting method redefines the casting running system and the pouring basin and down-sprue are no longer required. Because of the new running system, less metal is fed into the running system and thus, the casting yield increases. With regard to quality, the up-casting process provides a turbulence-free filling, which means that defects, such as air entrapment and DOF formation can be minimised. The quality of the casting can be improved to a new level and fewer rejections reduce the energy consumed by re-working.

2.4 Summary of chapter

This chapter has reviewed the different casting methods and casting defects and their formation mechanisms have been reviewed as well. In addition to the quality of the casting production, the energy management of the casting foundry has also been considered. Instead of significant capital investments on new technology and equipment, the CRIMSON process can be considered as more of a lean manufacturing approach, which offers both direct and indirect material savings.

In the remaining chapters, different approaches will be used to evaluate the performance of the CRIMSON process. These include investigations of quality through numerical simulation, investigations on environmental impact through LCA, production performance investigations based on process simulation and an examination of profitability through cost estimations. These four approaches will form a complete assessment validating the CRIMSON process in terms of quality, energy, productivity and cost. For decision makers, these data will be very useful in assessing the performance of the production process.

Chapter 3 : Validation of the CRIMSON process through numerical simulation

3.1. General introduction

The first approach is used of software validation method to validate the CRIMSON process. There are two sections in this chapter. The first concerns a comparison of the tensile test bar casting using different running systems: one for the traditional gravity sand casting running system and the other for the new CRIMSON casting running system. The Flow3D simulation package is used to simulate the filling processes in these two runner systems. The second section concerns the designing of the CRIMSON running system for making a filter housing. The development process involves the use of Flow3D and Magmasoft packages as standard tools.

3.1.1 Software validation

There were two computational fluid dynamics (CFD) software packages available at the beginning of the research project: FLOW3D (Version 9.4) and MAGMASOFT (Version 5). To ensure the accuracy of the simulation results, the suitable CFD software has to be used. Generally, FLOW3D is a commercial CFD package based on a finite volume / finite difference approach. FLOW3D can describe accurately transient free surfaces with large deformation (Barkhudarov, et al., 1995). On the other hand, MAGMASOFT 5 is commercial casting software used widely by foundry personnel. The well-developed thermal and fluid dynamic codes can be used to predict shrinkage and gas porosity as well as stress distribution during solidification (Sabatine, et al., 2005).

To establish which software is most accurate in predicting the fluid pattern during filling, a classic benchmark test was introduced. The original benchmark test developed at the University of Birmingham by Sirrel and his co workers (Sirrell, et al., 1996) was carried out in 1995, in which x-rays were used to record flow behaviour during filling (Appendix 3 shows the geometry of casting running system used). It is a special test intended to assess the abilities of computer models. For this reason, default settings are kept for both simulation packages to test their true potential.

3.1.1.1 Parameters used in the filling simulation

	Flow3d94	Magma5
Material	Al 356, Al-Si alloy	Al 356, Al-Si alloy
Liquid density (kg m ⁻³)	2385	2385
Kinematic viscosity (m ² s ⁻¹)	0.0012	0.45 x 10 ⁻⁶
Pouring pressure (Pa)	400 ⁷	400
Minimum mesh size (mm)	5	5
Total elements of mesh	95,200	91,285
Turbulence mode	Activated	Activated
Surface tension angle	160 ⁷	
Surface tension coefficient	1	

Table 3-1 Parameters used in the simulations

Table 3-1 shows the simulation parameter

The simulations are carried out using a Workstation with 16 GB RAM and eight 2.66 GHz CPUs. In addition to the accuracy of the results, the simulation time is another consideration in software selection. Thus, the maximum hardware performance was applied for each simulation. Flow3D took only 5 to 10 minutes to run the filling simulation, whereas Magmasoft 5 took about 30 minutes to perform the same task.

Under default settings, both simulation packages exhibit some difference compared with the benchmark results. However, Flow3D still has the most similar fluid pattern. Thus, considering both the accuracy and the execution time, Flow3D is selected as the better choice for the filling simulation. In addition to these two reasons, the Flow3D package offers additional useful functions. One of the most useful function is that offering a customised subroutine to track the oxide film in the liquid metal. The detailed results of the comparison result can be found in Appendix 5.

⁷ Pressure head work as pouring basin

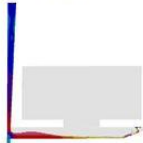
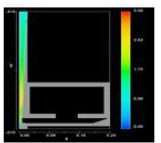
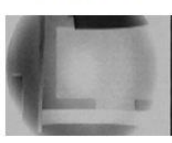
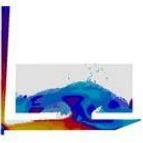
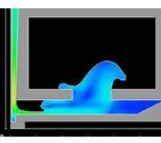

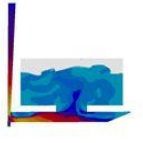
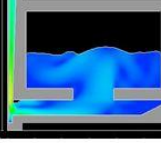

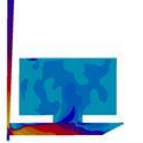
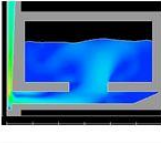
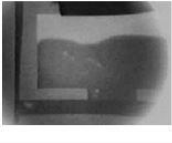
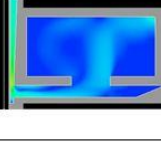
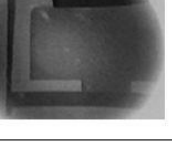
Time (s)	Magma5	Flow3D	X-Ray Data
0.25			
0.75			
1.25			
1.5			
2	NA		

Table 3- 2 Comparison of the benchmark and the different simulation results

3.1.1.2 Solidification & mechanical property

Ideally, it is possible to use Flow3D to perform the solidification and some stress analysis. However, that would have required more time and resources than was available to establish a proper database. Fortunately, Magmasoft5 contains reliable thermal data for most engineering metals; thus, Magmasoft5 is the ideal choice for the solidification and stress analyses.

In conclusion, on the topic of software selection, it is better to combine two software packages, using the strengths of Flow3D to model the filling and those of Magmasoft5 to perform the solidification. However, to ensure the precision of the solidification results, the filling simulation is also carried out under Magmasoft5⁸.

⁸ Magmasoft5 can perform solidification without filling by considering that all the liquids in the model are at a homogenous temperature. However, in a real situation, the temperature of the liquid is changing during the pouring. As a result, the filling simulation in Magmasoft5 can ensure that the solidification simulation is more accurate.

3.1.2 Process introduction

3.1.2.1 Gravity filling method

The gravity filling method is a relatively cheap and less skilful filling method for the casting process. It is probably the best-known and most common filling method used throughout the world.

To fill the casting cavity, the down-sprue length should be sufficient to maintain the pressure head. As mentioned in the literature section 2.1, the critical velocity for liquid aluminium is $0.5 \text{ m}\cdot\text{s}^{-1}$. By converting this critical velocity to height, gives a value of 12 mm (Jolly, 2002). This means that the critical free fall height for liquid aluminium alloy is 12 mm; beyond this height, the critical velocity will be exceeded. Therefore, the design of a sound gravity pouring running system to minimise defects will be introduced in this chapter.

3.1.2.2 The CRIMSON process

For the purpose of ameliorating the casting quality and related energy issues within the light-metal casting industry, the researchers and engineers from University of Birmingham, Cranfield University, and a local company, N-Tec LTD., have co-invented the patent Constrained Rapid Induction Melting Single Shot Method (CRIMSON) (Jolly, et al., 2010). Compared with traditional casting processes, the CRIMSON method uses a rapid induction furnace to melt just enough metal for a single shot. The melt metal is then transferred to a computer-controlled platform to finish the anti-gravity up filling (Jolly, et al., 2010). During this up filling process, the filling rate is the only parameter that needs to be considered. According to the conservation of flow rate, the velocity of the piston can be determined easily to fit the filling rate required for a given area of piston. As a result, the velocity control in the CRIMSON process can be achieved much more easily. The energy consumption is also considered. Owing to the minimised melting and holding time, energy is saved during the casting process (Jolly, et al., 2010). The layout of the CRIMSON facility shows as below.

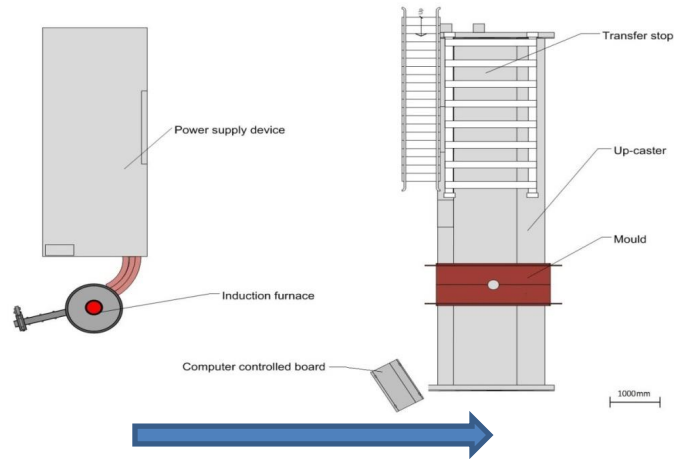


Figure 3-1 the entire CRIMSON facility (top view). The arrow represents operation sequence. + High resolution layout can be seen in Appendix 5

3.1.3 Methodology

3.1.3.1 CRIMSON casting running system

The mould design for the CRIMSON process is based on Gebelin's (Gebelin, et al., nd) up-casting running system for an ASTM (ASTM, 2003) standard tensile test bar. According to their simulation and experimental results, six test bars will be cast in one system. To prevent porosity and the unfurling of double oxide films (DFOs), a tube is added in the middle of the system to work as a riser (Figure 3-2). Gebelin derived a flow rate of $0.25 \text{ L}\cdot\text{s}^{-1}$ and 8500 pa pressure, which can provide turbulence-free filling for up-casting (Gebelin, et al., nd). In order to match the performance of the CRIMSON process, a gravity poured running system was designed to the highest specifications using the so-called Campbell guidelines, the details of which are introduced below.

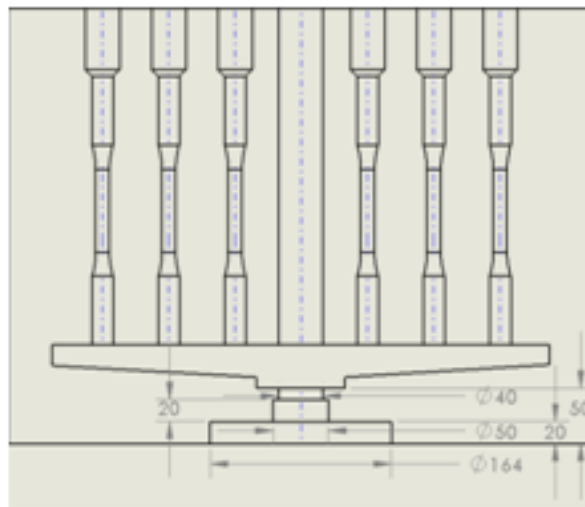


Figure 3-2 CRIMSON up-casting runner

3.1.3.2 Gravity pouring running system design

After the introduction on defects, it is clear that the quality of the casting relies on the quality of the filling and feeding. Firstly, a good running system should control the filling velocity inside the casting cavity to prevent surface turbulence. Secondly, a good casting system needs to provide effective gas flow, either through vents or holes or via mould permeability; otherwise, gas porosity can occur during solidification. Finally, a good casting system needs to provide sufficient feeding during solidification. In order to guarantee a directional solidification, eliminate localised shrinkage and micro-porosity and eliminate hot tears, a typical gravity poured running system looks like that depicted in Figure 3-3. It should have a pouring basin, down-sprue, a filter (optional), runner bar, ingate and casting. In addition to the casting itself, the cross sections of each element should be designed correctly.

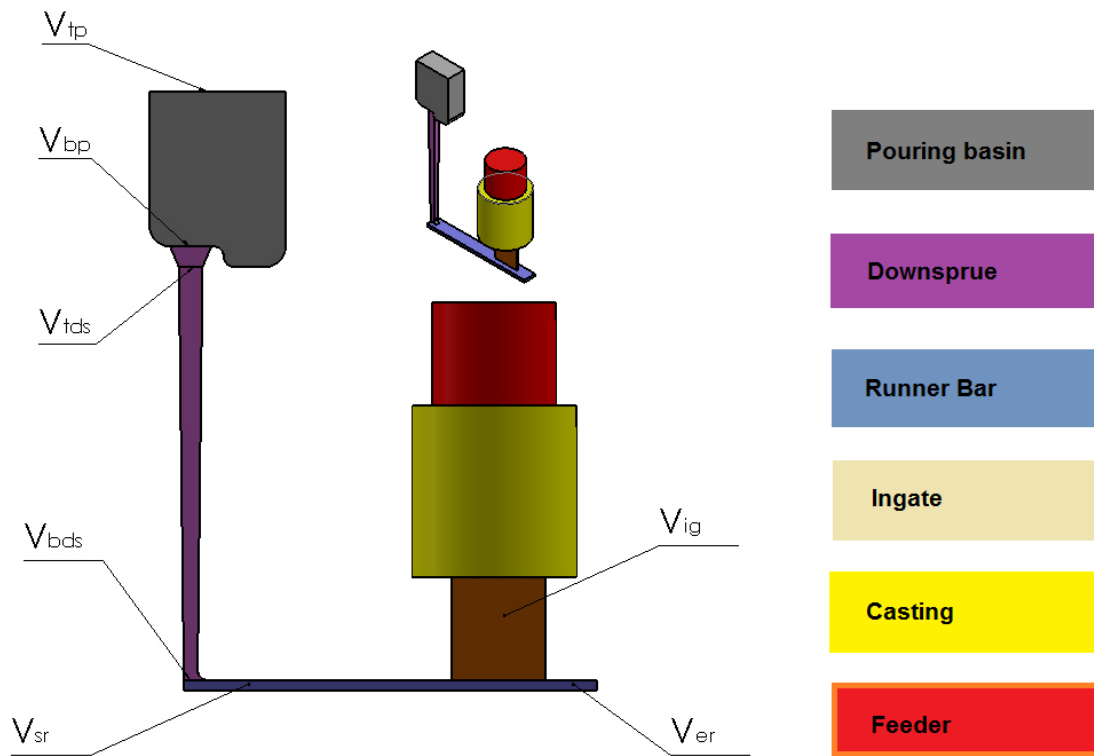


Figure 3-3 Typical gravity poured running system

Table 3-3 presents some parameters that can be used for gravity poured running systems design, obtained from the casting information of the CRIMSON process.

Alloy	Al354
Critical velocity for surface turbulence (m·s ⁻¹)	0.5
Process (Sand, LPD, GD, Investment)	Sand casting
Mass of casting and feeder (kg)	4.35
Solid density (g·cc ⁻¹)	2.65
Liquid density (g·cc ⁻¹)	2.385
Volume (cc)	1822
Filling time required (s)	5
Average mass fill rate (kg·s ⁻¹)	0.87
Initial mass fill rate (kg·s ⁻¹)	1.30
Initial volume fill rate (cc·s ⁻¹)	503
Average vol. fill rate (cc·s ⁻¹)	335

Table 3-3 Initial data for mould design

3.1.3.2.1 Pouring basin

Starting from the pouring basin, which is the initial part of the running system, a traditional design is a conical cup. However, this design requires a high rate of pouring; otherwise, the base of the down-sprue cannot be choked. The low pressure at the bottom will continue to suck air and dross into the system. Even though a desirable pouring rate can be achieved, a direct pouring (Conical pouring basin) will still cause the most oxides and bubbles to be carried into the casting (Campbell, 1991). Therefore, a new design of pouring basin should be used that can settle the liquid, arrest bubbles and provide a sufficient pouring rate.

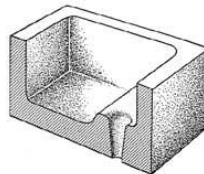


Figure 3-4 Schematic of the recommended pouring basin (Jolly, 2002)

The dimensions of the pouring basin have a relation with the average volume fill rate (table 3-3).

$$\mathbf{Length} = \sqrt{\frac{2.25 \times \text{average vol fill rate}}{2 \times \text{height}}} = 157 \quad \text{Equation 4}$$

$$\mathbf{width} = 0.5 \times \mathbf{length} = 78 \quad \text{Equation 5}$$

In Eq. 4, the height of the pouring basin can be decided by the designer. In this case, the height is 60 mm, which was decided upon by the author.

3.1.3.2.2 Down-sprue

The second part that has to be considered is the down-sprue, which needs to have a tapered shape in order to avoid defects, such as bubble entrapment and oxide film entrapment. From Table 3-3, the formula $\dot{m} = \frac{M}{t}$ can be used to calculate the required mass fill rate, where M is the mass of the casting, t is the time required to fill the casting and \dot{m} is the average mass fill rate. Typically, an initial pouring rate \dot{m}_{in} will be 1.5 times higher than an average pouring rate (Campbell, 1991).

$$\dot{m}_{in} = 1.5 * \dot{m} = 1.3 \text{ kgs}^{-1} \quad \text{Equation 6}$$

$$\dot{V}_{in} = \frac{\dot{m}_{in}}{\rho} = 503 \text{ ccs}^{-1} \quad \text{Equation 7}$$

Where \dot{V}_{in} is the initial volume fill rate and ρ is the density of the liquid metal.

As shown in Figure 3-3, v_{bp} is the velocity of the metal liquid reaching the bottom of the pouring basin. Therefore, the velocity at the bottom of the basin can be calculated by using Bernoulli's equation:

$$v_{bp} = \sqrt{\frac{(h_p+h_b)}{1000} \times 2 \times g} = 1.13 \text{ ms}^{-1} \quad \text{Equation 8}$$

Where h_p is the height above the pouring basin (the position of pouring activity) and h_b is the depth of the pouring basin. The value of h_p should be as small as possible to prevent splashing during the pouring. In this case, h_p is set at 5 mm above the pouring basin and as mentioned, the depth of the pouring basin is 60 mm.

It is assumed that each direction change can cause a 50% loss of the original energy. By transforming that lost energy to velocity, $1/\sqrt{2}$ or 71% of velocity will be lost during each right-angled turn (Jolly, 2002). As a result,

$$v_{tds} = \frac{v_{bp}}{\sqrt{2} \times \sqrt{2}} = 0.565 \text{ ms}^{-1} \text{ (Two right angles)} \quad \text{Equation 9}$$

In Eq. 9, v_{tds} is the velocity at the top of the down-sprue.

Therefore, the area of the top of the down-sprue is given by:

$$A_{tds} = \left(\frac{\dot{V}_{in}}{v_{tds}} \right) \times (1 + \text{discharge coefficient}) = 1259 \text{ mm}^2 \quad \text{Equation 10}$$

By using Bernoulli's equation again, the velocity of the liquid at the bottom of the down-sprue can be calculated. In Eq. 11, v_{bd} is the velocity at the bottom of the down-sprue and h_{ds}

is the height of the down-sprue. Again, there is no strict requirement regarding the height of the down-sprue; it is only required that the down-sprue be higher than the casting to provide suitable filling pressure. In this case, the height of the down-sprue is 368 mm.

$$V_{bd} = \sqrt{\frac{h_{ds}+h_p+h_b}{1000}} \times 2 \times g = 2.90 \text{ ms}^{-1} \quad \text{Equation 11}$$

Owing to conservation of mass theory, the flow rates are the same at the top and bottom of the down-sprue. The area of the base of the down-sprue can be calculated as:

$$A_{bds} = \frac{(A_{tds} \times v_{tds})}{A_{bds}} = 226 \text{ mm}^2 \quad \text{Equation 12}$$

3.1.3.2.3 Ingate

Clearly, the velocity of the liquid is too high at the bottom of the down-sprue. Therefore, the velocity must be reduced before entering the casting; otherwise, the casting will suffer quality problems. The runner bar and the ingate have the responsibility of reducing the velocity of the liquid to below the critical velocity.

As mentioned before, the critical velocity for aluminium is $0.5 \text{ m}\cdot\text{s}^{-1}$. The velocity of the liquid should be of a value equal to or less than this when it enters the casting cavity. Therefore, the target velocity at the ingate needs to be set at $0.5 \text{ m}\cdot\text{s}^{-1}$.

Figure 3-5 shows the flow chart for determining the size of the ingate. As with the down-sprue design, the calculation starts from the initial flow rate (Eq. 7). As the figure shows, by combining the target velocity and the initial flow rate together, the target area of the ingate can be established and then the shape of the ingate can be decided upon.

$$A_{ingate} = \frac{V_{in}}{v_{target}} = 252 \text{ mm}^2 \quad \text{Equation 13}$$

It is easy to understand the reason for using the initial volume flow rate to determine the target area of the ingate. In practice, the fill rate will decrease as the liquid metal fills the mould cavity due to the changing hydraulic pressure difference. This means that at the beginning of the filling, the fill rate is higher than the average fill rate. If the average flow rate is used, there is a chance that the velocity of the liquid metal will exceed the critical velocity at the beginning of filling. To avoid this kind of situation, the initial volume fill rate has to be used to satisfy the target velocity. Then, the initial fill rate and target velocity will work together to calculate the target ingate area.

3.1.3.2.4 Runner bar

After determining the target area of the ingate, the cross-sectional area of the runner bar can be established easily. Usually, the area of the runner bar should be one-half that of the ingate in order to reduce further the velocity of the liquid at the ingate (Jolly, 2002). The only suggestion about the runner bar is its height; it should be as thin as possible to prevent phenomena, such as a rolling back wave and hydraulic jumps (they can form DOFs). Additionally, the runner bar has to be located at the bottom of the running system. This arrangement can allow bubbles and slag to float out to the liquid surface. Beyond this requirement, there is no strict condition regarding the length of the runner bar; it is determined by the geometry of the casting.

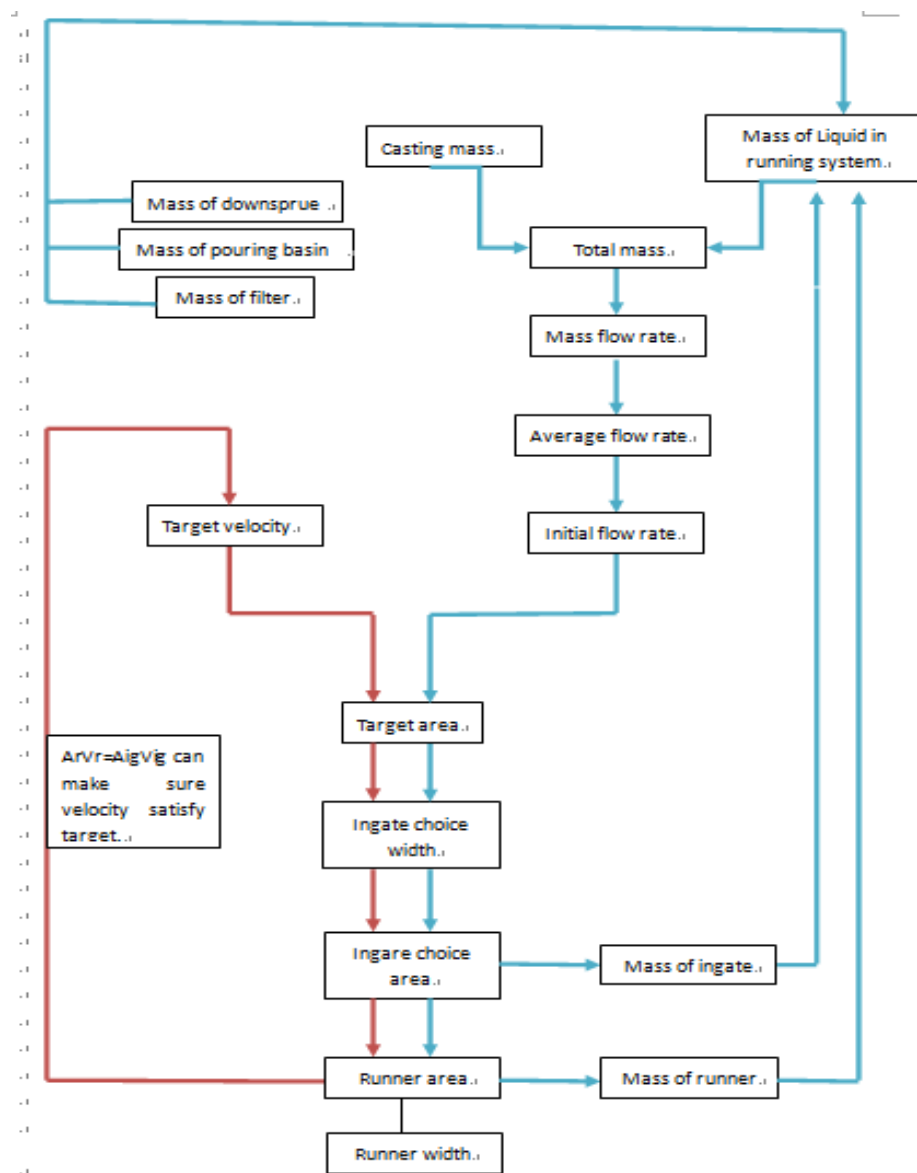


Figure 3-5 Flow chart of the velocity control in the gravity poured running system (Zeng, 2010). High resolution flow chart can be seen in Appendix 6 (pp185).

3.1.3.3 Summary

A gravity poured casting running system, designed to the highest specifications, has been introduced. According to this, a gravity poured tensile test bar with a five-second filling time has the parameters shown in Figure 3-6.

Casting	Al354
	Weight 4.35 kg with feeder
Pouring Basin	79x157x60 mm
Downsprue	Top area: 1158 mm ²
	Bottom area: 226 mm ²
	Height: 368 mm
Runner Bar	Cross section area: 547 mm ²
	Length: 120 mm
	Depths less than 10 mm
Ingate	Cross section area: 1093 mm ²
	Height: 20 mm

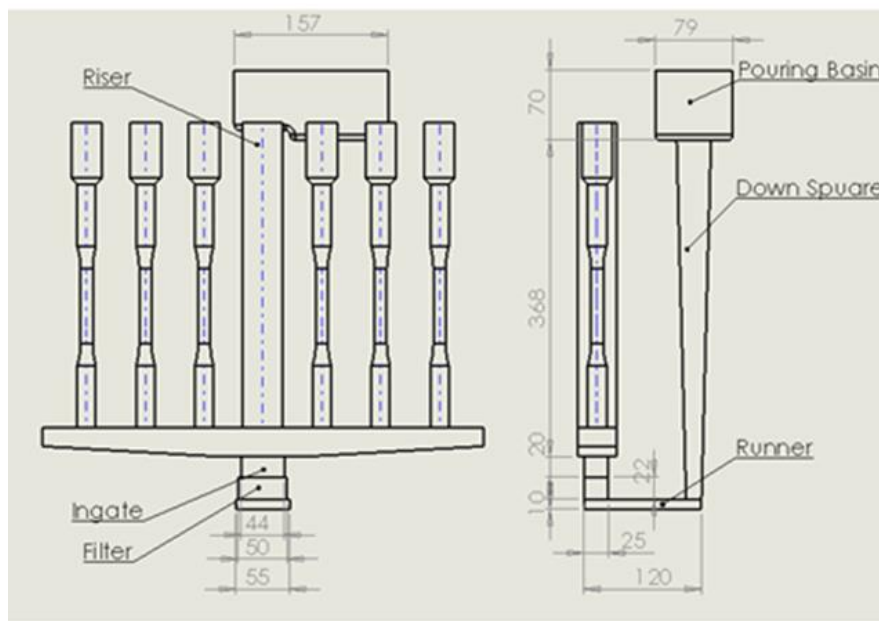


Figure 3-6 Key dimensions of the running system

3.1.4 Software and hardware introduction

From the validation results, the Flow3D package will be used for the filling simulation. In this project, a customised sub-routine is introduced into FLOW3D to track DOFs. This sub-routine was developed by researchers at the University of Birmingham (Reilly, et al., 2009). It allows the placement of particles at the point where the flow structure is likely to entrain

DOFs and tracks those particles (defects) to their final position. The density, size, co-efficient of restitution and initial velocity vector of the particles can be defined by the user. This allows particle behaviour to be tuned to exhibit specific behaviour defined by past research and theory. By using a velocity tracking sub-routine, the velocity and volume flow rate in the tensile test bars and the ingate are also recorded.

3.1.5 Results

By using the velocity tracking sub-routine in Flow3D, the flow velocities at the casting cavity were recorded. As [Figure 3-7](#) shows, the fluid flow velocities for both casting processes are around $0.25 \text{ m}\cdot\text{s}^{-1}$. This means that both processes can provide smooth filling in the casting cavity and no subsequent defects (air entrapment and DOFs, etc.) can be generated in the cavity. Although the flow rate in the CRIMSON process is slightly higher than that of the gravity casting process, both flow rates are reasonably well matched with the target flow rate of $0.25 \text{ L}\cdot\text{s}^{-1}$.

As discussed in section 3.3.2 in this chapter, falling under gravity causes surface turbulence during filling. The simulation results given in the tables below indicate the same problem as predicted. [Tables 3-4](#) and [3-5](#) show the amount of DOFs generated in the gravity sand casting running system and the CRIMSON running system, respectively. One thing that must be emphasised here is that the amount of particles shown here cannot represent the real amount of DOF (it is impossible to count real amounts of DOF by any method). However, such results can still qualitatively represent the DOFs in the casting.

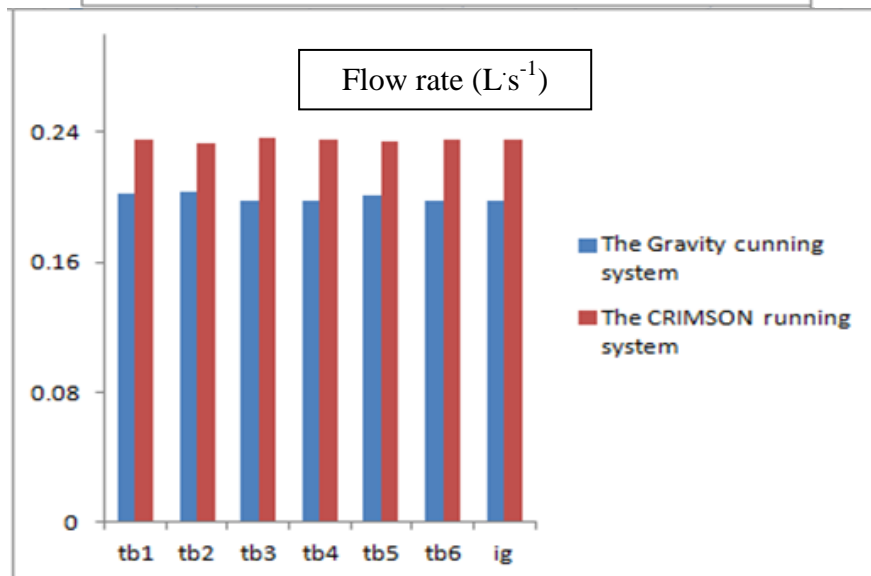
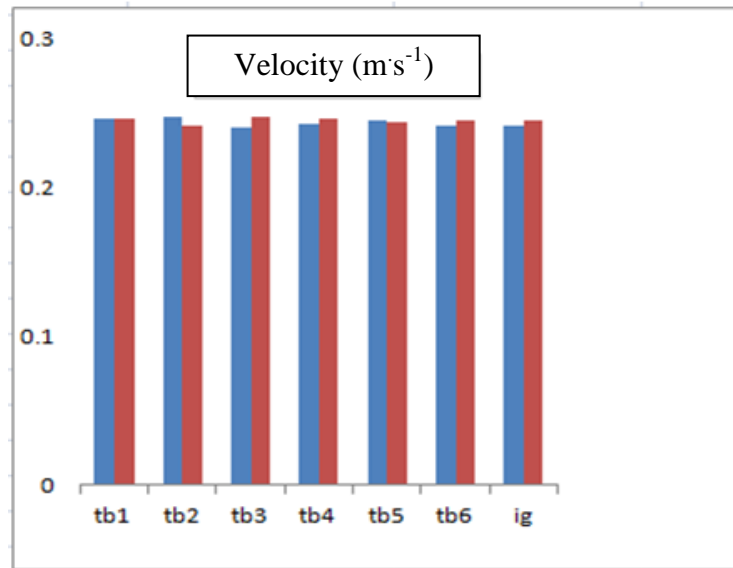


Figure 3-7 Tb stands for tensile test bar; it counts from left to right. ig represents ingate

	1	2	3	4	5	6
Particle in Test Bar (TB)	236	14	3	182	190	540
Particle NOW in TB	73	3	0	0	57	96
Particle in Gauge Length (GL)	66	3	1	13	33	75
Particle NOW in GL	8	1	0	0	7	12
Total Particle in System ⁹	124801					
Total particle NOW in system ¹⁰	12718					

Table 3-4 DOFs generated in the gravity sand casting running system

⁹ The system includes pouring basin, downsprue, runner bar, ingate, and feeder

¹⁰ The system includes pouring basin, downsprue, runner bar, ingate, and feeder.

	1	2	3	4	5	6
Particle in TB	15	8	27	15	21	21
Particle NOW in TB	0	0	3	0	1	19
Particle in GL	0	0	0	3	1	2
Particle NOW in GL	0	0	0	0	0	2
Total particle in system	1900					
Total particle NOW in system	763					

Table 3-5 DOFs generated in the CRIMSON running system

In the tables, the “Particle NOW” stands for those not on the wall. It represents the DOFs remaining in the liquid. Because it has similar density to liquid aluminium, it can stay anywhere within the casting running system. The “Particle NOW in GL” shows the number of particles within the gauge length. Because the gauge length is the thinnest section in the tensile test bar, it is the key performance indicator for the filling quality. Therefore, it is clear to see that the CRIMSON process has fewer particles in the gauge length. By contrast, four out of the six test bars made by the gravity filling method have DOFs, which means that the gravity tensile test bar is more likely to fail during the tensile test.

3.1.6 Discussion

Both the theoretical assumption and the simulation results indicate that the gravity filling method generates more DOFs than the CRIMSON method does during the filling. Generally, there are two sources for DOF formation in a gravity poured casting running system: the pouring basin and the down-sprue. From [Figure 3-8](#), it can be seen that when the liquid metal entering the pouring basin at $t = 0.1$ seconds, the velocity of the liquid metal flow has already exceeded the critical velocity. In particular, when the liquid metal steam hits the pouring basin, the sudden change of the velocity direction leads to the break-up of the oxide film surface, forcing it to become entrapped. As the liquid metal fills the pouring basin, a physical phenomenon called a plunging jet (Reilly, 2010) occurred at around $t = 0.3$ seconds. Such an impingement breaks up the surface oxide and entrains it at the point of impingement. As mentioned before, the aluminium is a film forming material, which means that it can react instantly with air to form an oxide. Therefore, the impingement point keeps breaking and reforming oxide films, which is why such chaos occurs in the pouring basin.

Pressure difference is the driving force for gravity filling. Therefore, the down-sprue should have sufficient length to maintain the pressure head. As discussed before, the critical height for the fall of aluminium is 12 mm. However, the down-sprue used in this system is 368 mm

in length. Thus, surface turbulence occurs almost immediately after the liquid metal enters the down-sprue, generating DOFs all of the way down the down-sprue (Figure 3-9b, 3-9c, 3-9d).

Fortunately, the well-designed taper-shaped down-sprue arrests most of the DOFs during the filling (Figure 3-9c, 3-9d); otherwise, the quality of the castings produced by the gravity runner system will be much worse.

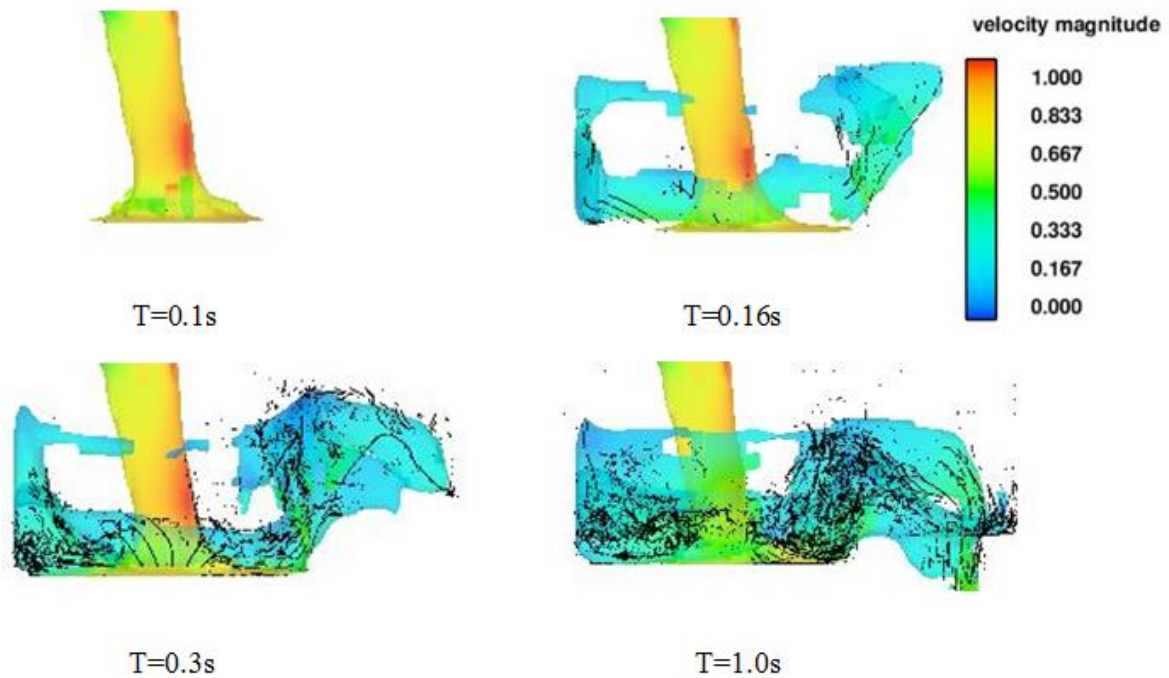


Figure 3-8 Schematics of the fluid behaviour in the pouring basin

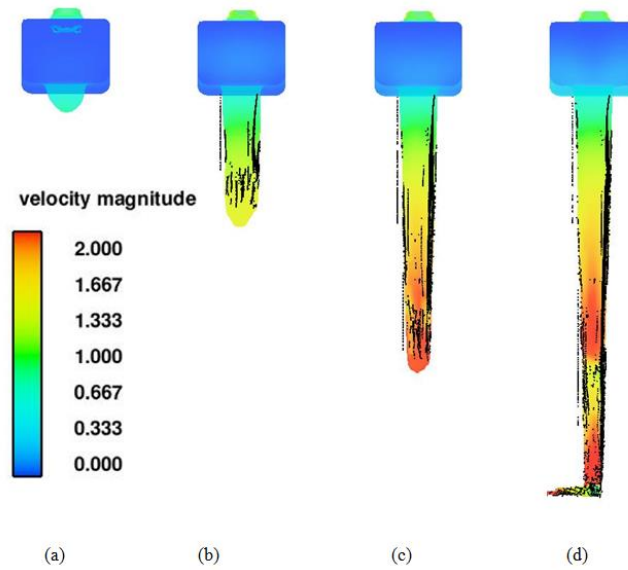


Figure 3-9 Schematic of DOF generation during falling. Parts c and d show DOFs stuck on the taper-shaped downsprue

On the other hand, the CRIMSON process tells a different story. To satisfy the $0.25 \text{ L}\cdot\text{s}^{-1}$ volume flow rate for the ingate and test bar, the piston only has to move at a velocity of $0.032 \text{ m}\cdot\text{s}^{-1}$ (determined from mass conservation theory, the diameter of the sleeve is 100 mm). With such a velocity, the surface tension dominates the flow and no surface turbulence is present. Thus, the liquid metal can be delivered smoothly into the ingate without any DOFs forming. Figure 3-10 below shows the filling of the running system.

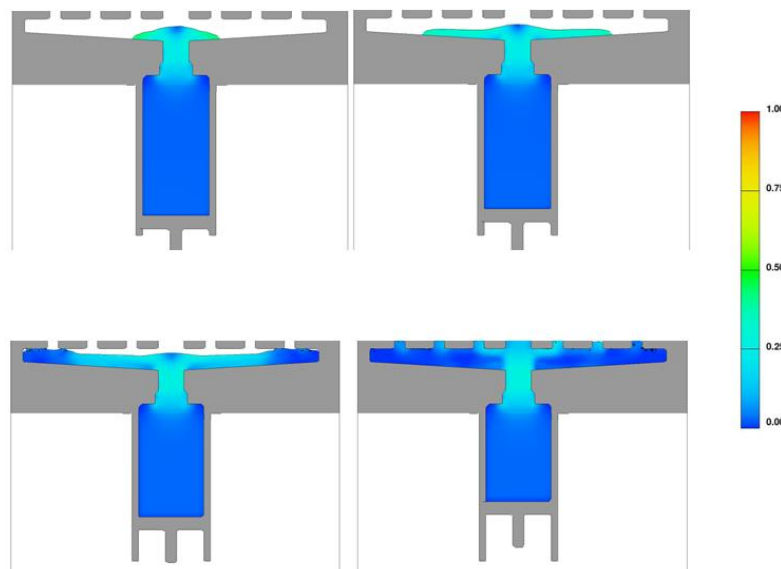


Figure 3-10 Demonstrating fluid behaviour during the CRIMSON filling process. Fluid is moving very smoothly in the runner.

3.1.7 Conclusion

From the simulation and investigation, the following conclusions can be made:

1. The gravity sand casting running system designed for this project is successful, because 90% of the oxide films generated in the running system are captured by the running system itself. This indicates that a good running system is very important for a casting process.
2. Because of the geometry requirements, the gravity casting running system cannot avoid DOFs during the filling process. No matter how sound the running system design is, there will always be DOFs entering the casting product and causing problems.
3. The CRIMSON up-casting process eliminates two major sources of DOF generation: the pouring basin and the down-sprue, which not only prevents DOFs defect but also increases the casting yield of the casting product.
4. In the CRIMSON process, all the important parameters are under control. Because of the conservation of flow rate, the piston needs only a very slow speed (0.032 m/s for this project) to deliver the liquid metal. This slow movement can ensure that the liquid metal is delivered smoothly, avoiding the formation and entrapment of DOFs.

3.2 Design and optimisation of an investment CRIMSON casting running system

Because of the advantages of the CRIMSON process, the next task is to apply CRIMSON to an investment casting process. As a partner of this project, AEROMET International PLC provided a thin-walled aluminium filter housing for research. AEROMET's traditional route is to use a massive investment casting running system to produce this filter housing, which only gives 5% to 10% casting yield. The running system of the filter housing was designed by using a combination of the casting software Magmasoft 5 and Flow3D. By working with AEROMET, various configurations of the casting running system were discussed and analysed. Ultimately, the optimum newly designed CRIMSON casting running system will be compared with the original.

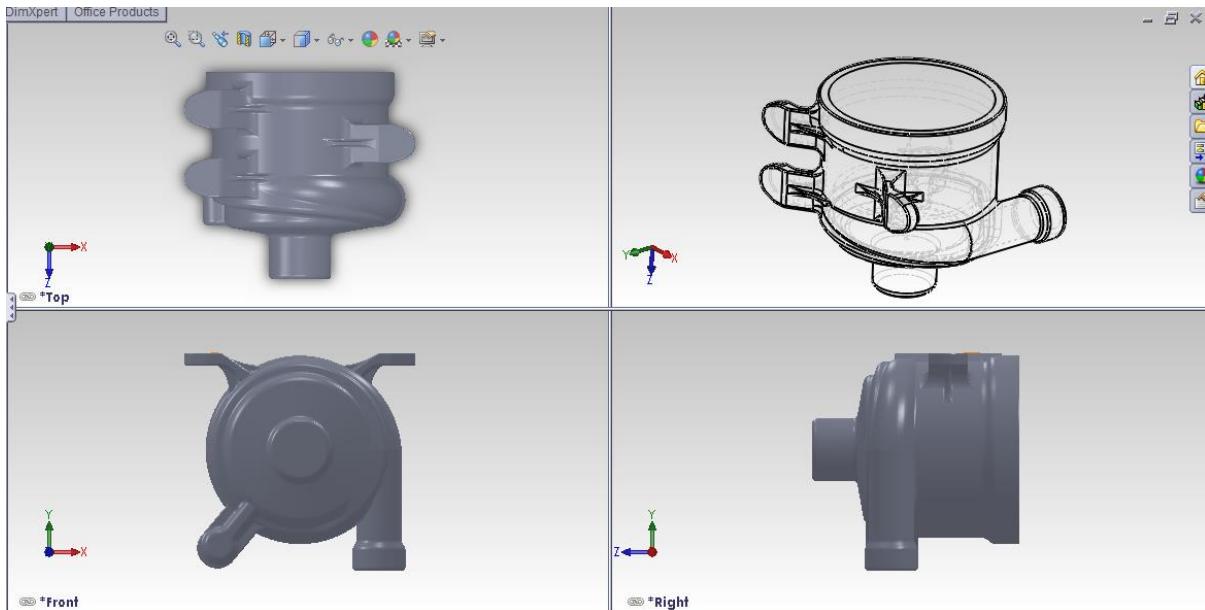


Figure 3-11 schematic of the geometry of the filter housing

Figure 3-11 shows the filter housing made by AEROMET. This filter housing has a thin middle section and a thick bottom. During the solidification stage, the thin wall in the middle solidifies first. Therefore, the natural feeding from the top is blocked by the solidified metal; thus, the thick bottom may suffer from shrinkage porosity. To eliminate the shrinkage problem, AEROMET has a massive feeding system to feed the shrinkage of the filter housing. It transpires that their casting yield is between 5% and 10%. Even with their maximum 10% yield, the manufacture of a 0.8 kg filter housing requires 8 Kg of raw Al356 alloy.

3.2.1 Methodology

Based on the comparison results of the gravity running system and the CRIMSON running system, the concept of an up-casting runner is adopted for the design of the new running system. By using the combination of Flow3D and Magmasoft 5, the geometry of the running system, pouring rate, pouring temperature and some other parameters can be determined.

Flow3D has already been introduced in previous sections. Its unique free surface model can describe accurately transient free surface flow with large deformations. According to benchmark tests performed at the University of Birmingham (Sirrell, et al., 1996) , Flow3D describes accurately the fluid behaviour inside the casting runner. According to the benchmark test and the author's experience (Zeng, 2010), Flow3D can be used to observe the behaviour of liquid and to optimise the shape of the running system.

On the other hand, Magmasoft 5 is commercial casting software package that is used widely by foundry personnel (1,800 active licenses). It can be used to perform numerical simulations of molten metal filling and solidification in different casting process, such as sand casting, investment casting and die casting. Its database not only contains the physical properties of the metals but also their thermal properties as well. Moreover, the well-developed thermal and fluid dynamic codes can be used to predict shrinkage and gas porosity, as well as stress distribution during solidification. For the design of the filter housing running system, Magmasoft 5 is used to focus mainly on the simulation of solidification, thermal properties correction and boundary condition justification.

3.2.2 First approach

Considering the advantage of the CRIMSON casting running system, the original test bar runner is used as a draft design (Figure 3-12). Two filter housings are attached to the runner bar: one on the left and the other one on the right. The first simulation is performed by Magmasoft 5. As mentioned before, the filter housing is a thin-walled casting product, which requires fine meshes for these parts. The author used the uniform mesh method to mesh the entire geometry. It transpires that this first approach has 50,974,440 mesh elements in total and takes about 30 hours to run. Some of the key settings, together with the simulation results are shown in Table 3-6 and in Figure 3-13.

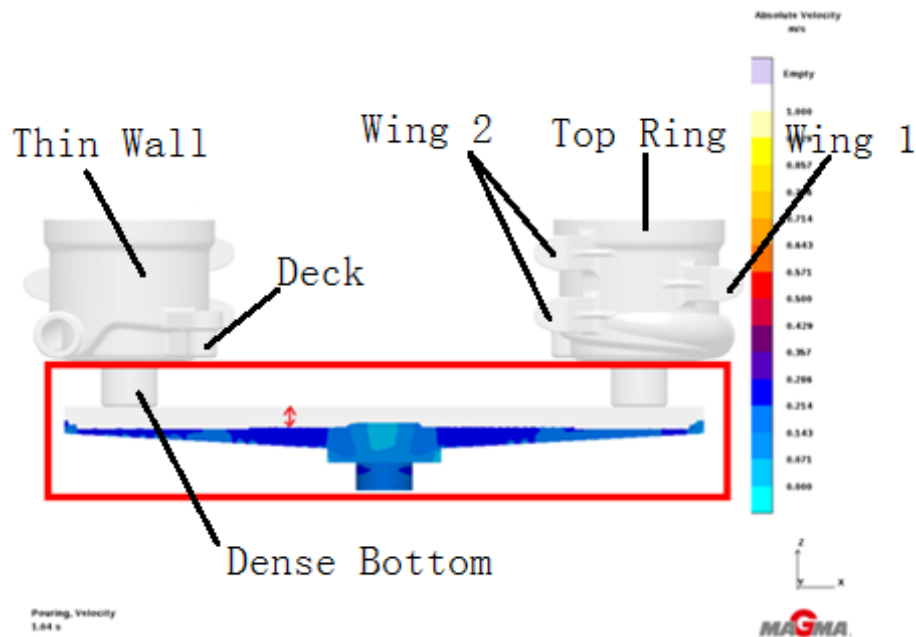


Figure 3-12 Ground design adapted from tensile test bar

Casting Method	Up-casting
----------------	------------

Casting Material	AlSi7Mg
Mould Material	Furan
Heat Transfer	Temperature dependent HTC
Pouring Temperature (°C)	700
Mould Temperature (°C)	20
Maximum Flow rate (l/s)	0.25
Time for solver (s)	108841.5
Time for solver (hour)	30.23
Filling time (s)	6.91
Solidification time (s)	1067.86
Porosity per housing (mm ³)	2832.42
Velocity at runner (m·s ⁻¹)	0.2
Velocity at ingate (m·s ⁻¹)	0.11
Mass of casting (kg)	1.6
Mass of casting system (kg)	1.36
Casting Yield (%)	54

Table 3-6 General settings and results

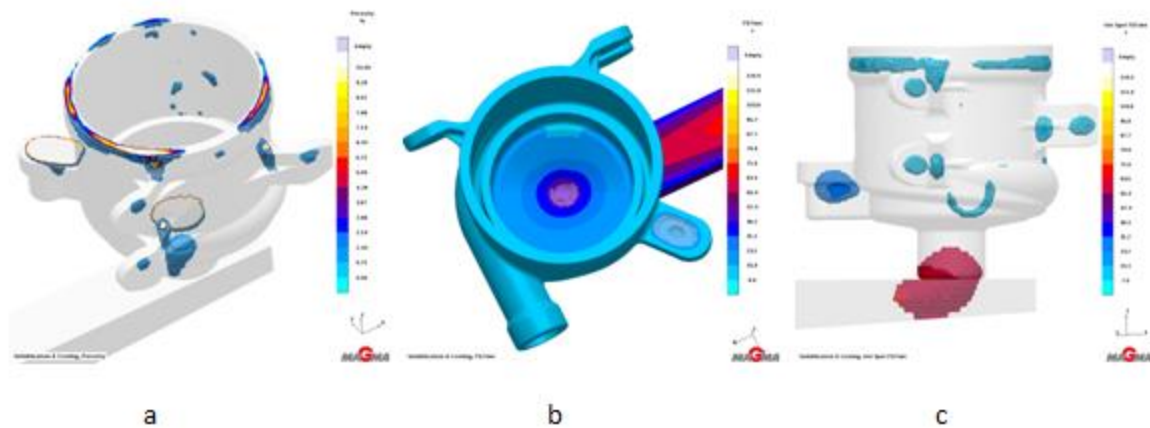


Figure 3-13 Solidification results. Left to right: porosity, FS time and Hot spot FS time

Table 3-6 shows that the velocity is not a problem during filling. In fact, the filling velocity is a little bit slow. The main concern from these results is porosity defects, as shown in Figure 3-13a. Eliminating these porosity defects is the major challenge to be addressed in the new running system design. Based on information from Figures 3-12 and 3-13 and from Table 3-6, several suggestions can be addressed here:

Firstly, the tensile test bar runner is oversized. As we know, the purpose of this design is to increase the casting yield. Thus, it is observed easily from Figure 3-12 that the distance between two filters can be reduced.

Secondly, as the metal enters the runner bar, it cannot reach the top of the runner and it leaves a gap. Because the filling is slow, the surface oxide film may be thicker due to longer oxidation. Eventually, the thick films can be a potential threat for the casting products. Therefore, reducing the height of the runner is essential.

Thirdly, because of the porosities found in the casting, various boundary conditions need to be tested. Feeders also need to be considered in the running system design. Their shape, size and location need to be calculated and proved. In order to assess the porosity in different locations, the filter housing is divided into six sections: the top ring, thin wall, dense bottom, deck and wings 1 and 2 (Figure 3-12).

Finally, the simulation took too long time to process. Therefore, a sensitivity analysis needs to be performed to establish the optimal mesh density for the simulation.

3.2.3 Running system design

3.2.3.1 Runner design

Filter housing running system design based on the CRIMSON tensile test bar runner due to its advantage. As the most important parameter for the sand casting running system, the velocity have to be under critical one for all cases. Therefore, the start point of the running system design is about discovering the thinnest cross section in the casting. For filter housing, the thinnest section is highlighted as below. It has the cross section area of 907 mm^2 . The target velocity through this section should be less than $0.5 \text{ m}\cdot\text{s}^{-1}$. Therefore, using the volume conservation theory $Fr=AV$, the critical filling rate (Fr) is about $453 \text{ cc}\cdot\text{s}^{-1}$, However, the author choose $250 \text{ cc}\cdot\text{s}^{-1}$ to demonstrate the flexibility of the CRIMSON process.

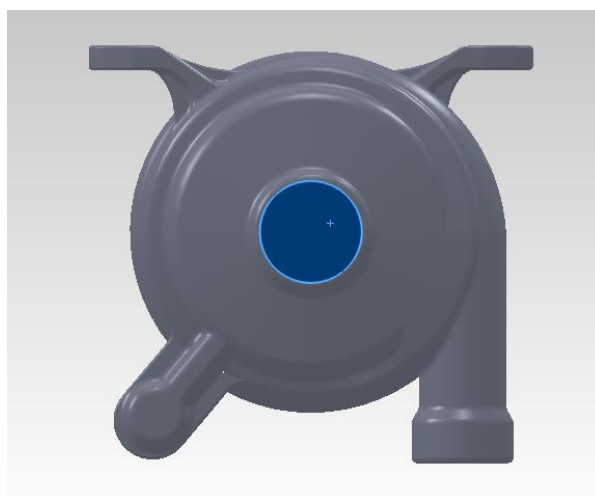


Figure 3- 14 shows the thinnest cross section area of the filter housing

In order to reduce the metal yield into the runner bar, the author decides to reduce the width of the runner bar. In this case, the width of the runner bar is same as the diameter of the bottom of filter housing, which is 40 mm. Assuming the runner bar is in rectangular shape. According to the observation, the idea runner bar should be a single pass runner bar (Reilly, 2010). The concept of the single pass runner is that the liquid enter into the runner can reach the top of the runner at first place. Therefore, there will be no gap between top surface of liquid and the runner and reduce the chance of the unnecessary contact. Therefore, a single pass runner in this case should have the thinnest thickness of 6.5 mm (volume conservation).

On the other hand, the condition to form single pass runner requires the runner must have the same or less height as the critical height the liquid can with stand. This critical height relates to the height of the sessile drop, which has relation with the critical velocity. It has been proved that the critical velocity has the relation with the height of the sessile drop (Campbell, 2004). The sessile drop is a stationary fluid droplet placed on the plain surface, which exhibits a specific height h defined by the balance between the surface tensional pressure and the gravitational pressure (Jolly, 2002) of the droplet.

$$p_1 = \frac{2\gamma}{r} \tag{Equation 14}$$

$$p_2 = \rho gh \tag{Equation 15}$$

Combining Eq. 14 and Eq. 15 together, the critical height of the sessile drop can be defined as:

$$h_{crit} = 2 \sqrt{\frac{\gamma}{\rho g}} \tag{Equation 16}$$

p is the pressure in Pa,

γ is the surface tension in Nm,

g is the acceleration due to gravity ms^{-2} ,

ρ is the density of the liquid in kgm^{-3} .

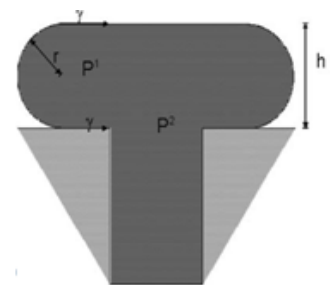


Figure 3-15 Critical height of the sessile drop (Jolly, 2002)

By using equation 16, the critical height of the aluminium is about 12 mm. This means the height of the single pass runner should be no more than 12 mm. Therefore, the runner bar thickness for this case should be in the range of 6.5 mm to 12 mm. Six different heights of the runner bars were simulated in Flow3D for the purpose identify the best thickness of the runner bar and also showcase the performance of the single pass runner. As usual, the

velocity and DOF defect tracking sub-routine are applied to check the quality of filling.

Figure 3-16 below shows the general shape and dimension of the runner bars

min Height (mm)	Max height (mm)	Length of runner (mm)	Width of runner (mm)	Tilt angle
3	7.44	280	40	3.25
5	9.44	280	40	3.25
8	12.44	280	40	3.25
10	14.44	280	40	3.25
15	19.44	280	40	3.25
18.7	24.44	280	40	3.25

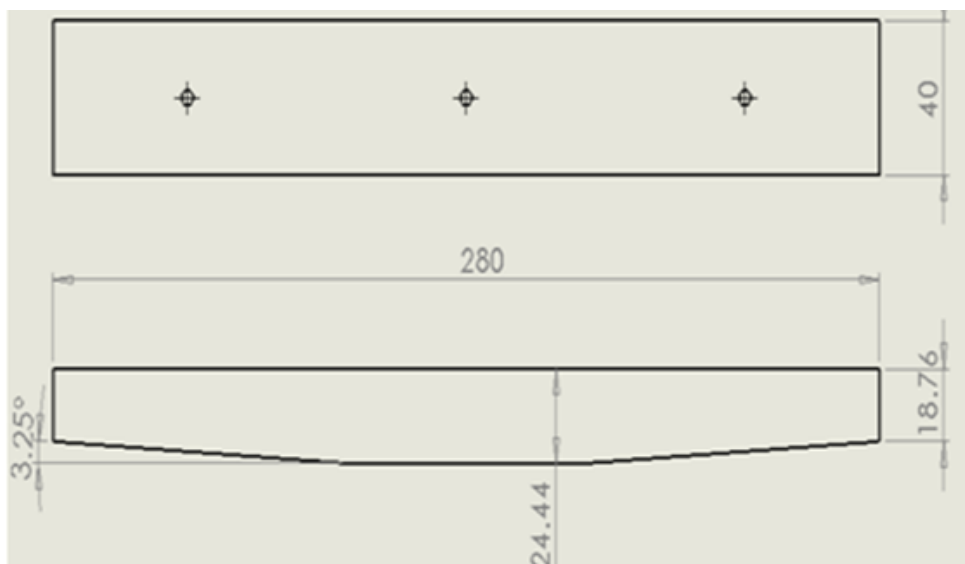


Figure 3-16 typical shape of the runner bar

The velocity of the liquid metal is always a big concern in the design of a running system. Maintaining the velocity of the aluminium below $0.5 \text{ m}\cdot\text{s}^{-1}$ is always good practice for maintaining casting quality. Because of the symmetrical structure, only half of the runner bar needs to be checked. By using simple mass conservation theory ($R = A_1 \times V_1 = A_2 \times V_2$) the liquid velocity along the runner can be determined. Figure 3-17 displays the velocity profile for different heights of runner. Clearly, if the height of the runner bar is reduced to 7.44 mm, the velocity of the liquid metal exceeds the $0.5 \text{ m}\cdot\text{s}^{-1}$ limit. It turns out that surface turbulence can occur. Therefore, reducing the runner height to 7.44 mm is probably unsuitable.

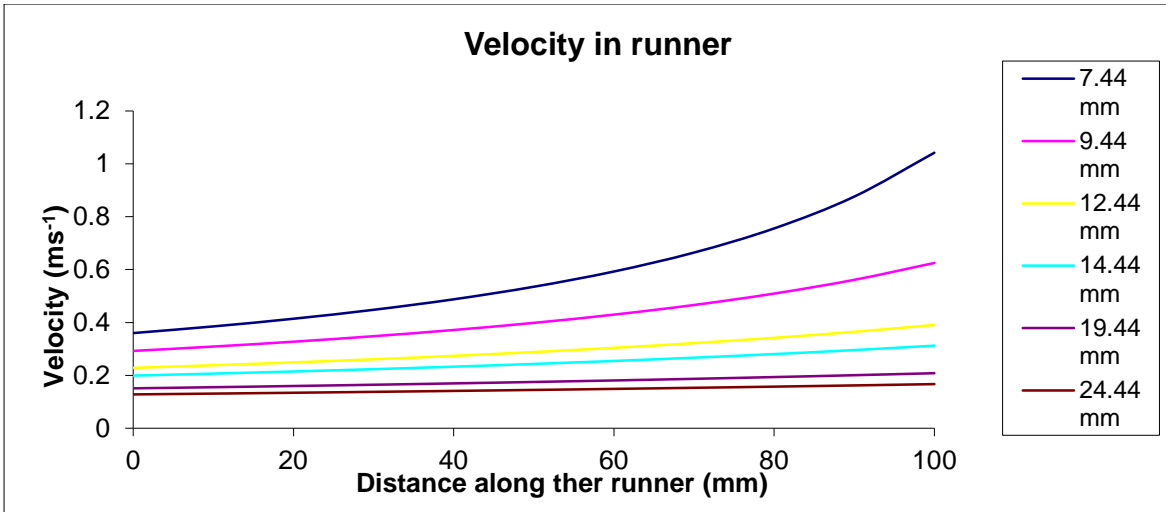


Figure 3-17 Velocity profile for different heights of runner

After the theoretical calculations, the runners were tested in Flow3D. Figure 3-18 shows the fluid pattern in the different runner bars at the same filling time. From the graph, it is easily to find that only the 12.44, 9.44 and 7.44 mm runner bars can form a single pass metal steam. In the remaining runner bars, the liquid cannot reach the top of the runner bar and their slow moving front (less than $0.2 \text{ m}\cdot\text{s}^{-1}$) increases the chance of oxidation. Therefore, the 12.44, 9.44 and 7.44 mm runner bars can considered further.

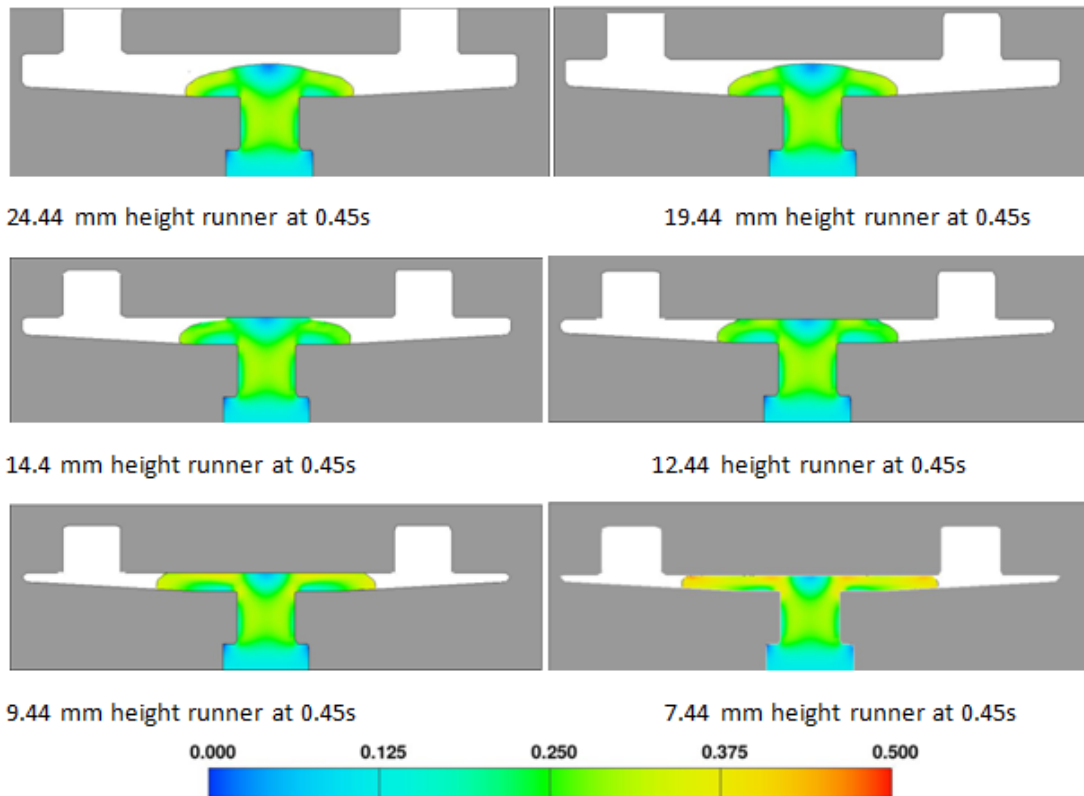


Figure 3-18 schematics of fluid pattern for different heights of runner

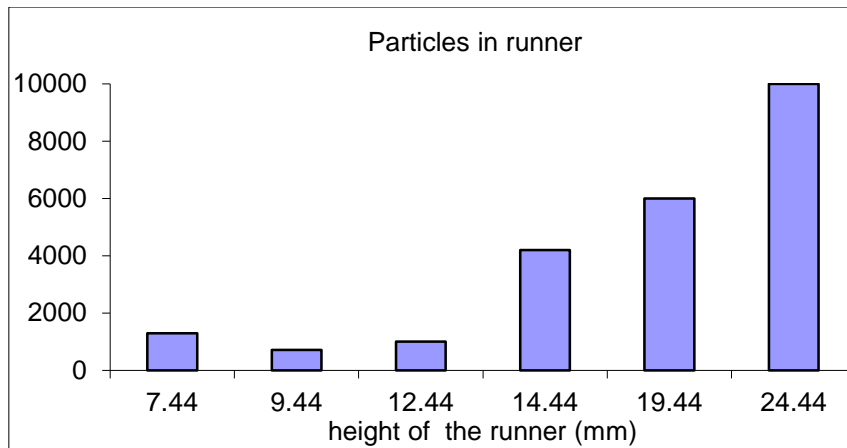


Figure 3-19 DOFs count for different casting running systems

Figure 3-19 shows the DOFs count for different heights of runner. Because the 22.44, 19.44 and 14.44 mm runner bars are not single pass runners, they generate more DOFs than the other runner bars, even though they have a slower velocity of liquid metal. Therefore, they cannot be used for the new filter housing running system. As discussed before, the 7.44 mm depth runner bar may suffer from DOF defects due to its velocity issue. The figure above tells the same story as expected; because of the velocity problem, it generates more DOFs than the 9.44 and 12.44 mm runner bars. Furthermore, the 7.44 mm depth runner may lose heat more quickly, causing a miss run in a filling. Therefore, the 7.44 mm depth runner is unsuitable for the new filter housing running system.

The 12.44 and 9.44 mm runner bars have similar performance on velocity control, single pass stream formability and DOF control. Clearly, the comparison of these two runners is focused on savings. According to the calculations, the 9.44 mm runner uses only 75% of the metal used by the 12.44 mm runner. Furthermore, comparing with the original 24.44 mm runner, the new runner bar saves about 62% of the aluminium. Considering both filling quality and the saving, the 9.44 mm runner bar is selected as the best runner design. This runner bar will be used as the standard runner bar for further optimisation.

3.2.3.2 Feeder design

As mentioned in the literature section 2.2, shrinkage is due to volume change during the solidification process. Figure 3-13 suggests several reasons that may cause porosity. The filter housing is in the vertical orientation and owing to the natural tendency of the flow; the liquid at the top will flow downward. This is why the top ring section suffers from porosity defects. The FS time result displayed in Figure 3-13b indicates another reason. FS time shows the time needed for a critical portion of liquid to solidify. This portion of liquid is related to

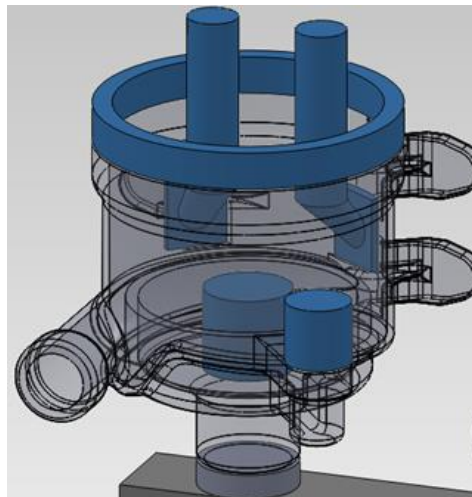
the feeding rate. For aluminium, the feeding rate is 30%. Thus, the FS time shown in [Figure 3-13b](#) indicates the time needed for 30% of the aluminium to solidify. From the graph, it is easily to establish that the centre of the thick bottom and the centre of the deck take a significant longer time to solidify than their surroundings. Therefore, when the surroundings solidify, the feeding passages are blocked and porosity defects can occur.

To eliminate porosity defects, feeders must be applied to the casting running system. The size of the feeder can be determined by modulus, which is the ratio of the volume to the cooling surface area. Normally, the modulus of $M_f = 1.2 \times M_c$ is applied to calculate the feeder size. For an L junction like the extruded deck, the modulus of $M_f = 1.33 \times M_c$ is used (Jolly, 2002). [Table 3-7](#) below shows the feeder size for filter housing casting.

	Modulus of casting (mm)	Modulus of Feeder (mm)	Feeder shape	Dimension (mm)
Top ring	6.45	7.74	ring	D120.5*d105*H30
Deck	5	6.65	cylinder	D26*H35
Bottom	7.5	8.99	cylinder	D40*H60

[Table 3-7](#) Dimensions of the feeders

[Figure 3-20](#) shows the first improvement of the feeder design. The highlighted parts are the feeders attached to the filter housing. In addition to those three feeders, two blank feeders are also attached in this design. They are used to feed the wing sections, as well as the thin wall.



[Figure 3-20](#) Schematic of the shape of the feeders and their locations

3.2.3.3 Parameter settings

After establishing the runner design and the feeder design of the running system, the next task is to determine the casting parameters for this investment casting that are most sound. Because the CRIMSON process is good at velocity control, defects caused by DOFs are

hardly to form. Therefore, the key performance indicator should be the shrinkage porosity in this case. Following factors can influence the volume of the porosity.

Pouring temperature is the first parameter needing consideration. Generally, the pouring temperature is around 700°C. However, the temperature can vary depends on the casting wall thickness. The second parameter need to be considered is the mould temperature. The casting will take longer to settle and may cause solidification defects at higher mould temperature. By contrast, a miss run may happen during a lower mould temperature. As the information provided by Aeromet, they keep the mould temperature at 400°C. The next parameter needing consideration is the filling rate, which is the key to surface turbulence-free filling. According to design specification, 0.25 l/s is the target flow rate for this case. Because the shell thickness will affect the cooling behaviour of the casting, this also needs to be considered. Currently, all investment castings have 6 mm shell at Aeromet.

Four factors had been discovered. It is make sense to investigate their influence to porosity level in terms of different variation. Therefore, a design of experiment method was used investigate such influence. However normal design of experiment method requires a certain amount of data to perform the analysis. In order to simplify the design of experiment analysis, a Taguchi¹¹ experimental design was adopted. A four factors and three levels (low, middle, and high) of Taguchi experiment were introduced. The factors, their levels and Taguchi combination is shown in [Table 3-8](#) and [Table 3-9](#).

		1	2	3
Pouring Temp (°C)	A	650	700	750
Flow rate (l·s ⁻¹)	B	0.15	0.25	0.5
Mould Temp (°C)	C	300	400	500
Shell thickness (mm)	D	3	6	10

[Table 3-8](#) Parameters that need to be tested for filter housing

¹¹ Taguchi methods have been used widely in engineering analysis to optimise the performance characteristics through the setting of design parameters. By applying Taguchi methods based on orthogonal arrays, the time and cost required to conduct experiments can be reduced. In addition, the Taguchi method recommends the use of the S/N ratio for the determination of the quality characteristics implemented in engineering design problems. The S/N ratio can be divided into three stages: the smaller the better, the normal the best and the larger the better.

Run	Factor			
	A	B	C	D
1	650	0.15	300	3
2	650	0.25	400	6
3	650	0.5	500	10
4	700	0.15	400	10
5	700	0.25	500	3
6	700	0.5	300	6
7	750	0.15	500	6
8	750	0.25	300	10
9	750	0.5	400	3

Table 3-9 Parameter combination of orthogonal array L9 (3*4) that needs to be tested

Because porosity is the key performance indicator, it should be as small as possible. Therefore, the response table for the signal-to-noise in the Taguchi method should be **smaller is better**.

Level	A	B	C	D
1	-101.11	-102.28	-102.25	-101.83
2	-93.65	-93.58	-94.16	-94.16
3	-95.37	-94.27	-93.72	-94.14
Delta	7.46	8.71	8.53	7.69
Rank	4	1	2	3

Table 3-10 Response table for signal-to-noise ratios Smaller

Table 3-10 shows that the flow rate has the most influence on the porosity level. The filling rate not only relates to the filling quality but also to the filling time. Too low a flow rate will need a longer time to fill the mould, which means that the liquid metal may lose significant amounts of heat that affects the feeding. On the other hand, a high value of flow rate causes a higher velocity of the flow in the casting. The surface turbulence can cause DOF defects and cause porosity in the casting. Once again, this result indicates that how important velocity control is; it not only affects DOF generation but also affects porosity formation.

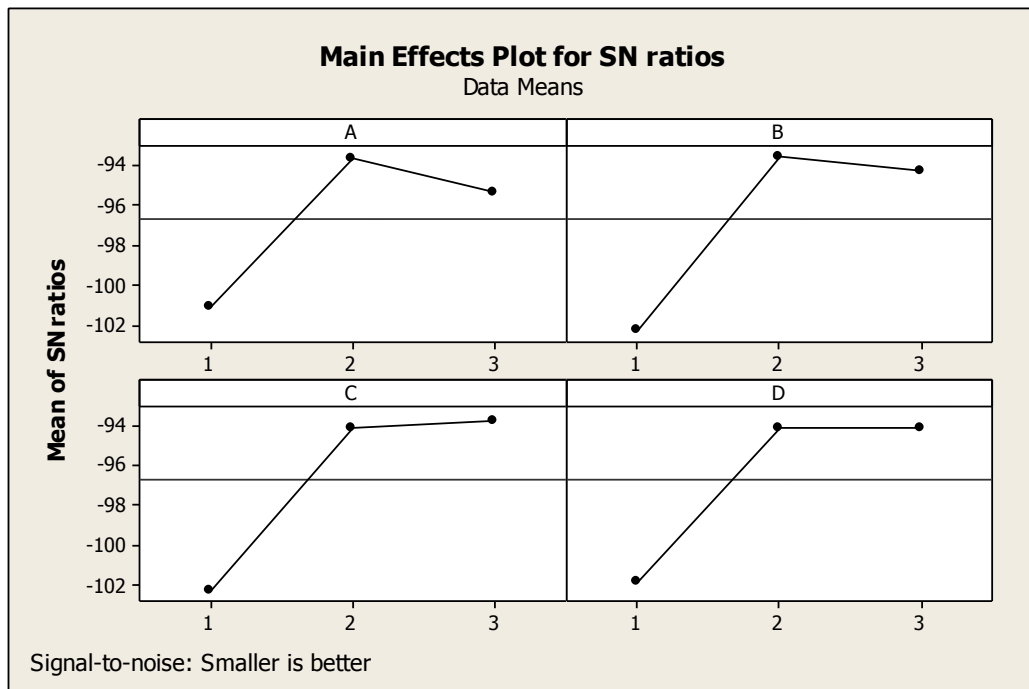
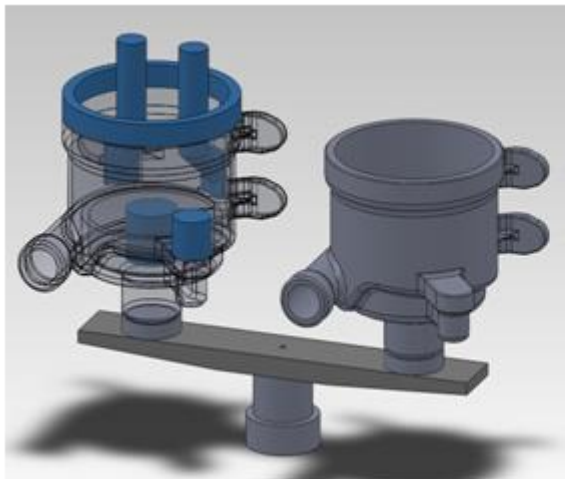


Figure 3-21 Main effects plot for SN ratios. Indicates that a good casting should have pouring temperature of 700 °C, a mould temperature of 500 °C, a filling rate of 0.25l/s and a 6-mm thickness shell

Optimisation is also carried out after the test. Figure 3-21 is the main effects plot for the SN ratios. It can be seen that the combination of A₂B₂C₃D₂ provides the best opportunity for reducing porosity. After the examination in Magmasoft 5, such a combination provides the minimum level of porosity. Furthermore, such results match with the normal parameters used. Especially the shell thickness, it matches with AEROMET’s own design. Therefore, the following set of parameters is used in the new design running system: pouring temperature, 700 °C; flow rate, 0.25 L·s⁻¹; shell temperature, 500 °C; and shell thickness, 6 mm.

3.2.4 Simulation results for version One

The assembly of the first version of the CRIMSON running system, shown in Figure 3-22, includes a new runner bar, filter housing and the feeders. The casting is in the vertical orientation and the metal will be pushed through the bottom gate. The highlighted parts are the feeder and attachments to the filter housing. In order to show the feeding capability only one housing has the feeder attachment.



casting method	Investment casting	Pouring Temperature @	700
Filling Method	Upfilling	Shell Temperature @	500
Casting Material	A356	Filling Rate (L/s)	0.25
Shell Material	Al2O3	volume element	4,139,300
Mass of Casting (Kg)	1.6	Mass of Casting system (Kg)	1.55
Advance Turbulence Mode	ON	Surface Tension	ON

Figure 3-22 First version of the filter housing design and key parameter settings

	With Feeder		Without Feeder	
	Porosity volume (mm ³)	No. of Porosities	Porosity volume (mm ³)	No. of Porosities
Dense Bottom	0	0	909	1
Deck	0	0	474	1
Wing 1	0	0	11	3
Wing 2	0	0	0	0
Top Ring	0	0	180	2
Other	0	0	4	1
Total	0	0	1577	8

Table 3-11 Porosity volume for Version One. The housing with the feeder shows massive improvement.

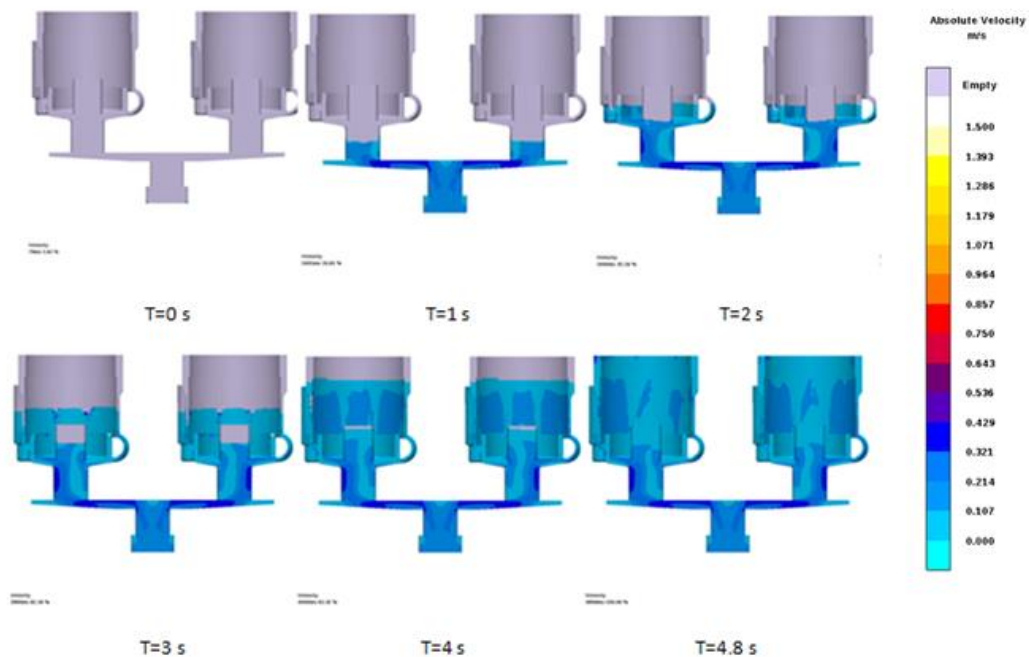


Figure 3-23 Schematics of the smooth and uniform filling process for Version One

By using the new configuration and parameters, the simulation takes about three hours to run. [Figure 3-23](#) shows the filling results for Version One. It is clear to see that the filling is very smooth throughout the entire process. The velocity has been kept under $0.5 \text{ m}\cdot\text{s}^{-1}$ for the entire filling process. Secondly, the melt rises almost uniformly until the casting cavity is filled. This filling pattern ensures a uniform temperature distribution inside the casting cavity. Therefore, the solidification rate can be consistent during the solidification stage. [Table 3-11](#) shows the comparison of porosity between the feeder and non-feeder filter housing; it indicates how important the feeders are. According to the results of velocity and porosity, this runner bar and the feeders are working very well in this design. The casting yield for this running system is about 51%.

3.2.5 Version Two

However, AEROMET did not approve of this design because of the location of the feeder. In their opinion, the feeders inside the filter housing are impossible to cut off in the fettling process. Furthermore, they highlight that they produce three filter housings per running system. Thus, the new running system should have the same or higher production rate compared with the existing one.

AEROMET also offered two suggestions based on their experience: try to reduce the cost and reinforce the wax pattern. Unlike other casting processes, investment casting needs to make the negative shape die to produce the wax pattern. Generally, the die can be made in any shape by machining. However, because of the costs of machining, it should be as simple as possible. After the wax injection, the wax pattern may deform in some way. If that happens, the final casting will be affected by the wax deformation. Therefore, it is important to prevent such deformation during the wax solidification and this requires that the entire structure of the casting running system be reinforced.

Thus, the design has to be changed to fit the fettling process. To overcome this problem, the author decided to change the casting orientation, such that the filter housing is cast upside down. In this new design, all of the feeders are located outside of the housing. This not only provides easy fettling in the post-machining process but it also permits more effective feeding (blank feeders are removed). The author also increased the production rate by incorporating a new configuration of the casting running system. Two crossed runner bars have been

introduced to the running system to produce four filter housings at a time, which means that the production rate can be increased by 25%.

After several design updates (full version of running system design can be seen under Appendix section), the final running system was approved by AEROMET, as shown in [Figure 3-24](#). The blue parts are the reinforced elements attached to the running system and the red parts are the feeders. The ingate is attached directly to the runner bar. This design ensures that the runner bar pattern can be produced directly without further assembly. The runner bar also works with the top blue rhombus frame, which fastens the running system in the correct location. Again, there are no filling and solidification defects from the simulation results. Because additional elements have been added to the running system, the casting yield of such design decreased to 42%.

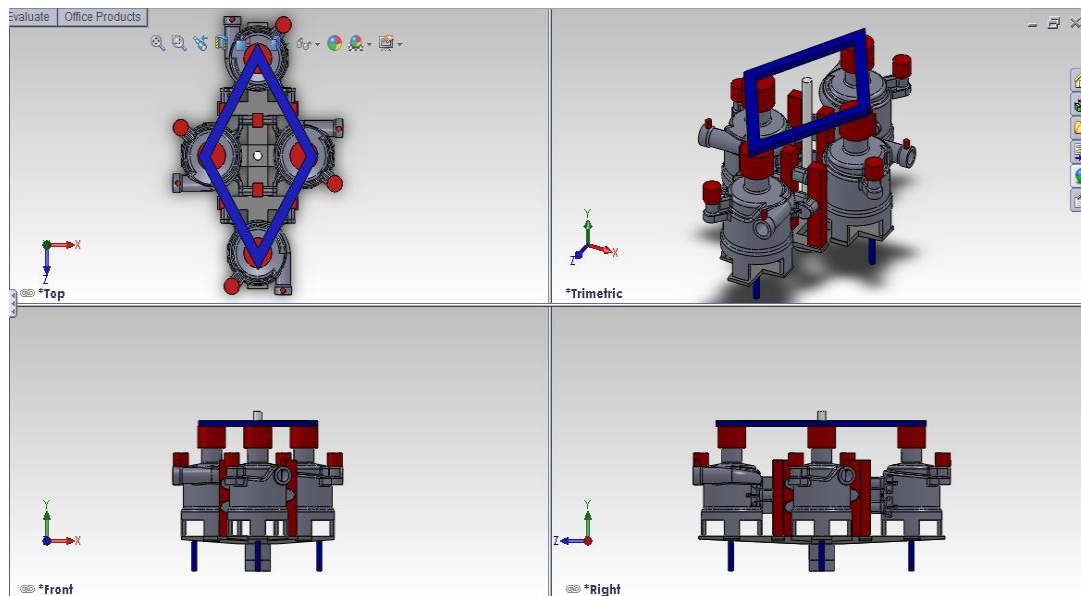


Figure 3-24 Configuration of Version Two. All of the feeders are located out of the filter housing

3.3 Development of the CRIMSON running system design spreadsheet

The CRIMSON running system is relatively easy to design. The designer only needs to focus on the volume conservation theory to control the filling velocity. However, as a new casting technology, no one has been working on the standardization of its running system design. Therefore, the author developed a CRIMSON running system designing spreadsheet to help future researchers or foundry engineers to design the CRIMSON running system.

The concept of the CRIMSON running system had been already introduced in section 2.3.

The sequence of the CRIMSON running system design shows in the [figure 3-25](#). From the flow chat, the logic of the CRIMSON designing sheet is clear. The major task of the user is to

identify the thinnest cross section of the casting and possible size of the casting feeder (can be done by simulation method). According to the target velocity input in the spreadsheet, the maximum flow rate pass through the thinnest section¹² can be calculated. The whole running system geometry is then decided by this flow rate to ensure the fill velocity of the liquid metal.

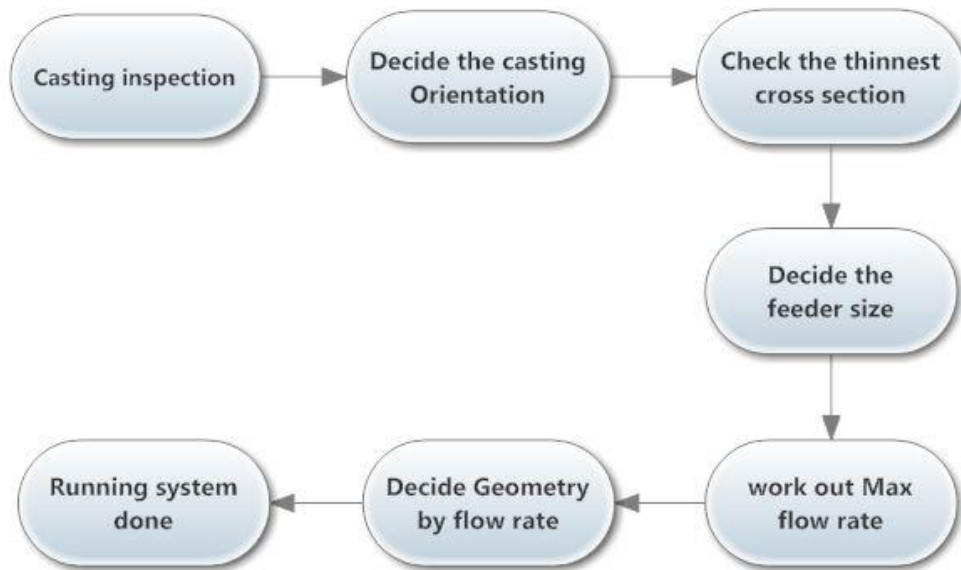
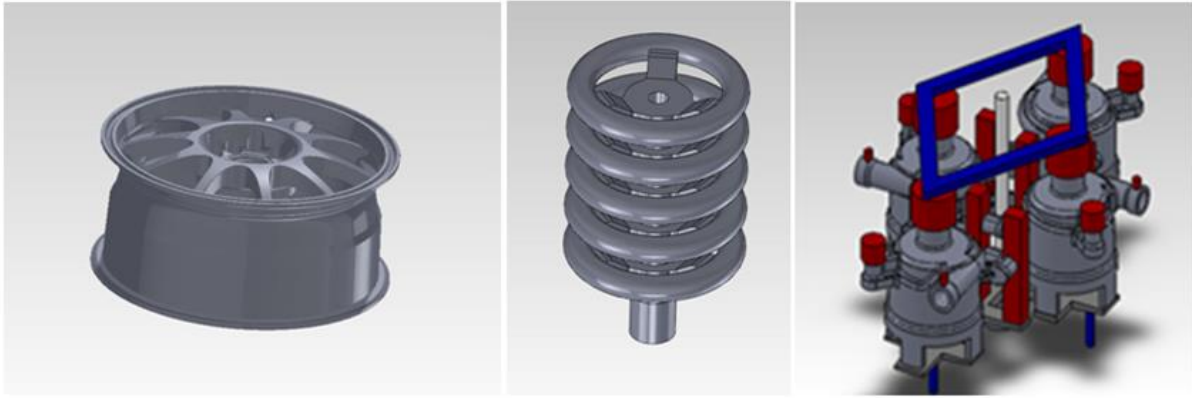


Figure 3- 25 schematics the system approach to design the CRIMSON running system

Decide geometry by flow rate shows in the figure 3-25 is the actual designing step of the running system. The author considered two kinds of situation at this stage. First scenario is for a big casting¹² which can only produced once a time. The second scenario is for multiple castings produced in one running system. Example shows in figure 3-26A can be used to demonstrate the situation one. Figure 3-26A shows a racing car wheel which has diameter around 400 mm. Due to the space limitation of the CRIMSON workstation, only one wheel can be cast at a time. Due to the advantages of the CRIMSON process, the wheel casting doesn't require traditional gating system such as inlet, runner bar. Instead of using ingate, runner bar to deliver metal into the wheel, it can be directly attached with the sleeve to receive metal.

¹² The dimension of the casting approach the upper limit of the CRIMSON up-casting workstation



A

B

C

Figure 3- 26 shows three different situations for the CRIMSON casting production

For scenario two, it can be divided into two sub-situations: produce all castings in line (along the filling direction) and produce all castings normally. Figure 3-26B can be used to represent sub-situation one. In this case, the valve wheel is cast by using the CRIMSON process. Similar to scenario one, no running systems are required by its configuration. The filter housing running system demonstrated before belongs to sub-situation two, which is the classical case of the CRIMSON process.

Decide geometry by flow rate show in the figure 3-25 refers to this kind of situation. The running system components such as in-gate, inlet, and runner have to satisfy the maximum flow rate.

Above all, a guideline was created in the spreadsheet to help user to design correct running system. In the spreadsheet, the user needs to answer following questions:

1. Does the running system produce more than one casting?
2. Does all castings filled in line (vertical orientation)?

By answering the questions, the spreadsheet gives proper advice to help user make the most efficient running system. Later, the validation of the spreadsheet will be take place at chapter 8. Please refer to the Appendix section for the full version of the spreadsheet. The appendix number is 11 (pp194).

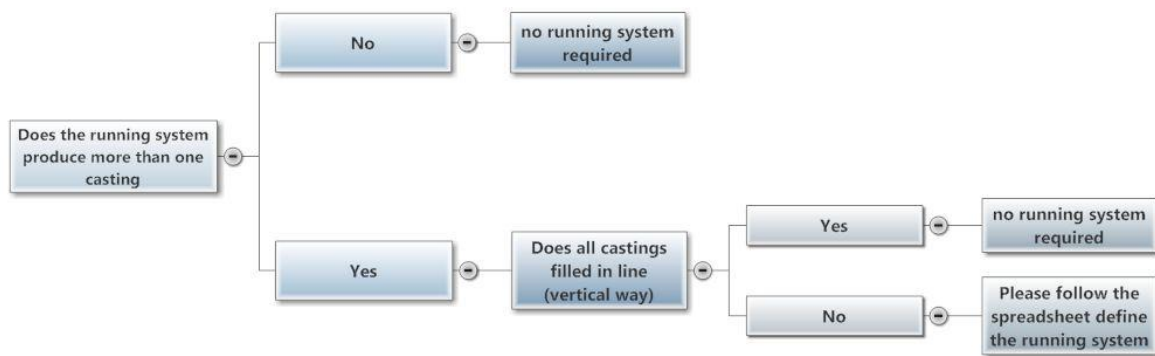


Figure 3- 27 shows the guide provided by the spreadsheet.

3.4 Summary of chapter

Compared with the conventional gravity filling method, the CRIMSON process adopts the up-casting method to fill mould. Because of the smooth and uniform behaviour of the filling, bubbles and DOF defects are hardly form in the CRIMSON running system. Furthermore, the up-casting method removes the pouring basin and the down-sprue from the running system. This not only eliminates the source of bubbles and DOF generation but also increases the casting yield.

The implementation of the CRIMSON process into investment casting production was investigated as well. Several CRIMSON running systems were developed for a filter housing. The approved version by AEROMET can increase casting yield from 10% to 42%. As part of the true yield, increasing the casting yield plays a vital role in energy saving. This means AEROMET can reduce their energy usage through metal reduction from 8 kg to 1.9 kg if they adopt the CRIMSON method.

Knowledge and experience of the CRIMSON running system design had also been developed through the filter housing running system design. A guideline and running system design spreadsheet was developed for future use.

Chapter 4 Validation of the CRIMSON process through Life Cycle Assessment

4.1 Introduction

As summarised in the summary, this research uses four different approaches to validate the CRIMSON process. In this section, the second approach using Life Cycle Assessment (LCA) is reviewed. According to the ISO 14040 standard, LCA can be defined as a four-phase process: goal definition and scoping, inventory analysis, impact assessment and interpretation. As the primary goal is to compare the CRIMSON process with other casting processes, only the goal definition and scoping, inventory analysis and impact assessment are important. This chapter focuses on the raw material and energy data collection for inventory analysis and the simulation approach for impact assessment.

4.1.1 About Life Cycle Assessment

Unlike some traditional analysis methods that focus on a particular machine or stage of the production/service, the LCA technique deals with the entire life of the product/service. The term ‘cradle to cradle’ refers to the entire life of a product or service from its raw material extraction, through manufacturing, usage, maintenance and final disposal. Therefore, the environmental impact of each stage is investigated. The cumulative effect on the environment of such a product or service can be established. By applying LCA to a product/service, the hidden impacts of material transportation, raw material extraction, etc., can be visualised. According to Curran’s report (2006), applying LCA throughout the life cycle of a product/service can provide a comprehensive view of the environmental aspects and thus, help decision makers select the correct process for the product/service.

4.1.1.1 Goal definition/scoping

Goal definition/scoping are the first steps and vital steps of LCA analysis. These affect directly the LCA depth and accuracy. Goal definition not only indicates the reasons for performing LCA but also identifies what type of results is essential. Scoping, on the other hand, determines the range of the analysis.

In this chapter, the goal of the LCA study is to assess the environmental impact of both the CRIMSON process and the conventional sand casting process. In contributing to this goal, a tensile test bar is used to assess the environmental impact of both casting processes. The life

cycle of the production system of the tensile test bar includes raw material production, manufacturing, production use and recycling. Because the same product is produced by both casting processes, the use phase of the tensile test bar (tensile test) is not included in this LCA.

4.1.1.2 System boundaries

The system boundaries for both casting processes have been defined according to the goal definition and scoping. For these casting processes, the material and energy requirements for each operation were investigated and the total material and energy usage will be determined.

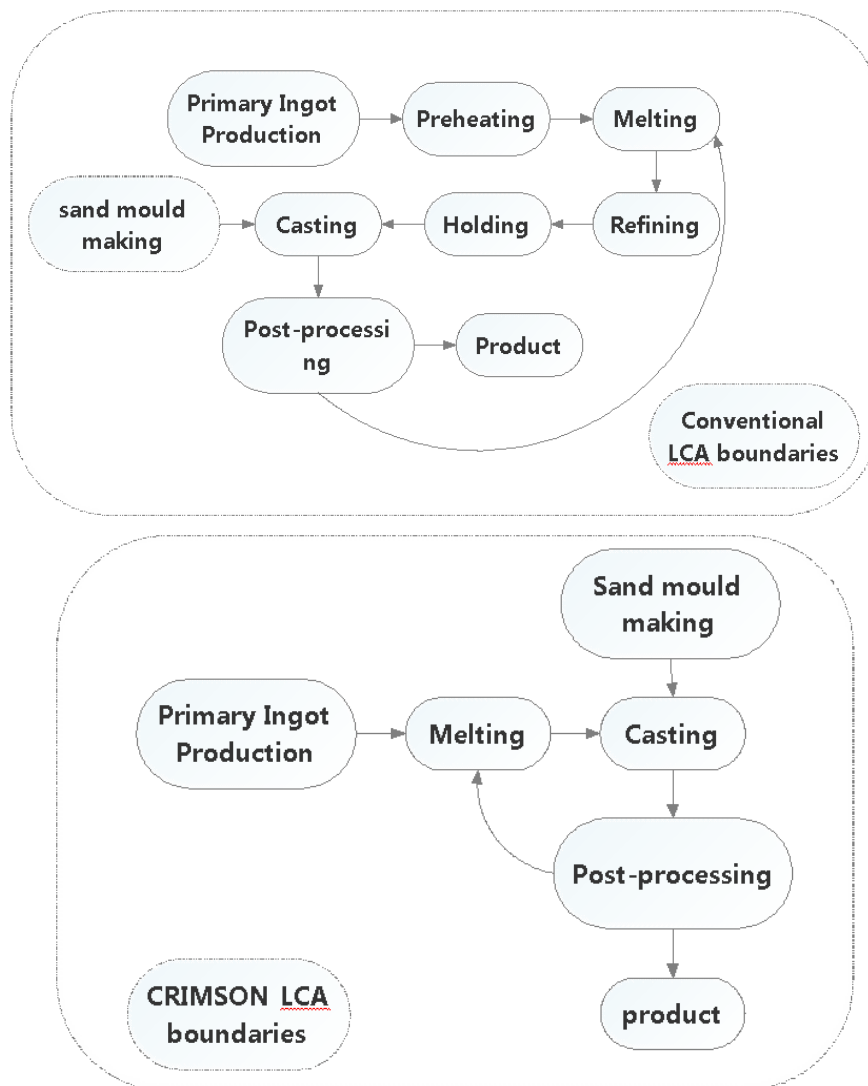


Figure 4-1 System boundaries for both casting process

4.1.1.3 Life cycle inventory data collection

Life cycle inventory (LCI) analysis is a process by which to complete and quantify the input and output of a product, service, or activity. The input refers to the initial design (Rebitzer, G. et al, 2004), energy and raw material. The output refers to atmospheric emissions, waterborne waste, solid waste, co-products and other releases throughout the entire life cycle (Curran, 2006). This means that all the resource inputs and emission outputs involved from raw material extraction to the final disposal of the product need to be understood.

Figure 4-2 demonstrates the entire life cycle of the sand casting product. As the colours indicate, the life cycle of a casting product can be divided into six phases: metal extraction¹³ (yellow), extraction of sand and its additives (green), casting¹⁴(red), mould making (light blue), use (dark blue) and disposal (purple). Meanwhile, the energy and material inputs are shown by black arrows and the emission outputs are shown by red arrows.

Every single step in the life cycle has inputs and outputs. Starting from the metal extraction process, the following factors need to be considered: the energy consumption for bauxite mining, alumina production, electrolysis and ingot casting; the material consumption of caustic soda, limestone, petrol coke, aluminium fluoride and so on. Similarly, each phase in the life cycle needs to go through the same investigation to collect data for the LCA.

By goal definition, the tensile test bars made by the CRIMSON process and by the conventional gravity sand casting process will be investigated by the LCI method. Because these processes produce the same product, the phases of use and disposal of the LCI are the same. Therefore, the LCA method only focuses on the metal extraction, the extraction of sand and its additives, casting and mould making phases of the casting process. The use and disposal phases of the tensile test bar are not included in this research project.

¹³ Also known as primary aluminium production

¹⁴ Casting can be treated as secondary aluminium production

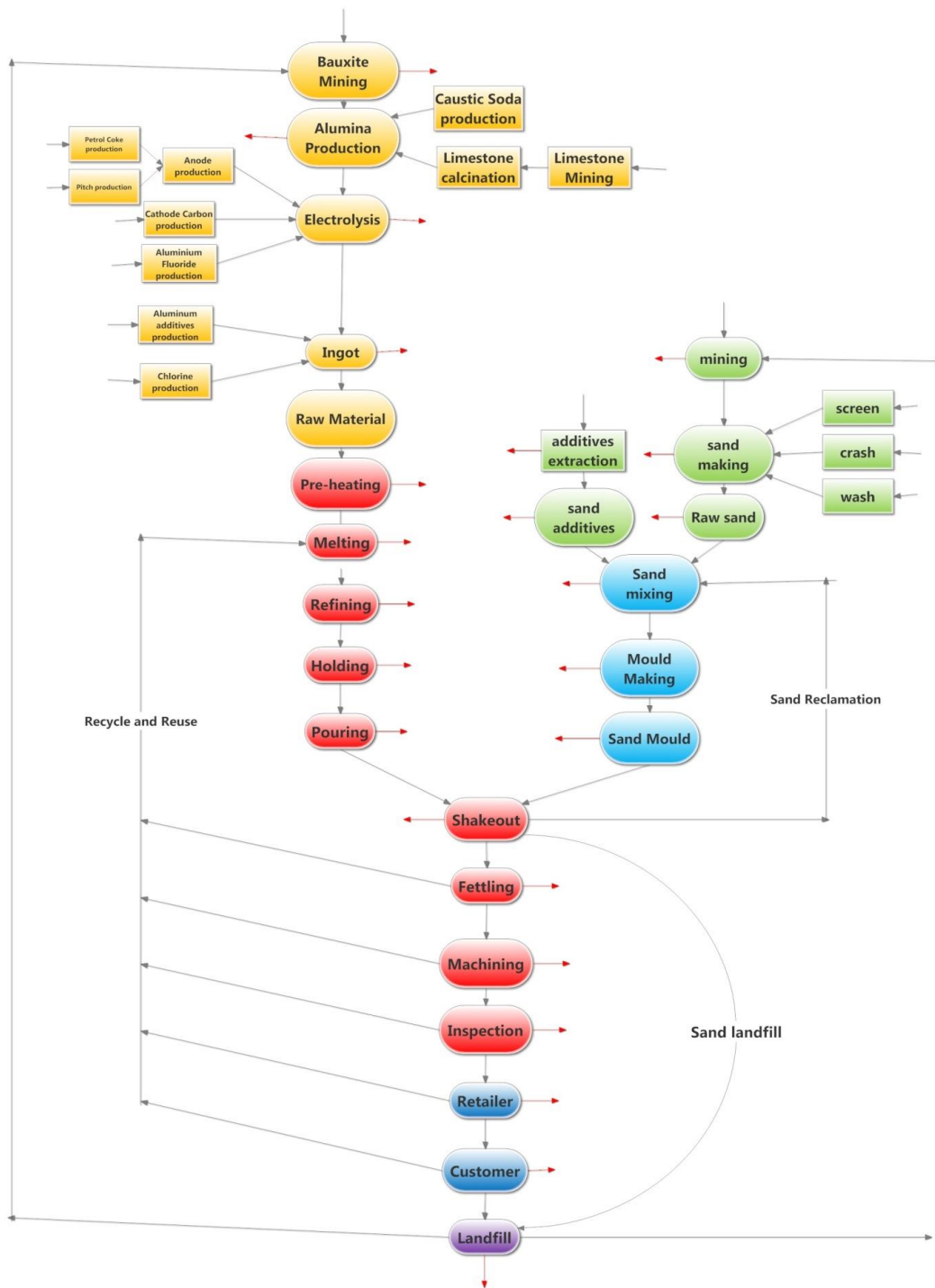


Figure 4-2 Schematic of the entire life cycle of the sand casting product. High resolution version can be found in appendix 12

4.1.1.4 Life cycle impact assessment

This is the third phase of the LCA. It is used to evaluate the potential impacts to human health and the environment by assessing the results of the LCI (Curran, 2006). The SimaPro LCA simulation package was used to assess the life cycle impact assessment.

Following the example of the flow chart shown in [Figure 4-2](#), the entire casting production process was modelled in SimaPro. The collected material and energy data are used with the SimaPro inventory data for a complete LCA model to assess the environmental impact of the casting process. Three impact assessment methods are considered in this study: Gas Protocol, Eco-indicator and Eco-points. All of the impact categories are used to assess the environmental impact throughout the complete life cycle.

4.2 Inventory data collection for casting

4.2.1 Energy input data collection for sand mould making

Following [Figure 4-2](#), the author decided to begin the investigation with the process of the making of the sand mould. In line with process of metal preparation, the making of the sand mould is essential for sand casting. The data collection is easy for the mould making because it only contains mixing and compaction processes. The difficulty in mould making is in the selection of the raw materials and the selection of the reclamation method. Depending on the casting applications, different sands can be used for moulding and different reclamation methods can be used later on. Therefore, this high degree of freedom over material selection makes it difficult to collect the input and output data. According to author's knowledge, not too many works have been carried out in this area.

To obtain the input data for the making of the sand mould, the author investigated every single step of the process, which included the following investigations:

1. The embedded energy of different sandstones.
2. The energy consumption for every single machine involved in sand making.
3. The energy consumption for every single machine involved in mould making.
4. The energy consumption for every single machine involved in sand reclamation.

4.2.1.1 Introduction

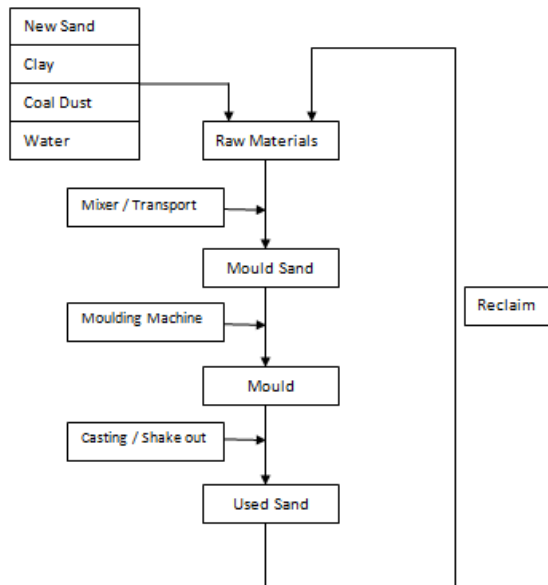


Figure 4-3 Process flow chart of sand mould construction

Generally, the process of making a sand mould can start with the mixing of the raw material. The mixed material is then transferred to the moulding machine. Subsequently, the mould is transferred to the pouring line for casting. Shakeout is the next step when the casting has solidified. At this step, the casting and the sand mould are separated. The casting is then transferred to post-process and the used sand is reclaimed for the next cycle of use. The process flow is shown in Figure 4-3.

According to Figure 4-3, the process starts with the preparation of the raw material. In this step, the preparation of the sand and its additives is required. Clearly, obtaining these raw materials requires energy input. Therefore, investigating the embedded energy of those raw materials is the first task.

However, this is a challenge because of the diverse materials available for sand moulding. Sand used for moulding can be divided into four categories: silica sand, zircon sand, olivine sand and chromite sand (Ramana, 1996). Silica sand is the most common, which can be found throughout the world. It is used for a wide range of applications, such as glass, fillers and casting moulds (SAMSA, 2012). It is a naturally occurring material and is extracted normally by surface quarrying (SAMSA, 2012). However, depending on the requirements of the application, silica sand can also be manufactured from sandstone. The following sections will explain how silica sand is made and how its embedded energy is calculated.

Silica sand is made from quartz stone, which is the most common stone found anywhere. According to CES2011's database¹⁵, the embedded energy of such stone is around $0.4 \text{ MJ}\cdot\text{kg}^{-1}$ to $0.6 \text{ MJ}\cdot\text{kg}^{-1}$ (including mining and transportation). To make silica sand, the quartz stone is delivered evenly by a vibrating feeder to a jaw crusher for primary crushing. The crushed stones are then transferred by a belt to a secondary crusher, such as a cone crusher, for further

¹⁵ CES EduPack is the world-leading teaching resource for materials in engineering, science, processing, and design. It includes General and mechanical engineering, Manufacturing, Materials science and materials engineering, and so on (Network, 2013)

crushing. Following the secondary crushing, the coarse sand is transferred to a vibrating screen for screening. The coarse sand can be screened into two major types of sand; one is transferred to the sand-making machine and the coarser material is sent back for re-crushing. The final step of sand making is sand washing. The cleaned sand is then delivered to the final products pile (Figure 4-4).

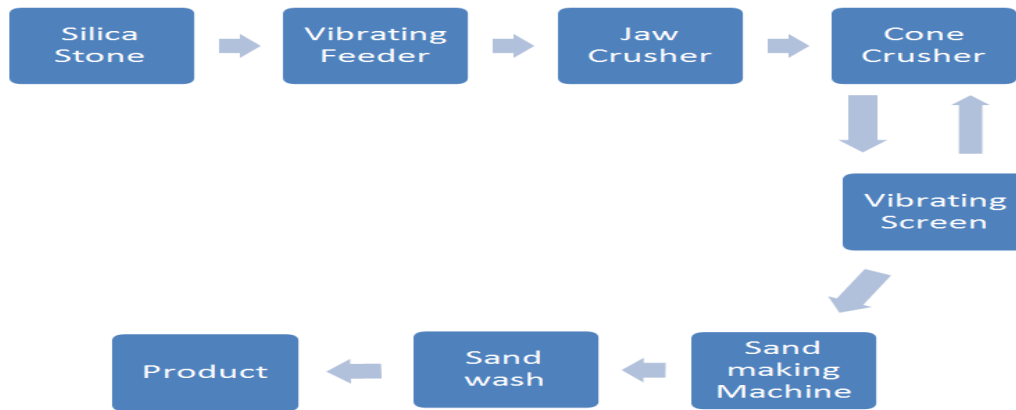


Figure 4-4 Process flow chart of sand making. Please note every arrow in this graph represents transportation by conveyor belt or bucket elevator

From Figure 4-4, the embedded energy of silica sand is calculated from the sum the energy burden of the entire process. The equation used to calculate the energy burden is:

$$\text{energy burden} = \text{Energy consumption} \div \text{processing capacity} \quad \text{Equation 17}$$

Model	Feeding Chute Size (mm)	Max. Feeding Size (mm)	Capacity (t/h)	Motor Power (kw)	Weight (kg)	Overall Dimension (mm)
GZD-750×2500	750×2500	300	50-80	3	1590	2580×1100×1400
GZD-850×3000	850×3000	400	80-120	2X2.2	3895	3110×1800×1600
GZD-960×3800	960×3800	500	120-210	11	3980	3850×1950×1630
GZD-1100×4200	1100×4200	580	200-430	15	4170	4400×2050×1660
GZD-1100×4900	1100×4900	580	280-500	15	4520	5200×2050×1700
GZD-1300×4900	1300×4900	650	450-600	22	5200	5200×2350×1750
GZD-1500×6000	1500×6000	800	500-700	30	8670	6082×2995×2095

Table 4- 1 Example shows various types of vibrating feeders (JOYAL, 2013). Please refer to appendix 37 for specification of each sand making machine.

According to this equation, the energy consumption and the processing capacity of the equipment must be determined. These data are normally displayed in the specifications of the equipment. However, there are various types and brands of equipment such as the vibrating feeder shown above that are available, which have different capacities and power outputs (Table 4-1). However, Eq. 17 indicates that the energy burdens of these feeders are normally of similar magnitude. Therefore, the normal distribution of their energy burden is investigated. In a normal distribution with a mean μ and standard deviation σ , the maximum and minimum energy burdens are adopted within 68% of the observations falling within σ and μ .

Similar to silica sand, zircon sand, olivine sand and chromite sand can also be made from stone. Assuming that similar mining techniques are used, the embedded energy of such stone also lies between 0.4 MJ/kg to 0.6 MJ/kg. Furthermore, by using same process to make the sand, the same embedded energy can be applied to all of these sands. As Table 4-2 shows, the embedded energy of the sand is between 406 kJ/kg and 616 kJ/kg.

	Minimum energy burden (KJ·Kg ⁻¹)	Maximum energy burden (KJ·Kg ⁻¹)	Average (KJ·Kg ⁻¹)
Vibrating feeder	0.13	0.26	0.2
Jaw crusher	1.3	5.5	3.4
Cone crusher	1.82	4.42	3.1
Vibrating screen	0.44	0.83	0.6
Sand making machine	2.47	4.76	3.6
Sand wash	0.23	0.71	0.5
sand	400	600	500
Total	406	616	511

Table 4-2 Embedded energy of sand

4.2.1.2 Sand additives

When classifying the sand mould by binder type, it can be categorised as a green sand mould or a chemical sand mould. The term green sand does not mean that the colour of the sand is green; it means using wet sand and clay to make the mould. Typically, a recipe for a green sand mould comprises 80% to 90% sand (silica, olivine and chromite sand), 5% to 10% clay, 2% to 4% water and 0% to 2% coal dust (Lost&Foundry, 2012). To determine the energy content of green sand requires an estimation of the embedded energy of all materials involved. Therefore, in addition to that of the sand, the embedded energy of the clay and other additives needs to be resolved.

The naturally occurring materials of sodium bentonite and calcium bentonite are normally used as clay in a green sand system. Therefore, these clays have to be mined by a certain method. Assuming that the same method is adopted, then the embedded energy of these natural clay lies between 0.4 MJ·kg⁻¹ and 0.6 MJ·kg⁻¹. Problems arise with the other additives such as coal dust. It is difficult to find useful information regarding how this product is produced. However, owing to its minor content (0% to 2%), it can be ignored in this situation.

For chemical bond sand, this issue becomes even more complicated. Firstly, the chemical bond sand mould can be classified as a self-hardening or a triggered-hardening mould. The chemical binder required for these two kinds of mould are different. A simple example for a self-hardening mould is the furan sand mould. This kind of mould is adopted widely in

ferrous and non-ferrous foundries. As a self-setting mould, furan resin and an acid catalyst are used as a binder system. The resin can be urea-formaldehyde, phenol-formaldehyde, or a combination of the two with additions of furfuryl alcohol (Brown, 1999). The catalyst can be phosphoric acid, sulphonic acids or some other mixed acid (Brown, 1999). Because the chemical reaction is complicated, the energy contents of the resin and the catalyst are hard to establish. In addition to the energy content of the materials, various recipes for the furan binder make the determination of the embedded energy even more un-predicable. Thus, as for the case of the triggered chemical binder, it is impossible to track every single additive.

After investigating different bonding resins, some reasonable assumptions have to be made for the purpose of simplification. Firstly, the average resin additions are 1% to 2.5% by mass. Secondly, by investigating the primary energy of the various resins using CES2011, the energy content of the resin is found to be between 87.63 and 116.28 MJ·kg⁻¹. Finally, the energy content of the catalyst can be ignored because of its negligible content (normally 0.38% by mass (Brown, 1999)).

The energy contents of the sands and their additives are given in [Table 4-3](#).

	Minimum energy burden (kJ·kg ⁻¹)	Maximum energy burden (kJ·kg ⁻¹)	Average (KJ·Kg ⁻¹)
Silica sand	406	616	511
Zircon sand	406	616	511
Chromite sand	406	616	511
Olivine sand	406	616	511
Nature clay	400	600	500
Resin binder	87630	116280	101955
Green sand	405¹⁶	615¹⁷	510
Chemical sand	1279¹⁸	3508¹⁹	2393.5

[Table 4-3](#) Energy contents of the sands, additives and mixed sands

4.2.1.3 Sand mix

The actual start point in making the sand mould is the mixing process. Prepared base sand, reclaimed used sand, clay/chemical binder and other additives are mixed in a mixer. For natural bonded sand (green sand), a muller is used. The main purpose of using a muller is to restore the ‘ready to use’ texture of the moulding sand. Calcium bentonites and sodium

¹⁶ Sand 90% and clay 10%

¹⁷ Sand 95% and clay 5%

¹⁸ Sand 99% and binder 1%

¹⁹ Sand 97.5% and binder 2.5%

bentonites are the most common clays used in the natural binder system (Brown, 1999). They have to work with water to bond the sand together and the only way to bond the clay and water properly is with a muller. Its wheel provides sufficient kneading and compression to the clay, which progressively exposes more clay flakes to the adsorption of water (Group, 2010). The plough blade then stirs the clay evenly around the sand grains (Brown, 1999).

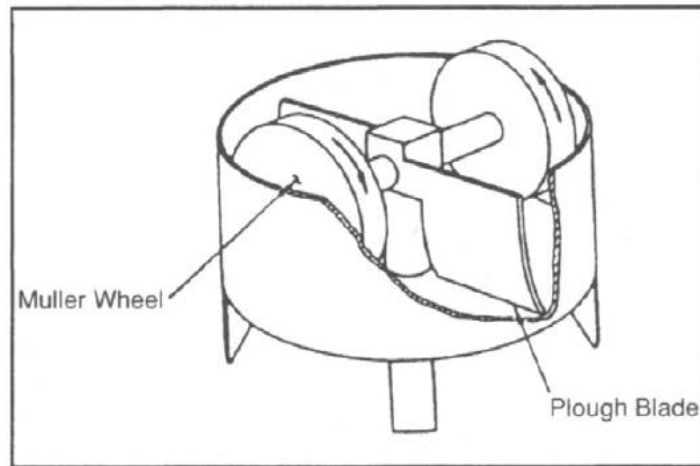


Figure 4-5 Schematic of a continuous mixer (muller) for chemical bonded sand (Brown, 1999)

For a chemical bond binder system, once the sand and binder are mixed, it begins to harden even inside the mixer. As a result, the mixer used for chemical bonded sand is a continuous sand mixer, as shown in Figure 4-6. Normally, a continuous sand mixer comprises two arms, a resin bucket, a catalyst bucket and a dust catcher. Firstly, the base sand from the sand bin is released to the conveying arm. The sand is then transferred to the mixing arm where the resin and catalyst from the other buckets are mixed together. Finally, the mixed sand is discharged for mould making.



Figure 4-6 Typical structure of a continuous mixer , containing a muller wheel and plough blade (A-Yite-group-Limited, 2012)

4.2.1.4 Mould making (compaction)

After the sand is fully mixed, it is ready for the mould making. Depending on the throughput, this can be either a manual operation for a minimal use or a highly mechanised operation for mass production (Brown, 1999). To investigate the energy content of the mould making process, it is better to focus on the mould for mass production. Therefore, this project considers only the mechanised operation of mould making. The principle of machine moulding is to use mechanical power to compact the mould. The compaction power can be categorised as squeeze power, impact power, vacuum power or vibration power (Brown, 1999). Depending on the application of the mould (size of the mould, hardness requirement, binder system of the mould), various types of moulding machines are available.

4.2.1.4.1 Green sand

A green sand mould uses natural clay to bond the sand mould. It requires large amounts of energy to compact the green sand evenly around the pattern. Only by such methods, can the green sand mould resist the friction of the molten metal and provide an inclusion-free casting (Brown, 1999). Jolting and squeezing are the most common compaction methods used. During jolting, the flask containing the loose sand is placed on a jolt table. The table then repeatedly jolts against a stopper to generate shocks that are largely absorbed by the sand (Brown, 1999). By using this method, the sand can be compact to some extent; the densest sand is always near the pattern plate (Brown, 1999). Consequently, the dimensions of the casting can be more accurate by using the jolting method. By contrast, squeezing employs a squeeze head to apply pressure to the surface of the mould. In this case, the density distribution of the sand is reversed; the densest sand is nearest the surface of the mould. According to the advantages of both compaction methods, most foundries combine the methods of jolt and squeezing compaction to produce a mould that is more uniform.

Similar to jolt and squeeze compaction, shoot squeeze compaction, impulse compaction and vacuum squeeze compaction can be used for green sand moulding (Brown, 1999). All of these methods require compressed air or vacuum to pre-compact the sand, and the squeeze head used for final compaction.

4.2.1.4.2 Chemical sand

Unlike green sand moulding, chemical sand requires less energy to compact the mould. Therefore, a slightly gentler force is used for chemical sand compaction. Instead of the jolt, a

vibration mould machine vibrates the flask while the chemical sand is charging. To intensify the compaction effect, squeezing is also used for final compaction.

4.2.1.4.3 Energy burden of mixing and compaction

DISA moulding machines are the most common moulding equipment used in foundries. The energy consumption of the mould making is based on DISA's machines.

	Minimum energy consumption (kJ·kg ⁻¹)	Maximum energy consumption (kJ·kg ⁻¹)	Average (kJ·kg ⁻¹)
Green sand mixer (muller)	4	9	6.5
Chemical sand mixer	3	7	5
DISA vertical	2	4	3
DISA flask	15	57	36
DISA match plate	2	5	3.5

Table 4-4 Energy burden of the mixer and moulding machines

4.2.1.5 Sand reclamation

The high cost of new sand and the growing cost of disposing of used sand, makes the reclamation and reuse of old sand increasingly important for the foundry sector. Reclamation is a process that returns the lumps of used sand back to sand grains in order to restore its working ability. During this process, it is important to reduce the contents of spilt metal, nails and spent binder inside the sand (Brown, 1999). There are three types of reclamation methods: mechanical (attrition), thermal and wet reclamation. Because the wet reclamation method requires expensive water treatment to permit safe disposal (Brown, 1999), it is not a technique commonly used for reclamation. Thus, this section focuses only on the mechanical and thermal methods.

4.2.1.5.1 Mechanical reclamation

Clay can absorb water continuously up to temperatures within the range 400–700 °C. The only permanent damage to the clay occurs at the interface immediately in contact with the pouring metal (Brown, 1999). This means that most of the original binder remains unchanged after the casting process. Owing to this feature, most of the green sand can be retrieved by mechanical reclamation.

The mechanical reclamation (also named primary reclamation) method is the technique most commonly adopted by foundries. It can work with a wide range of binder systems (green binder or chemical binder). This method also has the advantages of low capital cost and low operational cost. The reclamation begins with the shakeout. Sand moulds are placed in a

rotating drum or on a vibrating screen to separate the casting and the sand lumps. By further passage of the sand lumps through the drum or the screen, the sand lumps can be broken down into smaller pieces. For ferrous casting, such as cast iron, some metal spillages remain mixed with the sand (Hughes, nd). This metal can reduce the permeability and refractory resistance of the sand (Brown, 1999). Thus, magnetic separation needs to be employed following the initial sand and casting separation. After this classifying, the sands are transferred to a crusher to restore the sand to granular size. Depending on the equipment, the sand will go through a cooling and classifying process to cool the sand to ambient temperature and remove fine dust. Finally, the reclaimed sand will be transferred to a storage hopper for a new cycle.

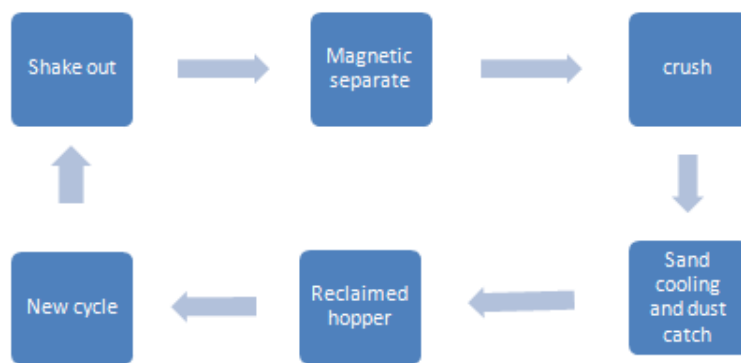


Figure 4-7 Process flow chart of primary mechanical reclamation. Every arrow in this graph represents a conveyor or bucket elevator, which means energy is consumed in the transportation

4.2.1.5.2 Secondary mechanical reclamation

However, primary reclamation is not efficient for chemical bonded sand. Dead binder on the sand grain acts as a coating that is hard to remove. If the residual coating builds up on the grains, it will reduce the bonding ability of the sand. Therefore, a secondary reclamation (more radical reclamation) to remove the coating of the spent binder is introduced.

Secondary reclamation requires mechanical systems that are more intensive. There are two kinds of secondary system: pneumatic scrubbing and a hammer mill (Brown, 1999) (Hughes, nd). The pneumatic device speeds up the sand streams and forces them against a target surface and each other. The impaction and the abrading of the sand grains remove the residual coating and fine dusts in the process (Hughes, nd). Similarly, the hammer mill forces the sand grains to spin, which causes them to impact with each other and thus, removes the binder coatings. Chemical sand systems are normally reclaimed by this method.

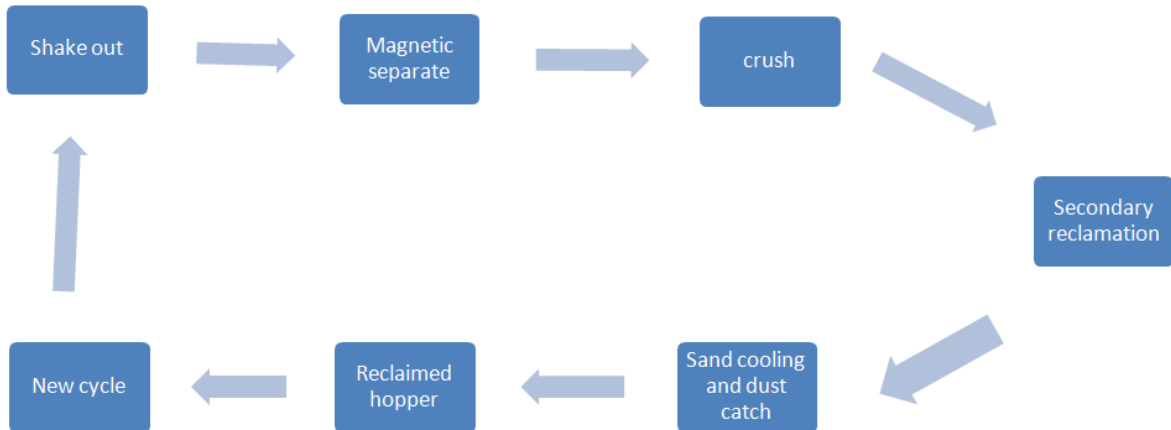


Figure 4-8 Process flow chart of full mechanical reclamation typical for resin bonded sand. Every arrow in the graph represents a conveyor or bucket elevator, which means energy is consumed by transportation

4.2.1.5.3 Thermal reclamation

The thermal reclamation method uses a gas furnace to heat the sand in an oxidising atmosphere to burn off the binder residuals (Brown, 1999). This is the most radical reclamation method for all types of the sand (except silicate bonded sands; the binder cannot tolerate high temperatures (Brown, 1999)), especially for organically bonded sand and the reclamation can reach 100%. Similar to mechanical reclamation, the starting point for the thermal method is shakeout and metal removal. Subsequently, the sand is transferred to a fluidised bed furnace, which is heated up to 800 °C for residual binder removal. Emissions carrying dusts are captured by a bag filter and the cleaned sand proceeds to a cooling stage. Finally, the reclaimed sand will be transferred to a storage hopper for a new cycle.

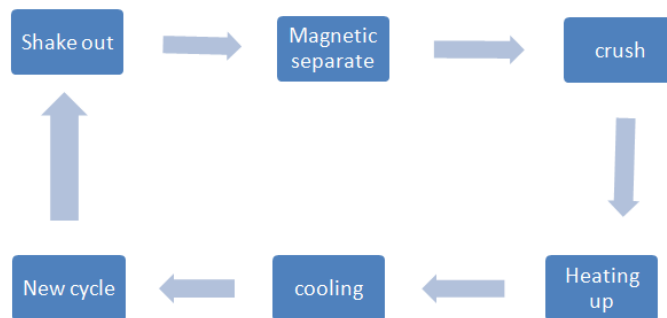


Figure 4-9 Process flow chart of full thermal reclamation. Every arrow in the graph represents a conveyor or bucket elevator, which means energy is consumed by transportation

A combustion furnace uses natural gas or LPG for thermal treatment. Using LPG as an example, to reclaim one tonne of used sand can consume 7 to 9 kg of fuel (WESMAN, nd).

The calorific value of LPG is between 46.6 and 50.1 MJ·kg⁻¹. Therefore, the heat required for thermal reclamation is between 326 and 451 MJ.

The energy burden of each reclamation method is presented in [Tables 4-5, 4-6 and 4-7](#).

		Minimum energy burden (kJ·kg ⁻¹)	Maximum energy burden (kJ·kg ⁻¹)	Average (kJ·kg ⁻¹)
magnetic separate		0.2	0.4	0.3
shake out	vibrating	3.3	13	8.2
	rotating	6.2	10.5	8.4
crusher	green sand	4.5	9.4	7
	chemical sand	2	4.2	3.1
sand cooling	fluid bed	5.1	13.5	9.3
	rotary kiln	7.9	11.9	9.9

Table 4-5 Energy burden of primary reclamation

		Minimum energy burden (kJ·kg ⁻¹)	Maximum energy burden (kJ·kg ⁻¹)	Average (kJ·kg ⁻¹)
magnetic separate		0.2	0.4	0.3
shake out	vibrating	3.3	13	8.2
	rotating	6.2	10.5	8.4
crusher	green sand	4.5	9.4	7
	chemical sand	2	4.2	3.1
secondary attrition	pneumatic	3.9	4.6	4.3
	hammer mill	7.2	18	12.6
sand cooling	fluid bed	5.1	13.5	9.3
	rotary kiln	7.9	11.9	9.9

Table 4-6 Energy burden of secondary reclamation

		Minimum energy burden (kJ·kg ⁻¹)	Maximum energy burden (kJ·kg ⁻¹)	Average (kJ·kg ⁻¹)
magnetic separate		0.2	0.4	0.3
shake out	vibrating	3.3	13	8.2
	rotating	6.2	10.5	8.4
crusher	green sand	4.5	9.4	7
	chemical sand	2	4.2	3.1
heat treatment	burning	326.3	455.5	391
sand cooling	fluid bed	5.1	13.5	9.3
	rotary kiln	7.9	11.9	9.9

Table 4-7 Energy burden of thermal reclamation

4.2.1.6 Transportation

Up to this point, the energy of transportation has not been discussed. In this project, transportation refers only to the sand transferred between each operation and does not include the transportation from its original source to the foundry (this is already included in the embedded energy of raw material). For example, the arrows appearing in Figures 4-4, 4-7, 4-8 and 4-9 represent the transportation involved within the process. In those cases, the equipment involved includes conveyor belts or bucket elevators. Unlike other the equipment used in the sand making process, the energy burden of the conveyor or elevator is influenced by multiple factors, such as the transfer velocity, distance and load capacity. Generally, the energy burden increases as the distance increases and decreases as the capacity increases. In order to investigate the energy burden, some other equations are introduced.

For a conveyor belt (DUNLOP, 2009):

$$\text{energy burden} = \left(\frac{F_c(L+t_f)(C+3.6Q \times S)}{367} \pm \frac{C \times h}{367} \right) \times t \div C \quad \text{Equation 18}$$

For a bucket elevator (CarlosIII_University, nd)

$$F = \frac{C}{3.6 \times S} (H + H_0) \quad \text{Equation 19}$$

$$\text{energy burden} = \left(\frac{F \times S}{75 \times n} \right) \times t \div C \quad \text{Equation 20}$$

where:

F_c is the equipment friction factor; its value is about 0.03, L is the horizontal centre-to-centre distance (m), t_f is the terminal friction constant (m), the value of which:

Up to 300 m = 60 m

From 300 m to 1200 m = 45 m

From 1200 m to 1800 m = 30 m

Above 1800 m, this influence is disregarded

C is the capacity ($t \cdot h^{-1}$); Q is the mass of moving parts expressed in kilograms per metre of the centre-to-centre distance (Appendix 13); S is the belt speed ($m \cdot s^{-1}$); h is the net height change during lift (for inclined conveyor belt); F is the force the driver pulley needs to move the belt; H is the lift height, H_0 is the friction height in metres; its value can be selected from 3.8, 7.6, 11.4 and 15.3; n is the efficiency of the motor; t is the time in this case it is 3600 seconds

Clearly, the energy burden of transportation is complex and various factors need to be considered. In fact, depending on the processing capacity and layout of the foundry, the transporting status between different processes is not same; it could be a conveyor belt or a bucket elevator with different delivery length/capacity/speed. This is why the arrows in Figure 4-4, 4-7, 4-8 and 4-9 are never the same.

Integrating all the information together, the average energy burden of the making of the sand mould is summarised in Table 4-8.

Sand mould type	Sand used	Energy burden (KJ·kg ⁻¹)
Green sand mould	Green sand	511
Chemical sand mould	Chemical sand	2393
Mould made by primary method	Green sand	565
Mould made by second method	Chemical sand	2448
Mould made by thermal method	Chemical sand	2448

Table 4-8 Summary of the energy burden of making sand moulds using different materials and processes

4.2.2 Energy input data collection for metal preparation

In this section, the inventory data collection for metal preparation is introduced. Following the flow chart shown in Figure 4-2, the metal extraction and casting phases are investigated in this section. However, how best to collect these data is a significant problem for this type of research project. Owing to reasons of confidentiality, data on energy, material and emissions are not available publicly. Unfortunately, this is true for the casting foundry sector and there are no specific statistical data regarding energy consumption or annual production available for the non-ferrous foundry sector since 1996 (DETR, 1997).

In addition to the difficulty of data collection from different industrial sectors, collecting data from within the casting foundry sector faces other troubles. Different foundries have different approaches to casting aluminium products. Thus, it is feasible that the energy consumption between foundries is different, even when producing similar products. Dalquist (2004a; 2004b) performed an LCI analysis for sand casting and die casting in 2004. Using mould making as an example, the results indicated that energy consumption can vary from 6% to 20% of the total energy. The Department of the Environment, Transport and the Regions published a report in 1997 (DETR, 1997), which suggest that the average energy burden of the casting process is about 40 GJ·tonne⁻¹. However, it also indicated that there was a significant difference between different casting sectors. For example, the energy burden of die casting foundries was in the range of 26 to 52 GJ·tonne⁻¹ (DETR, 1997). By contrast, the energy

burden of sand casting foundries was in the range of 30 to 130 GJ/tonne (DETR, 1997). Such widely scattered data is not helpful in this research.

However, it is impossible to use a detailed analysis method to investigate the energy burden of metal preparation. As mentioned previously, different foundries have different approaches to making sand casting products. Unlike the process of making the sand mould, the process of metal preparation is not as standardised. To avoid difficulties in the collection of energy data, a concept called embedded energy will be adopted to collect energy input data. Embedded energy is defined as the sum of the all the energy required to produce products or services (Jolly, 2010). In this case, the embedded energy of casting refers to the energy used to produce the casting, which includes the energy input of making the sand mould and preparing the metal (melting, holding, ventilation, fettling, etc.).

4.2.2.1 Aluminium foundry energy consumption investigation

First, the overall situation of production, energy consumption and energy price for aluminium foundries needs to be understood. The only data available for aluminium foundries was published in 1996 (DETR, 1997). At that time, 55 GJ of energy was required to produce one tonne of aluminium casting (Jolly, 2010). However, the aluminium foundry sector has not reported any useful data since then; thus. these data may outdated and unrepresentative of the current situation. For this reason, the energy burden of aluminium casting needs to be reinvestigated. Theoretically speaking, the concept of collecting the data is simple; find the annual energy consumption for the aluminium foundry sector and the annual production by weight. The energy burden can then be determined by dividing the energy consumption by the weight. In order to solve this issue, several different statistic datasets were compared and combined.

Data category	Time Range	Investigated sector
UK Industry Energy Consumption (2012)	1990--2010	Aluminium Production Energy Consumption
UK Monthly Digest of Statistics (2000) (2002) (2007)	1995--2007	Aluminium Casting percentage by weight
Census of World Casting Production	1996, 1999	UK Aluminium casting by weight

Table 4-9 Database used to collect data

From the UK Industry Energy Consumption data catalogue, the energy consumption for entire aluminium industry can be found. The data coverage is from 1990 to 2010. However, this data includes energy consumption for all aluminium production, which includes cast,

wrought and machined products, etc. Therefore, the UK Monthly Digest of Statistics was used to investigate the contribution of the casting products. The coverage of the data is from 1995 to 2007. For the annual production of aluminium castings, either the Monthly Digest or the Census of World Casting Production is used, from which the weight of production can be estimated.

year	1,993	1,994	1,995	1,996	1,997	1,998	1,999	2,000	2,001
Aluminium consumption (TJ)	61,838.43	62,805.46	61,959.95	63,089.14	60,695.08	70,439.07	66,480.71	70,061.32	73,517.54
Casting Contribution (%)	8.40	13.23	13.28	14.32	13.16	12.39	11.14	10.53	10.22
Casting energy consumption (TJ)	5,196.11	8,309.43	8,230.10	9,032.59	7,987.85	8,725.08	7,408.41	7,374.88	7,511.73
casting weight (thound tonne)	133.20	144.00	147.60	156.00	152.40	147.60	136.80	134.40	129.60
energy burden (MJ/kg)	39.01	57.70	55.76	57.90	52.41	59.11	54.16	54.87	57.96
year	2,002	2,003	2,004	2,005	2,006	2,007	2,008	2,009	2,010
Aluminium consumption (TJ)	70,866.44	76,885.74	70,852.50	76,335.15	76,912.60	72,898.00	72,898.31	60,894.18	59,940.68
Casting Contribution (%)	11.03	11.60	10.24	10.24	13.41	12.73	12.70	12.70	12.70
Casting energy consumption (TJ)	7,816.69	8,916.73	7,258.83	7,815.26	10,317.54	9,283.65	9,258.09	7,733.56	7,612.47
casting weight (thound tonne)	127.20	127.20	110.40	204.00	185.00	139.20	186.64	151.31	164.68
energy burden (MJ/kg)	61.45	66.00	65.75	38.00	65.14	66.69	49.60	51.11	46.23

Table 4-10 Energy burden result from 1993 to 2010. High resolution table can be seen in Appendix 14 (pp197)

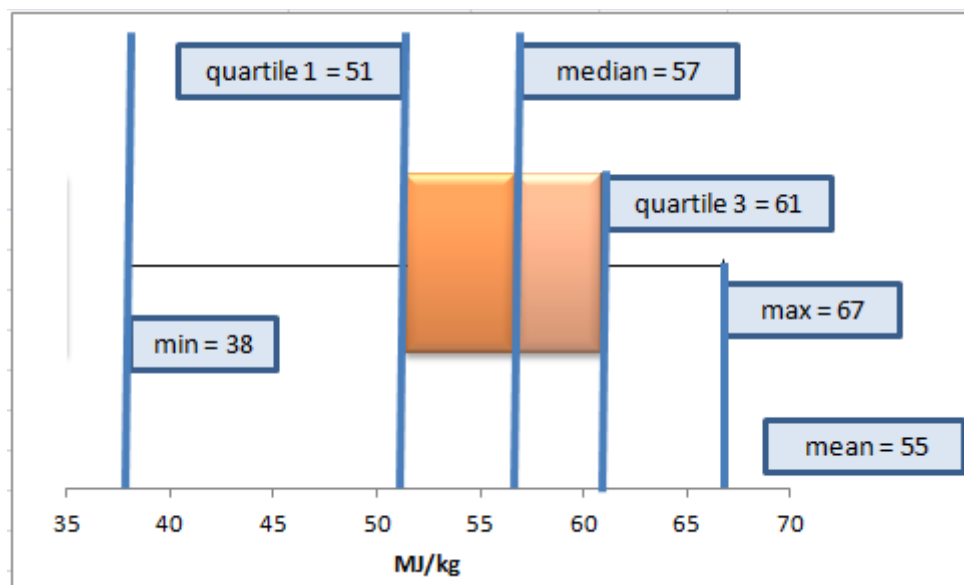


Figure 4-10 Box plot showing the distribution of energy burden from 1993 to 2010

Table 4-10 and Figure 4-10 present the results of the investigation of the energy burden of the aluminium casting foundry sector. The variation of the energy burden is between 38 and 67 MJ/kg. In fact, the average energy burden, determined from the table above, is 55 MJ·kg⁻¹. Therefore, the embedded energy used to produce an aluminium casting is 55 MJ·kg⁻¹.

Therefore, according to the energy burden of the sand mould making process, the energy burden of the casting process varies from 52 to 54 MJ·kg⁻¹.

4.2.3 Multiple recycling inventory data collection

The embedded energy investigated here only looks at a once-through product system. It does not consider the influence of recycling and reusing material in the casting process. A more relevant LCI analysis is required to take recycling into consideration. As a result, the multiple life cycle method is adopted for the LCI data collection. This method is used to calculate the environmental cost of a material that undergoes recycling and reuse (Brimacombe, et al., 2005). It focuses on the impact of the product production phase and not on the use of the product. It is a useful tool for investigating the material flow and energy burden over a series of life cycle stages (Brimacombe, et al., 2005).

4.2.3.1 Methodology for multiple life cycle method

In order to collect energy consumption data using the multiple life cycle method, it is important to measure or estimate the following factors:

Process yield (Y): This is used to describe the true mass loss from a unity, normally less than 1 (Jolly, 2010). The true mass loss in an aluminium foundry can be defined as the oxides loss during the melting, holding and degassing. The fettling, machining and scraps cannot be taking into consideration because they can be recycled.

Recovery Ratio (RR): This is the figure that considers the scrap that is recycled from the process as a percentage of the material put in (Jolly, 2010). It includes the fettling loss, the machining loss and the scraps. As research has shown, the worst case RR for a general/automotive foundry can be estimated at 64% (Jolly, 2010). For quality reasons, the RR can be as high as 86% in an aerospace foundry.

Recycling Efficiency (r): This factor represents how efficient the process is over one production cycle. It is the product of the process yield and the recovery ratio (Jolly, 2010).

$$r = Y \times R$$

Equation 21

To calculate the LCI for different foundry sectors by using the multiple life cycle approach, the following equations are required.

The total mass passing through the chosen number of cycles, M (Jolly, 2010)

$$M = 1 + r + r^2 + \dots + r^{n-1} \quad \text{Equation 22}$$

The total energy content for the chosen number of cycles can be calculated as follows (Jolly, 2010):

$$\text{Total Energy Content} = X_{pr} + rX_{re} + r^2X_{re} + \dots + r^{n-1}X_{re} \quad \text{Equation 23}$$

where X_{pr} is the energy from the primary process and X_{re} is the energy for the recycling process. Normally, the primary process energy is $55 \text{ MJ}\cdot\text{Kg}^{-1}$ and the secondary energy is only about 5% that of the primary energy ($2.754 \text{ MJ}\cdot\text{Kg}^{-1}$) (Jolly, 2010).

By dividing the total mass passing through the cycles by the total energy content, the life cycle inventory (X) can be defined as below (Jolly, 2010):

$$\text{LCI for the Whole system } X = \frac{X_{pr} + rX_{re} + r^2X_{re} + \dots + r^{n-1}X_{re}}{1 + r + r^2 + \dots + r^{n-1}} \quad \text{Equation 24}$$

By simplifying Eq. 37 the energy burden can be derived (Jolly, 2010):

$$X = (X_{pr} - X_{re}) \left[\frac{(1-r)}{(1-r^n)} \right] + X_{re} \quad \text{Equation 25}$$

4.2.3.2 Material flow during the casting process

The values of RR and r need to be determined in order to find the Process Yield (Y). Summarizing from section 2.3.3.2, the weight loss for different casting processes and products can be listed as in Table 4-11.

	CRIMSON test bar	Gravity test bar	CRIMSON housing	AEROMET housing
Weight loss during melting (%)	0.5	2	0.5	2
Weight loss during holding (%)	0	2	0	2
Weight loss during degassing (%)	0	5	0	5
Weight loss during fettling (%)	60	77.5	58	90
Weight loss during machining (%)	25	25	25	25
Weight loss by scrap (%)	10	20	10	20

Table 4-11 Summary of weight loss for different casting foundry sectors. Filter housing was introduced to demonstrate the multiple recycling method

Assuming that there is 1 Kg of virgin aluminium prior to melting, after the different stages of metal loss, the weight of the saleable casting, process yield, recovery ratio and recycling efficiency can be calculated.

	CRIMSON Test bar	Gravity test bar	CRIMSON housing	AEROMET housing	AEROMET housing with recycling
Virgin aluminum (kg)	1	1	1	1	1
Melting loss (kg)	0.005	0.02	0.005	0.02	0.02
Holding loss (kg)	0	0.02	0	0.02	0.02
Degassing loss (kg)	0	0.048	0	0.048	0.048
Fettling loss (kg)	0.597	0.707	0.577	0.821	0.821
Machining loss (kg)	0.099	0.051	0.105	0.023	0.023
Scrap loss (kg)	0.06	0.031	0.062	0.013	0.013
Good casting (kg)	0.239	0.123	0.25	0.055	0.055
Process yield (%)	99.50%	91%	99.50%	91%	91%
Recovery Ratio (%)	75.60%	79%	74.40%	0%	89%
Recycling Efficiency (%)	75%	72%	74%	0	81%

Table 4-12 Saleable casting per unit melting of aluminium, process yield, recovery ratio and recycling efficiency for different casting products. High resolution table can be found in appendix 16.

4.2.3.3 Energy burden for casting

Table 4-12 presents the process yield, recovery ratio and recycling efficiency for different foundry sectors. By applying these parameters in Eq. 25, the multiple LCI for different foundry sectors can be derived, as shown in Figure 4-11.

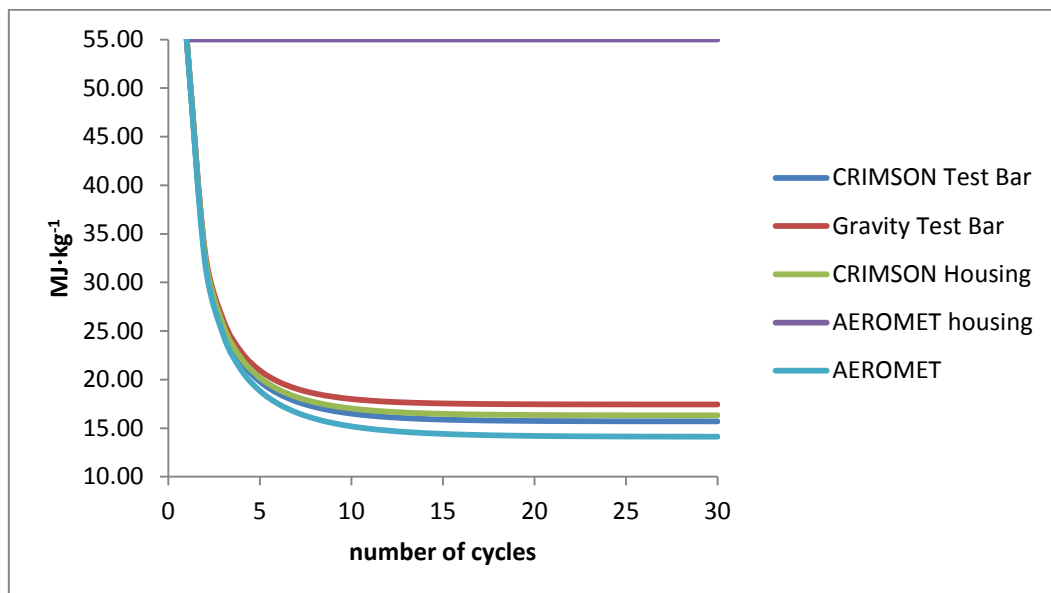


Figure 4-11 Energy burden for different foundry sectors

The figure 4-11 above shows the energy burden after taking the recycling into consideration. By using recycled aluminium from the fettling, machining and scrap, the environmental cost of making a new casting is reduced. From this graph, the average energy burden stabilises at 13.13 MJ/Kg after 10 production cycles for the CRIMSON test bar. Similarly, the gravity test

bar stabilises at $14.58 \text{ MJ}\cdot\text{Kg}^{-1}$, the CRIMSON housing stabilises at $13.65 \text{ MJ}\cdot\text{Kg}^{-1}$ and the AEROMET housing stabilises at $11.81 \text{ MJ}\cdot\text{Kg}^{-1}$. Compared with primary virgin aluminium, recycling uses in excess of 50% less primary energy. Especially for AEROMET with recycling, the energy burden is only 25% of that when using primary material. However, owing to the quality requirements, it is difficult for the AEROMET foundry to undertake any recycling and reusing. This means that they use only virgin alloy to make castings, which is why their energy burden remains at $55 \text{ MJ}\cdot\text{Kg}^{-1}$, as shown in the figure above.

It is also can also be determined that after several cycles of recycling and reuse, the energy burden of the process stabilises. Therefore, Eq. 25 can be simplified further by assuming that the recycling and reuse continues indefinitely: $n \rightarrow \infty$.

$$X = X_{pr} + r(X_{re} - X_{pe}) \quad \text{Equation 26}$$

It becomes obvious that the energy burden is influenced heavily by the recycling efficiency (r). The more material that can be recycled from the process, the lower the energy burden required to melt the metal.

4.2.3.4 Energy burden for saleable casting

The energy burden for multiple recycling methods shows that the aerospace foundries have the lowest energy burden for melting aluminium if they do recycle their internal scrap. However, this result only considers the melting energy for different foundry sectors. The energy burden of the saleable castings (the castings finally shipped to the customer) is not considered. In the following section, the operational material efficiency (OME) is introduced to calculate the energy burden for saleable castings. It represents how many materials have passed through the process and been shipped.

The OME is defined as:

$$OME = \frac{AlMt - AlWs - AlWr}{AlMt} \times 100\% \quad \text{Equation 27}$$

where AlMt stands for aluminium melted, AlWs stands for aluminium waste sold and AlWr stands for aluminium waste recycled in-house (Tharumarajah, 2008).

By using the OME, the efficiency of good casting per unit mass can be calculated. Based on the information provided by Table 4-12, the OME for different foundry sectors is presented in Table 4-13.

	CRIMSON test bar	Gravity test bar	CRIMSON housing	AEROMET housing
Virgin aluminium (Kg)	1	1	1	1
Good casting (Kg)	0.24	0.12	0.25	0.06
OME (%)	24%	12%	25%	6%
Casting weight (kg)	1.56	1.56	3.2	3.2
Melting weight (kg)	6.52	12.68	12.75	58.18

Table 4-13 Operational material efficiency of the different foundry sectors

First, considering the critical situation in which foundries use only virgin aluminium to produce casting products no recycling and reuse are involved in the process. As mentioned before, the energy burden for melting virgin aluminium is approximately $55 \text{ MJ}\cdot\text{Kg}^{-1}$. Thus, the CRIMSON process will use 359 MJ of energy to make the tensile test bars and 701 MJ of energy to make the filter housings. By contrast, the conventional process will use 697 MJ of energy to make the test bars and 3200 MJ of energy to make the filter housings. [Table 4-14](#) displays the energy burden for the saleable castings.

	CRIMSON test bar	Gravity test bar	CRIMSON housing	AEROMET housing
Casting weight (kg)	1.56	1.56	3.2	3.2
OME (%)	24%	12%	25%	5.5%
Energy burden ($\text{MJ}\cdot\text{kg}^{-1}$)	55	55	55	55
Energy consumption (MJ)	359	701	697	3200
Energy burden for saleable casting ($\text{MJ}\cdot\text{kg}^{-1}$)	230	449	208	1000

Table 4-14 Energy burden of saleable castings for different casting processes under critical condition

As calculated before, following recycling and reuse of the internal scrap, the energy burden of melting aluminium is reduced to $13.13 \text{ MJ}\cdot\text{kg}^{-1}$ for the CRIMSON test bar, $14.58 \text{ MJ}\cdot\text{kg}^{-1}$ for the gravity test bar, $13.65 \text{ MJ}\cdot\text{kg}^{-1}$ for the CRIMSON housing and $55 \text{ MJ}\cdot\text{kg}^{-1}$ for the AEROMET housing. The saleable energy burden can be seen from [Table 4-15](#).

	CRIMSON test bar	Gravity test bar	CRIMSON housing	AEROMET housing
Casting weight (kg)	1.56	1.56	3.2	3.2
OME (%)	24%	12%	25%	5.5%
Energy burden (MJ·kg ⁻¹)	13.13	14.58	13.65	55
Energy consumption (MJ)	85	174	185	3200
Energy burden for saleable casting (MJ·kg ⁻¹)	54	112	58	1000

Table 4-15 Energy burden of saleable castings for different casting processes under multiple recycling method

4.2.4 Spreadsheet

The embedded energy of sand and its additives, the energy burden of the mould making machines, the material flow of metal preparation and the embedded energy of the casting process have all been investigated. Therefore, following the objective of the project, it is time to discuss the environmental impact assessment. This can be achieved by simply modelling Figure 4-2 in the SimaPro simulation package using the collected inventory data. However, the variables of sand type, reclamation method and number of operations can influence the embedded energy of the mould making and entire casting process. Therefore, a spreadsheet was developed to estimate the embedded energy of making the sand mould and the energy burden under the multiple recycling method and material usage through the casting operation.

This spreadsheet is divided into three sections: sand mould making, total energy burden and recycling. For the sand mould making, it can be used to calculate the embedded energy of making the mould and the energy consumption of mould making under the multiple recycling method. The embedded energy of the casting process will be applied directly for the total energy burden and the spreadsheet focuses on calculating the energy burden of the multiple recycling method. In order to calculate the embedded energy for sand mould making, the sand mould making section can be divided into four parts: energy consumption of using new sand, primary reclamation, secondary reclamation and thermal reclamation.

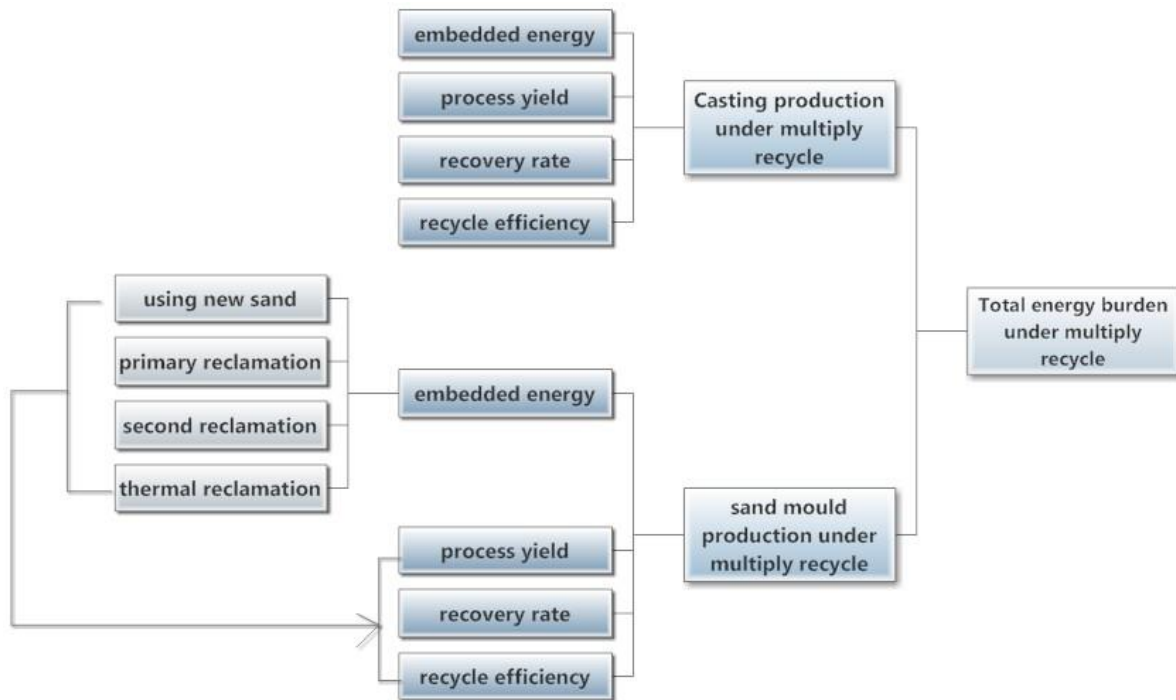


Figure 4-12 Process flow of sand in a foundry

As Figure 4-12 shows, the starting point is using new sand to make the mould. After the first cycle of mould making, pouring, solidification and shakeout, the used sand is transferred to a specified reclamation method. The energy burdens of those operations are calculated and added together to form the embedded energy. The process yield, recovery rate and recycling efficiency are also determined for the purposes of multiple recycling.

4.2.4.1 How the spreadsheet works

4.2.4.1.1 Sand mould making

The spreadsheet starts by using new sand and additives. The first step is to select what type of sand will be used for mould making. As with the assumption made previously, all sands have the same embedded energy; only the binder systems make a difference. Consequently, there are two choices available: green sand and chemical sand. The energy contents can be seen from Table 4-3.

The second step is the selection of the mixer. Depending on the binder system, the mixers that can be chosen are the muller and chemical sand mixers. The energy burden of these mixers can be verified in Table 4-4.

The third step is the transportation between the mixing and the next process. Again, the performance of the transportation depends on the layout and productivity of the foundry.

Therefore, two options are available for transportation. The user can choose either conveyor belt or bucket elevator and even activate both or deactivate both. Furthermore, depending on a specific transportation method, the user can decide upon factors, such as capacity, delivery length, lifting height and motor efficiency according to the real situation.

After the mixing, the sand is sent to the mould-making machine. According to the moulding mechanism, the moulding methods used are DISA vertical, flask and match plate. Their energy burdens are also presented in [Table 4-4](#).

Following the moulding, there is another transfer; the sand mould is transferred to casting, solidification and for shakeout. As with the first transfer, the user can decide on the transportation method and the corresponding parameters.

The sixth step is the shakeout, which depends on the process requirements. Two mechanisms are available for shakeout: vibrating screen and rotary drum. The energy burden of these machines can be found in [Table 4-5](#).

After the shakeout process, the sand goes through a reclamation process. As explained before, the reclamation process can be divided into three categories: primary reclamation, secondary reclamation and thermal reclamation. The logic behind each process is the same; the user selects the appropriate equipment for a particular operation. The energy burden of the reclamation can be found in [Tables 4-5, 4-6 and 4-7](#).

According to the literature (Brown, 1999) and author's experience, the mechanical reclamation method can achieve 90% reclamation and the thermal method can achieve almost 100% reclamation. Therefore, a reclamation rate of 90% is adopted for the primary and secondary reclamation and a reclamation rate of 98% (foundry experience) is adopted for thermal reclamation. Combining the energy burden information for sand processing, the user can determine the energy burden for a given number of recycling cycles.

4.2.4.1.2 Casting production

The energy burden calculation for the casting production is relatively simple. The purpose of the spreadsheet is to calculate the process yield, recovery rate and the recycling efficiency. The energy burden can then be calculated based on these data. To achieve this, the user need only know the amount of aluminium flow through each casting operation. After all the parameters have been worked out, the user only need decide on the number of operation

cycles and the corresponding casting production energy burden can be derived. For full version of the spreadsheet, please refer to the Appendix 16 on the DVD.

4.2.4.2 Results

In this section, the author will choose the most common equipment to perform the calculation of the energy burden of the mould making process. For the conveyor belt and bucket elevator, the capacity is 20 t·h⁻¹, the velocity of the belt is 3 m/s, the length/height of the delivery is 10 m and the motor efficiency is 85%. The tables below show the energy burden for the casting process for up to 10 recycling cycles. As expected, the CRIMSON process has less energy burden compared with the conventional casting process.

cycle	1	2	3	4	5	6	7	8	9	10
green sand primary reclaim (MJ/kg)	0.56	0.31	0.23	0.19	0.16	0.15	0.14	0.13	0.12	0.12
CRIMSON metal preparing (MJ/kg)	54.44	32.26	25.06	21.59	19.63	18.4	17.59	17.03	16.65	16.36
Conventional metal preparing	54.44	32.82	25.86	22.56	20.73	19.6	18.86	18.39	18.06	17.82
CRIMSON process (MJ/kg)	55	32.57	25.29	21.78	19.79	18.55	17.73	17.16	16.77	16.48
Conventional process (MJ/kg)	55	33.13	26.09	22.75	20.89	19.75	19	18.52	18.18	17.94

Table 4-16 Energy burden of sand mould making and total energy burden of casting. High resolution table can be found in appendix 17 (pp200)

cycle	1	2	3	4	5	6	7	8	9	10
chemical sand secondary reclaim (MJ/kg)	2.45	1.32	0.94	0.75	0.64	0.57	0.52	0.48	0.45	0.43
CRIMSON metal preparing (MJ/kg)	52.55	31.25	24.35	21.03	19.15	17.98	17.21	16.68	16.32	16.05
Conventional metal preparing	52.55	31.81	25.15	22	20.25	19.18	18.48	18.04	17.73	17.51
CRIMSON process (MJ/kg)	55	32.57	25.29	21.78	19.79	18.55	17.73	17.16	16.77	16.48
Conventional process (MJ/kg)	55	33.13	26.09	22.75	20.89	19.75	19	18.52	18.18	17.94

Table 4-17 Energy burden of sand mould making through secondary reclamation method and total energy burden of the casting. High resolution table can be found in appendix 18 (pp200)

cycle	1	2	3	4	5	6	7	8	9	10
chemical sand thermal reclaim (MJ/kg)	2.45	1.49	1.17	1.02	0.92	0.86	0.82	0.79	0.76	0.74
CRIMSON metal preparing (MJ/kg)	52.55	31.08	24.12	20.76	18.87	17.69	16.91	16.37	16.01	15.74
Conventional metal preparing	52.55	31.64	24.92	21.73	19.97	18.89	18.18	17.73	17.42	17.2
CRIMSON process (MJ/kg)	55	32.57	25.29	21.78	19.79	18.55	17.73	17.16	16.77	16.48
Conventional process (MJ/kg)	55	33.13	26.09	22.75	20.89	19.75	19	18.52	18.18	17.94

Table 4-18 Energy burden of sand mould making through thermal reclamation method and total energy burden of the casting. High resolution table can be found in appendix 19 (pp201)

4.2.4.3 Discussion

From the tables above, it is easy to see that the energy burden between green sand and chemical sand are quite different. This is because the binder systems are different. Natural clay is used for the green sand mould, which has low energy content. In contrast, chemical sand uses artificial binders to bond the sand. The chemical industry is another energy intensive industry, whose products normally have high energy content. In this case, the

energy burden of the resin is around 87.63–116.28 MJ·Kg⁻¹. Even with the small amounts of resin (2% by weight) in the chemical sand, it still has much higher energy content than green sand.

As described previously, clay can absorb water continuously up to temperatures within the range 400–700 °C. As a result, the aim of its reclamation is the removal of metal spillages and the breaking down of the sand lumps. This is why primary reclamation has the lowest energy burden. “Dead” resin coating is hard to remove by primary methods; thus, equipment that is more energy intensive, such as pneumatic scrubbing or hammer mills is required in secondary reclamation. However, compared with thermal reclamation, the energy burden of the mechanical method is only about 10%. The reason that thermal reclamation is intensive is because of the large amount of heat required. Although it is an expensive method, compared with using new sand, it is still less energy and material intensive.

For good sand casting, the sand to metal ratio is about 6:1 (Fenyés, 2010), which means 1 kg of metal requires 6 kg of sand. Using the CRIMSON tensile test bar as an example, 1.56 Kg of tensile test bar requires 39 kg of sand. Table 4-19 presents the energy consumption of mould making after continuous recycling. It shows that the average energy of using green sand reduces from 19913 to 3606 KJ, which saves 82% of the energy by using new green sand. For chemical sand, this figure can be 87% by the secondary method and 73% by the thermal method.

sand type	unit energy consumption after 25 recycling (kJ·kg ⁻¹)	energy consumption (kJ)
green sand	510	19919
chemical sand	2393	93336
primary reclaimed green sand	92.45	3605
secondary reclaimed chemical sand	322	12574
thermally reclaimed chemical sand	652	25466

Table 4-19 Table of the unit energy consumption and energy consumption of sand mould making for different mould making methods

In addition to the sand process and its treatment, transferring the sand also consumes energy. Although it is not a huge amount of energy compared with the total energy of the mould making, it still worth considering its energy and cost efficiency (driven by electricity, which is an expensive energy resource). For the conveyor belt, two factors influence the energy burden significantly: load capacity and belt speed. Load capacity has an inverse relation with the energy burden; the greater the capacity the belt has, the less energy burden it has. In

contrast, the speed of the belt is proportional to the energy burden; the faster the speed is, the more energy required to drive the belt. Moreover, according to the spreadsheet, the speed of the belt has the most influence on the energy burden. The energy burden reduces as the speed decreases. Thus, reducing the conveyor speed can reduce the energy burden of the conveyor belt dramatically. For a bucket elevator, the most influential factor is the lifting height. In comparison with the conveyor belt, lifting over the same distance costs three times more energy than horizontal transportation. As a result, reducing the lifting height or replacing the elevator with an inclined conveyor will save significant amounts of energy.

4.3 Simple impact assessments: greenhouse gas emission

To this point, the energy burden of the casting production, sand mould making and associated reclamation has been determined. In this section, a simple environmental impact assessment is carried out to investigate the greenhouse gas emissions caused by the CRIMSON and the conventional tensile test bar production. Four types of situations were investigated: the CRIMSON process with chemical sand mould without recycling, the CRIMSON process with chemical sand mould with recycling, the conventional process with chemical sand mould without recycling and the conventional process with chemical sand mould with recycling. Because the energy burden reduces to a constant value after 25 recycling operations, the operation cycle used was 25. The total energy burden for each situation is shown in Table 4-20.

Process		OME	Casting Weight (kg)	Melting Weight (kg)	Sand weight (kg)	Energy burden for sand (MJ/kg)	Energy burden for metal (MJ/kg)	Energy Consumption (MJ)
Non-recycle	CRIMSON	0.24	1.56	6.53	39.16	2.39	52.61	436.98
	Conventional	0.12	1.56	12.68	76.10	2.39	52.61	849.13
recycle	CRIMSON	0.24	1.56	6.57	39.16	0.65	15.05	124.48
	Conventional	0.12	1.56	12.68	17.38	0.65	16.73	223.50

Table 4-20 Total energy burden for different recycle and non-recycle models. High resolution table can be seen from appendix 20 (pp201)

As the table above shows, under a non-recycle situation, the CRIMSON process uses 437 MJ of energy and the conventional process uses 849 MJ of energy to produce the tensile test bar. In contrast, the CRIMSON process uses only 124 MJ and the conventional process uses 224 MJ under a recycle situation.

Carbon dioxide (CO₂) is the main greenhouse gas investigated in this simple impact assessment. Using the greenhouse gas equivalencies calculator (EPA, nd), the energy consumption can be converted into an amount of carbon dioxide emissions. Table 4-21 presents the emission data for these four situations.

Process		Emission by metal (kg)	Emissions by sand (kg)	Total (kg)	Total per kg of saleable casting (kg/kg of casting)
Non-recycle	CRIMSON	67	18	85	54.49
	Conventional	131	36	167	107.05
recycle	CRIMSON	19	5	24	15.38
	Conventional	42	10	52	33.33

Table 4-21 Equivalent CO₂ emissions for four different situations

4.4 Environmental impact assessment

SimaPro is the leading LCA software chosen by industry, research institutes and consultants. It has the most complete LCI database to carry out environmental impact assessment. For the casting foundry and smelter sectors, the material usage and energy consumption during alumina extraction, electrolysis and ingot casting can be determined. Taking advantage of its database, more environmental impact assessments are carried out. Furthermore, its complete database provides great opportunity to validate the material and energy inventory data collected thus far.

4.4.1 Data input for simulation

The purpose of the analysis is to compare the environmental impact for different casting processes. Same as previous simple impact assessment, four types of situations were investigated by the SimaPro simulation. For non-recycle models, the primary aluminium ingot²⁰ data from SimaPro database were used as the raw material input and for the recycle models, the secondary aluminium ingot²¹ data from the database were used as inputs.

4.4.2 Simulation setup

As introduced before, the SimaPro simulation package was used to assess the environmental impact of the casting process. A model formed by the assembly and waste scenario is used in the SimaPro simulation. The assembly deals with the production stage of the products and it should include all the resources, parts/components, distribution, and processes required to make the products. The waste scenario is the use and end of life phases of the products, which it includes different scenarios, such as use, landfill, recycle and incineration, etc.

²⁰ Only virgin aluminium alloy is used as raw material input. All the production, distribution, and use data are include. It is the best match case compared with collected inventory data

²¹ Combination of virgin metal and recycled scrap metal are used as raw material input. It is the best match case compared with collected inventory data

For a normal approach, the impact assessment is used to assess the production, use phase and end life environmental impact of the product. In other words, the normal approach assesses the impacts only related to the final products. Clearly, the recycling in this study refers to the reuse of the high-energy-content metal removed from the fettling, machining and scrap. It is not as simple as the reuse of the tensile test bar at its end of life phase. Therefore, a special LCA model was developed in SimaPro to assess the environmental impact of raw material extraction, production and in-house recycling.

In order to redefine the definition of recycle within SimaPro, a complex model needs to be developed. There are two difficulties in developing such model in SimaPro. The first difficulty is to separate the recyclable, non-recyclable and other material. In the normal approach, all material passes through the process without any classification. In fact, the material can be converted to recyclable material, non-recyclable material and others. The second issue is to make SimaPro understand that each material has a different waste scenario. Once the material is separated into different categories, these categories have to be defined with a waste scenario. In SimaPro, one assembly has only one corresponding waste scenario. In order to define the different waste scenarios with different categories, multiple assemblies are needed.

According to the literature (Jolly, 2010), the metal loss during the casting process has been presented in Table 4-22. The loss in the melting, holding and degassing operations is through oxidation and impurities, which can be treated as a permanent loss. The metal loss during fettling, machining and inspection is high-energy-content scrap metal, which can be recycled to reduce the virgin aluminium requirement. Therefore, the raw aluminium input can be divided into three categories: permanent loss, scrapped and final product, which refers to the non-recyclable, recyclable and others.

	CRIMSON test bar		Conventional test bar		Loss type
	Weight loss %	weight remain (kg)	Weight loss %	weight remain (kg)	
raw material	0	6.53	0	12.68	Permanent, can be disposed
melting	0.5	6.53	2	12.68	Permanent, can be disposed
holding	0	6.49	2	12.43	Permanent, can be disposed
degassing	0	6.49	5	12.18	Scraped, can be recycled
fettling	60	6.49	77.5	11.57	Scraped, can be recycled
machining	25	2.6	25	2.6	Scraped, can be recycled
scrap	10	1.95	20	1.95	NA
good casting	NA	1.56	NA	1.56	
OME	0.24		0.12		

Table 4-22 Metal loss during each step of casting operation for the CRIMSON and the conventional casting processes. High resolution table can be seen from appendix 21 (pp202)

In addition to the metal input, sand is also used to make the test bar. Assuming that the metal and sand ratio is 1:6 for the tensile test bar sand casting, the sand required for the sand mould is 40 kg for the CRIMSON test bar and 76 kg for the conventional test bar. The material input for the sand mould can also be split into two categories: sand that can be recycled and sand that can be disposed of. According to research, 90% of the sand can go back into the process and 10% can be disposed of in landfill. Assuming the metal and sand ratio is 1:6 for the tensile test bar sand casting, then based on Table 4-22, the total material input to make the casting test bar for both casting processes can be categorised as shown in Table 4-23.

	CRIMSON Test bar	Gravity test bar
permanent loss (kg)	0.03	1.12
scraped (kg)	4.94	10.01
Tensile test bar (kg)	1.56	1.56
Sand will dispose 10% (kg)	3.92	7.61
Sand will recycle 90% (kg)	35.26	68.53
Total Metal(kg)	6.53	12.69
Total Sand(kg)	39.18	76.14

Table 4-23 Total aluminium used to produce the test bar

After splitting the material into different assemblies, the process for each assembly can be established. For permanent loss metal, the process starts from the raw material extraction and finishes at the holding process. For scrapped metal, the process starts from the raw material extraction and ends at the inspection process. The tensile test bar is the only assembly that goes through the entire casting operation from raw material extraction to final shipment. Similarly, the process flow of the sand can be determined. Figure 4-14 shows the mind mapping of the simulation.

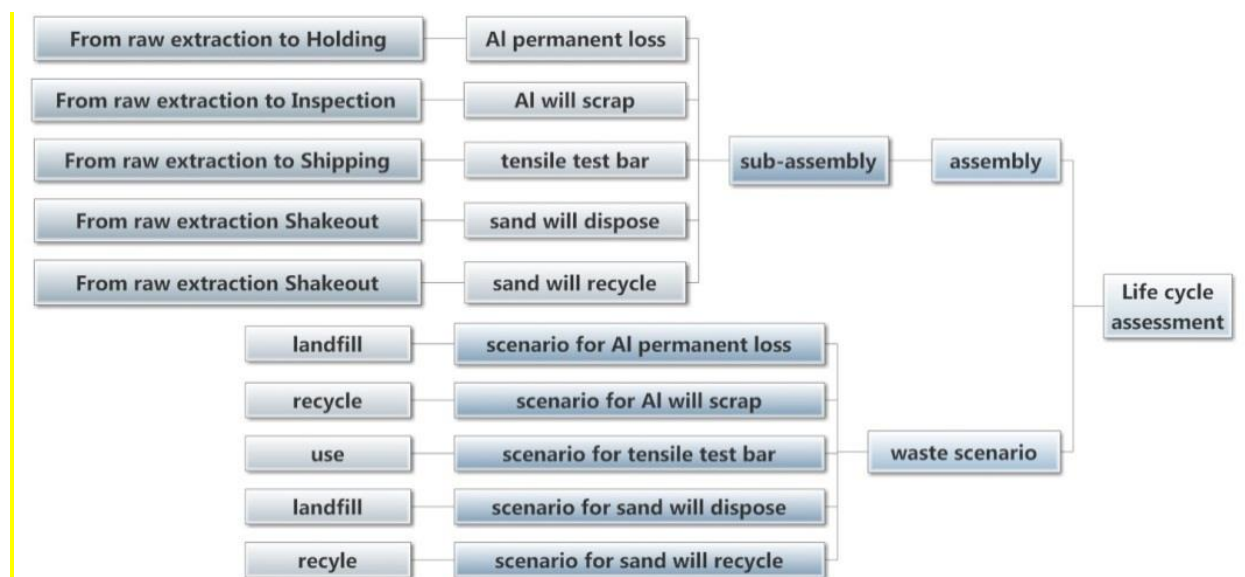


Figure 4-13 Flow chart of new simulation.

4.4.3 Life cycle impact assessment

Three environmental impact assessments were used to assess the environmental impact of the casting process. The first impact assessment is called Greenhouse Gas Protocol. It has been widely used to calculate and report the greenhouse gas emissions. In this section, it has been used as validation tool to check the accuracy of the collected inventory data. The second impact assessment method is called ECO-indicator 99. It calculates the environmental loads of the product / service from production, distribution, use, and end of life phase (Sustainable Manufacturing Protal, 2013). It expresses the emissions and resource extractions in 11 different impact categories (such as radiation, ozone layer, land use, and fossil fuels) (Salonitis, et al., 2006). The last impact assessment method used is called ECO-point 97. It also covers all life cycle stages include production, distribution, use, and end of life. The difference is that the ECO-point can be used to address environmental benefit of recycling and reusing materials (Bennett, et al., 1999).

4.4.3.1 Greenhouse gas emission

Table 4-24 presents the results of such a method. Clearly, there is some difference between spreadsheet and GHG gas protocol result. As introduced before, the spreadsheet use embedded energy owing to lack of raw material extraction data. By contrast, SimaPro provides complete inventory data for calculation. However, the spreadsheet still provides reasonable close results even the spreadsheet has such shortage. Therefore, the spreadsheet results and the simulation results are considerably close. The spreadsheet can be used for energy estimation.

Process		spreadsheet (kg/kg good casting)	simulation (kg/kg good casting)
non-recycle	CRIMSON	54	69
	Conventional	107	135
recycle	CRIMSON	15	21
	Conventional	33	40

Table 4-24 CO₂ emission resulting from the simulation and the spreadsheet

4.4.3.2 ECO-indicator

By applying the weighting factor, the result is shown in [Table 4-25](#), revealing that the ‘Resp. inorganics’, ‘Fossil fuels’ and ‘Climate change’ are the most significant problems, which contribute at least 66% of impact.

The total cumulative impact results are shown in [Figure 4-15](#), which gives the total environmental effect for each casting scenario. Firstly, recycled sand and metal can reduce the environmental impact of the casting process. The impact can be reduced by 62% by recycling in the CRIMSON process and 60% of the impact can be reduced by recycling in the conventional process. In addition to the influence of the recycling activity, the main purpose of the simulation is the comparison of the CRIMSON process and the conventional casting process. From the result, no matter whether the recycling activity is applied or not, the CRIMSON process has less impact than the conventional casting process: 49% and 47% of the impact can be reduced for non-recycling and recycling activity, respectively.

The impact caused by individual process, such as sand mould making and casting production, can also be seen from the simulation results. [Table 4-26](#) displays the environmental impact contribution by each production process.

Impact category /	Unit	life cycle assemble test bar conventional no recydl	life cycle assemble test bar CRIMSONno recydl	life cycle assembly test bar conventional	life cycle assembly test bar CRIMSON
Total	Pt	9.4	4.83	2.98	1.59
Carcinogens	Pt	0.122	0.0626	0.0613	0.0208
Resp. organics	Pt	0.00226	0.00116	0.000741	0.000403
Resp. inorganics	Pt	3.76	1.93	1.05	0.584
Climate change	Pt	1.13	0.581	0.337	0.183
Radiation	Pt	0.00336	0.00171	0.00164	0.000734
Ozone layer	Pt	0.000155	7.9E-5	5.42E-5	2.66E-5
Ecotoxicity	Pt	0.035	0.018	0.0269	0.00587
Acidification/ Eutrophication	Pt	0.306	0.157	0.0876	0.0486
Land use	Pt	0.00265	0.00136	0.00202	0.000789
Minerals	Pt	0.77	0.395	0.163	0.0965
Fossil fuels	Pt	3.27	1.68	1.25	0.654

Table 4-25 Impact assessment: GWP, AC, HTA due to emissions from the casting process and raw materials. High resolution table can be seen in appendix 23

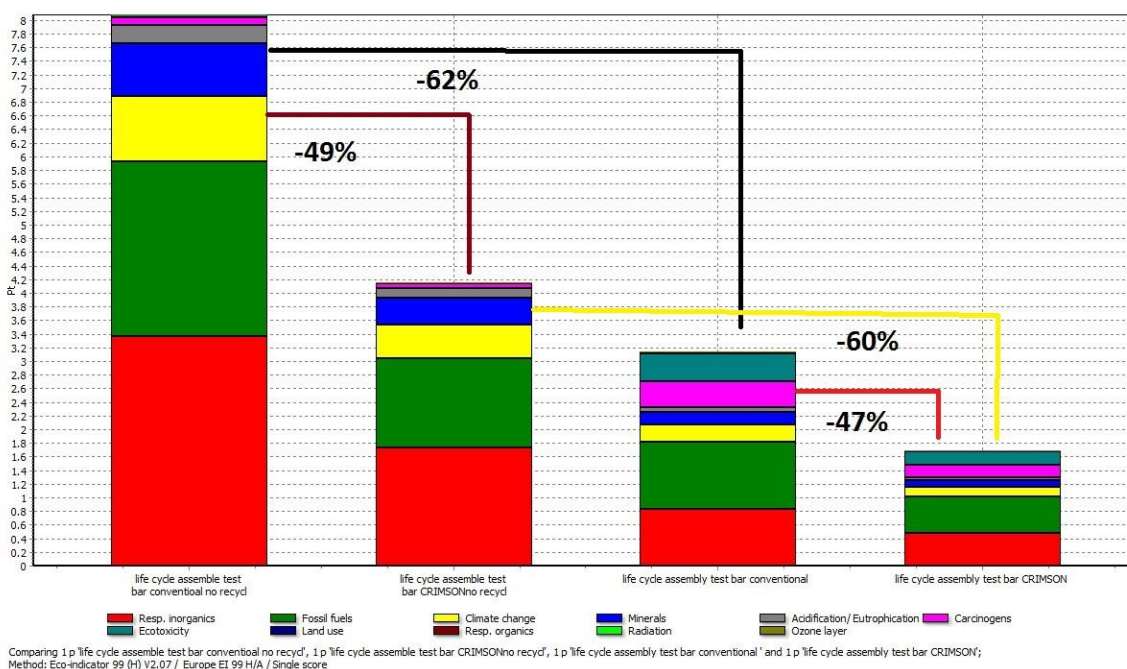


Figure 4-14 ECO-indicator single score results for four casting scenarios. High resolution table can be seen in appendix 24

Process		Metal processing (%)	Sand processing (%)
non-recycle	CRIMSON	83.6	14.6
	Conventional	83.5	14.7
recycle	CRIMSON	84.5	14.8
	Conventional	83.8	14.8

Table 4-26 Environmental impact contribution sorted by process type under ECO-indicator method

4.4.3.3 ECO-points 97

The comparison of the CRIMSON process and the conventional casting process, after the weighting factor is applied, is shown in Table 4-27. It can be seen that the major contribution to the environmental pollution is from NO_x, SO_x, NMVOC, NH₃, Dust PM10 and CO₂. Furthermore, these gases are the primary sources for global warming.

Table 4-27 below shows the single scores for the four casting scenarios. Again, the recycle activity reduces the environmental pollution by about 55%. As can be seen, the comparison between the CRIMSON process and the conventional casting process has similar results to the ECO-indicator. As with the ECO-indicator, the impact caused by individual processes, such as sand mould making and casting production, can also be seen from the simulation results. Table 4-28 presents the environment impact contribution for each production process.

Impact category	Unit	life cycle assemble test bar conventional no recycle	life cycle assemble test bar CRIMSON no recycle	life cycle assembly test bar conventional	life cycle assembly test bar CRIMSON
Total	Pt	169063.66	86719.35	76796.42	39440.90
SOx	Pt	53697.57	27587.13	12321.07	7179.03
Waste	Pt	45190.84	23081.14	18913.21	9497.21
CO2	Pt	35246.02	18107.11	9438.89	5322.39
NOx	Pt	28508.06	14645.38	7186.47	4128.35
Energy	Pt	1922.57	987.62	571.04	317.83
NMVOc	Pt	1703.32	875.09	577.14	317.68
Dust PM10	Pt	1196.79	614.64	664.40	349.96
Cd (water)	Pt	411.15	211.24	912.46	403.04
Hg (air)	Pt	351.10	180.38	425.22	216.84
COD	Pt	154.73	79.49	165.88	78.07
Cd (air)	Pt	153.15	78.68	331.77	166.57
Cu (water)	Pt	151.32	77.75	2091.61	371.79
Zn (water)	Pt	66.21	34.02	1021.86	402.36
Cr (water)	Pt	56.69	29.13	58.32	29.30
N	Pt	53.43	27.45	118.92	20.19
Pb (water)	Pt	52.13	26.79	92.32	13.33
HRAD	Pt	49.40	25.38	1397.52	693.19
NH3	Pt	35.41	18.19	98.83	49.64
Pb (air)	Pt	25.90	13.30	331.66	163.88
Hg (water)	Pt	16.50	8.48	623.51	151.59
LMRAD	Pt	16.31	8.38	397.54	197.01
Ozone layer	Pt	1.76	0.90	1028.34	506.42
Ni (water)	Pt	0.99	0.51	106.10	42.54
Nitrate (soil)	Pt	0.78	0.40	4.00	1.94
Metals (soil)	Pt	0.75	0.38	13.66	6.83
Zn (air)	Pt	0.47	0.24	738.79	363.86
P	Pt	0.22	0.11	12.23	1.76
Waste (special)	Pt	0.09	0.05	17153.09	8448.04
Pesticide soil	Pt	0.01	0.00	0.53	0.26
AOX (water)	Pt	0.00	0.00	0.04	0.02

Table 4-27 Weighting comparison using ECO-Points 97 method. High resolution table can be seen in appendix 25

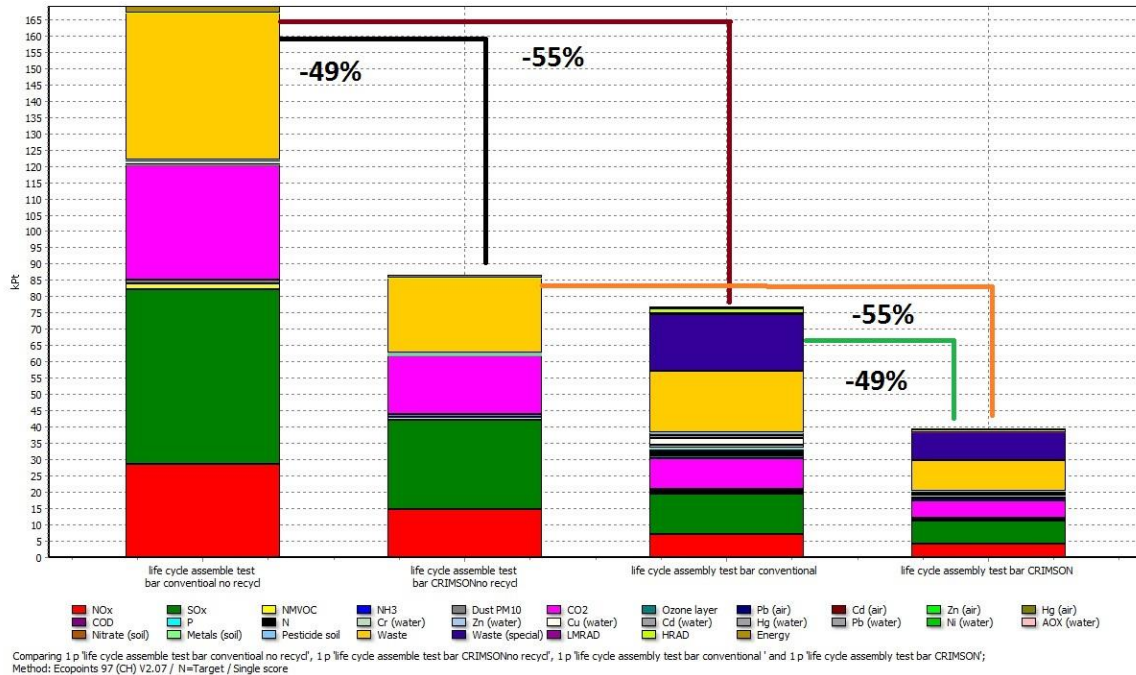


Figure 4-15 ECO-point single score results for four casting scenarios. High resolution table can be seen in appendix 26

Process		Metal processing (%)	Sand processing (%)
non-recycle	CRIMSON	58.4	28.2
	Conventional	58.2	28.4
recycle	CRIMSON	67.0	32.4
	Conventional	66.5	32.4

Table 4-28 Environmental impact contribution sorted by process type under ECO-point method

4.4.4 Discussion

The results of the simple impact assessment and the SimaPro impact assessment indicate the same phenomenon; that the CRIMSON process has less impact compared with the conventional casting sand process. In fact, irrespective of which impact assessment method is used, the environment impact for the CRIMSON process is only about half that of the conventional process. Such a result is quite interesting because it matches with the metal input, as Table 4-23 shows. This means that the environmental impact is influenced mainly by the metal input. In fact, this is as expected because the aluminium data used are for the primary ingot produced in the plant. In reality, such production also includes a refinery, a smelter and an ingot casting plant. Compared with ingot production from bauxite, the resources and energy input to make the tensile test bar (secondary production) is insignificant. According to the evidence given in the SimaPro inventory database, secondary production accounts for only about 2% of the energy consumption of the primary production. Therefore, the impact results are influenced mainly by the amount of primary ingot input.

Furthermore, if we investigate why there is a different metal input, it can be found that everything is related to the OME. The OME for the CRIMSON process and the conventional process is 23.9% and 12.3%, respectively. Therefore, the CRIMSON process uses only half the metal to produce the same casting compared with the conventional process (Table 4-22). The associated energy consumption is also halved. Meanwhile, because of the OME, the sand demand and associated process energy for the CRIMSON process is also halved (Table 4-22). As all the input data for the CRIMSON process were halved, its environmental impact is also halved.

4.5 Summary of chapter

4.5.1 Inventory data for mould making

For the sand mould making process, the energy content of the material and the energy consumption of the different machines are investigated. A special spreadsheet was developed to benchmark the energy burden for different mould making processes and methods of reclamation. From the spreadsheet, the following aspects have been discovered.

The energy burden of the green sand mould is between 434 and 695 $\text{kJ}\cdot\text{kg}^{-1}$ and the energy burden of the chemical sand mould is between 1307 and 3587 $\text{kJ}\cdot\text{kg}^{-1}$. The large difference between the two types of mould is due to the sand additives. For reclamation, as the process becomes radical, the energy burden of reclamation is increased. It was found that the energy burden of primary reclamation is 92 $\text{kJ}\cdot\text{kg}^{-1}$, the energy burden of secondary reclamation is 322 $\text{kJ}\cdot\text{kg}^{-1}$ and the most radical thermal reclamation is 653 $\text{kJ}\cdot\text{kg}^{-1}$. Because of reclamation, 82%, 87% and 74% of the mould making energy can be saved by green sand primary, chemical sand secondary and chemical sand thermal reclamation, respectively. By modifying the loading capacity, belt speed and the elevator lifting height, the energy burden of mould making can be reduced further by 1% or 2%.

4.5.2 Inventory data for casting production

Unlike the normal once-through inventory data collection, the influence of recycle and reuse is also taken into consideration. The method used in this study is called the multiple recycling method. It focuses on the impact of the product production phase rather than on the use of the product. It is useful for calculating the energy burden over a series of life cycle stages. By using this method, the energy burden of the casting process either with or without recycling can be derived.

For the casting production phase, it has been discovered that the energy burden of casting is influenced heavily by the recycling efficiency. The more metal removed from the fettling, machining and scrap, the higher the recycling efficiency. A typical example is shown in [Figure 4-11](#). The AEROMET foundry could have the highest recycling efficiency and lowest energy burden if they recycled their internal scrap. However, recycle efficiency only influences the energy burden of production. The energy burden of the saleable casting is influenced by the OME. The OME determines the true material requirements to perform good

casting. The higher the value of the OME is, the lower the demand for material. It is a good indicator by which to measure the material efficiency of the process.

	CRIMSON test bar	Gravity test bar	CRIMSON housing	AEROMET housing	AEROMET housing with recycle
Virgin Aluminium (kg)	1	1	1	1	1
Good Casting (kg)	0.2	0.2	0.3	0.06	0.06
Recycling Efficiency	0.8	0.7	0.7	0	0.8
OME (%)	0.2	0.2	0.3	0.06	0.06
Energy burden of virgin aluminum (MJ/kg)	55	55	55	55	55
Energy burden of good casting using virgin aluminum (MJ/kg)	230	447	219	1000	1000
Energy burden of recycle aluminum (MJ/kg)	16	17	16	55	14
Energy burden of good casting using recycle aluminum (MJ/kg)	66	142	65	1000	257

Table 4-29 Summary of the embedded energy of casting before and after recycling

4.5.3 Environmental impact assessment

In reality, materials that go through the casting process are not split. However, for the purposes of investigating the influence of recycling, it is useful to split the material flow, as presented in Table 4-24. This ensures that alumina and dead sand are sent to landfill, scrapped metal and reusable sand are sent for recycling and the test bar is sent to the customer. The difficulty of modelling the recycling model is solved and the mind mapping shown in Figure 4-13 displays the breakdown of the simulation model. Each sub-assembly has its process inputs and resource inputs according to the data shown in Table 4-24. By gathering all the sub-assemblies, the life cycle of the casting process can be assessed.

Using the spreadsheet, the energy consumption to make the sand casting bar can be calculated. In consideration of the aims of this study, four types of situations are calculated: CRIMSON test bar non-recycle, conventional test bar non-recycle, CRIMSON test bar recycle and conventional test bar recycle. The calculated energy consumption was converted to carbon dioxide emissions and compared with the SimaPro simulation results. Despite the limitation of the embedded energy, table 4-25 shows that the calculated results and the simulation results are similar, which indicates that the developed spreadsheet is reliable for use in a sand casting foundry.

In addition to the validation of the spreadsheet, the SimaPro life cycle assessment also assessed the environmental impact for both casting processes. The differences between the CRIMSON process and the conventional process are very significant. As with the good casting energy burden, the CRIMSON process has only half the environmental impact of the

conventional casting process. Once again, this is due mainly to the OME of the process. Because the CRIMSON process doubled the OME compared with the conventional process, it only requires half the amount of metal and associated sand and energy.

Therefore, the most important discovery from the inventory data collection and environmental impact assessment, is that the OME is the key for energy saving and sustainability. Because of the lower melting loss and higher casting yield, the CRIMSON process has a higher OME than the conventional casting sand process.

Chapter 5 Validation of the CRIMSON process through productivity investigation

Thus far, the quality and environmental impact of both casting processes have been investigated and the advantages of the CRIMSON process identified. In this chapter, the production performance of the casting process will be investigated. As the most important performance indicator, the labour productivity will be used to assess the performance of the CRIMSON casting process. Unlike previous chapters, some lean thinking will be adopted here to develop a more realistic model for the casting process. The performance indicator will be investigated in this model.

5.1 Assumptions for model development

In order to measure the labour productivity of the CRIMSON casting process, a complete casting model needs to be developed. Therefore, a casting foundry model was developed for this purpose. A survey was undertaken to investigate parameters such as cycle time, casting yield, operational material efficiency (OME) and recovery ratio (Appendix 27). This survey had been sent out to Cast Metal Federation (CMF) members and LinkedIn Aluminium casting user group. However, the response to the survey was poor; only 4% response rate (Appendix 28 –31 on DVD). Unfortunately, limited resources make it impractical to obtain additional data and therefore, to make the model more realistic, the survey results are combined with optimistic but reasonable estimates to build the foundry model. Sections 5.1.1- 5.1.6 describes the assumption made in the model.

5.1.1 Casting weight

The CRIMSON furnace can melt up to 30 kg of aluminium, it therefore sensible to investigate the influence of casting weight at the limit of production performance. As a result of metal loss during the casting operation, the actual weight of the casting is less than the 30 kg. Once again, OME is used to calculate the casting weight and associated melting weight. Unlike the OME used in Chapter 4, here the average OME was used for the general application. From the literature, the OME for the CRIMSON and conventional casting sand processes is 34% and 27%, respectively (Jolly, 2010). Under 34% OME, the CRIMSON process can produce a maximum 10 kg good casting. Therefore, it makes sense to investigate

the influence of casting weight on productivity from 1 to 10 kg for both casting processes (Table 5-1).

	good casting	1	2	3	4	5	6	7	8	9	10
OME (%)	CRIMSON	34	34	34	34	34	34	34	34	34	34
	conventional	27	27	27	27	27	27	27	27	27	27
weight for melting (kg)	CRIMSON	2.94	5.88	8.82	11.76	14.71	17.65	20.59	23.53	26.47	29.41
	conventional	3.70	7.41	11.11	14.81	18.52	22.22	25.93	29.63	33.33	37.04

Table 5-1 Depending on the capacity of the CRIMSON furnace, a maximum 10 kg aluminium casting can be produced. From 1 to 10 kg, the corresponding weights for the conventional casting sand process are also shown.

5.1.2 Cycle time for Melting

Melting is the most time-consuming operation of any casting process. Its cycle time determines the maximum number of operations that can be performed each day. For the CRIMSON process, a 300 kW induction furnace is used. However, for safety reasons, the author's team only used 40 kW. There is no lid to the furnace and conservatively assuming 50% efficiency, the time for melting is shown in Table 5-2.

good casting (kg)	1	2	3	4	5	6	7	8	9	10
Raw metal (kg)	3	5.9	8.9	11.8	14.7	18	21	23	26	29.4
Energy (KJ)	3907	7815	11723	15631	19538	23446	27354	31261	35169	39076
Time (min)	2	3	5	7	8	10	11.4	15	15	16

Table 5-2 Time required to melt different weights of metal to make one casting under the CRIMSON process

For the conventional casting sand process, a batch melting method is adopted. In this case, a 500 kg gas furnace is used for the melting operation. If it is assumed that the furnace is completely empty after each cycle of melting, then according to the survey results, two hours will be used to melt this amount of metal.

good casting (kg)	1	2	3	4	5	6	7	8	9	10
Raw metal (kg)	4	7.4	11	15	19	22	26	30	33.3	37
Casting can be produced (kg)	135	67	45	33	27	22	19	16	15	13
Time (min)	1	2	2.6	3	4	5	6	7	8	9

Table 5-3 Time required to melt different weights of metal to make one casting under the conventional process

5.1.3 Customer requirements

1. Casting products are delivered to the customer on a daily basis.

5.1.4 Supplier information

1. Supplier delivers raw materials twice a week to ensure sufficient supply for production

5.1.5 Information flow

1. All communication between customer and supplier is electronic.
2. Production control receives 30-day forecasts and daily orders from the customer.
3. Production control transmits monthly forecasts and weekly orders to supplier
4. There is a daily schedule released to the shop floor.
5. The combination of push and pull single is used in the production flow

5.1.6 Special assumptions for shop floor operation

1. Every month has 30 working days.
2. Foundry operates three shifts daily. Ignoring break times, the working time is 1440 minutes.
3. The conventional melting furnace can supply 500 kg of aluminium every 120 minutes. Depending on the weight, the CRIMSON melting furnace can supply up to 30 kg of aluminium every 16 minutes.
4. One-piece flow manufacturing method²² is adopted for both casting processes to eliminate the work in process. Therefore, there is no inventory during the casting process. There is no batch production required. Because of the speciality of the casting process, the one-piece flow starts from the shakeout operation, which is the cold end²³ of the casting process. For the conventional casting process, the raw material enters into production flow every 120 minutes. For the CRIMSON process, the raw material enters into production flow depending on the melting time.
5. Based on reasonable assumptions, each operation requires one operator, except for preheating, melting, refining, holding and casting operations in the conventional casting sand process. Preheating, melting and refining processes can share an operator in the conventional casting sand process and the holding and casting operation can share one operator as well.
6. The production time for both casting processes is set as one year
7. Setup time is ignored due to the long period of production.
8. Due to the uncertain shapes of the casting products, there is no point in investigating casting solidification for a particular casting shape. Therefore, an average solidification time is used for all castings.

The tables below present the assumptions of the setup time, cycle time, changeover time, availability and the up time for the two processes.

²² One-piece flow production is also called the Cellular Manufacturing Method. It aims to move the products through the production process one piece at a time, at a rate determined by customer demand (US Environmental Protection Agency, 2003)

²³ Casting can be divided into hot end and cold end processes. The hot end refers to the liquid state of the casting operation, in which all of the operations have to be continuous. The cold end refers to operations dealing with solidified metal. The processes at the cold end can be discrete.

	Preheating	Melting	Refining	Holding	Casting	Shakeout	Fettling	Machining	Inspection
operator	1	1	0	0	1	1	1	1	1
setup time (min)	30	30	30	30	30	30	30	30	30
cycle time (min)	30	120	15	0	1	5	1	1-10	1
Availability	480	480	480	480	480	480	480	480	480

Table 5-4 Assumptions of setup time, cycle time, changeover time, availability and up time for different equipment used in conventional sand casting process

	Melting	Casting	Shakeout	Fettling	Machining	Inspection
operator	1	1	1	1	1	1
setup time (min)	30	30	30	30	30	30
cycle time (min)	2-16	1	5	1	1-10	1
Availability	480	480	480	480	480	480

Table 5-5 Assumptions of setup time, cycle time, changeover time, availability and up time for different equipment used in the CRIMSON process

5.2 Simulation approach

Gathering all the assumptions above, the total output of the casing production can be determined by the melting time. The amounts of casting products that can be made in one year for different weights are shown in the table below.

casting weight (kg)	1	2	3	4	5	6	7	8	9	10
CRIMSON (min/set)	1.62	3.26	4.89	6.51	8.15	9.77	11.4	13.03	14.65	16.28
Conventional (min/set)	0.89	1.78	2.67	3.56	4.44	5.33	6.22	7.11	8	8.89
CRIMSON (set)	32444	161226	107484	80737	64514	53797	46105	40337	35877	32285
Conventional (set)	590561	295280	196853	147640	118378	98611	84501	73924	65700	59122

Table 5-6 Theoretical calculation results of casting products made in one year under the assumptions

However, such results are not accurate enough; the relation between cycle time and production output is not a simple linear relation. In fact, the size of the casting, the power output of the furnace and some other factors have an influence on the time of production. In this work, this is called a macroscopic relationship between time, size and shipments. In addition to the macroscopic relationships, the interconnected features of each operation also influence the production output (Robinson, 2004). As introduced in the life cycle approach, the casting process includes preheating, melting, refining, holding, shakeout, fettling, machining and inspection. The different machine cycle time and different production

capacities create a complex situation, which can influence the output variable of the production

Therefore, in order to investigate the production output of the casting production process, a process simulation needs to be introduced to this project. The process simulation model is able to represent the variability, interconnectedness and complexity of the system (Robinson, 2004). It is possible to predict the system performance with simulation. The simulation package used was WITNESS²⁴, which is a process simulation and modelling tool used to simulate full production runs over an arbitrary period (Markt, et al., 1997). WITNESS allows material flows to be modelled and tracked through each production process, which is a good way to discover problems and suggest improvements.

5.2.1 Simulation model setup

There are four types of basic elements in WITNESS: parts, buffers, machines and labour. Parts represent the input materials. Depending on the real situation, this can be set to any size and time. Buffers represent the storage for products or semi-finished products. Machines represent the production process. In WITNESS, the production process can be single, batch, production, general, multiple cycle and multiple station. For both casting processes, only single, batch and production are used. Single means processing the parts or products one at a time, batch means processing a certain amount of parts or products at one time and production means repetitive continuous production. Labour straightforwardly represents the work force required for the job.

In WITNESS, there are two types of output rules: push and pull. Push means the current process pushes output to the downstream process and pull means that the downstream process extracts input from upstream. A combination of push and pull are used to model the casting process.

Beginning with the conventional casting sand process, the model starts with the entry of raw metal into the foundry. Following the material flow, the metal passes through preheating, melting, refining, until holding with respective cycle times. After the holding operation, the molten metal is poured into 135 sets of casting moulds (assume 1 kg of good casting required). Moreover, the holding is used to supply liquid metal continuously for casting. It works as storage or a buffer to supply the downstream operations. In order to apply these two

²⁴ Witness is provided by Lanner simulation

characteristics into the simulation, the holding operation is set as a production process in WITNESS, which can produce 135 sets of casting moulds. However, as a buffer it is not assigned a cycle time.

Following the material flow, the parts then go through the casting process and the mould is transferred to the safety area for solidification. In WITNESS, a buffer is used to represent the safety area and a 30-minute delay applied to represent the solidification time. After the solidification buffer, the material is moved into the shakeout process, in which a work-in-process buffer was added to collect parts after the shakeout process. The purpose of this buffer is to supply parts continuously to the downstream operation. After the buffer, there is a container to collect a certain amount of parts and to await transfer to the next process (to simulate the batch production process). In the current situation, the container only collects one part to act as the one-piece flow. For future batch investigations, the container can collect any number of parts. Similarly, for fettling and machining, a work-in-process buffer and container are located at the end of each process before delivery to the next process.

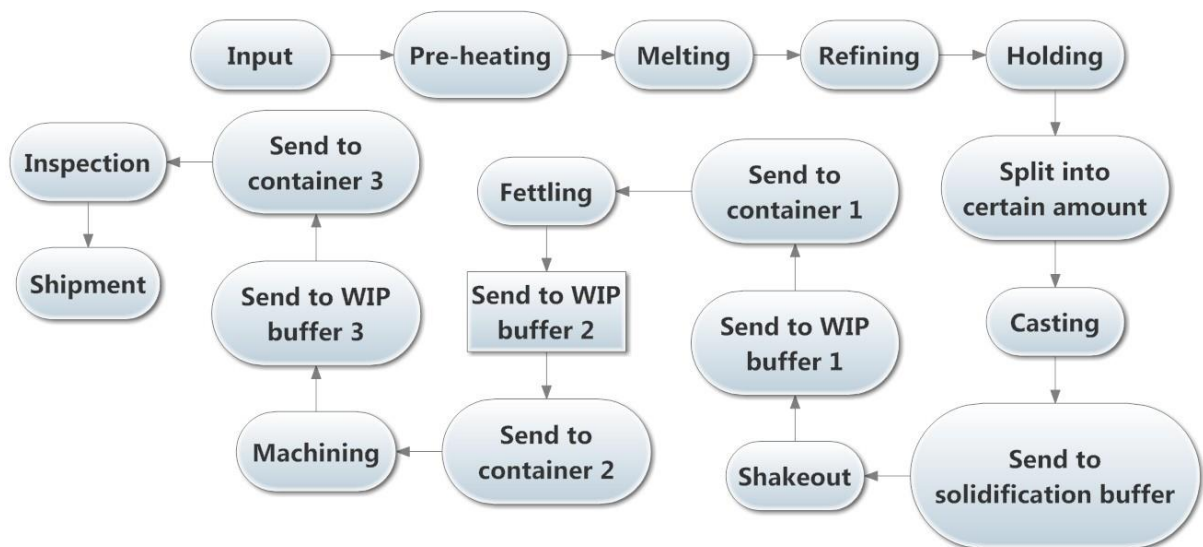


Figure 5-1 Process flow of the Witness simulation for conventional casting sand process. In current simulation, the container in the process only takes one piece at a time

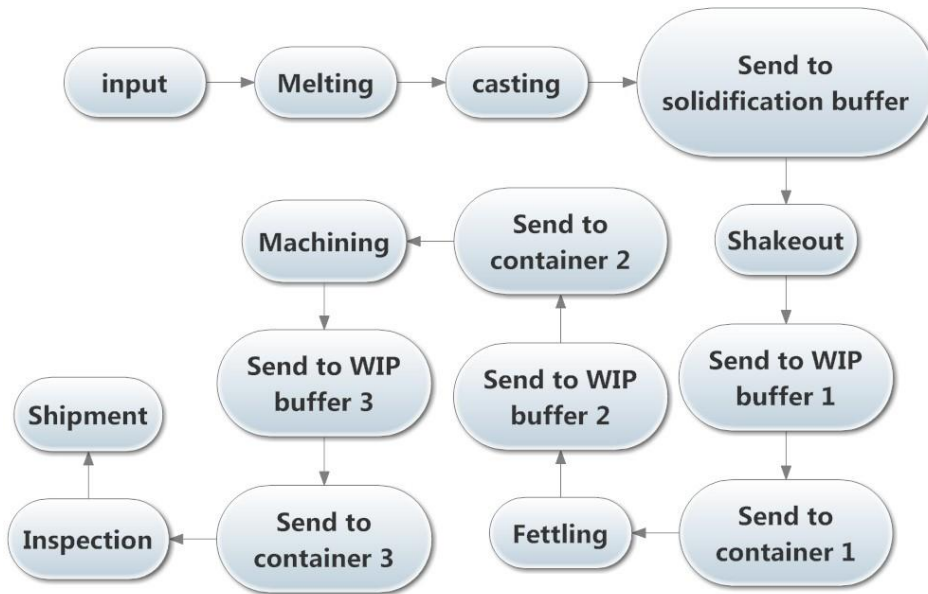


Figure 5-2 Process flow of the Witness simulation for the CRIMSON casting process. In current simulation, the container in the process only takes one piece at a time

A similar model was developed for the conventional casting sand process. However, the CRIMSON melts metal for a single shot and has no holding in the process. Therefore, there is no production required at the hot end and the raw material can enter into the production flow much more quickly than in the conventional casting sand process. Figures 5-3 and 5-4 represent the actual layout used in simulation for both casting process.

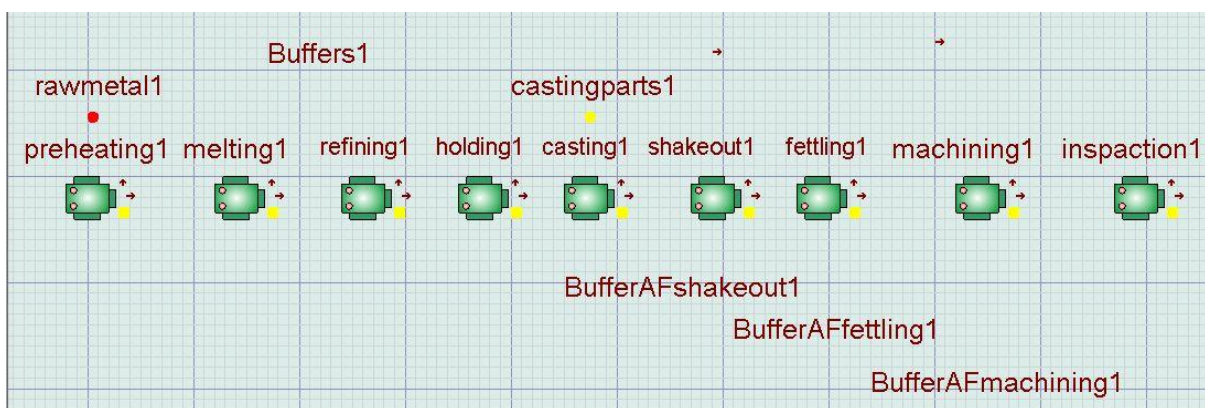


Figure 5-3 Layout of the conventional casting sand process in WITNESS. The process starts from raw metal 1 on the left side. Followed by the assumption there are no inventories from preheating to holding. After casting, buffers are applied to represent the work-in-process inventory

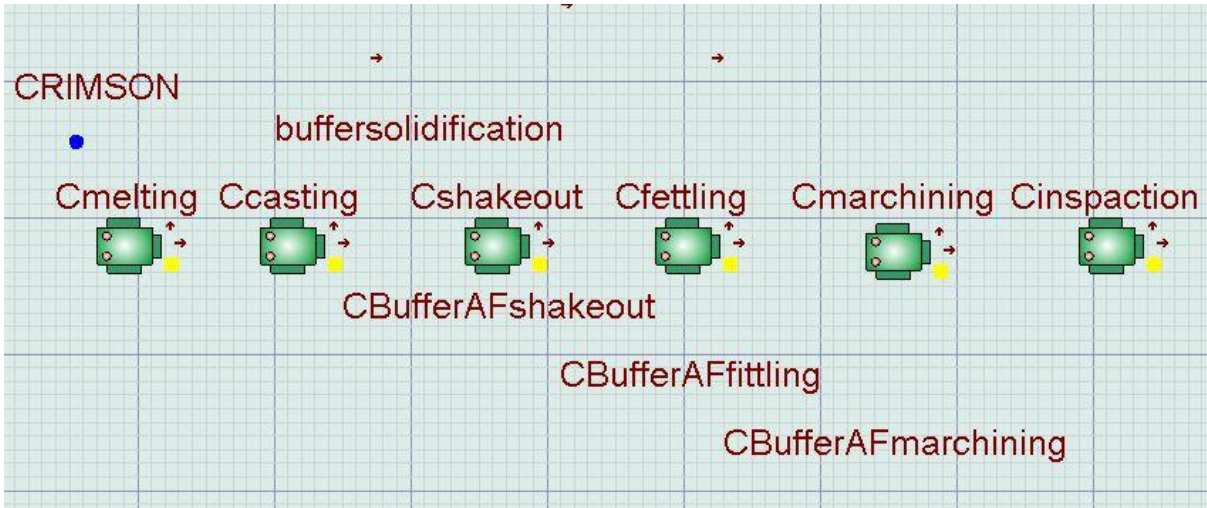


Figure 5-4 Schematic of the current state of CRIMSON process. A part arrives every 4.8 minutes. The capacity of the container is 20

5.2.2 Simulation results

Under the assumptions, the productivity of both casting processes for different casting weights has been investigated for a period of one year. The results of both casting processes are presented in Figure 5-5.

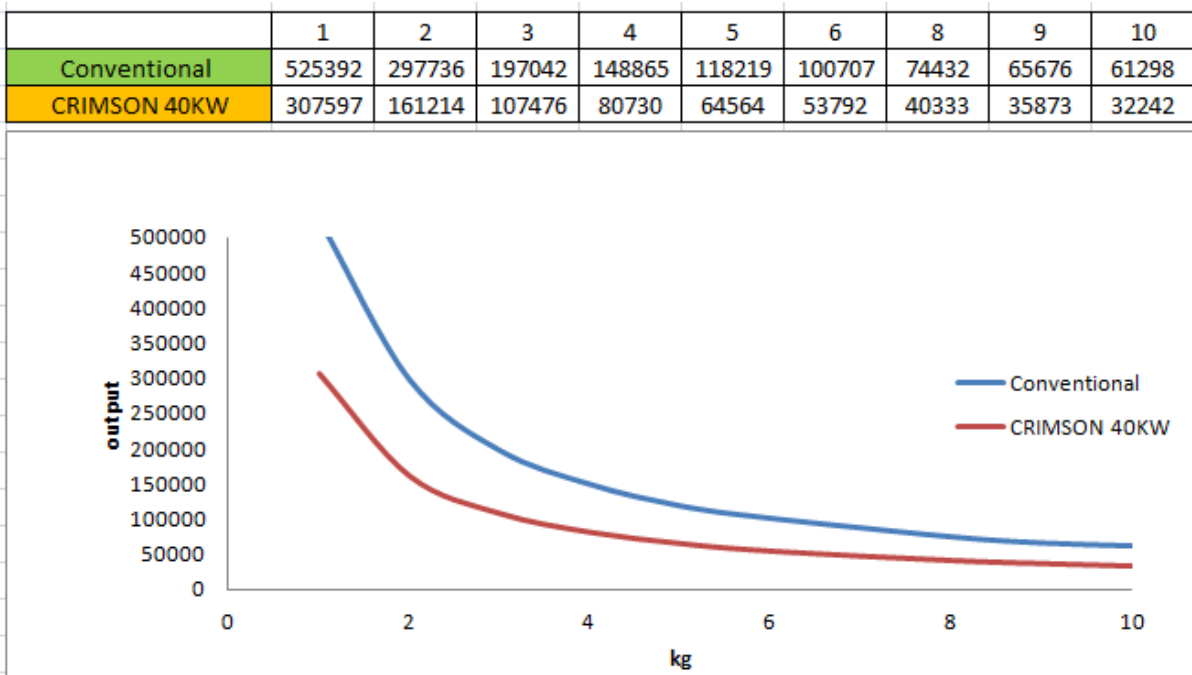


Figure 5-5 Simulation results of output for both casting processes under different casting weights for one-year period

In addition to the production output data, the machine availability is also investigated for both casting processes. The utilisation of the machine represents the availability of the machine. The higher the utilisation is, the higher the productivity of the machine is. Figure 5-6 shows

the machine utilisation comparison between the CRIMSON and the conventional casting processes.

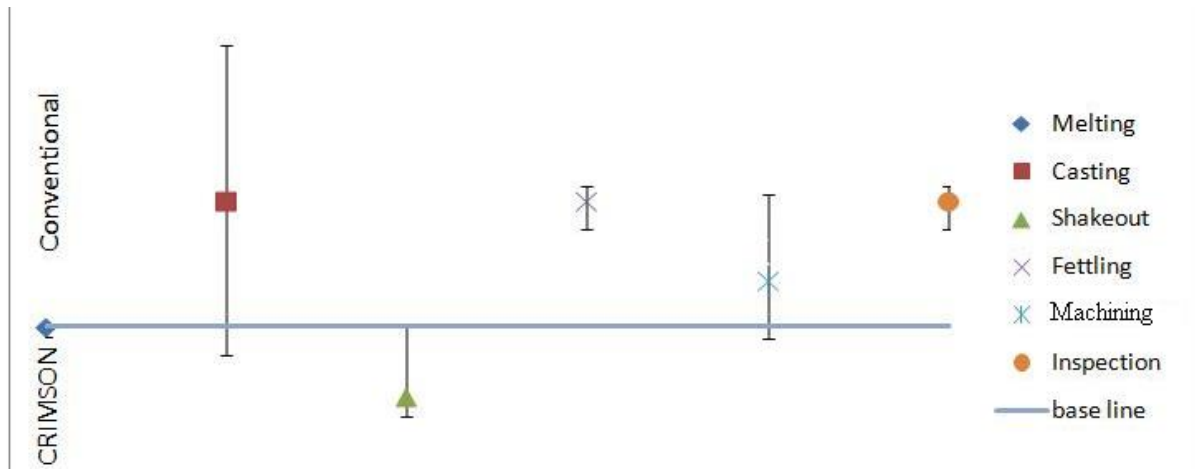


Figure 5-6 Comparison of busy status between the CRIMSON and the conventional casting processes. Maximum, minimum and mean difference between the processes are shown. Above base line means conventional has higher utilization, below base line means CRIMSON has higher utilization.

The maximum, minimum and the mean difference for each operation are shown in the graph. There is a base line in the figure, which represents the same performance for both casting processes. The conventional process has greater value above the base line and the CRIMSON process has greater value below the base line. Clearly, most of the operations are above the base line. This means that most of the conventional casting operations have higher utilisation than the CRIMSON process, no matter what the change in casting size.

Finally, the labour productivity can be seen from the [table 5-7](#).

casting size (kg)		1	2	3	4	5	6	8	9	10
output	Conventional	525392	297736	197042	148865	118219	100707	74432	65676	61298
	CRIMSON 40KW	307597	161214	107476	80730	64564	53792	40333	35873	32242
labour hour (h)	Conventional	61320	61320	61320	61320	61320	61320	61320	61320	61320
	CRIMSON 40KW	52560	52560	52560	52560	52560	52560	52560	52560	52560
labour productivity (set/h)	Conventional	8.57	4.86	3.21	2.43	1.93	1.64	1.21	1.07	1.00
	CRIMSON 40KW	5.85	3.07	2.04	1.54	1.23	1.02	0.77	0.68	0.61

Table 5-7 Labour productivity results for both casting processes. The conventional casting sand process is more productive than the CRIMSON process

5.2.3 More results and discussion

The data above are based on current furnace safety settings for power output up to 40 kW. In fact, the power output of the CRIMSON furnace can reach up to 300 kW. If the full power were used for melting the metal, the story would be different. Therefore, further results relating to the different power outputs will be presented in this section.

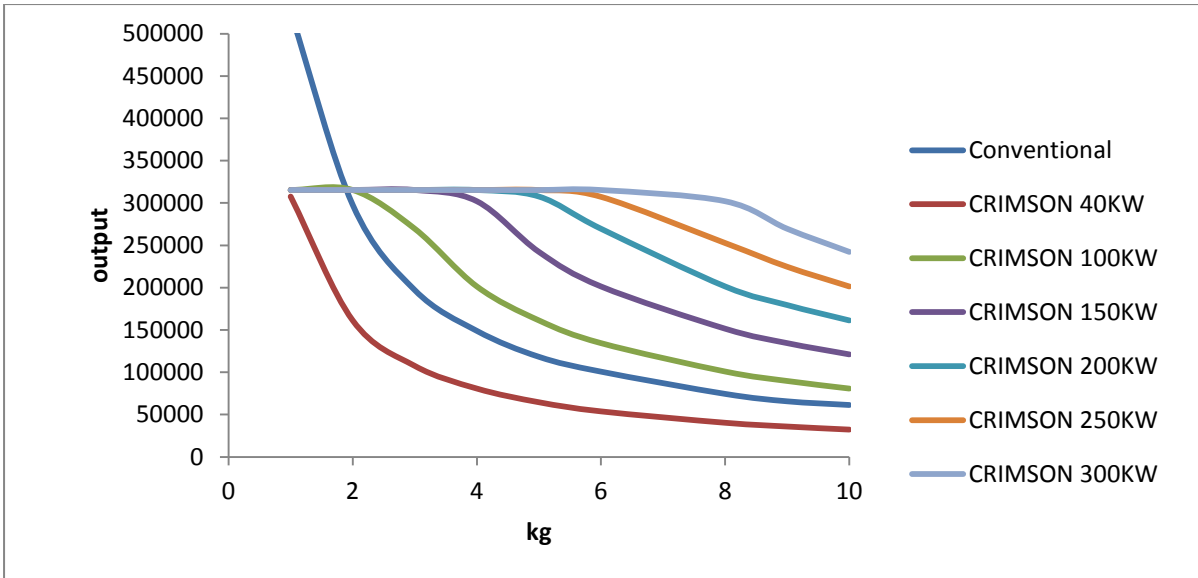


Figure 5-7 CRIMSON product output under different power outputs

Figure 5-7 lists the product outputs for different casting weights under different power outputs. Several things can be seen from these results. First, the conventional process is much more productive for small-sized casting products, especially those castings below 2 kg in weight. Secondly, the product outputs increase as the power output increases, especially for large-sized casting products. Finally, as the casting size increases, the product output decreases.

The reason why the conventional casting process is productive can be seen from Figure 5-8. This shows the utilisation of the major casting operations for 1 kg of casting products. Clearly, the conventional sand casting process has the smoothest operation compared with the other process. Furthermore, its operations also have the highest utilisation compared with the CRIMSON process. Because of these two advantages, the operations in the conventional sand casting process can be fully functional without any process interruption or delay.

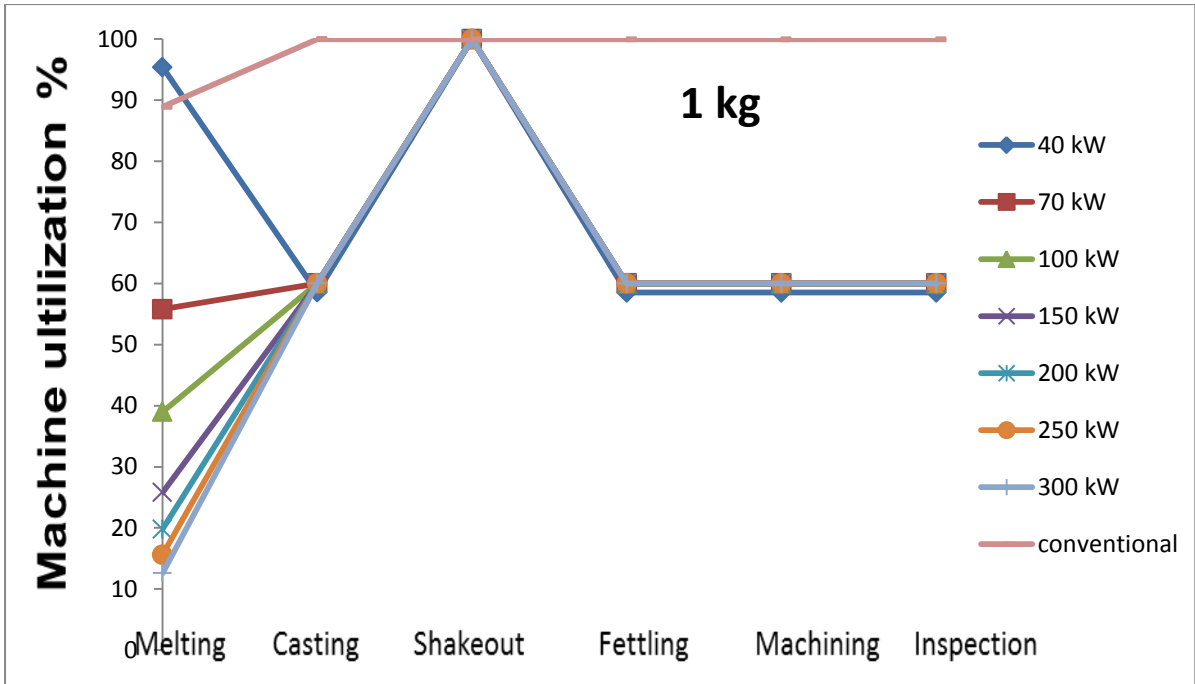


Figure 5-8 Machine utilisation for different casting settings; higher utilisation means higher productivity

Figure 5-9 shows the machining utilisation required to produce 3 kg castings under different furnace power outputs. As the power increases, the machine utilisation increases. Therefore, more products can be produced during the same period, which is why the output increases as the power output increases.

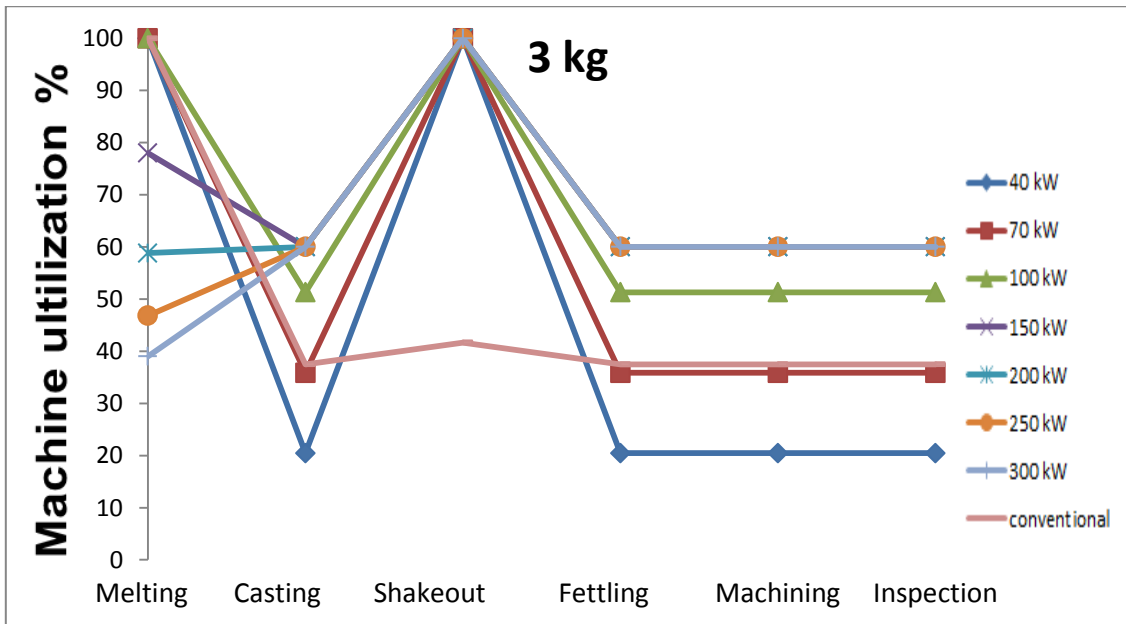


Figure 5-9 Machine utilisation in producing 3 kg castings under different power outputs

As the size of the casting increases further, the utilisation of machines changes. Figure 5-10 presents the utilisation in producing 8 kg castings under different furnace power outputs.

Unlike Figures 5-8 and 5-9, the pattern shown in Figure 5-10 is much rougher. Therefore, a trend can be seen from these three figures; as the casting size increases, the production becomes less smooth. It turns out the casting process is not fully operational and that the productivity is low, which is the reason why the productivity is reduced as the casting size increases.

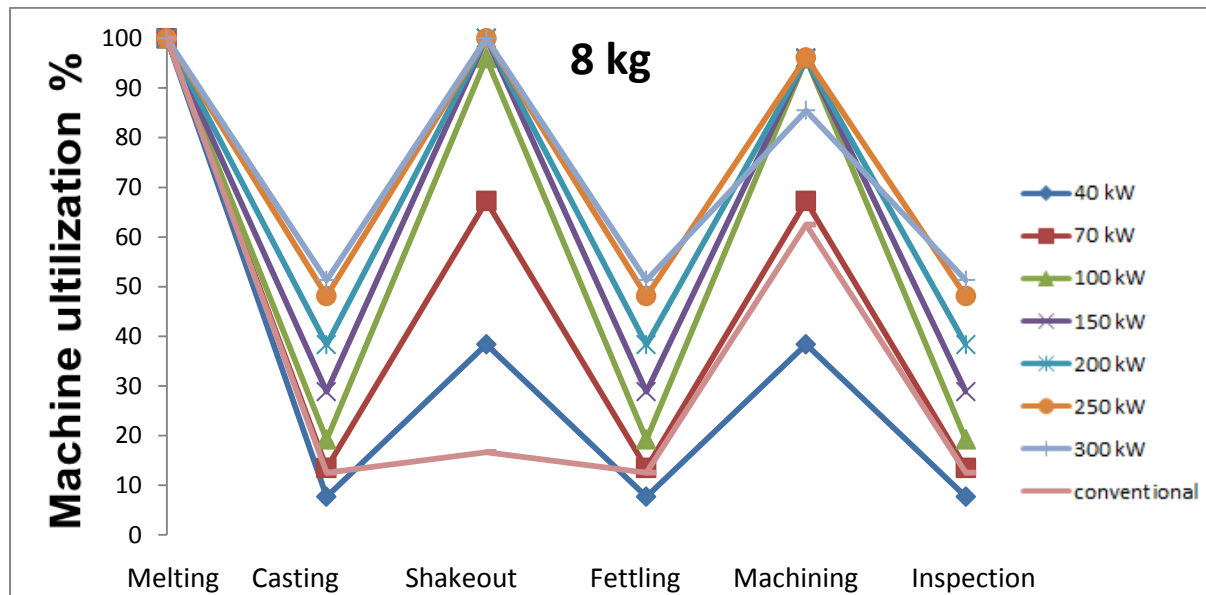


Figure 5-10 Utilisation to produce 8 kg castings under different power outputs

From these investigations, the labour productivity for all kinds of situations is displayed in Table 5-8. Once again, it tells a similar story to that shown in Table 5-7. The conventional sand casting can produce more when the casting size is less than 2 kg. However, in addition to the aspects indicated in Table 5-7, compared with the conventional sand casting processes, the CRIMSON process can be much more productive under high power output when making large castings. The best scenario can be found at 300 kW when making castings between 6 and 10 kg, which can be at least 2.5 times more productive compared with the conventional sand casting process.

Table 5-8 also indicates the production limit for the CRIMSON process. As the highlighted area shows, six sets per hour is the upper limit for the CRIMSON process. For castings up to 3 kg, an increase in the power output cannot help the productivity. This is because more metal can be melted under high power output; however, it only builds up the work-in-process inventory. Therefore, this table not only indicates the advantages of the CRIMSON process, it also gives good guidance about the power output selection for CRIMSON furnace.

casting size (kg)	1	2	3	4	5	6	8	9	10
Conventional (set/h)	8.57	4.86	3.21	2.43	1.93	1.64	1.21	1.07	1.00
CRIMSON 40KW (set/h)	5.85	3.07	2.04	1.54	1.23	1.02	0.77	0.68	0.61
CRIMSON 100KW (set/h)	6.00	6.00	5.13	3.28	2.63	2.19	1.65	1.46	1.32
CRIMSON 150KW (set/h)	6.00	6.00	6.00	4.31	3.46	3.28	2.16	1.92	1.73
CRIMSON 200KW (set/h)	6.00	6.00	6.00	4.50	4.39	3.85	2.55	2.28	2.04
CRIMSON 250KW (set/h)	6.00	6.00	6.00	4.50	4.50	4.38	2.88	2.56	2.55
CRIMSON 300KW (set/h)	6.00	6.00	6.00	4.50	4.50	4.50	3.13	2.80	2.76

Table 5-8 Labour productivity for different casting processes for different casting sizes and power outputs

5.3 Summary of chapter

In this chapter, the labour productivity was used as a performance indicator to investigate the production performance of the CRIMSON process. To achieve this, a complete casting foundry model was developed. In this model, the setup time and cycle time for different operations were defined through a survey investigation and reasonable assumptions. Working hours, labour availability and material flow were also defined. According to the OME results, the casting capacity of the CRIMSON process was also defined at 10 kg. Other factors such as cycle time, casting size and furnace output, were also used to investigate the influence of labour productivity on performance.

In order to achieve better productivity results, WITNESS simulation package was used to simulate the foundry model. Under the current situation, the CRIMSON only uses 40 kW to melt metal. It transpires that the conventional sand casting process is twice as productive when compared with the CRIMSON process. However, as the CRIMSON furnace power increases, the situation is changed. When full power is applied to make 10 kg casting products, the CRIMSON process is four times more productive than the conventional casting sand process. However, there is an exception. No matter whether the power output is increased or not, the conventional casting sand process has higher labour productivity if the casting is less than 2 kg.

Therefore, the simulation results suggest that the CRIMSON process should be used for casting sizes between 2 and 10 kg, using the correct power output, as shown in Table 5-8.

The conventional sand casting process should be used for casting sizes up to 2 kg, if the productivity is an issue.

Chapter 6 Validation of the CRIMSON process through cost analysis

Nowadays, the global market has become increasingly competitive. In the manufacturing industry in particular, such pressure forces the manufacturing organisations to seek continuously for opportunities to improve quality, reliability and productivity with a competitive manufacturing cost. In the previous chapters, the quality, reliability and productivity of the CRIMSON process have been investigated and the results are appealing. In this chapter, the manufacturing cost of the CRIMSON process will be investigated. Once again, a process simulation will be used to investigate the CRIMSON casting process and the results will be compared with the conventional sand casting process.

It is the author's contention that this chapter is the most important part of the validation the CRIMSON process. As discussed in the literature review, introducing new equipment or technology is difficult. Organisations may deliberate over time, production disruption, associated costs of production disruption and the cost of technology. In particular, the cost of production disruption and cost of technology can be the most significant barriers to an organisation becoming competitive. Even for the CRIMSON process, despite advantages such as low capital cost, high flexibility, quality and productivity, the foundry management will not be pay attention without realistic and accurate cost estimations.

6.1 Introduction to cost estimation

The aim of cost estimation in a manufacturing organisation is to estimate accurately the manufacturing costs prior to actually commencing manufacture (Shehab, et al., 2001). It can help an organisation understand the feasibility and value of a project. It plays a vital role in cost engineering, because it helps cost engineers with proposals of cost control.

As Layer (2010) indicated, from a methodological point of view, cost estimation techniques can be divided into qualitative and quantitative approaches. A qualitative estimation is based primarily on expert judgement and similarities between existing and new products (Caputo, et al., 2008). On the other hand, quantitative estimations are based on detailed investigations of product design, product' features and the manufacturing process (Niazi, et al., 2006). According to the literature, cost estimation techniques can be further classified, as shown in

Figure 6-1. Each method will be introduced and the most suitable chosen for the CRIMSON cost estimation.

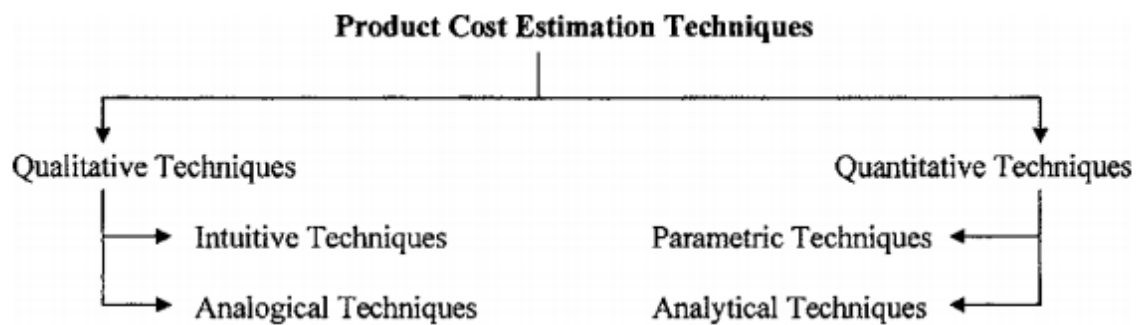


Figure 6-1 Typical classification of cost estimation techniques (Niazi, et al., 2006)

6.1.1 Intuitive cost estimation techniques

The intuitive cost estimation technique is based on an expert’s experience and knowledge. It retrieves data from past projects and experience, building up an extensive database for current processes or projects. Therefore, intuitive cost estimation can provide relatively quick and accurate estimations. However, it requires people and time to establish the database (Niazi, et al., 2006).

6.1.2 Analogical cost estimation techniques

The analogical cost estimation technique is based on historical cost data (Niazi, et al., 2006). The estimated cost of a new process or project is based on previous cost information (Agyapong-Kodua, et al., 2011). Such a technique is quite useful when a current process or project has similarities with a historical one. However, its accuracy depends on the integrity of the historical data and the validity of the relationship between the historical and current process or project (Agyapong-Kodua, et al., 2011).

6.1.3 Parametric cost estimation techniques

The parametric cost estimation technique is based on statistical methodologies, expressing cost as a function of its constituent variables (Niazi, et al., 2006). By using this technique, some information is needed (Zhai, 2012); however, this technique needs to identify the cost drivers because without cost drivers, this technique cannot work.

6.1.4 Analytical cost estimation techniques

The analytical cost estimation is a technique used to assess production costs by investigating the cost of each operation involved. This technique requires detailed understanding about the

production process. It is the most time consuming and costly approach; however, it is the most accurate (ASIEDU, 1998).

6.2 Suitable technique for current project

The advantages and disadvantages of the different cost estimation techniques have been introduced. The intuitive cost estimation technique can provide quick and optimised results; however, it requires accumulated experience and knowledge. For the CRIMSON process, such a cost estimation technique has its limitation. Despite the geometrical differences of casting products, different casting methods (sand casting or investment casting for example) and different metal alloys can be used. Thus, similarities are hard to find under such flexible production processes. Furthermore, the CRIMSON process is a relatively new process, for which time is required to build up experience and knowledge. Similarly, the analogical cost estimation technique is unsuitable for the CRIMSON process.

The accuracy of the parametric method depends on the identification of the cost drivers. This is easy for the CRIMSON process. The cost drivers are material cost, set-up cost, tool replacement cost, machining cost and transportation cost, etc. The problem is that the CRIMSON process is too young to have historical data and thus, the statistical cost estimation approach is impossible.

Therefore, the cost estimation method used in this chapter is the analytical cost estimation technique. By using this method, only the production time and hourly rate for the man, machine and resources need to be investigated. The associated manufacturing costs can be calculated by multiplying times and rates together. Traditionally, this approach to obtain the production information is time consuming and costly. However, because of the process simulation carried out in previous chapters, it is possible to use the simulation approach to investigate the production time.

As the production time is investigated by using the analytical cost estimation technique, it is easier to assess how cost varies with production quantity. Therefore, the cost estimation method used is the fixed cost and variable cost method. The fixed cost refers to the capital cost for machines, rental cost for site, development cost for new product and administration cost, etc. These costs are fixed even if there is no product output. Investigating such costs can be relatively simple and easy. Therefore, the cost estimation focussed mainly on the variable costs of the casting process.

Variable costs refer to process costs such as raw material cost, labour cost, the inventory cost and facility maintenance cost, etc. These costs are influenced by the amount of output of the products. Generally, as the output increases, the time for production increases, the raw material requirement increases and the price of material may decrease. The longer the machine is in operation, the possibility of breakdown increases and the cost of maintenance increases. Therefore, it is easy to see that most variables are inter-connected. Changing one variable may change in others. Therefore, to coordinate all the variables and to estimate the cost of the production, a cost estimation model will be developed.

6.3 Model development

The model developed in Chapter 5 is still useful for the cost estimation model. The casting size of up to 10 kg is used for both casting processes. The CRIMSON process uses a rapid melting furnace, which has 300 kW power output. The conventional process uses a 500 kg furnace all the time. However, there is one difference between the cost estimation model and the productivity model. The cost estimation model investigates the production time for different amounts of product output. Therefore, a new assumption is added to the model, which is that the customer requirement for casting products depends on real demand. The normal total demand is shown in the following table and the production time for each demand can be then recorded.

100	200	300	400	500	700	1000	1500	2000	2500
3000	4000	5000	7000	10000	15000	20000	25000	35000	50000

Table 6-1 Quantity of the shipment by customer requirement

6.4 Development of casting cost estimation model

According to the assumptions, the variable costs modelled are raw material cost, energy cost for melting and labour cost. The total variable cost can be calculated as below:

$$C_{Total\ variable} = C_{raw\ material} + C_{energy} + C_{labour} \quad \text{Equation 28}$$

6.4.1 Raw material cost

For the estimation of the raw material cost, the key element is the unit cost of the aluminium. For the CRIMSON process, pre-alloyed high-quality aluminium was used. Typically, the price of such metal is around £1.5·kg⁻¹ to £1.9·kg⁻¹. A database of the price of casting aluminium alloy was developed based on CES 2011. For the conventional casting sand

process, a normal ingot was used as the input metal for the purposes of cost reduction. From the metal price website (Alu13), an aluminium ingot costs about £1.22·kg⁻¹. From the data provided by the partner foundry, the sand cost can be as low as £0.03·kg⁻¹ for silica sand and can be as high as £1.8·kg⁻¹ for zircon sand.

Because this is a continuous production process, it is possible to use recycled material for the casting production. Therefore, the price of recycled metal and sand will be used. From Greengate Metals website (Scr13), the value of in-house aluminium scrap is about £0.65·kg⁻¹. From the partner foundry, the cost of reclamation is £0.015·kg⁻¹ for all kinds of sand. A melting weight of 3 kg (can produce 1 kg of good CRIMSON product) is assumed. After the first cycle of the casting process, 1.96 kg of metal can be used for the second cycle (65% recovery ratio) and only 1.04 kg of new metal is required to produce the second casting. By splitting the melting metal into recycled and new metal, as the recycling process continues, the original aluminium will be completely replaced by new metal after a certain number of operations. For this particular example, 3 kg of aluminium can be digested in 16 operation cycles. In these cycles, 47.65 kg of aluminium was melted and 8.73 kg of metal was contributed by recycled metal. Assuming CRIMSON metal is £1.5·kg⁻¹ and the in-house scrap is £0.65·kg⁻¹, the total cost of metal is £64, which is less than the £72 it would cost if only virgin aluminium was used.

According to this assumption, the cost equation of the raw material can be derived as below:

$$c_{metal} = \frac{total\ shipment}{n} \times [c_{unit\ cost\ of\ scrap} \times (\sum_1^n W_{mn} \times RR + W_{m1}) + c_{unit\ of\ new\ Al} \times \sum_1^n (W_{m1} - W_{mn} \times RR)] \quad \text{Equation 29}$$

$$W_{n+1} = W_n \times RR \quad \text{Equation 30}$$

where

c_{metal} is the cost of metal; $c_{unit\ cost\ of\ scrap}$ is the unit value of in-house scrap; $c_{unit\ of\ new\ Al}$ is the unit cost of new aluminium alloy; W_{mn} is the weight of the metal melted at a particular cycle; RR is the recovery ratio for the casting process; it represents how much metal can be recycled in one cycle; n is the number of operation cycles; it represents how many cycles before the recycled metal is fully replaced by new metal.

Through similar reasoning, the sand cost can be presented as below:

$$c_{sand} = \frac{total\ shipment}{n} \times [c_{unit\ cost\ of\ reclamation} \times (\sum_1^n W_{sn} \times RR + W_{s1}) + c_{unit\ of\ sand} \times \sum_1^n (W_{s1} - W_{sn} \times RR)] \quad \text{Equation 31}$$

where

c_{sand} is the cost of sand for the casting production; $C_{unit\ cost\ of\ reclamation}$ is the cost of reclamation; only thermal reclamation is considered in this cost model; W_{sn} is the weight of sand used at a particular cycle; RR is the recovery ratio for sand reclamation; it represents how much sand can be recycled in one cycle; n is the number of operation cycles; it represents how many cycles before the recycled sand is fully replaced by new sand.

6.4.2 Energy cost

Regarding the melting, the conventional sand casting process uses a gas furnace to melt the aluminium to its melting point (660°C), after which it is transferred to a holding furnace to be superheated to 700–750 °C. The energy efficiency for a gas furnace is about 50%. Using tensile test bar as example, 12.68 kg of aluminium will consume 14444 KJ. As the energy price shows on Europe’s Energy Portal website (Portal, 2013), natural gas in the UK costs £0.024·kWh⁻¹. Therefore, the conventional casting process costs about £0.12 per casting. For the holding operation, the literature indicates that it uses the same amount of energy as the melting process but costs more because it uses electricity. As the literature shows, the holding operation costs 1.2 times more than the melting process (DETR, 1997). Therefore, the holding cost is £0.13 per casting and the total cost is £0.25 per casting. By contrast, the CRIMSON process only uses electricity to melt metal up to 750 °C. Assuming 50% energy efficiency, its energy cost per casting is about £0.22.

$$C_{CRIMSON} = \{[c_{ps} \times (t_{melt} - t_{room}) + c_{pl} \times (t_{super} - t_{melt}) + E_f] \times m_{melt}\} \div e \times C_{unit\ energy}$$

Equation 32

$$C_{conventional} = 2.2 \times \{[c_{ps} \times (t_{melt} - t_{room}) + c_{pl} \times (t_{super} - t_{melt}) + E_f] \times m_{melt} \div e \times C_{unit\ energy}\}$$

Equation 33

where

$C_{CRIMSON}$ is the energy cost for the CRIMSON process; $C_{conventional}$ is the energy cost for the conventional process; c_{ps} is the specific heat of metal in the solid phase; c_{pl} is the specific heat of metal in the liquid phase; t_{room} is room temperature; t_{melt} is melting temperature; t_{super} is the superheated temperature; m_{melt} is the mass of molten metal; e is the melting efficiency ; $C_{unit\ energy}$ is the unit energy cost (electricity or gas); E_f is the heat of fusion, 389 kJ·kg⁻¹ (°C).

6.4.3 Labour cost

Labour cost is a function of the equipment, the labour and the time required to produce a certain amount of products. As stated previously in the assumptions, the CRIMSON process has six operators and the conventional process has seven operators. Assuming the national minimum wage is used, the labour costs will be:

$$C_{labour} = \sum_1^n (N_n \times Wage_n) \times t \quad \text{Equation 34}$$

where

C_{labour} is the cost of the labour; $Wage_n$ is the wage for particular job n ; N_n is the number of the operators for job n ; t is the time required for a certain amount of production; different casting processes have different ways to calculate this parameter.

Because the melting process has the longest cycle time, the labour hours will be determined by the melting time for the CRIMSON process. The melting time is calculated by the melting energy over the furnace power output.

$$t = E \div P \times shipment \quad \text{Equation 35}$$

By contrast, the conventional process uses a different approach because of the fixed furnace. For the conventional process, a 500-kg furnace with a two-hour melting time was used. Depending on the casting size, the number of moulds that can be poured is different:

$$t = t_m \times \frac{shipment}{n} \quad \text{Equation 36}$$

where

t_m is the time for melting; fixed at two hours in this study

n is the number of moulds needed for 500 kg of metal

For the same reason that the calculated product output will not be the same as in the simulation results, the actual time will not be the simple linear relation shown in the above equation. [Figure 6-2](#) shows the ratio between simulation results and the calculation results when 100 kW of power is applied. The higher the ratio means the higher the difference between simulation and calculation results. Clearly, the difference reduces as the casting weight is increased and it reduces as the output is increased. Therefore, the above equation works very well for heavy castings and high power output. However, for small castings, below 4 kg, the difference between the simulation and the calculation result is large. Similar

results can be seen for different furnace power outputs for the CRIMSON process (Appendix 31). To ensure the accuracy of the labour cost, the calculated time needs to match that simulated. To do this, a spreadsheet needs to be developed to analysis data.

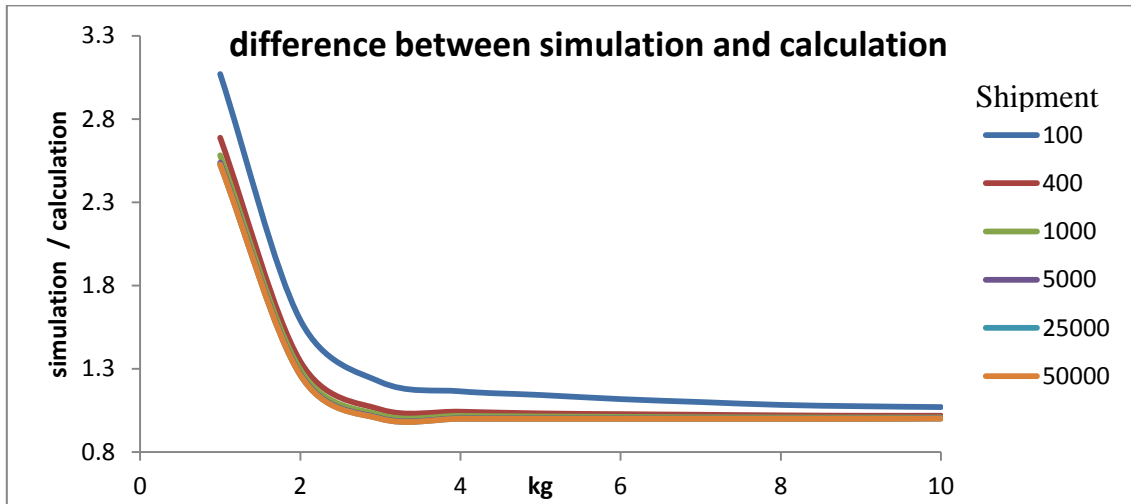


Figure 6-2 Ratio between simulated and calculated results for the CRIMSON process under 100 kW power output. The simulation and calculation results can be same only if the ratio equal to one. Otherwise, they are different.

6.5 Development of the cost calculation spreadsheet

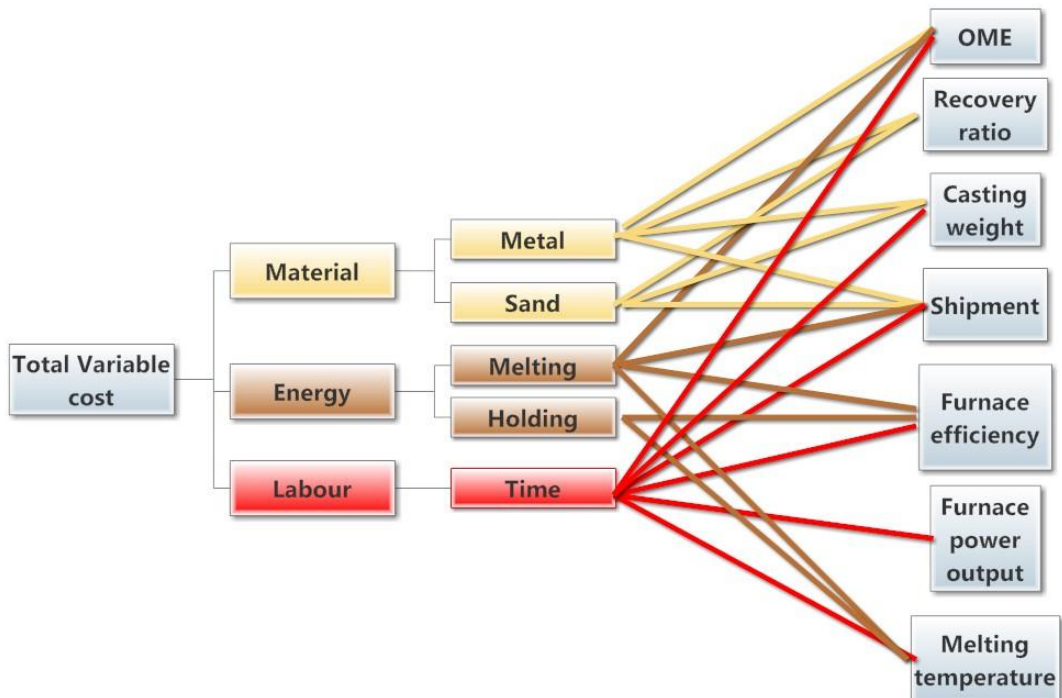


Figure 6-3 Schematic of the relation between variable cost and variables

Figure 6-3 shows the relation between the variable cost and the variables. Most of the variables are connected with more than one variable cost. Any change of a parameter might cause a different cost estimation result. Moreover, not only might the total cost of the production change but something like the time distribution and cost contribution might change as well. Therefore, in order to gain a complete view of the cost model, it was necessary to develop a spreadsheet that can integrate all the variables.

6.5.1 Calculation spreadsheet introduction

The spreadsheet can be divided into three sections according to the variable cost: raw material cost, energy cost and labour cost. There are three colours in the spreadsheet. The blue cells indicate optional data that can be decided upon by the user. These cells represent the variables in equations. The red cells represent the result according to the user input and the black cells show the fixed value according to literature and experience.

the CRIMSON Process	
Melting temperature °c	750
Energy consumption (kJ)	9772
Efficiency	0.5
Real energy consumption (kJ)	19545
Total energy consumption for all shipment (kJ)	195447122
energy (kWh)	54291

Figure 6-4 Illustration of the colour system in the spreadsheet

6.5.1.1 Raw material cost

For the estimation of raw material costs, only the costs of the sand and aluminium are collected. Because recycling and reuse are adopted, the cost of material is the sum of cost of the recycled materials and virgin raw materials. Therefore, the basic requirement is the weight of the material and the unit cost of the material. The operational material efficiency (OME) is used for the melting metal weight calculation. The user can decide the amount of metal input and loss during each process. The OME can then be calculated according to the input data and the true mass melted can be determined. For the sand consumption, the sand to metal ratio of 6: 1 is used. Because recycling and reuse are adopted for both casting processes, the weight of the recycled material and new material are calculated according to Equation. 29 and Equation. 31. For the unit cost of the material, the data come from three different resources. The price of the CRIMSON metal comes from the CES 2011, the price of the

conventional process metal comes from the Internet and the price of the sand comes from the foundry expert (appendix 32, pp208).

6.5.1.2 Energy cost for melting and holding

As [equation. 32](#) and [33](#) show, the energy cost is the product of energy consumption and unit energy cost. Energy consumption depends on the casting size, the OME, the shipment and the melting temperature, which can be defined according to the user requirements. The unit cost of the metal can be found on Europe's Energy Portal website (Portal, 2013).

6.5.1.3 Labour cost

The key to the calculation of labour cost is the time calculation. The production time is influenced by the casting size, the output size and the furnace power output. Therefore, a lookup function was used in the spreadsheet to locate matched simulation times. The user only needs to input the casting size, the desired output size and the furnace power output and then the spreadsheet will find automatically the best fitting production time. The labour cost can be calculated based on [Equation. 34](#).

Please refer to the Appendix 33 (pp210) for the full version of the cost estimation spreadsheet.

6.5.2 Case study

Two cases have been chosen to demonstrate how to use the spreadsheet. A variable cost comparison between the CRIMSON and the conventional processes has also been made.

6.5.2.1 Case study 1: tensile test bar

The tensile test bar has been chosen to demonstrate how to use the spreadsheet. According to a previous study, the following data can be input into the spreadsheet.

Step 1: recovery ratio and operational material efficiency

Step 1 is used to calculate the recovery ratio and operational material efficiency. The recovery ratio is used to calculate how much metal can be recycled. The operational material efficiency is used to calculate how much metal needs to be melt for the casting. According to real situations, the user can input into the spreadsheet the melting loss, holding loss, degassing loss, fettling loss, machining loss and the scrap rate. Consequently, the corresponding recovery ratio and OME can be determined. In this case, the recovery ratio for the CRIMSON process and conventional process is 0.76 and 0.79, respectively. The OME for the CRIMSON and conventional process is 0.24 and 0.12, respectively.

Step 2: material consumption and shipment

The user inputs the casting weight from 0 to 10 kg. According to the OME calculated in step 1, the weight of the melting metal can be calculated. In the spreadsheet, the metal to sand ratio 1: 6 is used to calculate the sand requirement. In this case, one set of tensile test bars (six pieces) weighs about 1.56 kg. The metal required for the CRIMSON process and conventional process is 6.53 and 12.67 kg, respectively. The sand required to make the mould is 40 and 76 kg, respectively. Finally, the user decides the total amount of castings that need to be produced.

Step 3: metal and sand selection

Step 3 is used to select the desired metal and sand for the casting. It will be used for the material cost calculation. In this section, the user selects the metal and the sand. Because recycling and reuse are adopted, the in-house value of the metal and the price of reclaimed sand are also valuable.

Step 4: breakdown material into new and recycled

The material is composed of new material and recycled material. As the example in Section 4.1 shows, a special method was developed in the spreadsheet to split them. According to the recovery ratio calculated in step 1 and the melting weight calculated in step 2, the operation cycle to consume all the recycled metal and sand can be calculated. For the CRIMSON process, the metal can be consumed within 26 cycles and the sand can be consumed within 86 cycles. For the conventional process, the metal can be consumed within 34 operations and the sand can be consumed within 92 operations. The cost of each material can be seen in the following table.

metal input during the recycle cycle			
CRIMSON		conventional	
<=26		<=34	
recycle (kg)	new metal input (kg)	recycle (kg)	new metal input (kg)
27	143	60	371
CRIMSON sand		conventional sand	
<=86		<=92	
recycle (kg)	new sand input (kg)	recycle (kg)	new sand input (kg)
391	2978	759	6231

Table 6-2 Operation cycles to consume the recycled metal and total weight of recycled metal and new metal

Step 5: time consumption for operation

Step 5 is used to determine the production time for the entire operation. It will be used for the calculation of the labour cost.

The CRIMSON process

As introduced before, the melting time can be the longest cycle time within the casting process. Therefore, the production time is based on the melting time for the CRIMSON process. However, the melting time is not accurate enough to predict the production time. Therefore, an equation was developed, based on the simulation results, to predict the production time. According to this equation, the spreadsheet will measure automatically the influence of the power output, casting size and shipment and thus, a proper production time can be calculated.

The conventional process

For the conventional process, the furnace is fixed at 500-kg capacity with a two-hour melting time. The production time calculation is slightly different. According to the melting weight calculated in step 2, the number of pourings can be calculated. In this case, 500 kg of melting metal can make 39 castings in two hours. Therefore, the time required for one mould can be calculated, as can the total time. Again, these calculated results are not accurate enough to predict the production time. The simulation was introduced to optimise the predicted results.

Step 6: energy consumption calculation

Step 6 is used to calculate the energy consumption required to melt the aluminium at the desired temperature. It will be used to calculate the energy cost. According to the energy calculation in step 5 and the shipment input in step 2, the total energy consumption of the CRIMSON process can be determined. Similarly, the conventional melting energy can be worked out.

Step 7: total variable cost

All calculated results are gathered in step 7 and the final cost of materials, labour and energy are displayed. For the tensile test bar case study, the total variable cost is shown in the following table:

	Recovery Ratio	OME	Melting Weight (kg)	Sand Weight (kg)	Shipment	Meal	Sand	Melting Time (min)
CRIMSON	0.75	0.24	6.53	39.19	1000	A356 T6	Silica Sand	3.77
Conventional	0.72	0.12	12.67	75.99				3.04

Table 6-3 Key variables used to calculate the variable cost

CRIMSON			Conventional		
metal	recycle £	670	metal	recycle £	1148
	new £	9025		new £	13296
sand	recycle £	68	sand	recycle £	124
	new £	1039		new £	2032
energy £		239	energy £		258
labour £		2640	labour £		2482
total £		13680	total £		19341

Table 6-4 Total variable costs for both casting processes

6.5.2.2 Case study 2: piston head

The geometry selected for case study 2 is an engine piston head, which can be produced by sand casting. The spreadsheet was used to design the casting running system in this case study. According to author's experience, four piston heads produced in one running system weigh about 1.93 kg. Figure 6-5 shows the casting running system for the piston head. The left-hand side is the CRIMSON running system and the right-hand side is the sand casting running system.

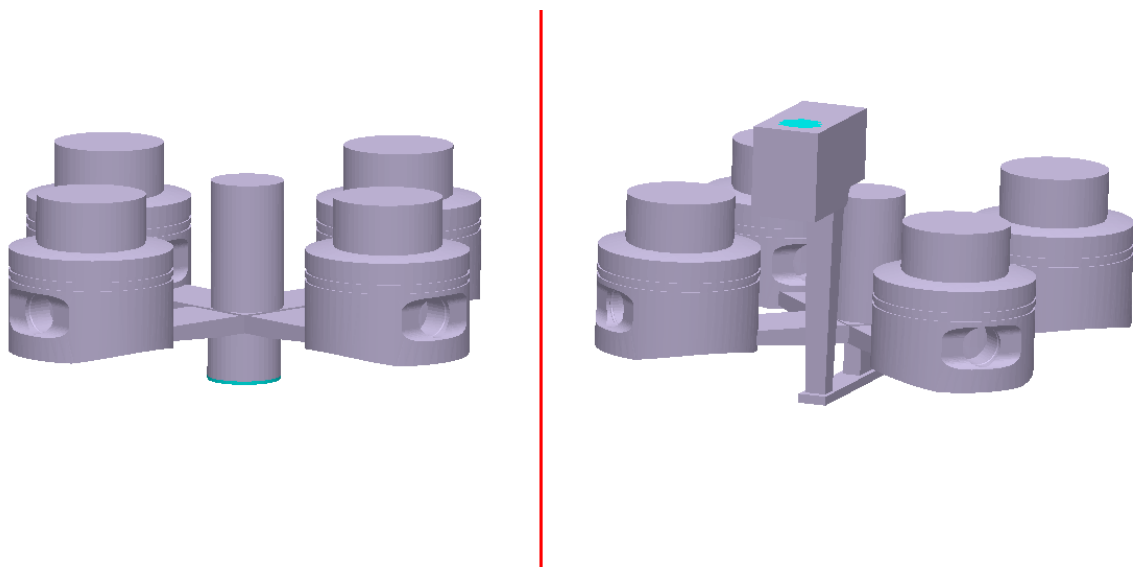


Figure 6-5 Schematics of the running system design for piston head. The left-hand side is the CRIMSON running system and the right-hand side is the conventional sand casting system. The casting yield for the CRIMSON system is 58% and the casting yield for the conventional system is 52%

Following the same steps as shown in case study 1, the piston head case study has the following variable input and cost results:

	Recovery Ratio	OME	Melting Weight (kg)	Sand Weight (kg)	Shipment	Meal	Sand	Melting Time (min)
CRIMSON	0.6	0.39	4.95	29.73	1000	A354 T6	Silica Sand	2.86
Conventional	0.57	0.28	6.78	40.68				1.63

Table 6-5 Key variables used to calculate the variable cost

CRIMSON			Conventional		
metal	recycle £	573	metal	recycle £	801
	new £	7562		new £	6905
sand	recycle £	73	sand	recycle £	97
	new £	744		new £	1047
energy £		180	energy £		140
labour £		1839	labour £		1707
total £		10974	total £		10698

Table 6-6 Total variable cost for case study 2

6.6 More results and discussions

Two case studies have been presented in the previous sections and their results are summarised in the following. The casting weight of the tensile test bar and the piston head is 1.56 and 1.93 kg, respectively. The cost of the tensile test bar is £13679 and £19340 for the CRIMSON and conventional sand casting processes, respectively. The cost of the piston head is £10974 and £10698 for the CRIMSON and conventional sand casting processes, respectively.

This is a surprising result because the lighter casting (tensile test bar) actually costs more than the heavier casting (piston head). Initially this result was unanticipated and so the results were re-examined to debug errors and establish whether the results were correct.

According to the information shown in Tables 6-3 and 6-5, the OME for the tensile test bar varies from 0.12 to 0.24 and it varies between 0.28 and 0.39 for the piston head. Therefore, even though the tensile test bar is lighter than the piston head, it still requires more metal to cast, which means that the cost of the metal becomes higher. Figure 6-6 shows the cost contribution of each variable cost. Clearly, the contribution of the metal cost is the most significant in the production cost. It comprises at least 70% of the total variable cost, which is why the tensile test bar has a higher cost than the piston head. This indicates the importance

of the OME; the higher the OME, the less material needed to make the casting and thus, the lower the associated material costs.

From these two case studies, it is found that the OME can influence the cost estimation results significantly. Such results prove that any parameter change can cause a different cost estimation result. In the following results section, the influence of different manufacturing methods, materials and process parameters will be discussed.

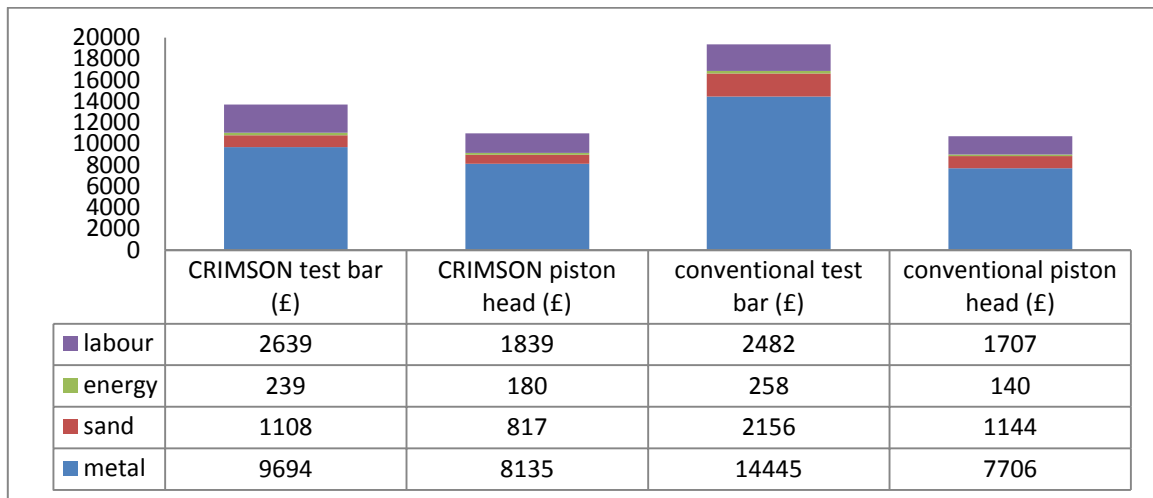


Figure 6-6 Cost breakdown for the two case studies

6.6.1 Recovery ratio influence

In addition to the OME, the recovery ratio may also influence the total variable cost. The metal recovery ratio has a relation with casting yield, machining loss and scrap rate. Any change in the recovery ratio requires a change in the casting design. Therefore, it is impractical to investigate the influence of the metal recovery ratio. In this section, only the sand recovery ratio is investigated. The parameters used to investigate the variable costs are listed in Table 6-7 and the results shown in Figure 6-7.

	CRIMSON		Conventional	
	type	price (£/kg)	type	price (£/kg)
metal	A201 T7	1.7	A201 T7	1.22
sand	Chromite	0.65	Chromite	0.65
OME	34%		27%	
Metal Recovery ratio	0.66		0.64	
furnace power	100 KW		NA	
sand reclaim method	Thermal reclaim which gives 98% recovery			
shipment	10,000			
casting weight	3 kg			

Table 6-7 Parameters used to investigate the influence of recovery ratio

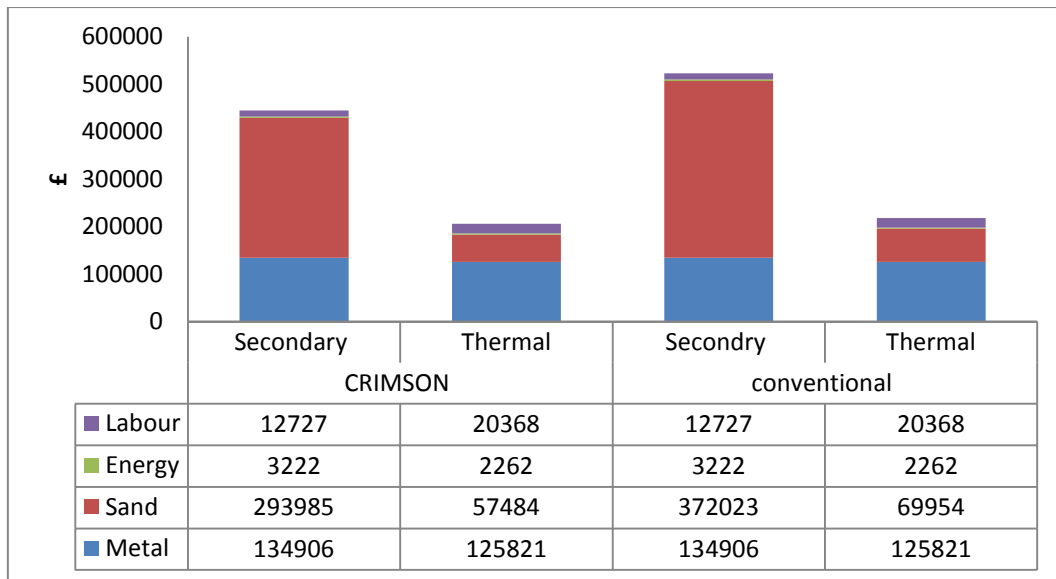


Figure 6-7 Cost contribution for different sand reclamation methods (different recovery ratios)

The influence of the sand recovery ratio can be easily found in Figure 6-7. Clearly, sand costs can be high when radical reclamation methods are used (secondary reclamation). This is especially true when high-cost sands such as chromite and zircon are used (very rare in foundries). Therefore, the correct reclamation method not only reduces the sand costs but also brings down the total variable cost.

6.6.2 Material influence

Currently, 22 aluminium alloys and 4 types of sand can be chosen from the spreadsheet. In order to show the material influence on the total variable cost, the same product produced by three different material groups was carried out. The three material groups were a low price combination of sand and metal, a middle price combination of sand and metal and a high price combination of sand and metal. The parameters used to investigate the variable costs are listed in Table 6-8 and the results are shown in Figure 6-8.

	CRIMSON		Conventional	
	metal	price (£/kg)	metal	price (£/kg)
low	pure s1s0: LM0-M	1.5	pure s1s0: LM0-M	1.22
middle	A201 T7	1.7	A201 T7	1.22
high	A357 T7	1.86	A357 T7	1.22
	sand	price (£/kg)	sand	price (£/kg)
low	silica	0.03	silica	0.03
middle	Chromite	0.65	Chromite	0.65
high	zircon	1.8	zircon	1.8
OME	34%		27%	
Recovery ratio	0.66		0.64	
furnace power	100 KW		NA	
shipment	1000			
casting weight	3 kg			

Table 6-8 Parameters used to compare the variable costs

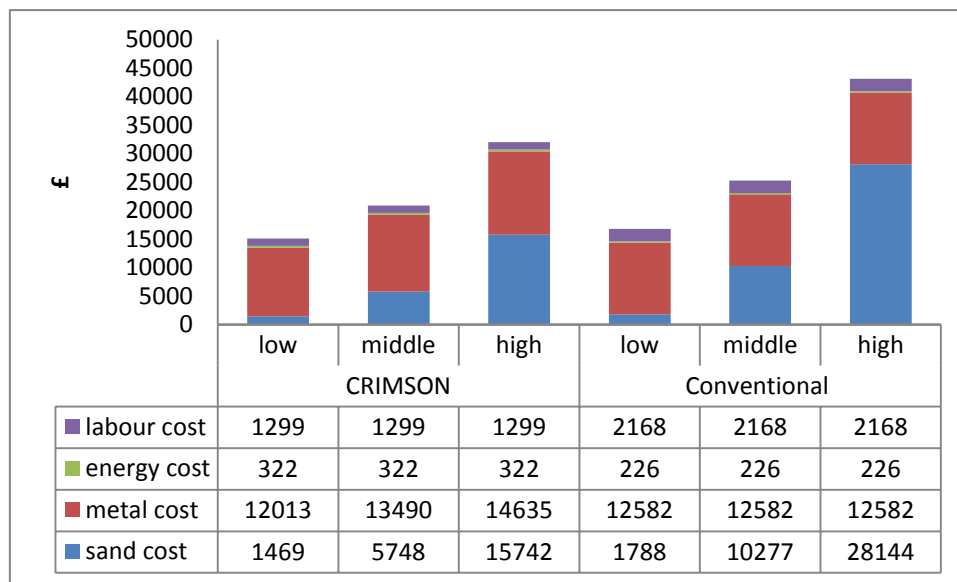


Figure 6-8 Contribution of the different variable costs

From Figure 6-8, it can be seen easily that the material cost is the major contributor to the total variable cost. However, for different categories, the cost contribution is slightly different. For low cost material, the major contributor is the metal cost. For middle cost material, the cost of sand increases and for high cost material, the major contribution shifts to the sand cost. Overall, the material cost contributes the largest effect on the variable cost. Therefore, choosing the correct material for the job is quite important.

6.6.3 Casting size influence

Casting size determines the total amount of melted metal needed and the total amount of sand needed for the mould. Therefore, it makes sense to investigate its influence on the total

variable cost. The parameters used to compare the variable costs are listed in Table 6-9 and the results are shown in Figure 6-9.

	CRIMSON		Conventional	
	type	price (£/kg)	type	price (£/kg)
metal	A201 T7	1.7	A201 T7	1.22
sand	Chromite	0.65	Chromite	0.65
OME	34%		27%	
Metal Recovery ratio	0.66		0.64	
furnace power	100 KW		NA	
sand reclaim method	Thermal reclaim which gives 98% recovery			
shipment	10000			
casting weight	1 kg to 10 kg			

Table 6 -9 Parameters used to investigate the influence of size

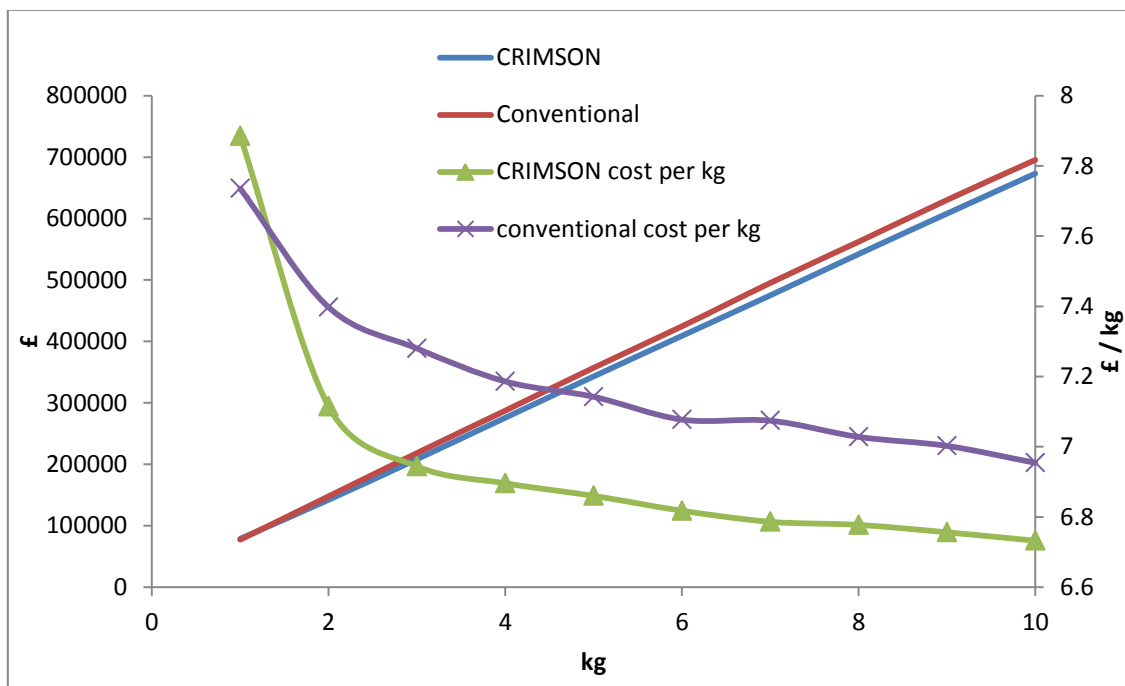


Figure 6-9 Total variable cost for different sizes of casting and the cost per kg as the casting size increases

It can be seen that the total variable cost increases as the casting size increases. However, as the casting size increases, the cost per kilogram of the casting decreases. The CRIMSON process has the lower unit cost in producing 1 kg of good casting.

6.6.4 Batch size influence

Batch size also determines the total amount of melted metal needed and the total amount of sand needed for the mould. Therefore, it makes sense to investigate its influence on the total

variable cost. The parameters used to investigate the variable costs are listed in Table 6-10 and the results are shown in Figure 6-10.

	CRIMSON		Conventional	
	type	price (£/kg)	type	price (£/kg)
metal	A201 T7	1.7	A201 T7	1.22
sand	Chromite	0.65	Chromite	0.65
OME	34%		27%	
Metal Recovery ratio	0.66		0.64	
furnace power	100 KW		NA	
sand reclaim method	Thermal reclaim which gives 98% recovery			
shipment	100 to 30000			
casting weight	3 kg			

Table 6-10 Parameters used to investigate the influence of batch size

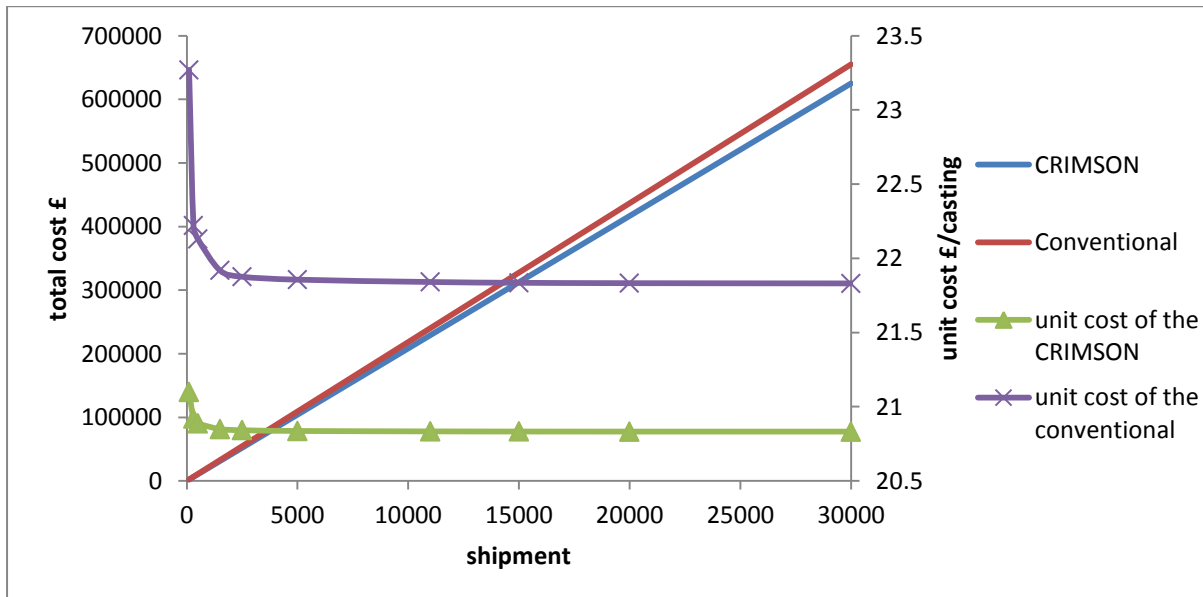


Figure 6-10 Results show total variable costs vary with batch size and unit cost to produce one casting

As with the size, the total variable costs increase as the batch size increases. However, as the batch size increases, the unit cost to produce one casting decreases. The unit cost for the CRIMSON process can be stabilised when the shipment increases to 1500. For the conventional casting sand process, the unit cost can be stabilised when the shipment increases to 2500.

When the shipment number increases 1500, the curve tends to stabilise for the CRIMSON process.

6.6.5 Power output influence

The CRIMSON furnace can supply power up to 300 kW. It has been made clear that the productivity of the CRIMSON process is influenced significantly by the furnace power output. Therefore, it is worth investigating the influence of the power output on the total variable costs. The parameters used to investigate the variable costs are listed in Table 6-11 and the results are shown in Figure 6-11.

	CRIMSON		Conventional	
	type	price (£/kg)	type	price (£/kg)
metal	A201 T7	1.7	A201 T7	1.22
sand	Chromite	0.65	Chromite	0.65
OME	34%		27%	
Metal Recovery ratio	0.66		0.64	
furnace power	40 KW to 300 KW		NA	
sand reclaim method	Thermal reclaim which gives 98% recovery			
shipment	10,000			
casting weight	3 kg			

Table 6-11 Parameters used to investigate the influence of power

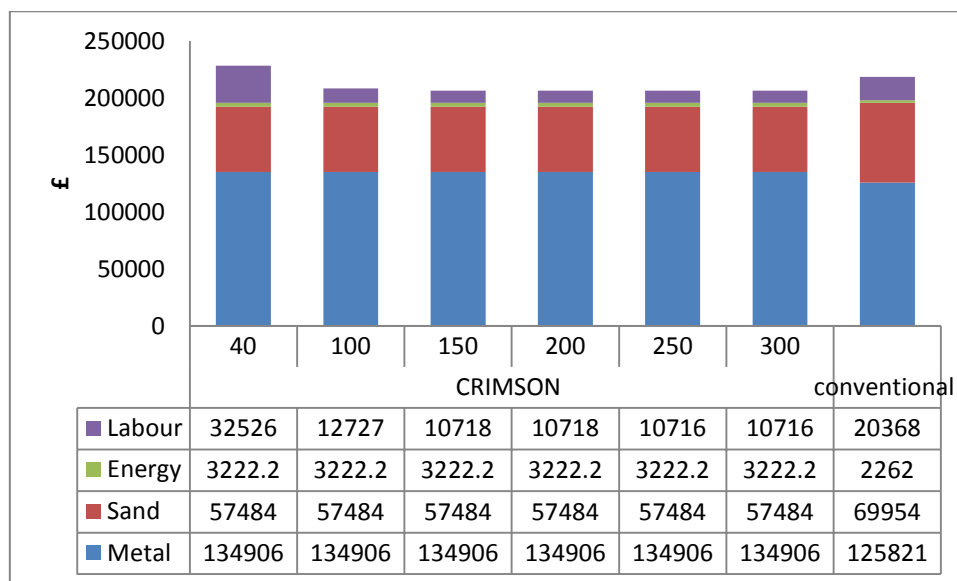


Figure 6-11 Total variable costs for different power outputs for the CRIMSON process

From Figure 6-11, it is easily to see that the power output has no effect on the raw material costs. It only influences the labour cost; the higher the power output, the lower the labour cost. This is probably because the productivity increases with an increase of power output. However, as discovered in the last chapter, there is a critical point beyond which, for any

additional increase in power output, there is no further increase in productivity. In this case, the critical power output is 150 kW.

6.7 Summary of chapter

In this chapter, a cost estimation spreadsheet was developed to estimate the total variable costs for the CRIMSON and conventional sand casting processes. By using this spreadsheet, the cost of the casting production could be estimated under different casting sizes, shipment sizes, furnace power outputs, OME and more. The case studies carried out in the last section covered all the variables that can influence the variable costs of casting. Based on those results, a box plot has been used to illustrate the distribution of the cost comparison of the CRIMSON and conventional sand casting processes.

This box plot is the result of the CRIMSON costs divided by the conventional casting costs. Therefore, the CRIMSON process can be seen as expensive when the result is greater than 1. Conversely, the conventional casting process can be deemed expensive when the result is less than 1. From [Figure 6-12](#), it is easy to see that most data lie to the left-hand side of the base line. This means that the conventional casting process has higher total variable costs in most circumstances. However, there is an exception to this. The CRIMSON process can be expensive in certain cases. For instance, the CRIMSON process can be expensive when a low furnace power output is adopted, because low power output prolongs the production time, which increases the labour cost.

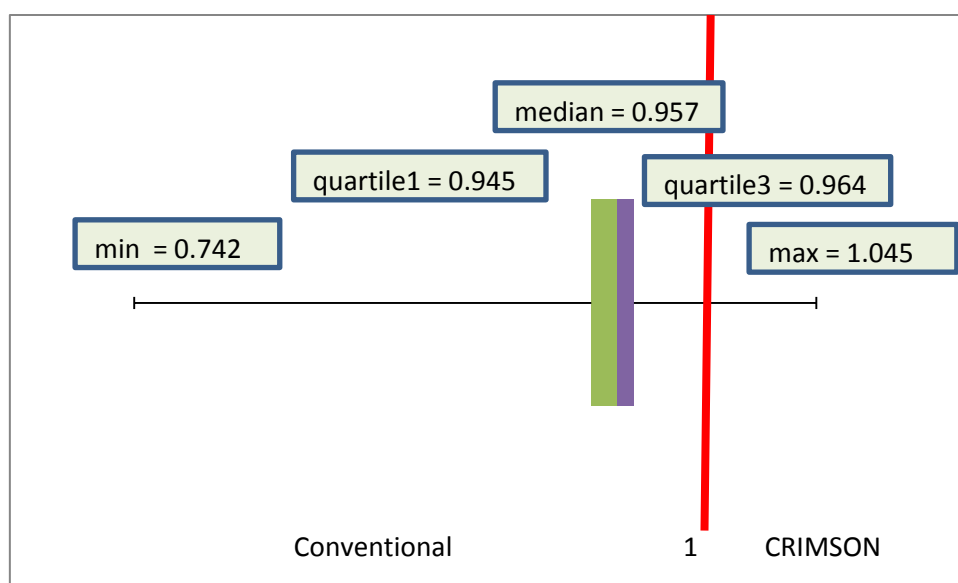


Figure 6-12 Comparison of the CRIMSON and conventional sand casting processes. The red line is the base line of the comparison. Left-hand side of the red line means that conventional casting is expensive, the right-hand side of the

red line means that the CRIMSON process is expensive and the red line means both casting processes have the same cost

Based on the case study results, the average cost contribution for each variable cost can also be plotted (Figure 6-13).

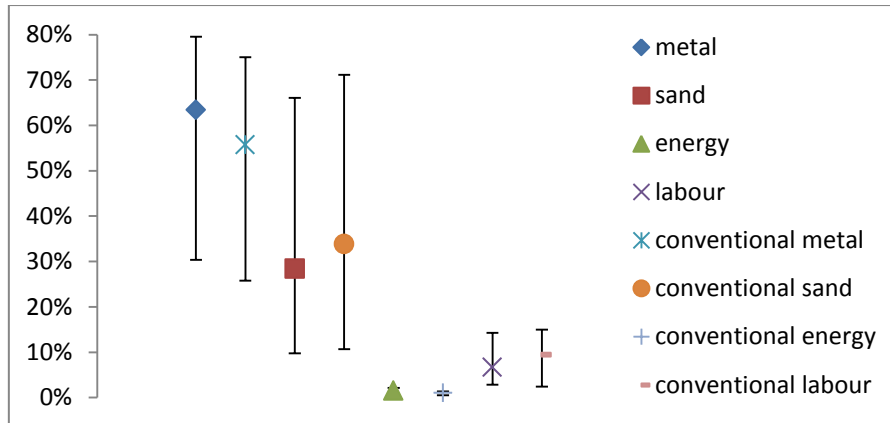


Figure 6-13 Average cost contribution and distribution of each variable cost

Irrespective of whether the CRIMSON or the conventional sand casting process is used, the energy costs only contribute about 1% of the total variable costs. In contrast, the metal costs contribute the greatest effect on the variable costs. In particular, the CRIMSON process has the highest cost contribution due to the high cost of the raw material. Because less material is required by the CRIMSON process, the CRIMSON process has low sand costs compared with the conventional sand casting process. According to the results shown in the last chapter, the CRIMSON process is more productive than the conventional sand casting process. Therefore, the labour costs can be cheaper because of the lower lead-time.

In addition to the average results of the variable costs, the above figure also indicates the distribution of each variable cost. The sand cost has the widest distribution because of the sand price. It can be as low as 10% when silica sand is used and as high as 70% when zircon sand is used. Because the sand has such a wide distribution, it affects the overall contribution of the metal cost. In contrast to the sand cost, the metal contribution is high when the sand cost is low and the metal contribution is low when the sand cost is high. Therefore, the metal has a similar distribution to the cost contribution.

Finally, several conclusions can be drawn from the case studies:

1. The influence of raw material is significant; it contributes at least 80% of the total variable cost.

2. The OME is a very important parameter. It decides the amount of metal and sand required for the casting process. Improving the OME can reduce the cost of the materials.
3. Irrespective of whether green sand or chemical sand is used, the thermal reclamation method is recommend for sand recycling. This is because thermal reclamation has the highest recovery ratio, which increases the utilisation of the used sand. In particular, for high-quality sand such as Zircon and Chromite sand, thermal reclamation can reduce the sand cost by up to 80% compared with the secondary reclamation method.
4. As the casting size and the shipment increase, the unit cost of casting decreases. This is exactly what happens when batch production is adopted.

The power output of the furnace influences only the productivity and labour cost of the production process.

Chapter 7 All-In-One spreadsheet development

The CRIMSON process has been compared with the conventional sand casting process through numerical simulation, life cycle assessment, productivity comparison and variable cost comparison. A running system design spreadsheet was used to design the casting running system in the numerical simulation comparison chapter. A spreadsheet was developed to estimate the embedded energy of sand mould making and casting making in the life cycle assessment section. Another spreadsheet was developed to estimate the casting variable cost in the cost estimation chapter. In this chapter, the author will introduce a new spreadsheet which can be used by industry people to design casting running system, to estimate the energy consumption and to estimate the production cost at early stage.

7.1 The all in one spreadsheet

After finish in of the development and comparison, the author realised that there are some connections between each spreadsheet. A parameter in one spreadsheet can influence the result of the other spreadsheet. Therefore, the author considered the idea to integrate all the spreadsheets together to form an all-in-one spreadsheet. To do so, it will be very useful at early stage of the product development. Then foundry people not only get idea about casting running system design, but also understand the energy consumption and cost estimation of the corresponding design.

Basically, the principle of the all in one spreadsheet can be seen from the figure. Different functions are connected by the shared information. By default, the information used in running system design will eventually influence the result of the cost estimation. However, the user can break the link between each function to use any function individually. By clicking the reset button, each function can be reconnected.

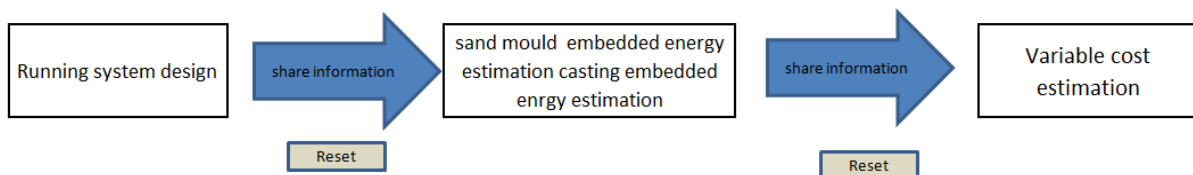


Figure 7- 1 schematics the flow chart of the all in one spreadsheet. Because of the shared information, each function can be connected

7.2 Share information

7.2.1 Casting weight

Starting from the casting weight, this is the first shared information identified. As introduced, it is the key information links everything together. Once the casting size is determined, the general size of the running system can be determined and amount of sand required can be determined as well. Based on this information, the energy consumption of the sand and metal can be estimated. The cost of sand, metal, energy, and possible labour time also can be estimated.

7.2.2 Casting yield

Casting yield is a ratio between casting weight and the pouring weight. Originally, this parameter is a performance indicator in the casting running system design spreadsheet. In the energy estimation spreadsheet, the casting yield also used to determine how much metal need to be chopped off (fettling operation). Because the fettling loss influences the recovery ratio (RR) and the operational material efficiency (OME), the casting yield has a relationship with these parameters aswell.

7.2.3 OME and RR

The operational material efficiency (OME) is a ratio between *good* casting product and metal melted (i.e considering casting yield, fettling and scrap rates as well). The Recovery ratio (RR) is a ratio that represents how much metal can be recycled in the process. These are two important parameters are used to estimate casting energy consumption in the energy estimation spreadsheet. However, these two parameters play vital roles in the cost estimation spreadsheet as well. The OME can be used to determine the actual amount of metal and sand required. The RR can be used to determine how much recycled metal can be used to replace the raw metal requirement.

7.3 Running system design

Running system design is the first part of the all in one spreadsheet. It can be used to determine the geometry of the gravity pour running system and CRIMSON up-casting running system. Jolly (appendix 34, pp211) developed the gravity pour running system spreadsheet and the author developed the CRIMSON up-casting running system spreadsheet. Originally, the user interface of such spreadsheet is not very user friendly. Considering the user experience, it is better to simplify it. As [figure 7-2](#) shows below, the input data and

output data are separated and the output data are categorized according to geometry feature. By doing this, the user can easily find any information they desired.

	A	B	C	D	E	F
25						
26						
27	CRIMSON user input				Out Put	
28		alloy	AI			inlet
29		density (cc/g)	2.385			diameter
30		casting weight (kg)	1.56	reset casting weight		50.00
31		feeder weight (kg)	1.4			inlet hight (mm)
32		casting and feeder (kg)	2.96			39.27
33						
34		inlet				vertical runner
35		inlet hight (mm)	20			diameter (mm)
36						50.00
37		Vertical runner				height
38		diameter (mm)	50			30.00
39		height	30			volume of vertical runn
40						58.90
41		runner				
42		number of runer	1			runner
43		width (mm)	50			number of runer
44		target height in the centre (mm)	10			width (mm)
45		choose height in the centre (mm)	20			50.00
						choose height in the ce
						length at bottom (mm)
						80.00
						length of the runner ba
						450.00
						volume of the runner (c
						239.91

Figure 7- 2 schematics the simplified spreadsheet for gravity running system design, the blue cells are the user input data, the red cells are the output results, the green one are the shared information with other sheet, and the black cell is the default value.

7.4 Energy consumption estimation

The function of the energy consumption spreadsheet has been introduced in chapter 4 section 4. The main function of the spreadsheet is same as before: estimate the energy consumption of the sand mould making and casting under multiple recycling method. In the all in one spreadsheet, the energy consumption spreadsheet was connected with the running system designing sheet by casting weight, yield, and recovery ratio (RR).

7.5 Variable cost estimation

Like the running system designing spreadsheet, the cost estimation spreadsheet wasn't user friendly. Therefore, the cost estimation spreadsheet was reformatted in a smart way. In the all-in-one spreadsheet, the cost estimation is separated into three tabs named as: cost information, production process information, and costing sheet. Cost information tab contains information such as cost of the raw material, labour rate, and energy cost. Production process information tab contains information such as casting weight, shipment, sand reclamation method, and energy consumption. Costing sheet is the summary sheet of the total variable cost.

Please refer to the Appendix 35 (pp212) for full version of the all-in-one spreadsheet

7.6 Case study

7.6.1 Calliper production

An aluminium calliper weight about 1.28 kg. The calliper is sand cast in an olivine sand mould. The customer requires 10000 callipers.

Running system design

First of all, the calliper is assessed by Magmasoft to determine possible casting orientation and size of the feeder. As figure shows below, such calliper has many curve surfaces and thick body. Considering the feeding and fettling, the calliper is cast in the vertical orientation as figure shows below. According to the Magmasoft results, hot spots are formed at the junction area. Therefore, cooling fins are introduced to increase the cooling rate at junction area to achieve more effective feeding. Figure 7.3 b on the right shows the casting with the feeder and the cooling fins. The feeder is about 0.43 kg by weight.

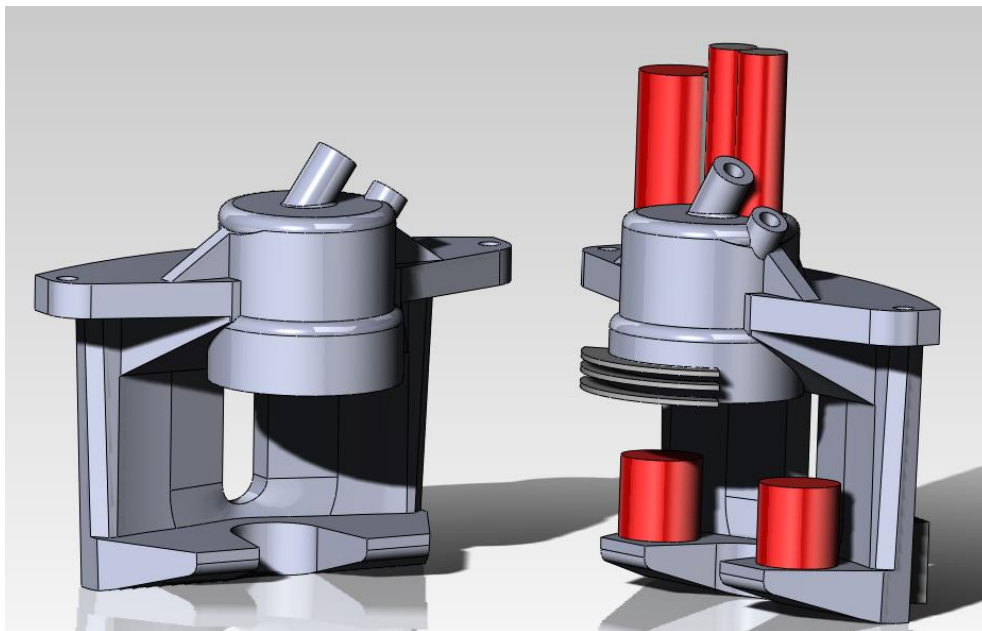


Figure 7- 3a left side is the geometry of the calliper. Figure 7- 3b right side is the casting orientation with feeder and cooling fin

Put casting and feeder information into designing spreadsheet. The high specification casting running system can be worked out. In order to maximise the productivity of the casting process, four callipers are produced in one running system.

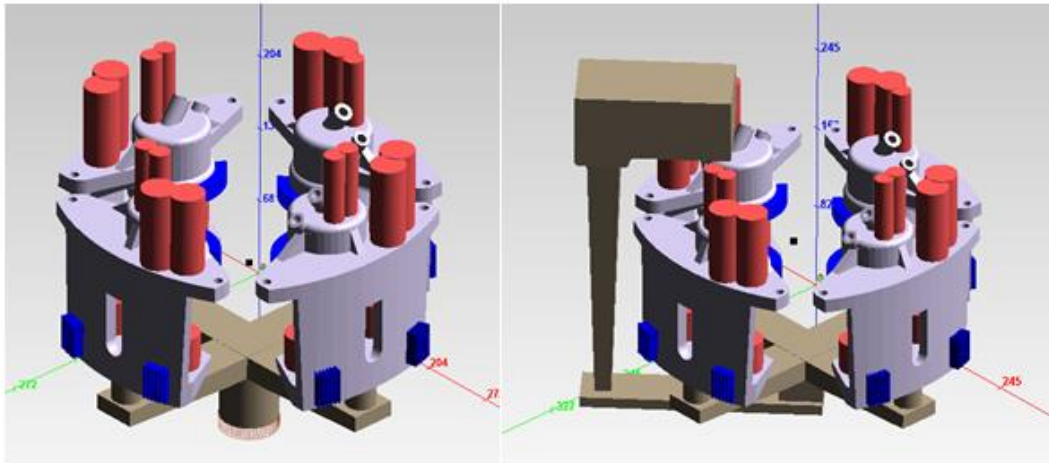


Figure 7- 4 running system on the left is for the CRIMSON process, the running system on the right is for the gravity sand casting process. Both are designed to the highest specification

According to the running system showed here. The casting yield, OME, energy consumption of this casting, the possible production lead time and the variable cost of the production can be estimated.

	casting yield	OME
CRIMSON	68%	46%
Conventional	58%	32%

Table 7- 1 the casting yield and OME results from the spreadsheet

energy burden (MJ/kg)		material consumed (kg)		energy consumption (MJ)	
		CRIMSON	conventional	CRIMSON	conventional
green sand energy	0.56	16.57	23.81	9.28	13.34
chemical sand energy	2.44	16.57	23.81	40.42	58.1
green sand primary reclamation after stable ²⁵	0.09	16.57	23.81	1.49	2.14
chemical sand secondary reclamation after stable	0.31	16.57	23.81	5.14	7.38
chemical sand thermal reclamation after stable	0.64	16.57	23.81	10.6	15.24
CRIMSON after stable	15.69	2.76		43.32	
Conventional after stable	17.38		3.97		68.98

Table 7- 2 energy burden and energy consumption of each operations

²⁵ The energy burden of the casting reduces to a constant level after certain number of recycling operation. Please refer to chapter 4, section 4.2.3.3 and figure 4-11 for more detail (pp90).

	CRIMSON	Conventional
production time (h)	213	641
sand cost (£)	10294	14111
metal cost (£)	150757	180782
energy cost (£)	4051	3252
labour cost (£)	9671	29188
total variable cost (£)	174773	227333

Table 7- 3 the production time and variable cost estimation

7.6.2 Sliding block

An aluminium sliding block weight 1.9 kg. The block is cast in silica sand mould. The customer requires 10000 blocks.

Running system design

Ideally, this sliding block can be produced by milling process. However, it requires a solid block has at least 180 x 85 x 120 mm. considering the material utilization, only 40% of the metal is used by machining method. Therefore, sand casting is introduced to produce this sliding block

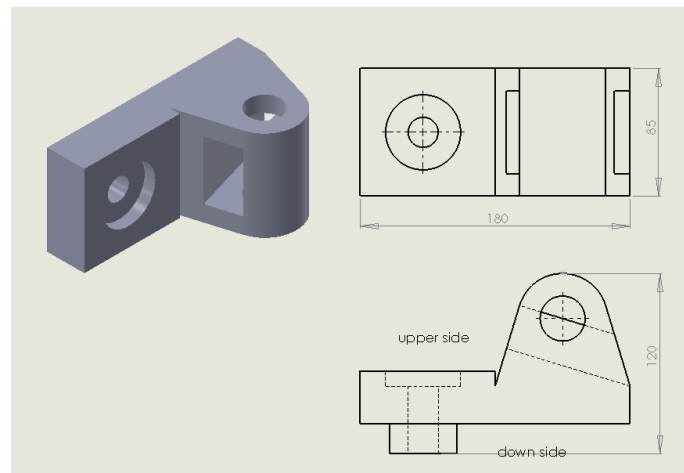


Figure 7- 5the geometry of the sliding block

Again, the block was assessed by Magmasoft to determine possible casting orientation and the feeder. Because the block has a curved surface, feeders should be avoided (hard for fettling and machining). Therefore, the casting is cast in the vertical orientation. As the entire casting is a solid block, hotspots can easily occur at thermal centre and cause porosity (circled in figure). According to the Magmasoft simulation results, the hot spot is circled in the following figure. A cooling fin is therefore used to improve cooling at thermal centre. As figure 7.6 showed below, the casting is cast in a vertical orientation, the feeders are on the top

of the casting, and the cooling fin is at centre of the casting. The feeder is weight 0.86 kg in total.

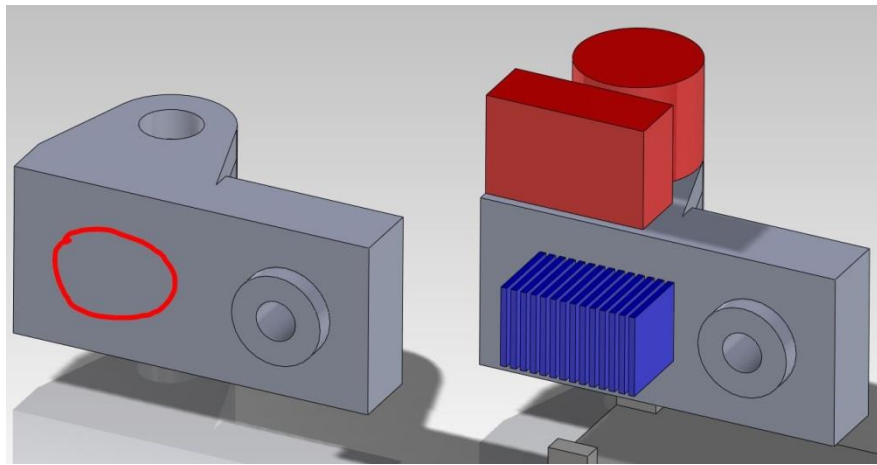


Figure 7- 6 the left side shows the casting orientation and the right side shows the casting feeder and cooling fin location

Input the casting and feeder information into the casting running system design spreadsheet. The casting running system for both casting process can be worked out.

According to the running system showed here. The energy consumption of this casting, the possible production lead time, the variable cost of the production can be estimated.

	casting yield	OME
CRIMSON	60%	41%
Conventional	49%	27%

Table 7- 4 the casting yield and OME results from the spreadsheet

energy burden (MJ/kg)		material consumed (kg)		energy consumption (MJ)	
		CRIMSON	conventional	CRIMSON	conventional
green sand energy	0.56	27.80	42.22	15.57	23.64
chemical sand energy	2.44	27.80	42.22	67.84	103.02
green sand primary reclamation after stable	0.09	27.80	42.22	2.50	3.80
chemical sand secondary reclamation after stable	0.31	27.80	42.22	8.62	13.09
chemical sand thermal reclamation after stable	0.64	27.80	42.22	17.80	27.02
CRIMSON after stable	15.69	4.63		72.71	
Conventional after stable	17.38		7.04		122.30

Table 7- 5 energy burden and energy consumption of each operations

	CRIMSON	Conventional
production time (h)	297	1132
sand cost (£)	6863	9752
metal cost (£)	202688	295027
energy cost (£)	6792	5661
labour cost (£)	13526	51517
total variable cost (£)	229869	361957

Table 7- 6 the production time and variable cost estimation

7.6.3 Casing

An aluminium casing is weight about 0.7 kg. The casing is casted in chromite sand mould. The customer requires 10000 castings.

Running system design

Unlike previous case studies, this casing is a very thin casing. Ideally, such casing can be easily cast by high pressure die casting method. However, let's see how this casing can be cast by the sand mould. The casting was assessed by the Magmasoft to determine the casting orientation and possible feeder location and size. figure below shows the casting orientation of the casing. The right side figure is the casting with the feeders.

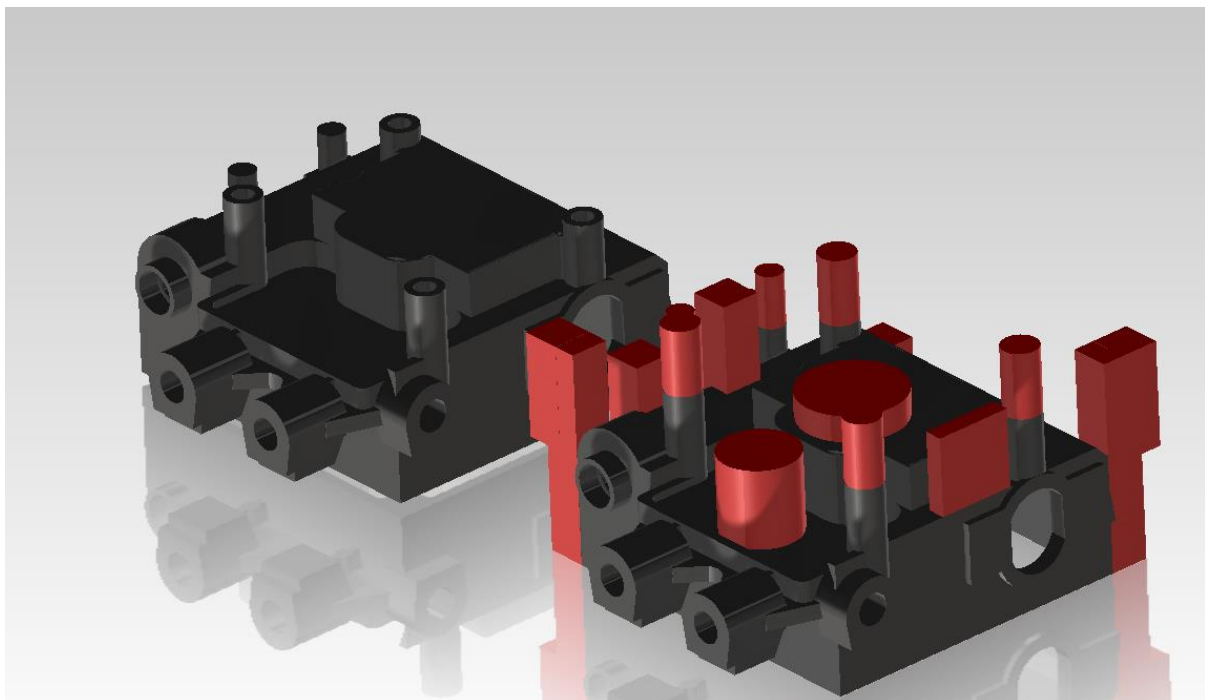


Figure 7- 7 shows the geometry and casting orientation of the casing.

Input the casting size and feeder information to the casting running system design spreadsheet. The casting running system for both casting process can be worked out.

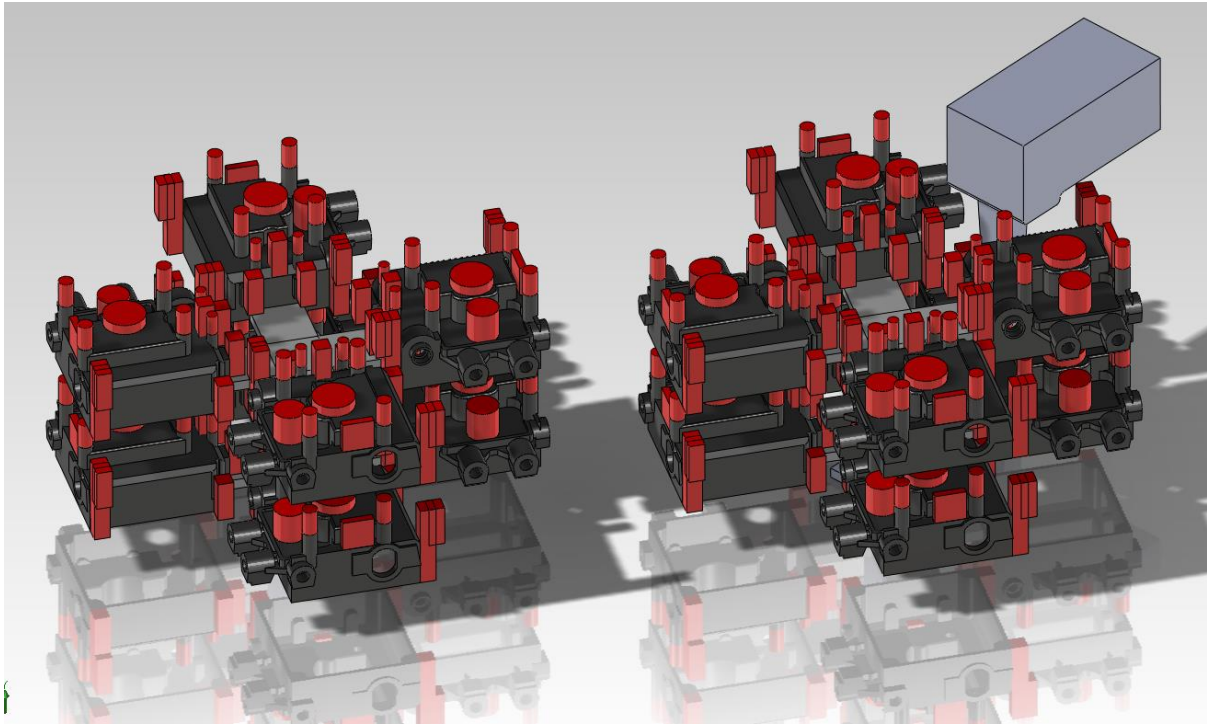


Figure 7- 8 the left side is the CRIMSON running system, and the right side is the gravity poured running system

According to the running system showed here. The energy consumption of this casting, the possible production lead time, the variable cost of the production can be estimated.

	casting yield	OME
CRIMSON	56%	38%
Conventional	45%	25%

Table 7- 7 the casting yield and OME results from the spreadsheet

energy burden (MJkg ⁻¹)		material consumed (kg)		energy consumption (MJ)	
		CRIMSON	conventional	CRIMSON	conventional
green sand energy	0.56	11.05	16.80	6.19	9.41
chemical sand energy	2.44	11.05	16.80	26.97	40.99
green sand primary reclamation after stable	0.09	11.05	16.80	0.99	1.51
chemical sand secondary reclamation after stable	0.31	11.05	16.80	3.43	5.21
chemical sand thermal reclamation after stable	0.64	11.05	16.80	7.07	10.75
CRIMSON after stable	15.69	1.84		28.90	
Conventional after stable	17.38		2.80		48.66

Table 7- 8 energy burden and energy consumption of each operations

	CRIMSON	Conventional
production time (h)	281	942
sand cost (£)	90686	131609
metal cost (£)	205504	261681
energy cost (£)	5481	4684
labour cost (£)	12817	42045
total variable cost (£)	314488	440019

Table 7- 9 the production time and variable cost estimation

7.7 Summary of chapter

A running system design spreadsheet was developed to design the casting running system in the numerical simulation comparison chapter. A spreadsheet was developed to estimate the embedded energy of sand mould making and casting making in the life cycle assessment section. Another spreadsheet was developed to estimate the casting variable cost in the cost estimation chapter. Because the shared information was discovered in each spreadsheet, the author developed an all-in-one spreadsheet which contains all information. Typical case studies have been used to exam the performance of the spreadsheet. It has been showed that the all-in-one spreadsheet not only can design the casting running system, but also can estimate the energy consumption and cost of the casting production. From this point of view, the all-in-one spreadsheet is a convenient and powerful tool for early stage product design and development.

Chapter 8 conclusions

The purpose of this project is to validate the novel CRIMSON process for foundry industries. Four different approaches have been used to validate the CRIMSON process. First of all, the casting simulation method was introduced to investigate the casting quality of the CRIMSON process. Secondly, the Life Cycle Assessment (LCA) method was used to assess the environmental impact of the CRIMSON process. Thirdly, using process simulation method, the productivity of the CRIMSON process had been investigated. Finally, and most importantly, the total variable cost of the CRIMSON process was investigated. Comparing with the conventional sand casting process, this research project has been found specifically that:

8.1 Simulation approach

- There are two double oxide film sources for gravity poured casting running system. The first one is in the pouring basin due to plunging jet, the second one is in the down-sprue due to surface turbulence. Both sources are hard to avoid due to the geometry requirement of the gravity poured running system.
- In the casting quality simulation, the gravity poured sand casting running system designed for the tensile test bar is quite successful. 90% of the oxide films generated during the filling are trapped by the running system itself. This indicated that a good running system is very important for a casting process.
- In the CRIMSON process, all the important parameters are under control. The up-casting piston only needs to move at very low velocity to deliver liquid metal. This low velocity can assure the liquid metal is smoothly delivered avoiding double oxide film formation and entrainment. The CRIMSON process also removes the pouring basin and downsprue from the casting running system. It not only eliminates the source of double oxide film generation, but also improves the casting yield.

8.2 Life Cycle Assessment approach

- Life Cycle Assessment method was introduced to investigate the environmental impact of the CRIMSON process. Regarding the inventory data collection of the casting process, the embedded energy of the casting process had been introduced. Due

to the difficulty of the data collection, the data investigated in this research project were sand mould making embedded energy and total embedded energy. According to the investigation, the embedded energy of sand mould making varies from $0.5 \text{ MJ}\cdot\text{kg}^{-1}$ to $2.4 \text{ MJ}\cdot\text{kg}^{-1}$. The total embedded energy of the casting is about $55 \text{ MJ}\cdot\text{kg}^{-1}$. Therefore, the embedded energy of metal preparing is about $52.6 \text{ MJ}\cdot\text{kg}^{-1}$ to $54.5 \text{ MJ}\cdot\text{kg}^{-1}$.

- Instead of using virgin aluminium in all cases. Recycling and reusing of the aluminium also takes into consideration. The method used to calculate the energy burden of the recycling and reusing is called multiple recycling method. After the recycling, the energy burden of the CRIMSON tensile test bar can be reduced to $13.13 \text{ MJ}\cdot\text{kg}^{-1}$, and the energy burden of the conventional sand tensile test bar can be reduced to $14.58 \text{ MJ}\cdot\text{kg}^{-1}$.
- However, these results only consider the energy burden of casting production. The real energy burden for saleable casting is not clear. As a result, the Operational Material Efficiency (OME) was introduced to investigate the energy burden for saleable casting. In order to calculate the OME of the casting process, the material usage during each casting operation need to be investigated as well. After the investigation, the OME for CRIMSON and conventionally cast test bars are 24% and 12% respectively. The energy burdens for saleable castings are $230 \text{ MJ}\cdot\text{kg}^{-1}$ and $449 \text{ MJ}\cdot\text{kg}^{-1}$ respectively.
- Using the collected energy and material inventory data, the environmental impact assessment was carried out by SimaPro LCA simulation package. Greenhouse gas emission, ECO-indicator, and ECO-points were the impact assessment used. All the impact assessment results indicate that the CRIMSON process has less environmental impact compared with the conventional sand casting process.

8.3 Productivity investigation

- Besides the casting quality and environmental impact of the process. The productivity of the CRIMSON process was investigated as well. The key performance indicator used was the labour productivity. According to survey and reasonable assumptions, a foundry model was developed to investigate the labour productivity. The foundry model was then modelled in the WITNESS simulation package. For the CRIMSON process, the casting size investigated from 1 kg to 10 kg. The furnace power out investigated from 40 KW to 300 KW. The period of the investigation is one year. For

Conventional sand casting process, the casting size investigated also from 1 kg to 10 kg. A 500 kg capacity furnace was used for all casting size. The period of the investigation also is one year.

- Several things can be found by the WITNESS simulation. As the CRIMSON furnace power increase, the labour productivity increase as well. For large size casting, the labour productivity of the CRIMSON process can be two times higher than the conventional process. However, the casting size can influence the performance of the power output. Small casting with high furnace power output can not increase the productivity. By contrast, it only builds up the work in process inventory. Therefore, the WITNESS simulation not only indicates that the CRIMSON process is productive, but also establishes the guides for the CRIMSON power output selection.

casting size (kg)	1	2	3	4	5	6	8	9	10
Conventional (set/h)	8.57	4.86	3.21	2.43	1.93	1.64	1.21	1.07	1
CRIMSON 40KW (set/h)	5.85	3.07	2.04	1.54	1.23	1.02	0.77	0.68	0.61
CRIMSON 100KW (set/h)	6	6	5.13	3.28	2.63	2.19	1.65	1.46	1.32
CRIMSON 150KW (set/h)	6	6	6	4.31	3.46	3.28	2.16	1.92	1.73
CRIMSON 200KW (set/h)	6	6	6	4.5	4.39	3.85	2.55	2.28	2.04
CRIMSON 250KW (set/h)	6	6	6	4.5	4.5	4.38	2.88	2.56	2.55
CRIMSON 300KW (set/h)	6	6	6	4.5	4.5	4.5	3.13	2.8	2.76

Table 8- 1 shows the guides of the power selection for the CRIMSON process

- No matter increase the power output or not, the conventional casting sand process has higher labour productivity if the casting is less than 2 kg. If the productive or lead time is very important for casting less than 2 kg. The conventional sand casting process should be used.

8.4 Cost estimation

- Beside other advantage of the CRIMSON process. Cost estimation is the most realistic performance indicator for industries. Analytical cost estimation techniques was used to estimate the total variable cost of the casting production. By using this technique, the cost estimation spreadsheet was developed. Varies of case study were carried out by the spreadsheet. As expect, the CRIMSON process is cheaper than the conventional sand casting process in most cases.
- The case studies also indicate that the raw material influence is significant. It contributes at least 80% of the total variable cost.

- The OME is a very important parameter. It decides the amount of the metal and sand need to be used for the casting process. Improve the OME can significantly reduce the total variable cost.
- No matter green sand or chemical sand, thermal reclamation method is recommend for sand recycling. This is because the thermal reclamation has higher recovery ratio, which increase the utilization of the used sand. Especially for high quality sand like Zircon and Chromite sand, the thermal reclamation can reduce the sand cost by 80% compared with the secondary reclamation method.
- As the casting size and the shipment increase, the unit cost of casting decrease. This is exactly what happed when batch production is adopted.

8.5 Final conclusions

This research project is about validating the novel CRIMSON casting process. In order to achieve this goal, the author decided to validate the CRIMSON process through quality investigation, productivity analysis, environmental impact assessment, and estimate cost of the production. As the findings conclude here, the CRIMSON process does have more advantages compared with the conventional sand casting process. It has better casting quality due to great filling rate control; it saves energy through holding free casting production and high OME; under the CRIMSON capacity, it has higher productivity compared with the conventional sand casting process; most importantly, it costs less to produce same casting products compared with the conventional sand casting process.

According to these approaches, a special spreadsheet also was developed to assess the entire production process of the CRIMSON and conventional sand casting process. The user can use this spreadsheet to design the high specification casting running system, evaluate the environmental impact of such running system, and estimate the cost to produce such casting. It is a convenient and powerful tool for early stage product design and development.

Chapter 9 Future Work

- Further quality investigation of the CRIMSON process would benefit from mechanical property testing to ensure product quality.
- The spreadsheet designed for this research project can design sound CRIMSON casting running system easily. However, the shape of the casting running system is limited at moment. A more flexible CRIMSON running system needs to be designed.
- This research project only validates the CRIMSON process for sand casting production. Considering the potential of the CRIMSON process, validating the CRIMSON process for investment casting process and block moulding process wide the market for the CRIMSON process.
- For the cost estimation, more detailed and accurate material database needs to be developed. For example: the price lists of copper alloy, magnesium alloy, investment slurry, wax, and so on.
- Considering further increase the casting yield of the CRIMSON process, rollover mechanism needs to be assessed.
- To further increase the productivity of the CRIMSON process, an automatic crucible handing / loading device needs to be developed. It can reduce the setup time for every casting and reduce the hassle for operators.

Chapter 10 Reference

- 34 census of world casting production, (2000), Modern Casting, AFS.
- 38 census of world casting production, (2003), Modern Casting, AFS.
- 39th Census of World Casting Production, (2004), Modern Casting, AFS.
- 40 census of world casting production, (2006), Modern Casting, World Foundry Organization (WFO).
- 41 census of world casting production, (2007), Modern Casting, WFO.
- 42 census of world casting production, (2008), Modern Casting, AFS.
- 43 census of world casting production, (2009), Modern Casting, AFS.
- 44 census of world casting production, (2010), Modern Casting, WFO.
- 45 census of world casting production, (2011), Modern Casting, WFO.
- Abdulmalek, F. A. and Rajgopal, J. (2007), "Analyzing the benefits of lean manufacturing and value stream mapping via simulation: A process sector case study", *International Journal of Production Economics*, vol. 107, no. 1, pp. 223-236.
- Agyapong-Kodua, K., Wahid, B. and Weston, R. (2011), "Towards the derivation of an integrated process cost-modelling technique for complex manufacturing systems", *International Journal of Production Research*, vol. 49, no. 24, pp. 7361-7377.
- Anderson, S. T. (2004), "Information programs for technology adoption: the case of energy efficiency audits. *Resource and Energy Economics*", *Resource and Energy Economics*, vol. 26, no. 1, pp. 27-50.
- Anderson, Soren T. & Newell, Richard G (2004), "Information programs for technology adoption: the case of energy-efficiency audits", *Resource and Energy Economics*, vol. 26, no. 1, pp. 27-50.
- Ann, C. M. (2006), *Life Cycle Assessment: Principles and Practice*, Scientific Applications International Corporation.
- Asiedu, Y. and Gu, P. (1998), "Product life cycle cost analysis: state of the art review", *International Journal of Production Research*, vol. 36, no. 4, pp. 883-908.
- ASM Handbook Committee (1979), *Metals Handbook - Ninth Edition (Volume 2 - Properties and Selection: Nonferrous Alloys and Pure Metals)*, 9th ed, American Society for Metals.

A-Yite-group-Limited (2012), Resin sand mixer, available at:
http://www.ayite1973.com/sdp/1094510/4/pd-5248457/7189001-2146260/Resin_Sand_Mixer.html. (accessed 03/04/2012).

Barkhudarov, M. and Hirt, C. (1995), "Casting simulation: Mold filling and solidification: Benchmark calculations using FLOW-3D", Modeling of Casting, Welding and Advanced Solidification Processes (MCWASP VII), London, pp. 935-946.

BCS Incorporated (2005), Advance Melting Technologies: Energy Saving concepts and Opportunities for the Metal Casting Industry, Office of Energy Efficiency & Renewable Energy.

BUCKET ELEVATOR, (nd), Carlos III University.

Besta, P., Stoch, M. and Haverland, J. (2011), Lean manufacturing concept in metallurgical industry, Metal 2011.

Brimacombe, L., Coleman, N. and Honess, C. (2005), "Recycling, reuse and the sustainability of steel", MilleniumSteel International.

Brown, J. (1999), "The moulding material: Properties, preparation and testing", in Foseco Non-Ferrous Foundryman's Handbook, Butterworth-Heinemann.

Brown, J. (1999), "Reesin bonded sand", in Foseco Non-Ferrous Foundryman's Handbook, Butterworth-Heinemann.

Brown, J. (1999), "Sands and sand bonding systems", in Foseco Non-Ferrous Foundryman's Handbook, Butterworth-Heinemann.

Brown, J. (1999), "Sand casting process", in Foseco Non-Ferrous Foundryman's Handbook. , Butterworth-Heineman.

Brown, J. (1999), "Production techniques 1: The manufacture of sand castings", in Foseco Non-Ferrous Foundryman's Handbook, Butterworth-Heinemann.

Bennett, M., Hughes, A., & James, P. (1999). Evaluating the Whole-Life Environmental Performance of Products. Sustainable Measures: Evaluation and Reporting of Environmental and Social Perf, 1(90), 283-312.

Cambridge Network (2013), CES EduPack for materials teaching, available at:
<http://www.cambridgenetwork.co.uk/directories/companies/368/products/843/> (accessed 015/05/2013).

Campbell, J. (1991), Casting, Butterworth-Heinemann, London.

Climate Change Agreements: Results of the Fifth Target Period, (2011), Department of Energy & Climate Change (DECC).

Campbell, J. and Richard, A. (1994), Solidification Defects in Castings, European Aluminium Association (EEA).

Caputo, A. C. and Pelagagge, P. M. (2008), "Parametric and neural methods for cost estimation of process vessels", *International Journal of Production Economics*, vol. 112, no. 2, pp. 934-954.

Chan, D. Y., Yang, K., Hsu, C., Chien, M. and Hong, G. (2007), "Current situation of energy conservation in high energy-consuming industries in Taiwan", *Energy Policy*, vol. 35, no. 1, pp. 202-209.

Dalquist, S. and Gutowski, T. (2004), "Life cycle analysis of conventional manufacturing techniques: die casting", USA: MIT, (2007-09-06).<http://web.mit.edu/ebm/www/Publications>.

Dahlquist, A., (2011), *Breaking Down the US numbers*, Modern Casting.

DECC Fossil Fuel Price Projections,, (2012), Department of Energy & Climate Change.

Dai, J. S., Balabani, S. and Seneviratne, L. (2006), "Product cost estimation: technique classification and methodology review", *Journal of manufacturing science and engineering*, vol. 128, pp. 563.

Dai, X., Jolly, M. and Zeng, B. (2011), "The Capability Enhancement of Aluminium Casting Process by Application of the Novel CRIMSON Method", in *Shape Casting*, John Wiley & Sons, Inc., pp. 265-272.

Dalquist, S. and Gutowski, T. (2004), "Life cycle analysis of conventional manufacturing techniques: die casting", USA: MIT,(2007-09-06).<http://web.mit.edu/ebm/www/Publications>.

Dalquist, S. and Gutowski, T. (2004), "Life cycle analysis of conventional manufacturing techniques: sand casting", ASME International Mechanical Engineering Congress and RD&D Exposition, Anaheim, California, USA.

Di Sabatino, M., Arnberg, L. and Bonollo, F. (2005), "Simulation of fluidity in Al-Si alloys", *Metallurgical Science and Technology*, vol. 23, no. 1, pp. 3-10.

Divandari, M. and Campbell, J. (1999), "The Mechanisms of bubble damage in casting", proceeding of: 1st International Conference on Gating , Filling and Feeding of aluminum castings, 11/10/1999, Opryland Hotel , Nashville TN, American Foundrymen's Society, .

Dunlop, F. "Conveyor Handbook conveyor belting," Australia (2009), pp. 1-32.

Earth Shift (2013), *Ecopoint 97 Impact Assessment Method*, available at: <http://www.earthshift.com/software/simapro/ecopoints97> (accessed 18/04/2013).

Environment Protection Agency (EPA) (2013), *Greenhouse Gas Equivalencies Calculator*, available at: <http://www.epa.gov/cleanenergy/energy-resources/calculator.html> (accessed 15/05/2013).

Energy Consumption Guide 38 Non-ferrous foundries 2nd Edition, (1997), DETR.

Environmental management – Life cycle assessment – Principles and framework, International Organisation for Standardisation (ISO), (2006), ISO.

ETSU (1998), Induction Melting of Aluminum, Department of the Environment, Transport and the Regions (DETR).

Falkovich, G. (2011), Fluid Mechanics, a short course for physicists, Cambridge University Press.

Fossil fuel (30/05/2012), available at: http://en.wikipedia.org/wiki/Fossil_fuel (accessed 12/11/2012).

Fenyés, M. (2010). Maximising Sand Recovery in the Foundry. Transactions of 58th IFC, 49-54.

Gebelin, J. (2006), "Simulation Of Tensile Test Bars: Does The Filling Method Matter?", Simulation of Aluminum Shape Casting Processing: From Alloy Design to Mechanical Properties, pp. 299-310.

Girish, C. P., Naik, G. R. and Naik, P. G. (2012), "Application Of Process Activity Mapping For Waste Reduction A Case Study In Foundry Industry", International Journal of Modern Engineering Research, vol. 2, no. 5, pp. 3482-3496.

Green, N. and Campbell, J. (1994), "Influence of Oxide Film Filling Defects on the Strength of Al-7Si-Mg Alloy Casting", Transactions of the American Foundrymen Society, pp. 341-348.

Greengate metals (2013), Scrap Aluminium in Manchester, available at: <http://greengatemetals.co.uk/scrapmetal/Aluminium.html> (accessed 20/05/2013).

Hughes, D. (nd), Reclaimed sand in foundries, Foseco Australia.

Induction furnace(12/08/2012), available at: http://en.wikipedia.org/wiki/Induction_furnace (accessed 27/11/2012).

IndiaMART (2012), History of Metal Casting., available at: <http://sourcing.indiamart.com/engineering/articles/history-metal-casting/> (accessed 05/28/2012).

Investopedia (2013), What is the relationship between oil prices and inflation?, available at: <http://www.investopedia.com/ask/answers/06/oilpricesinflation.asp> (accessed 07/05/2013).

Campbell, J. (2004), Casting, 2nd ed, Elsevier Butterworth-Heinemann, Oxford.

Jolly, M. R. (2010), "Energy Saving in the Foundry Industry by Using the CRIMSON Single Shot Up-Casting process", **Energy Conservation in Metals**, 14/02/2012, Seattle, TMS2012, .

Jolly, M. R. (2002), "Casting Chapter", in Milne, I. R., Ritchie, O. and Karihaloo, B. (eds.) Comprehensive Structural integrity, Elsevier, Oxford.

Jolly, M. R., Reilly, C. and Green, N. R. (2010), "Assessment of Casting filling by Modelling Surface Entrainment Events using CFD", General Abstracts: Light Metals Division, 14/02/2010, Seattle, TMS2010, .

Jolly, M. and Dai, X. "Energy Efficiency Improvement by Implementation of the Novel CRIMSON Aluminium Casting Process", Energy Technology 2011: Carbon Dioxide and Other Greenhouse Gas Reduction Metallurgy and Waste Heat Recovery, pp. 55-64.

JOYAL (2013), Vibrating Feeder, available at http://www.joyalcrusher.com/products/Feeding-Conveying/Vibrating-Feeder.html?clid=CL7UyO_z17ECFcYmtAodfAYAwg (accessed 01/03/2013)

Kabir, G., Abubakar, A. I. and El-Nafaty, U. A. (2010), "Energy audit and conservation opportunities for pyroprocessing unit of a typical dry process cement plant", Energy, vol. 35, no. 3, pp. 1237-1243.

Klopffer, W. (1997), "Life cycle assessment from the beginning to the current state.", WG Assessment of Chemicals, Products and Systems, ESPR-Environ.Sci.& Pollut., pp. 223-228.

Klugman, S., Karlsson, M. and Moshfegh, B. (2007), "A Scandinavian chemical wood pulp mill. Part 1. Energy audit aiming at efficiency measures", Applied Energy, vol. 84, no. 3, pp. 326-339.

Kukla, S. (2011), "Maintenance system improvement in cast iron foundry", ARCHIVES of FOUNDRY ENGINEERING, vol. 11, no. 3, pp. 185-188.

Layer, A., Brinke, E. T., Houten, F. V., Kals, H. and Haasis, S. (2002), "Recent and future trends in cost estimation", International Journal of Computer Integrated Manufacturing, vol. 15, no. 6, pp. 499-510.

Legislation (2012), Clean Air Act 1993, available at: <http://www.legislation.gov.uk/ukpga/1993/11/contents> (accessed 20/11/2012).

Lost&Foundry (2012), Foundry facts- Learning Links, available at: <http://www.foundry101.com/archive.htm> (accessed 20/11/2012).

monthly digest of statistics, (2007), Office for National Statistics.

Monthly Digest of Statistics, (2000), Office for National Statistics.

Monthly Digest of Statistics, (2002), Office for National Statistics.

Mark, F. (2010), Maximising Sand Recovery in the Foundry, Omega Foundry Machinery Ltd.

Markt, P. L. and Mayer, M. H. (1997), "WITNESS simulation software: a flexible suite of simulation tools", Winter Simulation Conference: Proceedings of the 29 th conference on Winter simulation, Vol. 7, pp. 711.

Mefferta, W. A. (1999), "Energy Assessments in Iron Foundries", Energy Engineering, vol. 96, no. 4, pp. 6-18.

METALPRICES (2013), Aluminum, available at: <http://www.metalprices.com/metal/aluminum/aluminum-old-cast> (accessed 15/05/2013).

Niazi, A., Dai, J. S., Balabani, S., & Seneviratne, L. (2006). Product cost estimation: Technique classification and methodology review. *Journal of manufacturing science and engineering*, 128(2), 563-575.

NPC (2012), What is 'Lost Wax' Investment Casting, available at: <http://cc.bingj.com/cache.aspx?q=%22many+wartime+needs+and+during+the%22&d=4713735790461893&w=cdf4f3c4,7423d0dd> (accessed 12/03/2012).

Otsuka, R. (2003), "Molten Metal Processing. ", in George, E., Totten, D. and Scott MacKenzie (eds.) *Handbook of Aluminum: Vol. 1: Physical Metallurgy and Processes*, CRC Press, .

Portal Europe's Energy (2013), Fuel Prices, available at: <http://www.energy.eu> (accessed 29/04/2013).

PREVAIL (2012), process-lost wax process, available at: <http://www.investmentcasting-india.com/process-lost-wax.html> (accessed 10/12/2012).

Ramana Rao, T. V. (1996), **Metal Casting: Principles and Practice**, New Age International (P) Ltd.

Re-allocated energy by industry, (2012), Office for National Statistics.

Rao, T. R. (2007), *Metal casting: Principles and practice*, New Age International.

Reallocated Energy and Energy Intensity 1990-2010, (2012), Office of National Statistics.

Rebitzer, G., Ekvall, T., Frischknecht, R., Hunkeler, D., Norris, G., Rydberg, T., Schmidt, W., Suh, S., Weidema, B. and Pennington, D. (2004), "Life cycle assessment: Part 1: Framework, goal and scope definition, inventory analysis, and applications", *Environment international*, vol. 30, no. 5, pp. 701-720.

Reilly. (2010), *Development Of quantitative Casting Quality Assessment Criteria Using Process modelling* (unpublished PhD Thesis), University of Birmingham.

Reilly, C., Jolly, M., Green, N. and Gebelin, J. (2010), "Assessment of casting filling by modeling surface entrainment events using CFD", *TMS Annual Meeting & Exhibition (Jim Evans Honorary Symposium)*, Seattle, Washington, USA, .

Robinson, S. (2004), *Simulation: the practice of model development and use*, Wiley. com.

Salonitis, K., Tsoukantas, G., Drakopoulos, S., Stavropoulos, P. and Chryssolouris, G. (2006), "Environmental impact assessment of grind-hardening process", *Proc 13th CIRP INT CONF on Life Cycle Engineering*, pp. 657.

Standard Specification for Aluminum-Alloy Permanent Mold Casting, (2003), B108-03a, ASTM.

Shehab, E. and Abdalla, H. (2001), "Manufacturing cost modelling for concurrent product development", *Robotics and Computer-Integrated Manufacturing*, vol. 17, no. 4, pp. 341-353.

Silica and Moulding Sands Association (2012), what is silica, available at: <http://www.samsa.org.uk/silica.htm> (accessed 20/11/2012).

Silica and Moulding Sands Association (2012), Where is it found, available at: http://www.samsa.org.uk/sil_where01.htm (accessed 04/11/2012).

Simpson Group (2010), Sand Preparation: Simpson Mix-Muller Batch Mixer, available at: <http://www.simpsongroup.com/sandprep/mixmuller.htm> (accessed 10/09/2012).

Sirrell, B., Holliday, M. and Eng, J. C. D. (1996), "Benchmark testing the flow and solidification modeling of AI castings", JOM, vol. 48, no. 3, pp. 20-23.

Smithells, C. J. (1976), Smithells Metals Reference Book, 5th ed, Butterworth–Heinemann, London and Boston.

Sustainable Manufacturing Portal (2013), Eco-indicator 99, available at http://www.centreforsmart.co.uk/smp/tools_ecoindicator99.php (accessed 04/03/2013)

Subrahmanya, M. H. B. (2006), "Energy intensity and economic performance in small scale bricks and foundry clusters in India: does energy intensity matter?", Energy Policy, vol. 34, no. 4, pp. 489-497.

Tharumarajah, A. (2008), "Benchmarking aluminium die casting operations", Resources, Conservation and Recycling, vol. 52, no. 10, pp. 1185-1189.

Thollander, P. and Ottosson, M. (2010), "Energy management practices in Swedish energy-intensive industries", Journal of Cleaner Production, vol. 18, no. 12, pp. 1125-1133.

Thollander, P. and Ottosson, M. (2008), "An energy efficient Swedish pulp and paper industry—exploring barriers to and driving forces for cost-effective energy efficiency investments", Energy Efficiency, vol. 1, no. 1, pp. 21-34.

Thollander, P. and Ottosson, M. (2010), "Energy management practices in Swedish energy-intensive industries", Journal of Cleaner Production, vol. 18, no. 12, pp. 1125-1133.

Trianni, A., Cagno, E., Thollander, P. and Backlund, S. (2012), "Barriers to industrial energy efficiency in foundries: a European comparison", Journal of Cleaner Production, .

U.S.EPA (2003), Lean manufacturing and the Environment: Research on Advanced Manufacturing Systems and the Environment and Recommendations for Leveraging Better Environmental Performance, U.S.Environmental Protection Agency (EPA).

UKcasting (2013), Why Foundries are vital, available at: [http://www.ukcastings.org/page.asp?node=71&sec=Why Foundries are vital](http://www.ukcastings.org/page.asp?node=71&sec=Why_Foundries_are_vital) (accessed 11/10/2013).

UKFoundries (2013), UK Foundries., available at: <http://www.ukfoundries.co.uk/> (accessed 11/10/2013).

UNFCCC (2012), Kyoto Protocol, available at:
http://unfccc.int/kyoto_protocol/items/2830.php (accessed 20/11/2012).

WESMAN (2013), WESMAN THERMAL SAND RECLAIMER, available at:
<http://www.wesman.com/products/foundry-equipment/no-bake-sand-systems/thermal-sand-reclamation.html> (accessed 4/01/2013).

Yih-Liang Chan, D., Yang, K., Lee, J. and Hong, G. (2010), "The case study of furnace use and energy conservation in iron and steel industry", *Energy*, vol. 35, no. 4, pp. 1665-1670.

Zeng. (2010), Comparison of analytical model and numerical simulation for calculation of casting running systems (unpublished Final Year Project), University of Birmingham.

Zhai, Y. (2012), "Early cost estimation for additive manufacture".

Appendix 2 knowledge of the lean manufacturing

Cellular manufacturing

Work stations are arranged in a product- aligned sequence to support a smooth flow of production with minimal transport or delay. It normally used in one piece flow production.

5S

Sort, Set in order, Shine, Standardize, and Sustain are called 5S. It encourages workers to improve the physical setting of work, and reduce waste. Basically, it can reduce the space required for work.

Value stream mapping

Requires understand all the processes involved. So that non-value-added activity can be identified and eliminated. It involves cycle time, inventory, setup time, changeover time investigation. After the current VSM, the problem and waste can be addressed. Plan or future VSM need to be developed to solve the problems.

Just in time

It is a production planning method. Aim to provide product the customer want, when they want. Based on cellular manufacturing and pull method, levelling the production, spreading production evenly over time. Normally, visual signal / Kanban are used to assist JIT.

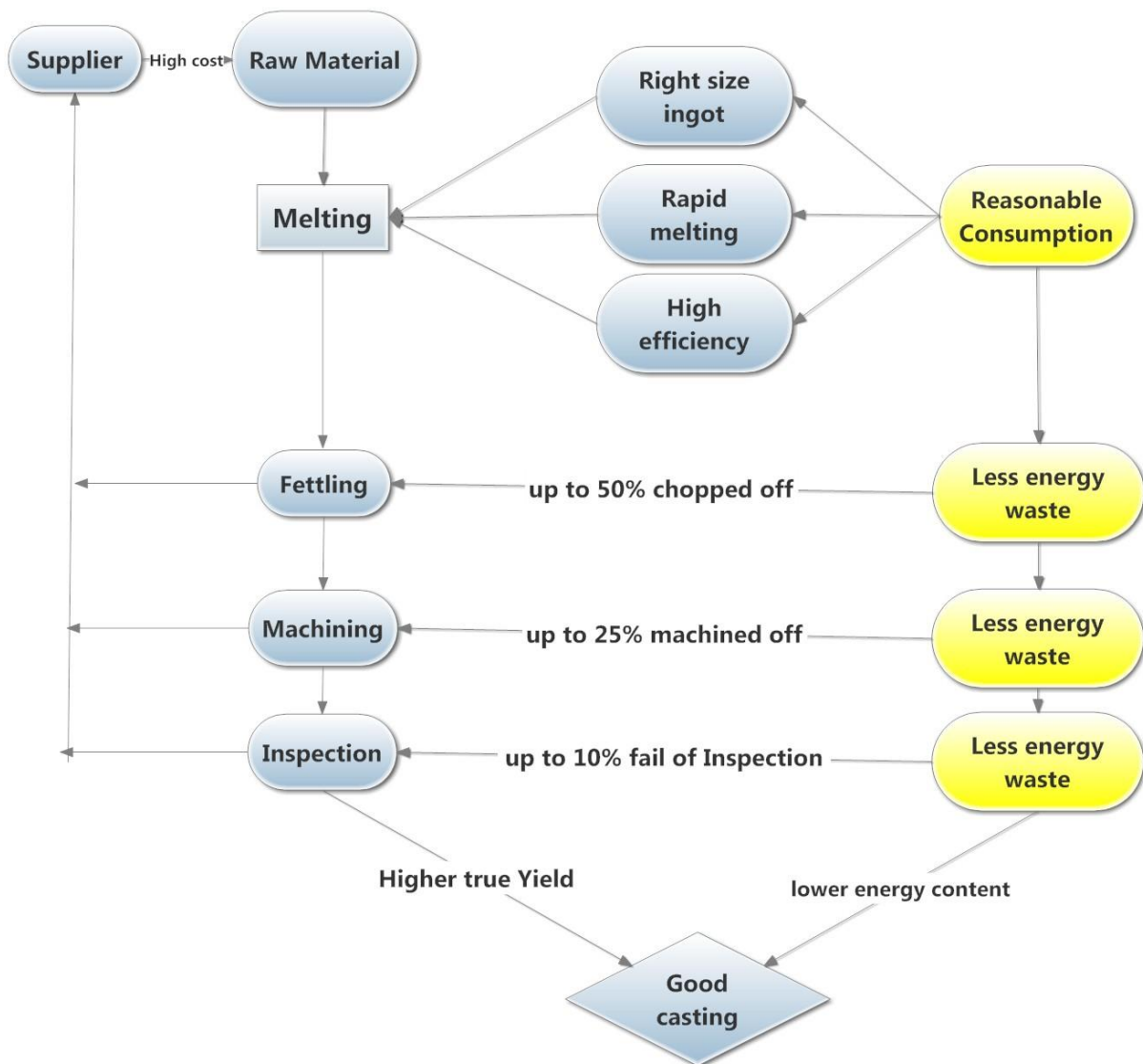
Production levelling

Mix different products within the same production line.

Total productive maintenance

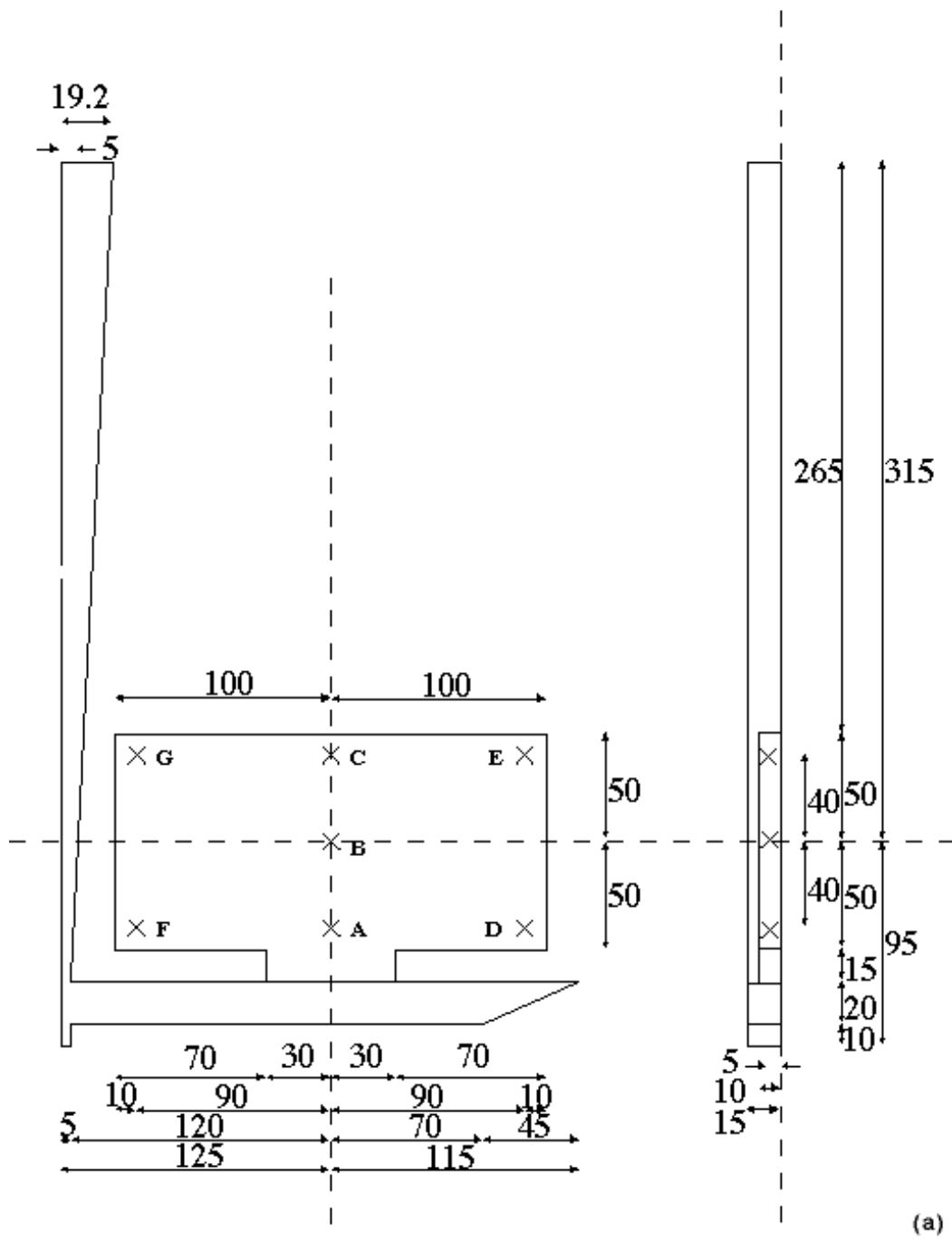
The operators know their machine better than others. Give them responsibility to look after their machine, do daily maintenance. Also Involves senior concept such as prevent / reduce maintenance through initial equipment design.

Appendix 3 Material and energy flow chart of the CRIMSON sand casting

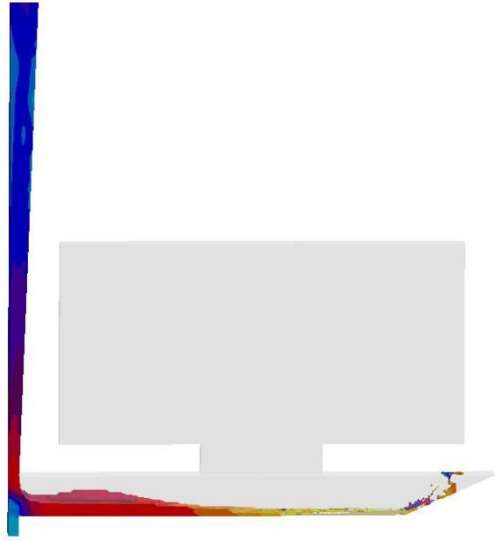
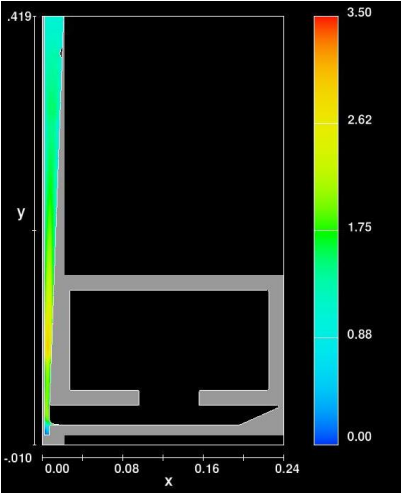



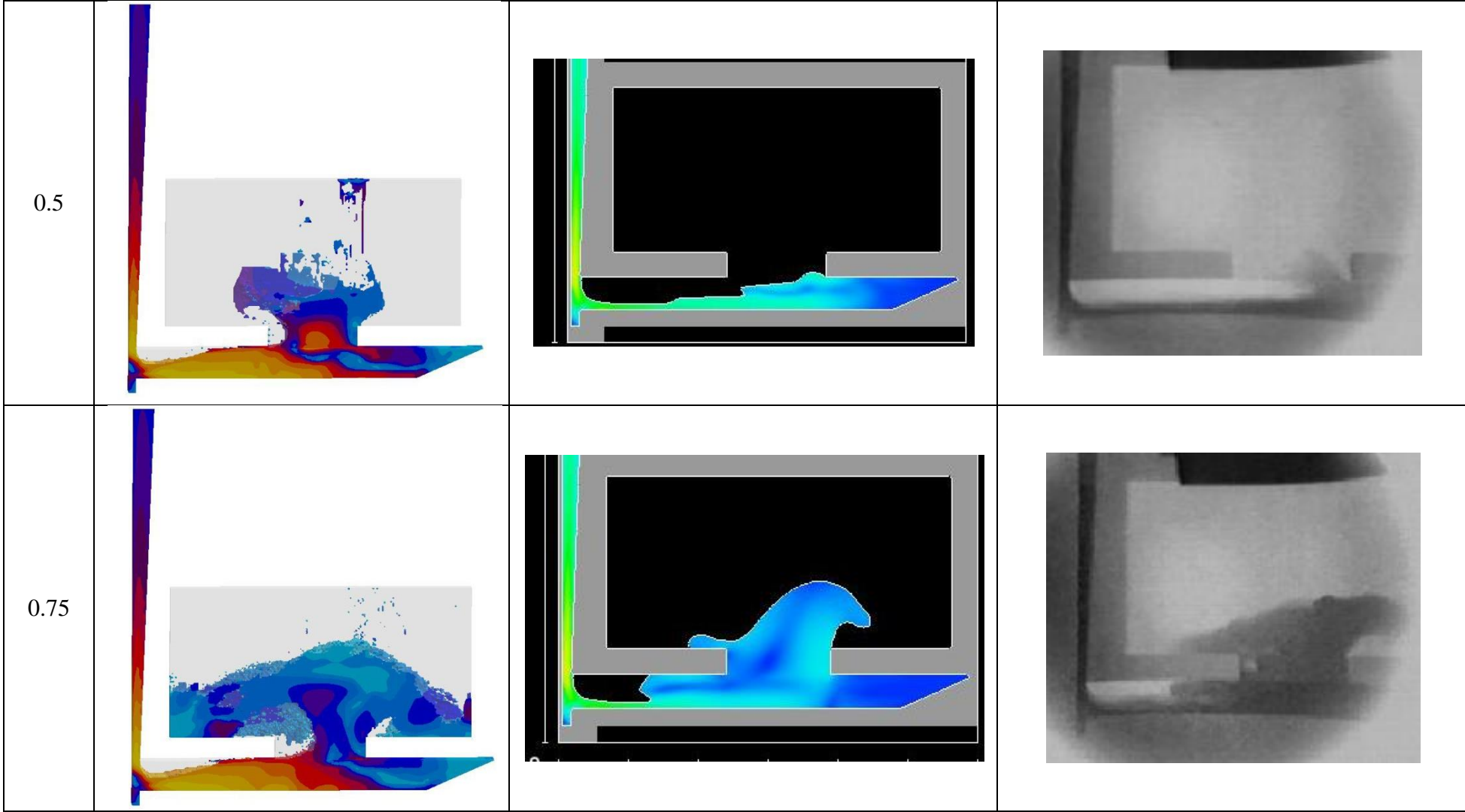
11.2 Numerical casting simulation

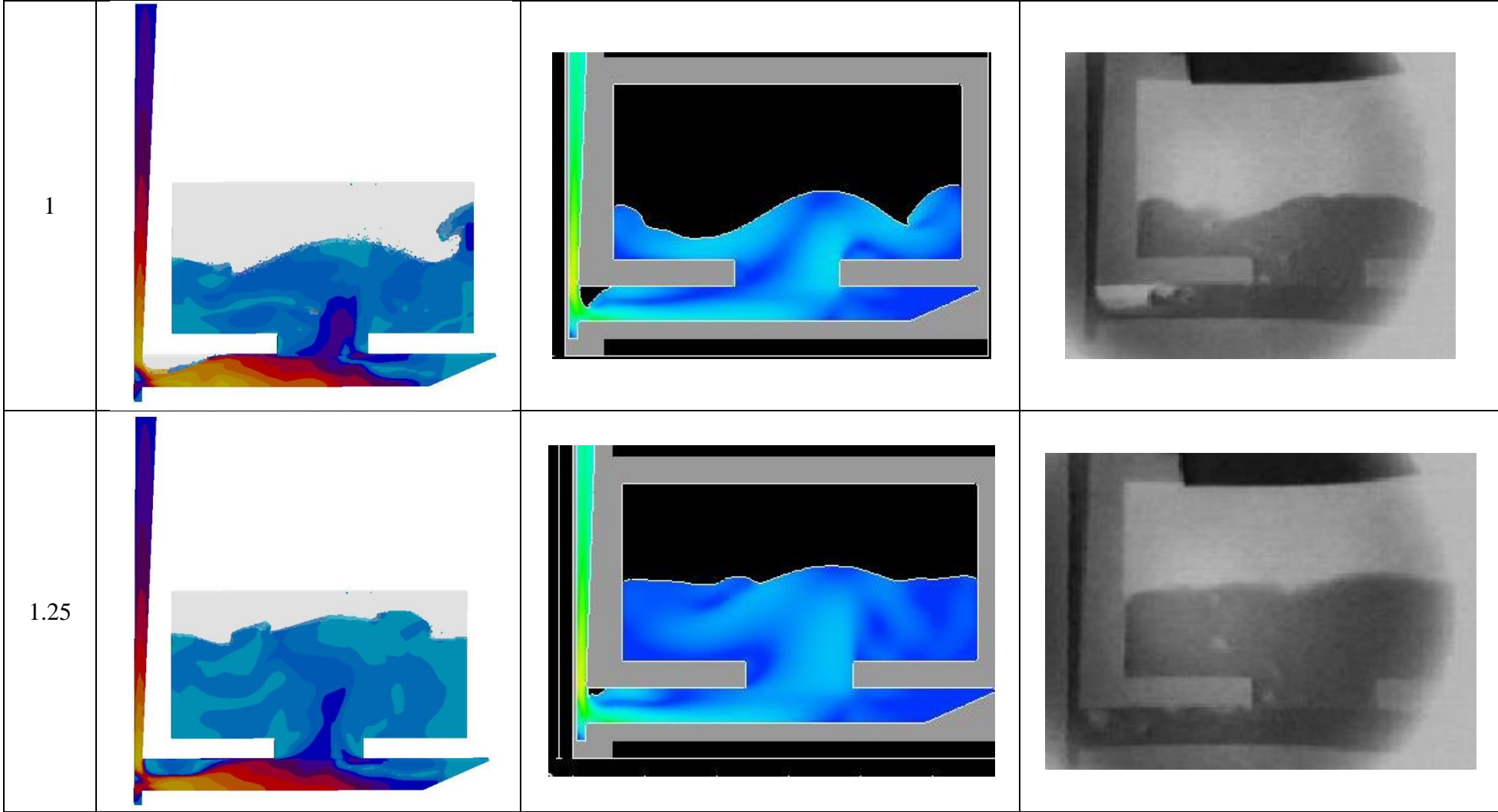
Appendix 4 the geometry of benchmark test

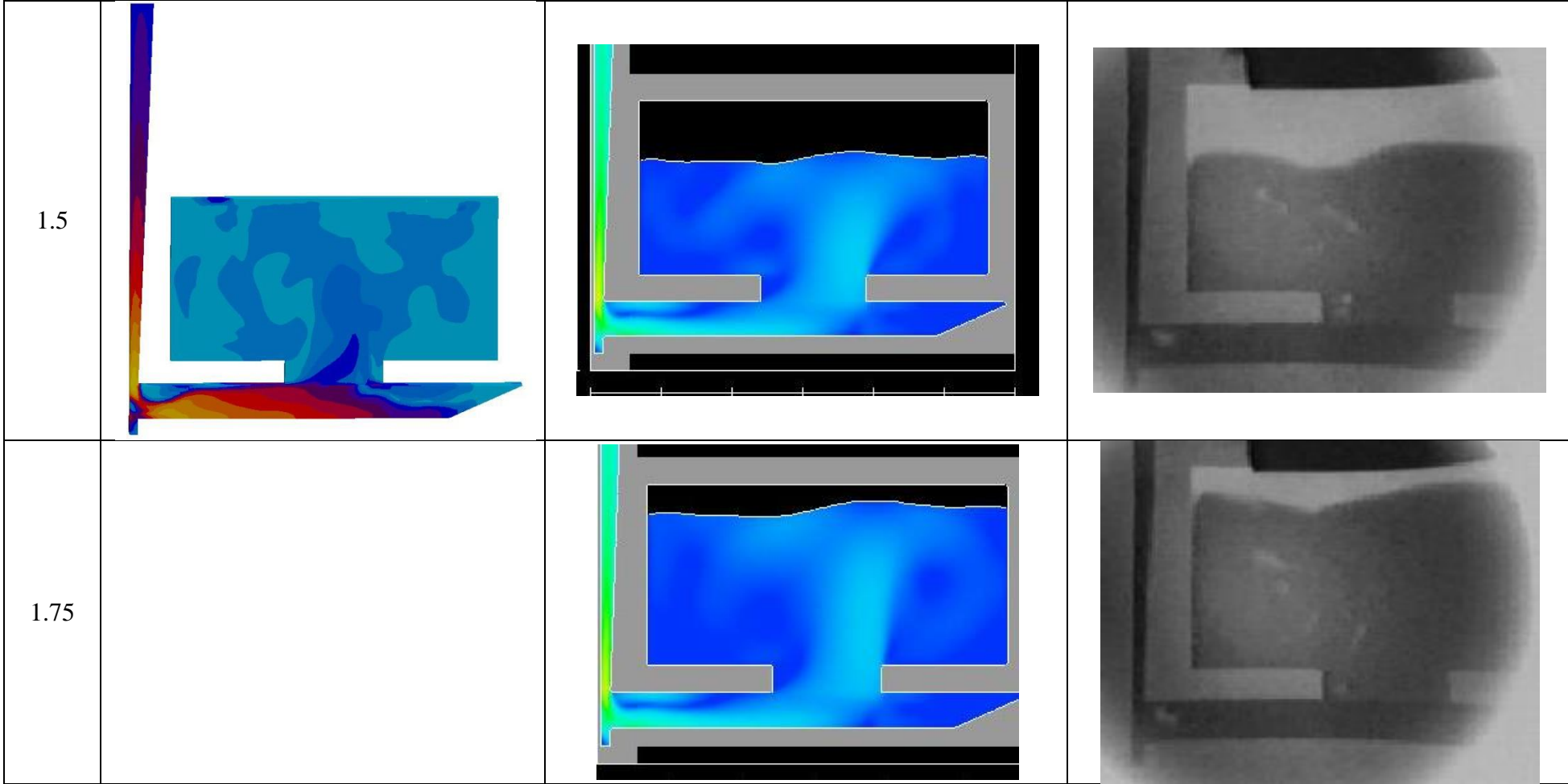


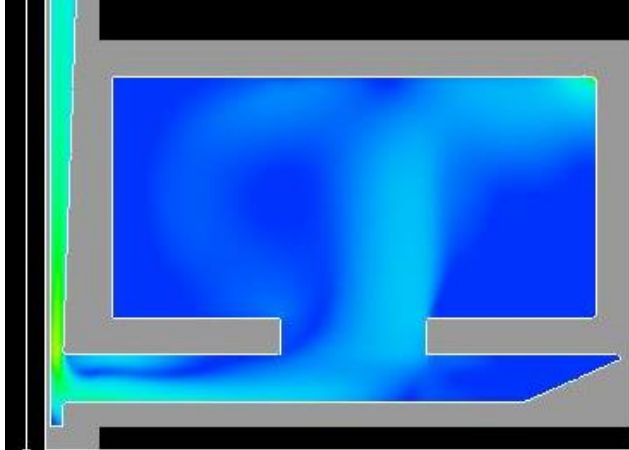
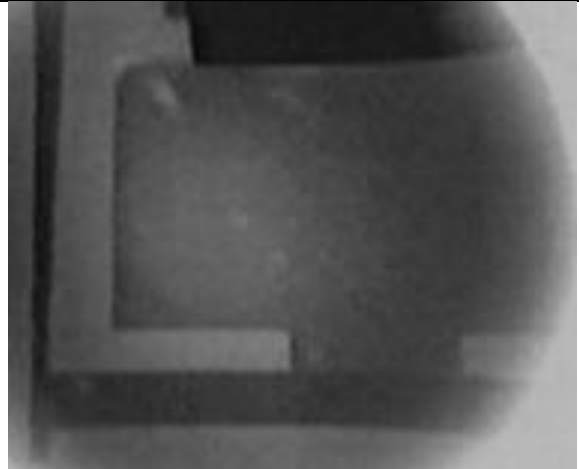
Appendix 5 the simulation results

Time (s)	Magma5	Flow3D	X-Ray Data
0.25			

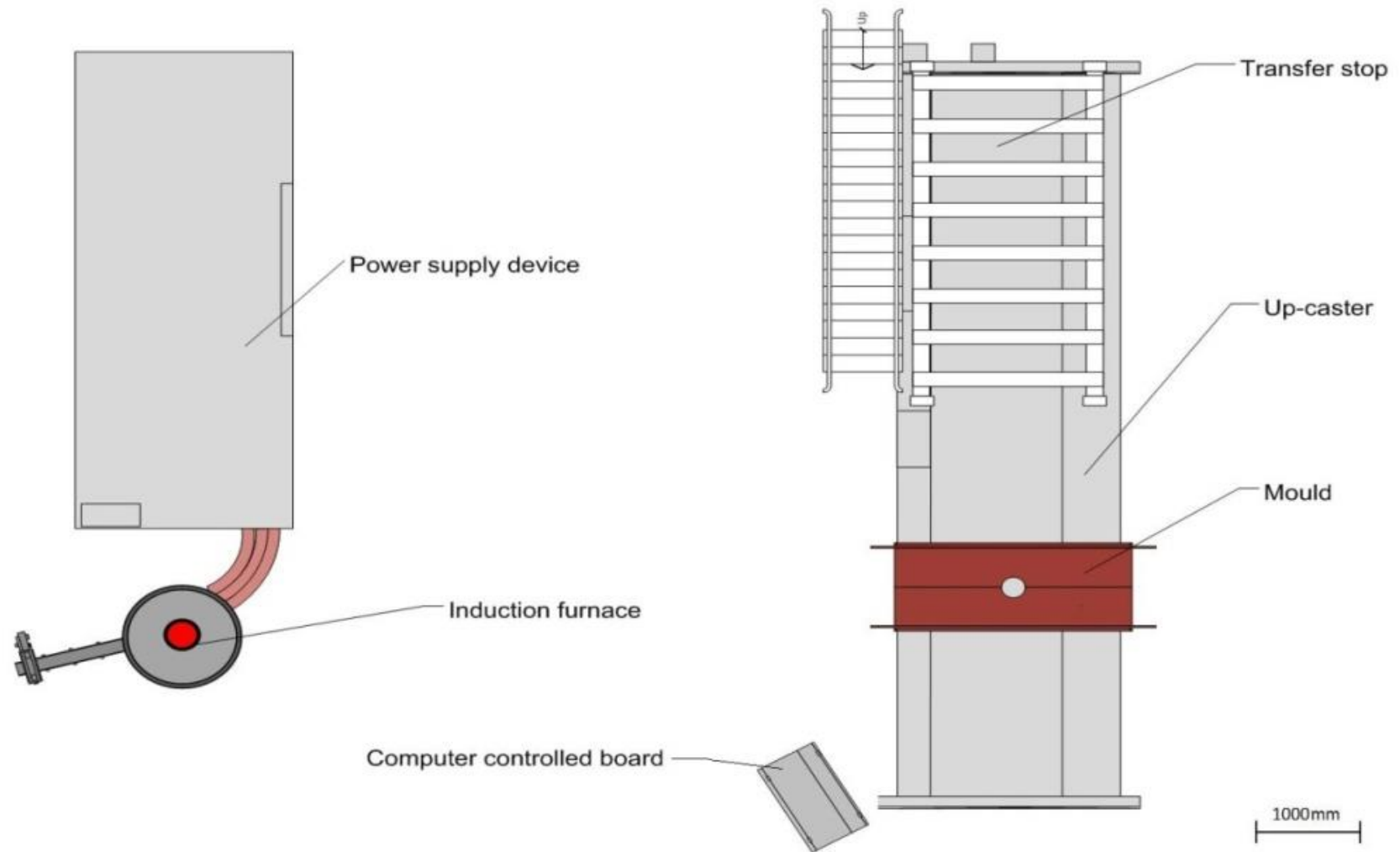




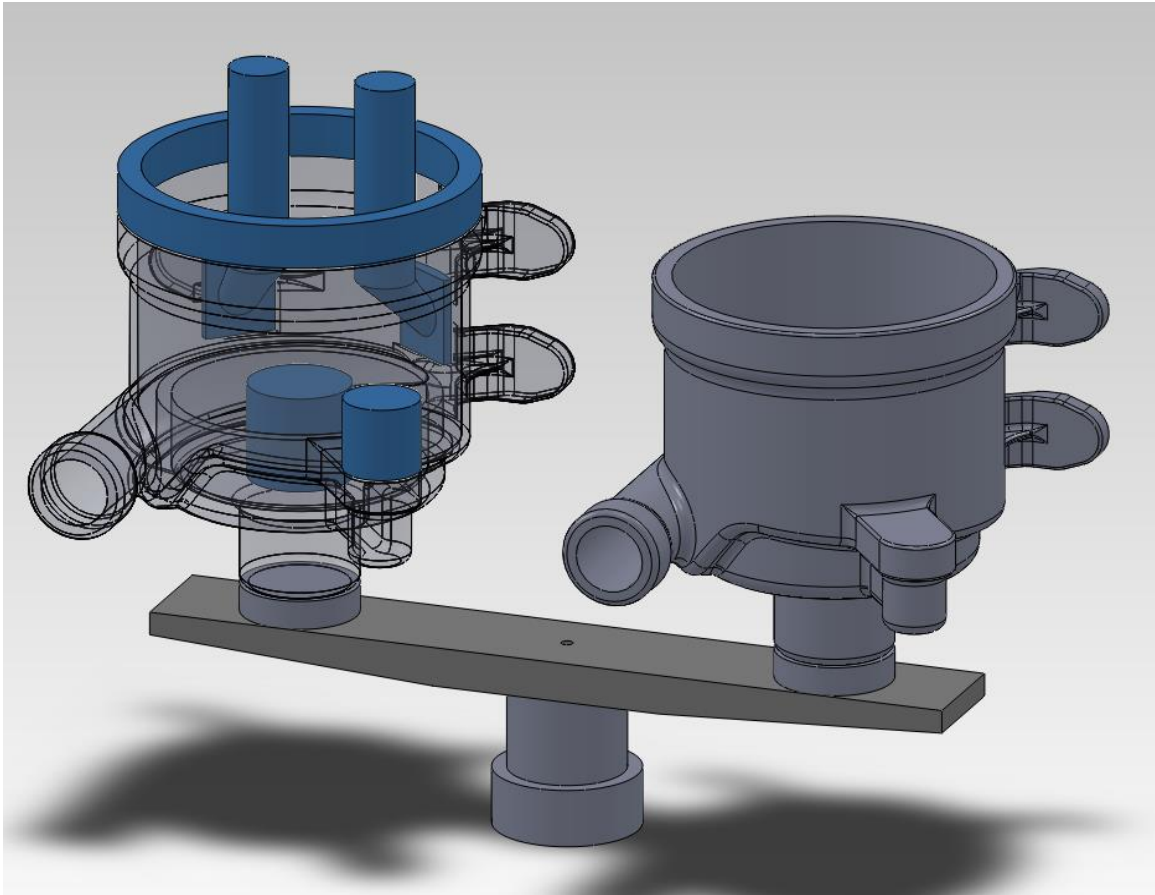


2			
Finish Time	1.5	1.938	2

Appendix 6 layout of the CRIMSON facility

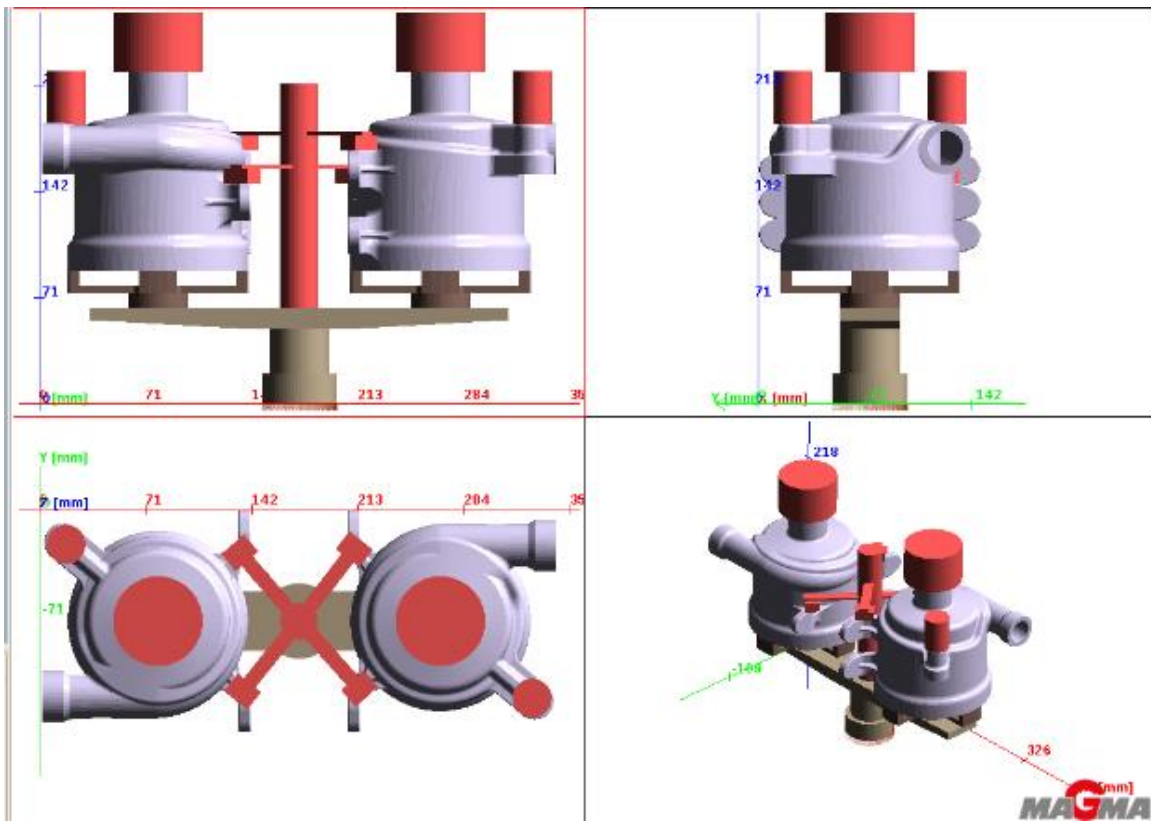


Appendix 8 First version of the running system design



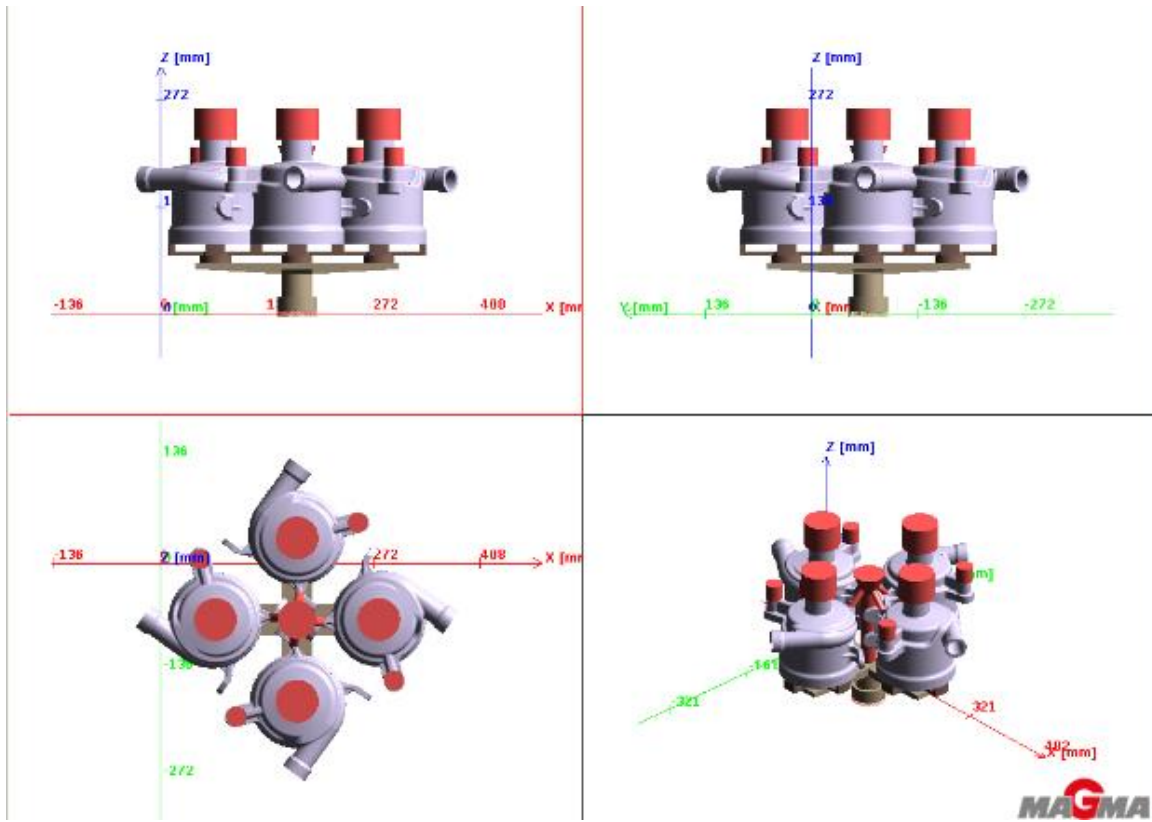
Casting Method	Up-casting
Casting Material	AlSi7Mg
Mold Material	Furan
Heat Transfer	Temperature dependent HTC
Pouring Temperature (°c)	700.00
Mold Temperature (°c)	20.00
Maximum Flow rate (l/s)	0.25
Time for solver (s)	9584.00
Time for solver (hour)	2.66
Filling time (s)	4.18
solidification time (s)	812.82
No feeder housing porosity (mm³)	4641.53
Feeder housing porosity (mm³)	77.71
velocity at runner (m/s)	0.32
velocity at ingate (m/s)	0.19
Mass of casting (kg)	1.60
Mass of casting system (kg)	1.48
Yield (%)	51.95

Appendix 9 Second approach of the CRIMSON filter housing system



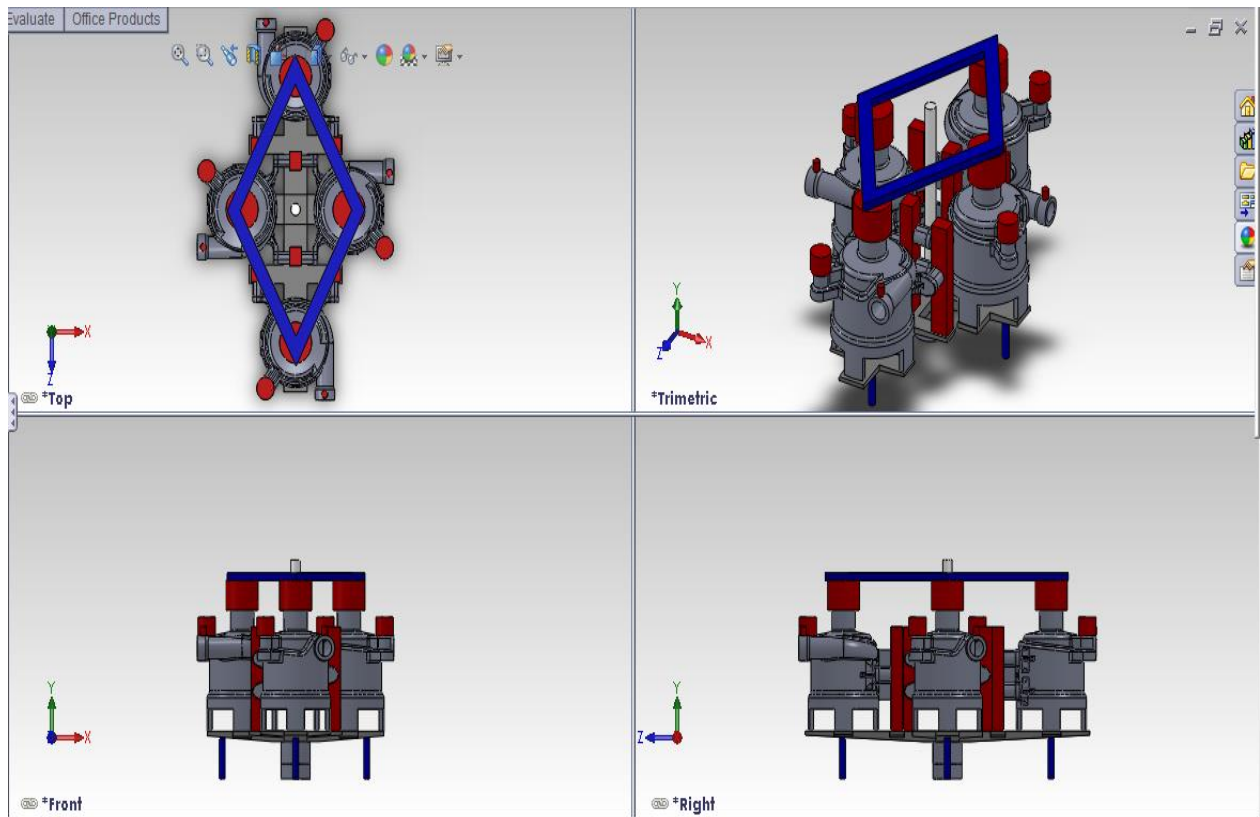
Casting Method	Up-casting
Casting Material	AlSi7Mg
Mold Material	AL2O3
Heat Transfer	Temperature dependent HTC
Pouring Temperature (°c)	700.00
Mold Temperature (°c)	500.00
Maximum Flow rate (l/s)	0.25
Time for solver (s)	176374.72
Time for solver (hour)	49
Filling time (s)	8.95
solidification time (s)	1112.20
housing porosity (mm ³)	0
velocity at runner (m/s)	0.18
velocity at ingate (m/s)	0.15
Mass of casting (kg)	3.24
Mass of casting system (kg)	2.71
Yield (%)	54.45

Appendix 10 The third approach for filter housing running system design



Casting Method	Up-casting
Casting Material	AlSi7Mg
Mold Material	AL203
Heat Transfer	Temperature dependent HTC
Pouring Temperature (°c)	700.00
Mold Temperature (°c)	500.00
Maximum Flow rate (l/s)	0.25
Time for solver (s)	176374.72
Time for solver (hour)	49
Filling time (s)	8.95
solidification time (s)	1112.20
housing porosity (mm ³)	0
velocity at runner (m/s)	0.18
velocity at ingate (m/s)	0.15
Mass of casting (kg)	3.24
Mass of casting system (kg)	2.71
Yield (%)	54.45

Appendix 11 the final design of the filter housing design



Casting Method	Up-casting
Casting Material	AlSi7Mg
Mold Material	AL203
Heat Transfer	Temperature dependent HTC
Pouring Temperature (°c)	700.00
Mold Temperature (°c)	500.00
Maximum Flow rate (l/s)	0.25
Time for solver (s)	176374.72
Time for solver (hour)	49
Filling time (s)	8.95
solidification time (s)	1112.20
housing porosity (mm ³)	0
velocity at runner (m/s)	0.18
velocity at ingate (m/s)	0.15
Mass of casting (kg)	3.24
Mass of casting system (kg)	4.42
Yield (%)	42.32

Appendix 12 the CRIMSON running system design spreadsheet

Appendix 11 the CRIMSON running system design spreadsheet.xlsx - Microsoft Excel

Home Insert Page Layout Formulas Data Review View Add-Ins Team

Clipboard Font Alignment Number Styles Cells

C1

	A	B	C	D	E	F	G	H	I	J	K	L	M	N	O	P	Q	R	S
1	Birmingham University Spreadsheet											Metal	Liquid Density	Liq Den					
2	Alloy		Al									Al	2346	2346					
3	Mass of Method		0.00	0.00	0.00	0.00	0.00	0.00											
4	Poured Mass		0.00	0.00	0.00	0.00	0.00	0.00											
5	Yield		0%	0%	0%	0%	0%	0%											
8	Process (Sand, LPD, GD, Investment)		Sand	Sand	Sand	Sand	Sand	Sand											
9	1 Mass of Casting & Feeders (kg)		4.78	4.78	4.78	4.78	4.78	4.78											
10	2 Mass of Runner & Ingates & Filter Print (kg)		0.00	0.41	0.41	0.41	0.41	0.41											
11	3 Total Mass (kg)		4.78	5.19	5.19	5.19	5.19	5.19											
12	4 Volume (cc)		2004	2175	2175	2175	2175	2175											
13	Solid density		2.650	2.650	2.650	2.650	2.650	2.650											
14	liquid density (g/cc)		2.385	2.385	2.385	2.385	2.385	2.385											
15	5 fixed inlet diameter (mm)		50.000	50.000	50.000	50.000	50.000	50.000											
16	thinnest section area in the casting (mm ²)		907.00	907.00	907.00	907.00	907.00	907.00											
17	target filling velocity (m/s)		0.50	0.50	0.50	0.50	0.50	0.50											
18	target filling rate (cc/s)		453.50	453.50	453.50	453.50	453.50	453.50											
19	chosen filling rate (cc/s)		250.00	250.00	250.00	250.00	250.00	250.00											
20	time for filling (s)		8.02	8.70	8.70	8.70	8.70	8.70											
22	inlet											Ce	6685	6.685					
23	inlet height (mm)		20	20	20	20	20	20				Co	7760	7.76					
24	volume of inlet (cc)		39.27	39.27	39.27	39.27	39.27	39.27				Cr	6280	6.28					
25												Cs	1854	1.854					
26	Vertical runner											Cu	8000	8					
27	diameter (mm)		50	50	50	50	50	50				Fe	7015	7.015					
28	height		30	30	30	30	30	30				Hg	13691	13.691					
29	volume of vertical runner (cc)		58.90	58.90	58.90	58.90	58.90	58.90				In	7023	7.023					
30	Does the running system produce more than one casting		yes	yes	yes	yes	yes	yes				K	827	0.827					
31	continue											Li	525	0.525					
32	Does the all castings filled in one single vertical line		yes	yes	yes	yes	yes	yes											
33	You may only use inlet and vertical runner to form casting system																		

vertical runner

runner

vertical runner

Inlet

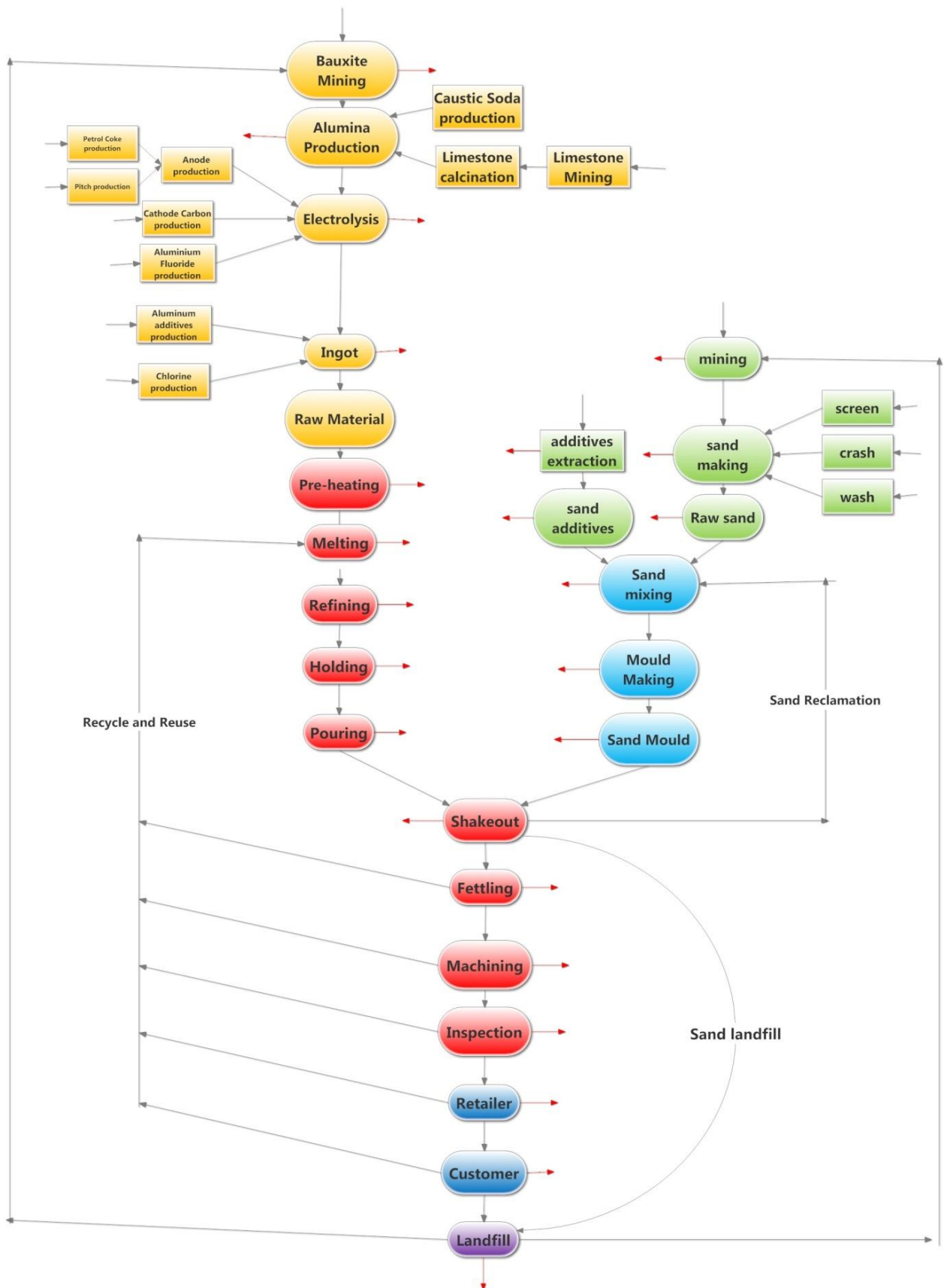
3.25

50

Please refer to the attached DVD for the spreadsheet

11.3 LCA Investigation of the casting process

Appendix 13 life cycle of the sand casting product (also can be found on DVD)



Appendix 14 Average values for “Q” for Fabric Belts

**AVERAGE VALUES FOR “Q” FOR FABRIC BELTS
(MASS OF MOVING PARTS, KILOGRAMS PER METRE)**

Belt width (mm)	Idler diameter			
	102 mm	127 mm	152 mm	178 mm
300	—	—	—	—
350	18	19	—	—
400	21	23	—	—
450	22	26	—	—
500	24	29	35	—
600	30	34	41	—
650	33	40	47	—
750	36	46	52	—
800	39	49	53	—
900	45	54	64	86
1000	50	59	68	100
1050	52	61	70	107
1200	—	70	84	125
1350	—	—	100	143
1400	—	—	103	150
1500	—	—	110	164
1600	—	—	118	175
1800	—	—	133	196
2000	—	—	148	217

Appendix 15 Energy burden result from 1993 to 2010

year	1,993	1,994	1,995	1,996	1,997	1,998	1,999	2,000	2,001
Aluminium consumption (TJ)	61,838.43	62,805.46	61,959.95	63,089.14	60,695.08	70,439.07	66,480.71	70,061.32	73,517.54
Casting Contribution (%)	8.40	13.23	13.28	14.32	13.16	12.39	11.14	10.53	10.22
Casting energy consumption (TJ)	5,196.11	8,309.43	8,230.10	9,032.59	7,987.85	8,725.08	7,408.41	7,374.88	7,511.73
casting weight (thound tonne)	133.20	144.00	147.60	156.00	152.40	147.60	136.80	134.40	129.60
energy burden (MJ/kg)	39.01	57.70	55.76	57.90	52.41	59.11	54.16	54.87	57.96
year	2,002	2,003	2,004	2,005	2,006	2,007	2,008	2,009	2,010
Aluminium consumption (TJ)	70,866.44	76,885.74	70,852.50	76,335.15	76,912.60	72,898.00	72,898.31	60,894.18	59,940.68
Casting Contribution (%)	11.03	11.60	10.24	10.24	13.41	12.73	12.70	12.70	12.70
Casting energy consumption (TJ)	7,816.69	8,916.73	7,258.83	7,815.26	10,317.54	9,283.65	9,258.09	7,733.56	7,612.47
casting weight (thound tonne)	127.20	127.20	110.40	204.00	185.00	139.20	186.64	151.31	164.68
energy burden (MJ/kg)	61.45	66.00	65.75	38.00	65.14	66.69	49.60	51.11	46.23

Appendix 16 Saleable casting per unit melting of aluminium, process yield, recovery ratio and recycling efficiency for different casting products 15

	CRIMSON Test bar	Gravity test bar	CRIMSON housing	AEROMET housing	AEROMET housing with recycling
Virgin aluminum (Kg)	1	1	1	1	1
Melting loss (Kg)	0.005	0.02	0.005	0.02	0.02
Holding loss (Kg)	0	0.02	0	0.02	0.02
Degassing loss (Kg)	0	0.048	0	0.048	0.048
Fettling loss (Kg)	0.597	0.707	0.577	0.821	0.821
Machining loss (Kg)	0.099	0.051	0.105	0.023	0.023
Scrap loss (Kg)	0.06	0.031	0.062	0.013	0.013
Good casting (Kg)	0.239	0.123	0.25	0.055	0.055
Process yield (%)	99.50%	91%	99.50%	91%	91%
Recovery Ratio (%)	75.60%	79%	74.40%	0%	89%
Recycling Efficiency	0.752	0.719	0.74	0	0.81172

Appendix 17 sand casting energy consumption calculation spreadsheet

Q22																		
	A	B	C	D	E	F	G	H	I	J	K	L	M	N	O	P	Q	
1	1						Minimum energy burden (KJ/Kg)	Maximum energy burden (KJ/Kg)		3	Melting	CRIMSON sand casting			Conventional sand casting			
2		sand	chemical sand				1278.627934	3507.848483				Weight loss during %	weight loss (kg)	weight remain (kg)	Weight loss during %	weight loss (kg)	weight remain (kg)	
3		Transport	conveyor on	100	3	5	0.09491346	0.09491346				raw material input	0	0	1	0	0	1
4			elevator off	20	0.8	10	0	0				melting	0.5	0.005	0.995	2	0.02	0.98
5		mik	muller				4.457	9.41				holding	0	0	0.995	2	0.0196	0.9604
6		Transport	conveyor on	100	2	5	0.068057657	0.068057657				degassing	0	0	0.995	5	0.048	0.9124
7			elevator off	100	0.85	5	0	0				fettling	60	0.597	0.398	77.5	0.7071	0.2053
8		compaction	flask				14.71	56.51				machining	25	0.100	0.299	25	0.0513	0.154
9		Transport	conveyor on	100	3	5	0.09491346	0.09491346				scrap	20	0.060	0.239	20	0.0308	0.1232
10			elevator off	100	0.85	5	0	0				good casting	0	0	0.2388	0	0	0.1232
11		shake out	rotating				6.232501502	10.49676221				Process yield	0.995			0.912		
12		Transport	conveyor on	100	3	5	0.143959782	0.143959782				Recovery Ratio	0.756			0.789		
13			elevator off	20	0.85	5	0	0				Recycling Efficiency	0.752			0.720		
14		transport total					0.40184436	0.40184436				OME	0.239			0.123		
15		energy without transport					1304.027436	3584.265245										
16		Total					1304.42928	3584.667089										
17																		
18											4	total energy burden						
19		reclamation									energy burden of using reclaimed sand				cycle of reclamation	energy burden (KJ/kg)		
20		2 primary reclaim									green sand					510.597		
21		shake out	rotating				6.232501502	10.49676221			chemical sand					2393.24		
22		Transport	conveyor on	20	3	5	0.417183106	0.417183106			by primary method		green sand	25		32.45		
23			elevator off	20	0.85	5	0	0			by second method	chemical sand	25		322.422			
24		magnetic separa	ferrous				0.178125	0.404977			thermally	chemical sand	25		652.988			

Please refer to the attached DVD for the spreadsheet

Appendix 18 Energy burden of sand mould making and total energy burden of casting

cycle	1	2	3	4	5	6	7	8	9	10
green sand primary reclaim (MJ/kg)	0.56	0.31	0.23	0.19	0.16	0.15	0.14	0.13	0.12	0.12
CRIMSON metal preparing (MJ/kg)	54.44	32.26	25.06	21.59	19.63	18.4	17.59	17.03	16.65	16.36
Conventional metal preparing	54.44	32.82	25.86	22.56	20.73	19.6	18.86	18.39	18.06	17.82
CRIMSON process (MJ/kg)	55	32.57	25.29	21.78	19.79	18.55	17.73	17.16	16.77	16.48
Conventional process (MJ/kg)	55	33.13	26.09	22.75	20.89	19.75	19	18.52	18.18	17.94

Appendix 19 Energy burden of sand mould making through secondary reclamation method and total energy burden of the casting

cycle	1	2	3	4	5	6	7	8	9	10
chemical sand secondary reclaim (MJ/kg)	2.45	1.32	0.94	0.75	0.64	0.57	0.52	0.48	0.45	0.43
CRIMSON metal preparing (MJ/kg)	52.55	31.25	24.35	21.03	19.15	17.98	17.21	16.68	16.32	16.05
Conventional metal preparing	52.55	31.81	25.15	22	20.25	19.18	18.48	18.04	17.73	17.51
CRIMSON process (MJ/kg)	55	32.57	25.29	21.78	19.79	18.55	17.73	17.16	16.77	16.48
Conventional process (MJ/kg)	55	33.13	26.09	22.75	20.89	19.75	19	18.52	18.18	17.94

Appendix 20 Energy burden of sand mould making through thermal reclamation method and total energy burden of the casting

cycle	1	2	3	4	5	6	7	8	9	10
chemical sand thermal reclaim (MJ/kg)	2.45	1.49	1.17	1.02	0.92	0.86	0.82	0.79	0.76	0.74
CRIMSON metal preparing (MJ/kg)	52.55	31.08	24.12	20.76	18.87	17.69	16.91	16.37	16.01	15.74
Conventional metal preparing	52.55	31.64	24.92	21.73	19.97	18.89	18.18	17.73	17.42	17.2
CRIMSON process (MJ/kg)	55	32.57	25.29	21.78	19.79	18.55	17.73	17.16	16.77	16.48
Conventional process (MJ/kg)	55	33.13	26.09	22.75	20.89	19.75	19	18.52	18.18	17.94

Appendix 21 Total energy burden for different recycle and non-recycle models.

Process		OME	Casting Weight (kg)	Melting Weight (kg)	Sand weight (kg)	Energy burden for sand (MJ/kg)	Energy burden for metal (MJ/kg)	Energy Consumption (MJ)
Non-recycle	CRIMSON	0.24	1.56	6.53	39.16	2.39	52.61	436.98
	Conventional	0.12	1.56	12.68	76.10	2.39	52.61	849.13
recycle	CRIMSON	0.24	1.56	6.57	39.16	0.65	15.05	124.48
	Conventional	0.12	1.56	12.68	17.38	0.65	16.73	223.50

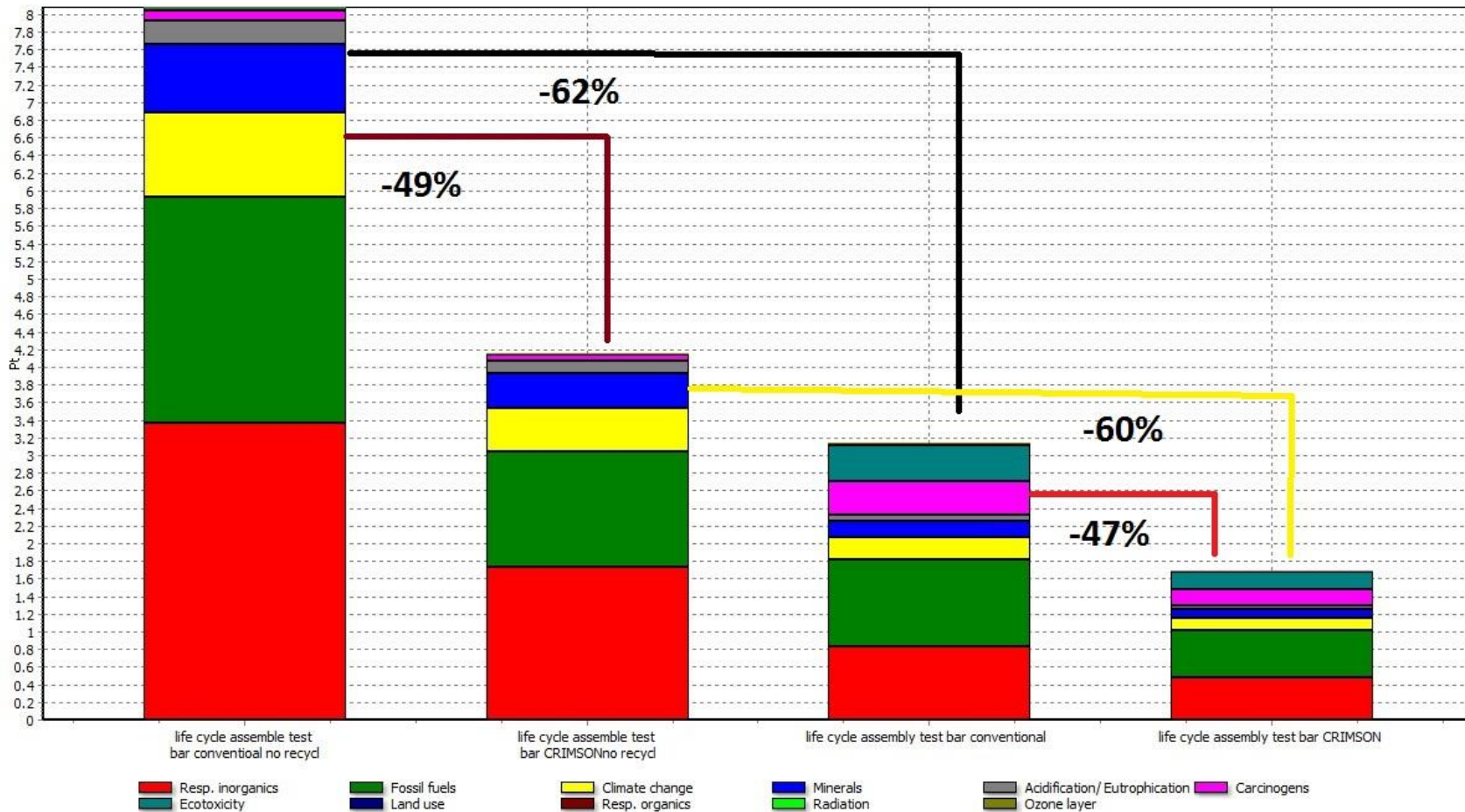
Appendix 22 Metal loss during each step of casting operation for the CRIMSON and the conventional casting processes

	CRIMSON test bar		Conventional test bar		Loss type
	Weight loss %	weight remain (kg)	Weight loss %	weight remain (kg)	
raw material	0	6.53	0	12.68	Permanent, can be disposed
melting	0.5	6.53	2	12.68	Permanent, can be disposed
holding	0	6.49	2	12.43	Permanent, can be disposed
degassing	0	6.49	5	12.18	Scraped, can be recycled
fettling	60	6.49	77.5	11.57	Scraped, can be recycled
machining	25	2.6	25	2.6	Scraped, can be recycled
scrap	10	1.95	20	1.95	NA
good casting	NA	1.56	NA	1.56	
OME	0.24		0.12		

Appendix 23 Impact assessment: GWP, AC, HTA due to emissions from the casting process and raw materials.

Impact category	Unit	life cycle assemble test bar conventioal no recydl	life cycle assemble test bar CRIMSONno recydl	life cycle assembly test bar conventional	life cycle assembly test bar CRIMSON
Total	Pt	9.4	4.83	2.98	1.59
Carcinogens	Pt	0.122	0.0626	0.0613	0.0208
Resp. organics	Pt	0.00226	0.00116	0.000741	0.000403
Resp. inorganics	Pt	3.76	1.93	1.05	0.584
Climate change	Pt	1.13	0.581	0.337	0.183
Radiation	Pt	0.00336	0.00171	0.00164	0.000734
Ozone layer	Pt	0.000155	7.9E-5	5.42E-5	2.66E-5
Ecotoxicity	Pt	0.035	0.018	0.0269	0.00587
Acidification/ Eutrophication	Pt	0.306	0.157	0.0876	0.0486
Land use	Pt	0.00265	0.00136	0.00202	0.000789
Minerals	Pt	0.77	0.395	0.163	0.0965
Fossil fuels	Pt	3.27	1.68	1.25	0.654

Appendix 24 ECO-indicator single score results for four casting scenarios

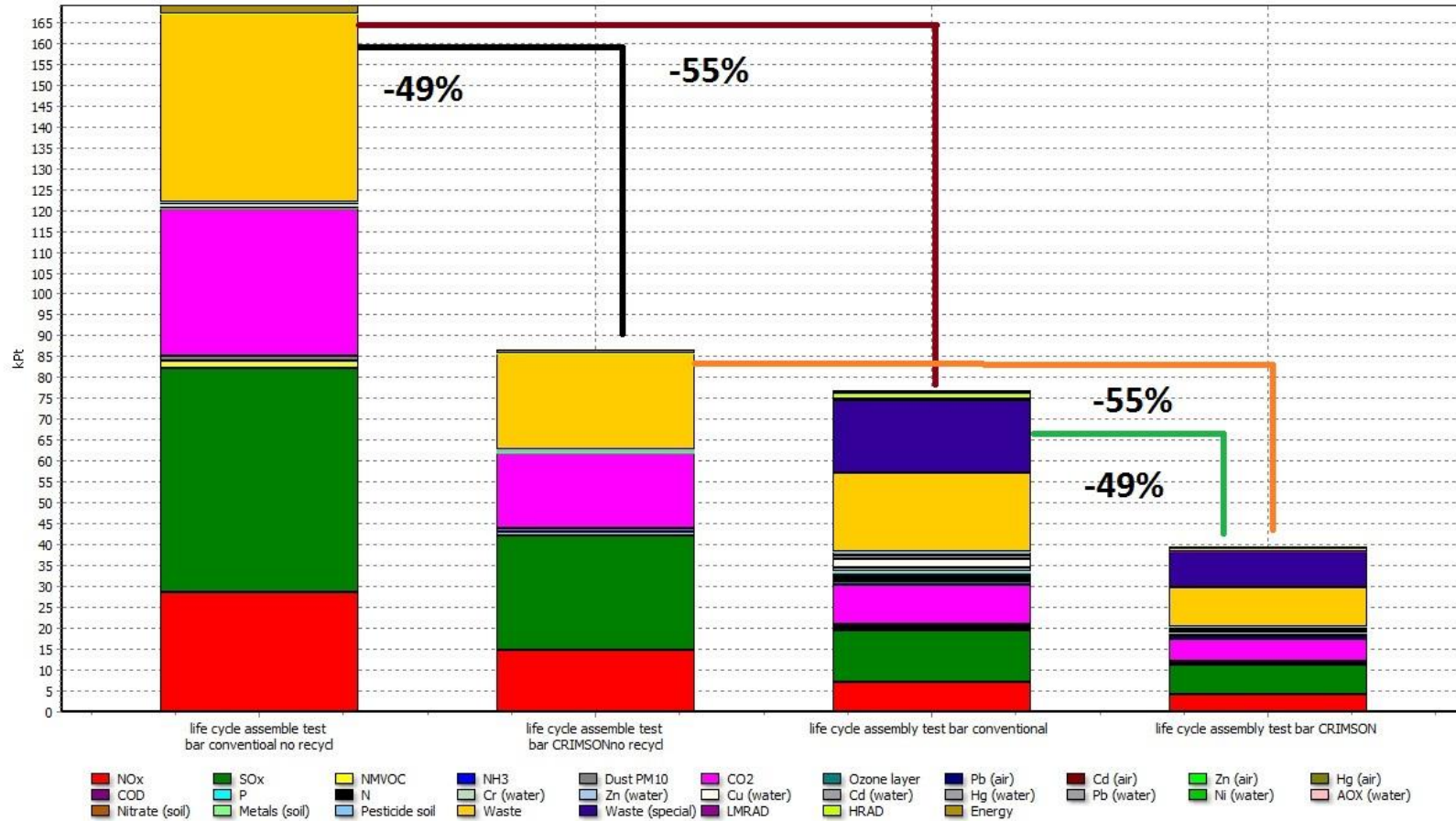


Comparing 1 p 'life cycle assemble test bar conventioal no recydl', 1 p 'life cycle assemble test bar CRIMSONno recydl', 1 p 'life cycle assembly test bar conventional' and 1 p 'life cycle assembly test bar CRIMSON';
Method: Eco-indicator 99 (H) V2.07 / Europe EI 99 H/A / Single score

Appendix 25 Weighting comparison using ECO-Points 97 method

Impact category	Unit	life cycle assemble test bar conventional no recycle	life cycle assemble test bar CRIMSON no recycle	life cycle assembly test bar conventional	life cycle assembly test bar CRIMSON
Total	Pt	169063.66	86719.35	76796.42	39440.90
SOx	Pt	53697.57	27587.13	12321.07	7179.03
Waste	Pt	45190.84	23081.14	18913.21	9497.21
CO2	Pt	35246.02	18107.11	9438.89	5322.39
NOx	Pt	28508.06	14645.38	7186.47	4128.35
Energy	Pt	1922.57	987.62	571.04	317.83
NMVOc	Pt	1703.32	875.09	577.14	317.68
Dust PM10	Pt	1196.79	614.64	664.40	349.96
Cd (water)	Pt	411.15	211.24	912.46	403.04
Hg (air)	Pt	351.10	180.38	425.22	216.84
COD	Pt	154.73	79.49	165.88	78.07
Cd (air)	Pt	153.15	78.68	331.77	166.57
Cu (water)	Pt	151.32	77.75	2091.61	371.79
Zn (water)	Pt	66.21	34.02	1021.86	402.36
Cr (water)	Pt	56.69	29.13	58.32	29.30
N	Pt	53.43	27.45	118.92	20.19
Pb (water)	Pt	52.13	26.79	92.32	13.33
HRAD	Pt	49.40	25.38	1397.52	693.19
NH3	Pt	35.41	18.19	98.83	49.64
Pb (air)	Pt	25.90	13.30	331.66	163.88
Hg (water)	Pt	16.50	8.48	623.51	151.59
LMRAD	Pt	16.31	8.38	397.54	197.01
Ozone layer	Pt	1.76	0.90	1028.34	506.42
Ni (water)	Pt	0.99	0.51	106.10	42.54
Nitrate (soil)	Pt	0.78	0.40	4.00	1.94
Metals (soil)	Pt	0.75	0.38	13.66	6.83
Zn (air)	Pt	0.47	0.24	738.79	363.86
P	Pt	0.22	0.11	12.23	1.76
Waste (special)	Pt	0.09	0.05	17153.09	8448.04
Pesticide soil	Pt	0.01	0.00	0.53	0.26
AOX (water)	Pt	0.00	0.00	0.04	0.02

Appendix 26 ECO-point single score results for four casting scenarios.



11.4 Productivity investigation: foundry survey and response

Appendix 27 the foundry survey

To whom it may concern

My name is Binxu Zeng. I am a PhD at Cranfield University supervised by Professor Mark Jolly and funded by the UK government on a project entitled “Energy saving in the Foundry Industry”. The CMF are representing the sector by being partners in the programme. I am working on the novel casting process called the CRIMSON (constrained rapid induction melting single up-casting) process. The aims of this new process are to improve casting quality and reduce energy consumption within the light-metal casting industry. The philosophy of the new process is to melt just enough mass of alloy in a closed crucible of an induction furnace and to use a counter-gravity filling method to fill a single mould and thus ensure smooth liquid alloy flow behaviour and at the same time avoid unnecessary energy consumption.

Currently I am working on validation such process through productivity analysis and cost estimation. For productivity analysis, I am planning to use process simulation method to compare normal casting process (sand casting, investment casting) with CRIMSON. For cost estimation, I will carry out a break even analysis both processes. To do this analysis I require some input data such as typical cycle times and fixed costs of equipment. If possible, please spend 5 to 10 minutes to finish this survey. It will help me a lot to validate such process.

In return, I can show you the possibility to improve casting quality, energy saving and cost saving as well.

Looking forward your reply

Best Regards

Binxu Zeng

<p>This survey aims to find the process cycle time for casting product up to 10 kg. The second goal is to find the fixed cost of the machines used for production. In this research, the casting process has been divided into eight steps: pre-heating, melting, melt-treatment, holding, shakeout, fettling, machining, and inspection.</p> <p>Please select one typical casting below 10 kg.</p>
<p>General information about the cast products</p>
<p>1 what is your alloy and casting size?</p>
<p>2 how much do you cut off during fettling? (kg)</p>
<p>3 roughly, how much metal do you remove during the machining process? (kg)</p>
<p>4 roughly, what is the scrap rate during inspection? (%)</p>
<p>5 roughly, how much is the raw material cost? £/tonne</p>
<p>about the casting process</p>
<p>1 what is batch size of the pre-heating? What is the cycle time of pre-heating? If possible, how much is the pre-heating equipment cost?</p>
<p>2 what is the capacity of the melting furnace? Ideally, how long will take to melt? If possible, how much is the furnace cost?</p>
<p>3 what is the cycle time of refining, degassing and drossing? If possible, how much is the degassing unit cost?</p>
<p>4 what is the capacity of the holding furnace? Ideally, how long will take to empty it? If possible, how much is the furnace cost?</p>
<p>5 what is the batch size of the shakeout? What is the cycle time to shakeout one batch? If possible, how much is the unit cost?</p>
<p>6 how long will fettling take? If possible, how much is the equipment cost?</p>
<p>7 how long will it take to machine one casting? If possible, how much is the equipment cost?</p>
<p>8 how long will it take to inspect one casting? If possible, how much is the equipment cost?</p>

Appendix 28 the foundry survey response from GKN

Appendix 29 the foundry survey response from himangshu patel

Appendix 30 the foundry survey response from RD casting

Appendix 31 the foundry survey response from zac ulsinger

Above appendices are located on the attached DVD

11.5 Data of cost estimation

Appendix 32 the comparison of the simulation results and the calculation results for different power output.

Above appendix is located on the attached DVD

Appendix 33 the conversation with Martin Wood from GW Cast about sand cost

Good morning Binxu,

The Cosworth process we operate uses Zircon sand. The cost for this material is around £1800 per tonne. Typical Silica sand is around £30 per Tonne. The Chromite sand you mentioned is around £650 per tonne. All of these sands are recycled using thermal reclamation. The recycling cost per tonne is around £15-20. Sand losses are somewhere between 3 and 5% per cycle.

Regards

Martin

From: Zeng, Binxu [<mailto:b.zeng@cranfield.ac.uk>]
Sent: 21 May 2013 19:45
To: Martin Wood
Subject: need little help about chromite sand price

Hi Martin

I am doing some break even analysis for the CRIMSON process and conventional casting process. I know GW use COSWORTH process which will use chromite sand.

Can you give me any information about the price of the chromite sand? It is hard to find it on line.

Thank very much

Best Regards

Binxu

This email has been scanned by the Symantec Email Security.cloud service.
For more information please visit <http://www.symanteccloud.com>

This email has been scanned by the Symantec Email Security.cloud service.
For more information please visit <http://www.symanteccloud.com>

Appendix 35 gravity pour casting running system design spreadsheet

C21														50	
A	B	C	D	E	F	G	H	I	J	K	L	M	N	O	
1	Birmingham University Spreadsheet										Metal	Liquid Density	Liq Den		
2	Alloy	Al									Ag	9346	9.346		
3	Mass of Method	0.55	0.65	0.67	0.68	0.68	0.68								
4	Poured Mass	1.55	1.65	1.67	1.68	1.68	1.68								
5	Yield	65%	60%	60%	60%	60%	60%								
6															
7															
8	Process (Sand, LPD, GD, Investment)	Sand	Sand	Sand	Sand	Sand	Sand				Al	2385	2.385		
9	1 Mass of Casting & Feeders (kg)	1.00	1.00	1.00	1.00	1.00	1.00				Au	17360	17.36		
10	2 Mass of Runner & Ingates & Filter Print (kg)		0.19	0.23	0.23	0.24	0.24				B	2080	2.08		
11	3 Total Mass (kg)	1.00	1.19	1.23	1.23	1.24	1.24				Ba	3321	3.321		
12	4 Volume (cc)	419	500	515	518	518	518				Be	1690	1.69		
13	5 Filling Time required (s)	5	5	5	5	5	5				Bi	10068	10.068		
14	6 Solid density	2.650	2.650	2.650	2.650	2.650	2.650				Ca	1365	1.365		
15	7 liquid density (g/cc)	2.385	2.385	2.385	2.385	2.385	2.385				Cd	8020	8.02		
16	8 average mass fill rate (kg/s)	0.200	0.239	0.246	0.247	0.247	0.247				Ce	6685	6.685		
17	9 initial mass fill rate (kg/s)	0.300	0.358	0.368	0.370	0.371	0.371				Co	7760	7.76		
18	10 initial volume fill rate (cc/s)	126	150	154	155	155	155				Cr	6280	6.28		
19	11 average vol fill rate (cc/s)	84	100	103	104	104	104				Cs	1854	1.854		
20	Height of pour above basin (mm) (lip of ladle or total height of bottom pour ladle plus vertical distance above basin)	50	50	50	50	50	50								
21	Depth of Basin (mm)	50	50	50	50	50	50								
22	11 Basin head (mm)	100	100	100	100	100	100				Cu	8000	8		
23	12 Basin velocity (m/s)	1.401	1.401	1.401	1.401	1.401	1.401				Fe	7015	7.015		
24	13 Top of Sprue velocity	0.700	0.700	0.700	0.700	0.700	0.700	35%			Hg	13691	13.691		
25	14 Discharge coefficient	30%	30%	30%	30%	30%	30%				In	7023	7.023		
26	15 Number of sprues	1	1	1	1	1	1				K	827	0.827		
27	16 Initial volume down each sprue (cc/s)	126	150	154	155	155	155				Li	525	0.525		
28	17 Average volume down each sprue (cc/s)	84	100	103	104	104	104				Mg	1590	1.59		
29											Mn	5730	5.73		
30	19 Area of top of Downsprue (sq mm)	233	279	287	288	289	289				Mo	9340	9.34		
31	20 Sides if square (mm)	15.3	16.7	16.9	17.0	17.0	17.0				Na	927	0.927		
32	21 Diameter if round (mm)	17.2	18.8	19.1	19.2	19.2	19.2				Ni	7905	7.905		
33											Os	20100	20.1		

Please refer to the attached DVD for full version of the spreadsheet

Appendix 36 All-in-one spreadsheet

Please refer to the attached DVD for full version of the spreadsheet

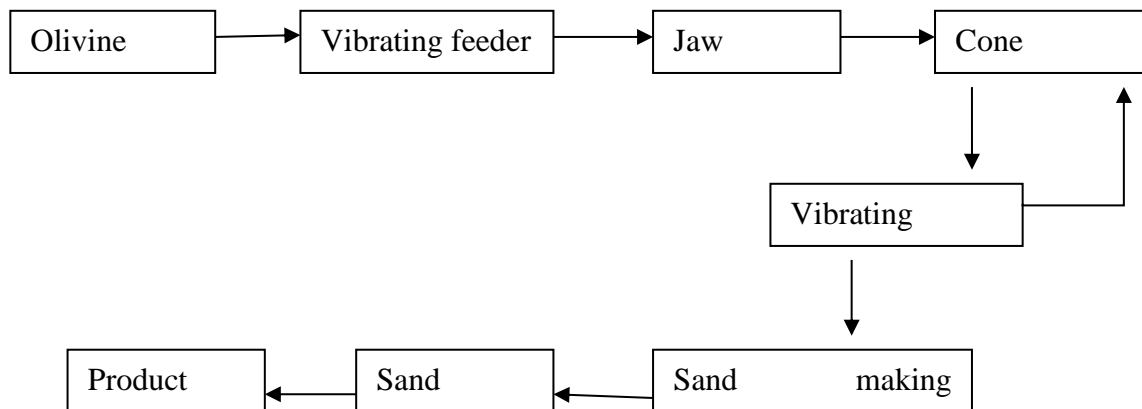
11.6 Machineries for sand making

Appendix 37 specification of machineries for sand making

Sand making line contains vibrating feeder, jaw crusher, cone crusher, sand making machine, vibrating screen and belt conveyor and some other equipment.

Silica sand making

The raw material (silica stone) is evenly delivered by the vibrating feeder to jaw crusher for primary crushing. The crushed materials are then sent by the belt to the secondary crusher such as cone crusher for further crush. After the second crush the coarse sand is transferred to a vibrating screen for screening. Then the coarse sand can screen out two major sand, one can be transferred to sand making machine and the other one sent back for re-crush. The final step of the sand making is the sand washing. The cleaned sand then send to the final products pile.



Vibrating feeder output

Model	Feeding Chute Size (mm)	Max. Feeding Size (mm)	Capacity (t/h)	Motor Power (kw)	Weight (kg)	Overall Dimension (mm)
GZD-750x2500	750x2500	300	50-80	3	1590	2580x1100x1400

GZD-850×3000	850×3000	400	80-120	2X2.2	3895	3110×1800×1600
GZD-960×3800	960×3800	500	120-210	11	3980	3850×1950×1630
GZD-1100×4200	1100×4200	580	200-430	15	4170	4400×2050×1660
GZD-1100×4900	1100×4900	580	280-500	15	4520	5200×2050×1700
GZD-1300×4900	1300×4900	650	450-600	22	5200	5200×2350×1750
GZD-1500×6000	1500×6000	800	500-700	30	8670	6082×2995×2095

http://www.joyalcrusher.com/products/Feeding-Conveying/Vibrating-Feeder.html?gclid=CL7UyO_z17ECFcYmtAodfAYAwg

Model	Max. feeding (mm)	Processing capacity(t/h)	Motor power(kw)	Obliquity of material trough	Total weight (kg)	Trough size (mm)	Dimensions (L*W*H)(mm)
GZD-650*2300	300	80	1.5*2	10	2798	650*2300	2300*1360*780
GZD-750*2500	350	100	1.5*2	10	3260	750*2500	2500*1460*780
GZD-850*3000	400	120	3*2	10	3607	850*3000	3110*1800*1600
GZD-1000*3600	500	150	5.5*2	5	3895	1000*3600	3850*1950*1630
GZD-1100*4200	580	240	5.5*2	5	4170	1100*4200	4400*2050*1660
GZD-1100*4900	580	280	7.5*2	5	4520	4900*1100	5200*2050*1700
GZD-1300*4900	650	450	11*2	5	5200	4900*1300	5200*2350*1750
ZSW-380*95	500	96-160	11	0	4082	3800*960	3920*1640*1320
ZSW-490*110	630	120-280	15	0	5352	4900*1100	4980*1830*1320
ZSW-600*130	750	400-560	22	0	7800	6000*1300	6082*2580*2083

<http://www.china-crusher.com/vibrating-feeder1.html>

Model	Max feed size(mm)	Processing capacity(t/h)	Speed(r/min)	Motor Model	Motor power(KW)	Motor NO.	Hopper size (mm)	Motor weigh(t)	Overall dimension (LxWxH)(mm)
GZD-180×80	300	30-80		YZO-20-6	1.5×2	2	1800×800	0.8	2200×1100×800
GZD-220×120	300	80-220		YZO-30-6	2.2×2	2	2200×1200	1.59	2200×1200×855
GZD-300×90	300	40-100		YZO-30-6	2.2×2	2	3000×900	1.5	3050×1430×1550
GZD-500	500	90-200	500-714	Y180L	11	1	3800×960	3.98	3882×2224×2121

380x96				6					
GSW-420x110	580	150-350	500-800	Y180L-6	15	1	4200x1100	5.0	4250x2500x1365
GSW-490x110	580	180-380	500-800	Y180L-6	15	1	4900x1100	5.32	5100x2500x1365
GSW-490x130	720	200-300	500-800	Y180L-6	22	1	4900x1300	5.9	4960x2580x1870
GSW-600x130	750	450-800	500-800	Y180L-6	30	1	6000x1300	7.8	6150x2580x2083

<http://www.alibaba.com/product->

[gs/578987527/Supply_complete_vibrating_feeder_specification.html](http://www.alibaba.com/product-)

Jaw crusher

Model	Feed Opening Size (mm)	Max. Feeding Size (mm)	Adjustable Range of Output Size (mm)	Capacity (t/h)	Motor Power (kw)	Weight (t)	Overall Dimension (mm)
PE250x400	250x400	200	20-50	5-20	15	2.9	1430x1310x1340
PE400x600	400x600	350	40-100	15-60	30-37	6.8	1700x1732x1653
PE500x750	500x750	425	50-100	40-100	45-55	11.2	2035x1921x2000
PE600x900	600x900	480	65-160	60-140	55-75	16.5	2290x2206x2370
PE750x1060	750x1060	630	80-150	80-230	90-110	29	2655x2302x3110
PE900x1200	900x1200	750	95-165	140-320	110-132	54.5	3789x3050x3025
PE1000x1200	1000x1200	850	105-185	180-400	160-200	56.5	3900x3320x3280
PE1200x1500	1200x1500	1020	150-300	250-650	220-250	99.6	4300x3540x4043
PEX150x250	150x250	125	10-40	1-3	5-5	0.85	896x745x935
PEX150x750	150x750	125	12-45	5-16	15	3.8	1205x1495x1203
PEX250x750	250x750	210	25-60	10-40	22-30	5	1667x1545x1020
PEX250x1000	250x1000	210	25-60	15-50	30-37	6.8	1964x1550x1380
PEX250x1200	250x1200	210	25-60	20-60	37-45	8.5	2192x1605x1415
PEX400x1200	400x1200	320	35-95	28-95	45-55	11.7	2256x2100x1960
JC180x1300	180x1300	150	10-30	12-40	30-37	6	1320x2150x1175
JC250x1000	250x1000	220	20-40	15-55	30-37	5.6	1400x1850x1310

JC250×1300	250×1300	220	20-40	20-65	37-45	6.8	1450×2150×1310
JC400×600	400×600	350	35-85	15-80	30-37	10	1920×1460×1840

<http://www.greatwallmill.com/product/jawcrusher.html>

Model	Max. Feed Size(mm)	Adjustable Range of Discharging Opening(mm)	Capacity(t/h)	Motor Power(kW)	Feed Opening(mm)	Weight(t)
PE-150×250	125	10-40	1.5	5.5	150×250	0.81
PE-250×400	210	20-60	5.20	15	250×400	2.8
PE-400×600	340	40-100	25-65	30	400×600	6.5
PE-500×750	425	50-100	45-80	55	500×750	10.1
PE-600×900	500	65-160	70-150	55-75	600×900	15.5
PE-750×1060	630	80-140	130-260	110	750×1060	28
PE-900×1200	750	95-165	220-500	110-132	900×1200	50
PE-1000×1200	850	195-265	250-700	132	1000×1200	57
PE-1200×1500	1020	150-300	400-1000	160-220	1200×1500	100.9

<http://www.quarrycrusher.com/jaw-crusher/>

Model	Max. Feeding Size (mm)	Adjustable Discharge opening (mm)	Capacity (t/h)	Motor Power (kW)	Overall Dimensions (mm)	Weight (t)
PEW200×1300	150	10-30	12.35	30	1320×2150×1175	6
PEW250×1000	220	20-40	15-50	30	1400×1850×1310	5.6
PEW250×1200	220	20-40	20-50	37	1450×2150×1175	6
PEW400×600	350	35-85	15-70	37	1920×1460×1840	6.5
PEW860	720	100-225	200-500	132	3300×2320×3120	32
PEW1100	940	150-275	300-650	185	4140×2660×3560	59.2

[http://www.shanghai-crusher.com/European Jaw Crusher/?googleUK-jawcrusher&gclid=CPnh2pCF2LECFUcKtAodZk4AMQ](http://www.shanghai-crusher.com/European_Jaw_Crusher/?googleUK-jawcrusher&gclid=CPnh2pCF2LECFUcKtAodZk4AMQ)

Cone crusher

[Standard CS Cone Cruser Technical Data]										
Type	Dia. of cone mm (inch)	Cavity	Feed Opening (mm)	Discharge Setting (mm)	Capacity (t/h)	Counter Shaft (r/min)	Power (kw)	Weight (t)	Overall Dimension (mm)	
Closed Side "B"	Opening Side "B"									
CSB75	900(3')	Fine	83	102	9-22	45-91	580	75	15	2821x1880x2164
		Coarse	109	175	13-38	59-163				
CSB110	1200(4')	Fine	127	131	9-31	63-188	485	110	20	2821x1974x2651
		Medium	155	156	13-38	100-200				
		Coarse	178	191	19-51	141-308				
CSB160	1295(4 1/4')	Fine	109	137	9-31	109-181	485	160	27	2800x2342x2668
		Medium	188	210	13-38	132-253				
		Coarse	215	241	19-51	172-349				
CSB240	1650(5 1/2')	Fine	188	209	16-38	181-327	485	240	55	3911x2870x3771
		Medium	213	241	22-51	258-417				
		Coarse	241	268	25-64	299-635				
CSB315	2134(7')	Fine	253	278	19-38	381-726	435	315	110	4613x3251x4732
		Medium	303	334	25-51	608-998				
		Coarse	334	369	31-64	789-1270				
[Short Head CS Cone Cruser Technical Data]										
Type	Dia. of cone mm (inch)	Cavity	Feed Opening (mm)		Discharge Setting (mm)	Capacity (t/h)	Counter Shaft (r/min)	Power (kw)	Weight (t)	Overall Dimension (mm)
			Closed Side "B"	Opening Side "B"						

CSD75	914(3')	Fine	13	41	3-13	27-90	580	75	15	2821×1880×2410
		Coarse	33	60	3-16	27-100				
CSD110	1218(4')	Fine	29	57	5-16	50-132	485	110	20	2560×1942×2928
		Medium	44	73	10-16	90-145				
		Coarse	56	89	13-19	141-181				
CSD160	1295(4 1/4')	Fine	29	64	3-16	36-163	485	160	27	2800×2342×2668
		Medium	54	89	6-16	82-163				
		Coarse	70	105	10-25	109-227				
CSD240	1676(5 1/2')	Fine	35	70	5-13	90-209	485	240	55	3917×2870×3771
		Medium	54	89	6-19	136-281				
		Coarse	98	133	10-25	190-336				
CSD315	2134(7')	Fine	51	105	5-16	190-408	435	315	110	4130×3251×445

<http://www.quarrycrusher.com/cone-crusher/symons-cone-crusher.php>

Standard	Chamber	Max feedsize (mm)	Min discharge opening (mm)	Power	Capacity(t/h)											Weight(kg)	
					Close discharge size(mm)												
					6	10	13	16	19	22	25	38	51	64			
ZYC600	C	95	10	37 45	20	25	30	35	45	50	76						5300
	M	72	6	37 45	18	20	25	30	35	40	45	60					5300
ZYC1000	C	160	13	90 110			80	100	135	150	175	235					10800
	M	115	10	90 110	65	75	90	120	135	150							10800
	F	80	8	90-110	52	62	72	78	115								10510
	EF	50	6	90-110	50	55	65	70	102								10510
ZYC1160	C	180	13	110-132			115	135	150	180	200	260					15500
	M	130	10	110-132	100	110	120	135	165	175							15500
	F	90	10	110-132	80	105	110	140									15500
	EF	60	6	110-132	60	74	105	110	130								15500

ZYC1300	C	200	16	132-160				150	180	200	230	310	390		22300
	M	150	13	132-160			115	140	160	190	210				22300
	F	102	10	132-160	90	115	145	160							22300
	EF	70	8	132-160	88	110	135	155							22300
ZYC1380	C	215	19	185-220					200	220	260	350	440		26300
	M	160	16	185-220				155	180	200	220				26300
	F	115	13	185-220			150	190	210	230					26300
	EF	76	8	185-220	122	148	185	200							26300
ZYC1500	C	235	22	185-220						265	310	420	525	580	37750
	M	175	19	185-220					215	240	265	320			37750
	F	130	13	185-220			180	210	235	255	275				37750
	EF	90	10	185-220	148	178	200	220							37750
ZYC1680	C	267	22	250-300						330	390	525	655	725	44300
	M	203	16	250-300				230	270	300	330				44300
	F	140	13	250-300	185	225	265	340							44300
	EF	95	10	250-300	180	220	260	335							44300

http://www.joyalcrusher.com/products/Crushing/ZYC-Cone-Crusher.html?clid=CLS_osyG2LECFQUOfAodtIQAfg

Vibrating screen

Type	Screen Spec .mm	Layers	Sieve Pore mm	Max. Feed Size mm	Capacity t/h	Power KW	Vibrating Frequency HZ	Double Amplitude mm
YA1230	1200×3000	1	3-50	200	7.5-70	5.5	800-970	8

2YA1230	1200×3000	2	3-50	200	7.5-80	5.5	800-970	8
2YA1230	1200×3000	3	3-50	200	7.5-80	7.5	800-970	8
YA1237	1200×3700	1	3-50	200	7.5-70	5.5	800-970	8
2YA1237	1200×3700	2	3-50	200	7.5-80	5.5	800-970	8
3YA1237	1200×3700	3	3-50	200	7.5-80	7.5	800-970	8
2YA1548	1500×4200	2	5-50	400	50-208	15	970	8
3YA1548	1500×4800	3	5-50	400	50-250	15	970	8
3YA1848	1800×4800	3	5-80	400	50-300	18.5	970	8
3YA1860	1800×6000	3	5-80	400	50-350	22	970	8
3YA2160	2100×6000	3	5-100	400	100-500	30	730	8
2YA2460	2400×6000	2	5-150	400	150-700	30	730	8

<http://www.chinavibratingscreen.com/Vibrating-screen-Specification.html>

sand making machine (silica sand)

Model		VSI5X7615	VSI5X8522	VSI5X9532	VSI5X1145
Capacity (t/h)	Feed Both at Center and Sides	150~280	240~380	350~540	500~640
	Feed at Center	70~140	120~200	180~280	250~360
Max Feed Size (mm)	Soft Material	<35	<40	<45	<50
	Hard Material	<30	<35	<40	<45
Rotation Speed (r/min)		1700~1900	1500~1700	1300~1510	1100~1310
Double Motor Power (kW)		110~150	180~220	260~320	400~440
Overall Dimension L×W×H (mm)		4100×2330×2300	4140×2500×2700	4560×2600×2900	5100×2790×3320
Weight (t)		8.6	11.8	17.5	27.5
Power Supply		380v, 50Hz			
Lubrication and Hydraulic Station	Double Motor Power	2X0.31kW			
	Safety Assurance	Double oil pumps assure enough oil supply, automatic switch off with no oil stream or hydraulic strength, lower the temperature with cool water in summer, raise the temperature with motor in winter.			
	Power of Oil Tank Heater	2kW			
	Overall Dimension L×W×H (mm)	820X520X1270			

<http://www.quarrycrusher.com/sand-making-machine/>

Model	Rolling Speed(r/min)	Max.Feed Size(mm)	Power(kw)	Capacity(t/h)	Overall Dimention(m)
JYS-6020	1460-2100	30	60-110	60-140	3.60×2.15×2.80

JYS-8623	1380-1810	40	150-220	120-280	4.52×2.58×3.30
JYS-9928	1200-1580	40	180-320	150-360	4.72×2.70×3.46
JYS-1238	1100-1360	40	220-400	200-400	4.98×2.97×3.68

http://www.mineral-grinder.com/pro_details_34.html

11.7 Publication

Appendix 38 Publications

Journal papers:

1. Xiaojun, D. A. I., Jolly, M., & Binxu, Z. E. N. G. (2012). Reduction of Energy Consumption and GHGs Emission in Conventional Sand Casting Process by Application of a New CRIMSON Process. *Energy Science & Technology*, 3(1).
2. Jolly, M. R., Dai, X., & Zeng, B. (2012). Energy saving in the foundry industry by using the CRIMSON single shot up-casting process. *Foundry Trade Journal International*, 186(3700), 317-324.

Conference papers:

1. Zeng, B., Jolly, M. and Dai, X. (2013) Designing Novel CRIMSON Running System Through Numerical Simulation Method for the Purpose of Reducing the Energy Content of Aluminium Investment Casting, in *Energy Technology 2013: Carbon Dioxide Management and Other Technologies* (eds S. Pati, J. Drelich, A. Jha, N. Neelameggham, L. Prentice and C. Wang), John Wiley & Sons, Inc., Hoboken, NJ, USA. doi: 10.1002/9781118658352.ch5
2. Dai, X., Jolly, M., Zeng, B. (2012) Implementation of Energy Saving and GHGs Emission Reduction in Investment Casting Process by Practical Application of a New Casting Method, *International Conference on Applied Energy*, Suzhou, China
3. Dai, X., Jolly, M., & Zeng, B. (2012, July). The improvement of aluminium casting process control by application of the new CRIMSON process. In *IOP Conference Series: Materials Science and Engineering* (Vol. 33, No. 1, p. 012009). IOP Publishing.
4. Dai, X., Jolly, M., & Zhang, B. (2012). Reduction of Energy Consumption and GHGs Emission in Investment Casting Process by Application of a New Casting Method. *Energy Technology 2012: Carbon Dioxide Management and Other Technologies*, 15-22.

5. Dai, X., Jolly, M., & Zeng, B. (2011). The Capability Enhancement of Aluminium Casting Process by Application of the Novel CRIMSON Method. In Shape Casting: 4th International Symposium 2011 (pp. 265-272). John Wiley & Sons, Inc..
6. Zeng, B., Salonitis, K., & Jolly, M. (2013). comparison of the enviromental impact of the CRIMSON process with normal sand casting process, Proceedings of the 11th International Conference on Manufacturing Research, Cranfield University, UK
7. Zeng, B., Jolly, M., & Salonitis, K. (2013, December). Manufacturing Cost Modeling of Castings Produced with CRIMSON Process. In Shape Casting: 5th International Symposium 2014 (p. 201). John Wiley & Sons.